A ROLE FOR PARKINSON'S-LINKED *LRRK2*, *SNCA*, AND *GBA1* GENES IN MODULATING THE COURSE OF DISEASE DUE TO RNA VIRUS INFECTIONS

Michaela Lunn

Thesis submitted to the University of Ottawa
in partial Fulfillment of the requirements for the
Doctor of Philosophy in Cellular and Molecular Medicine

Department of Cellular and Molecular Medicine
Faculty of Medicine
University of Ottawa

© Michaela Lunn, Ottawa, Canada, 2024

Thesis Abstract

Parkinson's disease (PD) is a complex motor neurodegenerative disorder with heterogenous disease pathology and symptomatology. We and others believe PD to be a complex disease, requiring a combination of genetic susceptibility, sex, ageing, and environmental trigger(s) for disease initiation. For over a century, viral exposures have been correlated to PD risk. In this thesis, we sought to investigate a role for three PD-linked genes, *Snca*, *Lrrk2*, and *Gba1*, in the host's response to virulent, microbial pathogens in mice. We also sought to explore the neuropathological consequences in the brains of adult mice that survived infections. We previously reported that endogenous expression of *Snca* (encoding α-synuclein) and allelic variants of *Lrrk2* (both a hyper-kinase variant, p.G2019S, and a kinase-dead variant, p.D1994S) could perturb the course of illness, as measured by survival rate and viral titres in target tissues, following nasally acquired reovirus, serotype T3D, in mouse pups. To delineate the involvement of these two proteins in peripheral- *vs.* brain-specific immune responses, we employed a direct brain inoculation method using reovirus T3D. In this case, all mutant neonates had the same disease course as their wild-type littermates, suggesting that both α-synuclein and Lrrk2 contribute to the host response during acute reovirus T3D-induced encephalitis primarily via peripheral rather than CNS-based immune mechanisms. Next, we investigated the role of Lrrk2 in the host's response to nasally inoculated adult mice using two distinct RNA viruses: neurotropic vesicular stomatitis virus (VSV), Indiana strain, and pneumotropic influenza A virus, serotype H1N1. Intriguingly, mice carrying a homozygous *Lrrk2* p.G2019S genotype had higher mortality following VSV infection -but not following H1N1 infection- with a female sex bias. We next investigated the commonest PD-risk gene, *Gba1*, in the same viral paradigms. Homozygous mutant Gba1 p.D409V mice (with associated decreased GCase activity) were relatively protected against VSV infection

-but not against influenza A virus serotype H1N1 or bacterial *Salmonella typhimurium* infection- with a male sex bias. Taken together, we found that three PD-linked genes could alter survival rates following nasally acquired encephalitis (*Snca*: reovirus T3D; *Gba1*: VSV; *Lrrk2*: both viruses). Next, the second goal of this thesis was to explore downstream effects of resolved viral infections on brain health. As such, we measured neuropathology-linked biochemical changes in the brains of wild-type and Lrrk2 p.G2019S mice that survived either VSV or H1N1 infection 6 weeks after inoculation. We observed that both viruses led to a significant increase of oxidative stress, but surprisingly, had opposing effects on α-synuclein concentration: the neurotropic virus decreased it, but H1N1 increased it, although the effects were not dependent on the p.G2019S mutation. Notably, we also identified a strong induction of tau phosphorylation (p-Tau) in the brain following these viral exposures. In reovirus T3D-infected neonates, the abundance of p-Tau protein was elevated during peak infection at 8 days post inoculation, when compared to mock-treated animals, with a further rise in Lrrk2 p.G2019S mutant pups. In adult mice, p-Tau remained high in VSV- or H1N1-infected brains at least until six weeks post inoculation. In summary, this thesis demonstrates a complex interplay between three PD-linked genes and viral infections in mice, showing that their loci can alter the course of illness in these infection models. We also found that viral infections, even those without neurotropism, such as H1N1, can lead to neurodegeneration-linked, biochemical changes in the brain of wild-type and mutant mice. These observations suggest that viral exposures could act as facilitators in the development of numerous neurodegenerative diseases that include tauopathies and PD.

Acknowledgements

This thesis has been a labour of love requiring a lot of blood, sweat, and (sad and happy) tears, and wouldn't have been completed without the support of a full community.

Firstly, to my supervisor Dr. Michael Schlossmacher, thank you for always motivating and supporting me to be the best scientist I can be, and always encouraging me to take every opportunity. Your fascination with science and discovery is infectious. To an equally important mentor, Dr. Julianna Tomlinson, I feel blessed to have been trained by you - beyond what a brilliant scientist you are, I admire how you bring joy, inclusivity, and enthusiasm to every situation you are in. These are skills that I hope to continue to emulate for the rest of my career. Thank you to Dr. Earl Brown and Dr. Qiubo Jiang for tremendous expertise and support in all things, but especially viruses and mice, respectively. Further, thank you to my thesis advisory committee members: Dr. Subash Sad, Dr. Angela Crawley, and especially Dr. Stephen Ferguson, who has supported me as a TAC member since 2017.

Thank you to all members of the Schlossmacher lab spanning from 2017 to present who have had a positive impact not only on my science but also my well-being. I've thoroughly enjoyed all the potlucks, playing 'geography' and trivia in the lunchroom, HQ trivia times, and crying together over bad and good experimental outcomes. To Daniel, you are a lifelong best friend and our time together in lab was so incredibly chaotic and joyful, I would do it all again with you. I blame (thank?) you that I did a PhD. To Nathalie, this thesis would not exist without you. I can't make a single decision, lab-related or otherwise, without you, and I thank you for listening to me literally hours on end. You are the second co-author on this entire thesis, and I value your friendship out of lab just as much.

To all the friends in other labs that I've met throughout my studies at uOttawa, Carleton, and Algonquin: you've all pushed me to be a better scientist but more than that you've been wonderful friends and a source of joy.

A tremendous thank you to the funding bodies that have believed in me as a scientist and supported my research. Specifically, thank you to everyone at the Parkinson Research Consortium and the Larry Haffner family, who kindly gifted me my first ever graduate scholarship, which then helped me get further government fellowships and continue this research. It has been a pleasure to be involved in the PRC and I look forward to continuing my support in my future endeavors.

To my family: my mom, Christine; my dad, Allan; my sister, Yvonne; and my fiancé, Zac, thank you for celebrating all my wins and helping me weather all my losses. I truly, truly, truly could not have managed without the support of each of you. I can't wait to see where the next chapter takes all of us together!

Finally, this thesis is dedicated to my grandpa, Michael Hynes. My grandpa always told me that when I finished my PhD, he would fly us to Paris, and he would buy me a designer Dolce & Gabbana dress. Grandpa, I'll meet you there.

"I had written this book because it was so difficult to do that the idea had fascinated me (...) I wrote the book after a tremendous amount of planning, and I was pleased with what I had made of it (...) It was well received and reviewed, but ***the person who was really pleased with it was myself, for I knew better than any how difficult it had been.****"*

- Agatha Christie, And Then There Were None (Author's Note)

Table of Contents

Acknowledgements ..... *iv*

List of Abbreviations ..... *viii*

List of Figures ..... *xi*

List of Tables ..... *xiii*

Chapter 1: General Introduction *1*

1. Parkinson's Disease **2**

2. Clinical Manifestations **2**

3. Genetics of Parkinson's Disease **4**

4. Molecular Pathology of Parkinson's Disease **6**

4.1. Dopaminergic Neuronal Cell Loss 6

4.2. α-Synuclein 7

5. Environmental Risk Factors for Parkinson's Disease **9**

6. Inflammation and Parkinson's Disease **11**

6.1. Inflammation 11

6.2. Cytokines in Parkinson's Disease 14

6.3. Epidemiological Evidence of Pathogen Exposure and Parkinson's Disease 15

6.4. Evidence from Mouse Models of Pathogen Exposure and Parkinson's Disease 16

7. LRRK2 ..... **17**

7.1. LRRK2 Structure 17

7.2. Genetics of LRRK2-PD 18

7.3. LRRK2 Variants in Other Diseases 20

7.4. LRRK2 Physiological Function 24

7.5. A Role for LRRK2 in the Immune System 25

7.5.1. LRRK2 in Innate Immunity 25

7.5.2. LRRK2 in Microglia 27

7.5.3. LRRK2 in Adaptive Immunity 27

7.5.4. LRRK2 and Pathogen Interactions 28

7.6. LRRK2 Kinase Inhibition as a Therapeutic Target 30

8. *GBA1* in Parkinson's Disease **31**

8.1. Physiological Role of Glucocerebrosidase 32

8.2. *GBA1* in the Immune System 34

8.3. *GBA1* and *LRRK2* 35

9. Pathogen Selection **36**

9.1. Reovirus T3D 36

9.2. Vesicular Stomatitis Virus 37

9.3. Influenza A Virus Serotype H1N1 39

9.4. *Salmonella typhimurium* 39

10. Statement of Research **40**

10.1. Rationale 40

10.2. Hypothesis 42

10.3. Objectives 42

Chapter 2: Lrrk2 variants do not alter course of primary encephalitis due to neurotropic reovirus T3D in newborn mice but the p.G2019S mutant elevates phosphorylated tau *44*

Statement of Author Contribution **45**
Abstract **47**
Introduction **48**
Methods **52**
Results **55**
Discussion **67**
Supplementary Information **74**
Chapter 3: Variable outcomes for phospho-tau, α-synuclein, and oxidative stress in adult mice including in Lrrk2 p.G2019S mutants after nasally acquired viral infections ***76***
Statement of Author Contribution **77**
Abstract **79**
Introduction **80**
Methods **83**
Results **90**
Discussion **122**
Supplementary Materials **129**
Chapter 4: Gba1 p.D409V Mutant Alleles Confer Protection During Acute Infection by a Neurotropic RNA Virus Following Nasal Inoculation ***133***
Statement of Author Contribution **134**
Abstract **136**
Introduction **137**
Methods **140**
Results **145**
Discussion **168**
Supplementary Materials **175**
Chapter 5: General Discussion ***178***
1. Summary **179**
2. Principal Findings **183**
3. Future Directions **191**
4. Conclusion **199**
References Cited ***201***

List of Abbreviations

AD	Alzheimer's disease
ALS	Amyotrophic lateral sclerosis
ANK	Ankyrin repeat
ANOVA	Analysis of Variance
APC	Antigen presenting cell
ARM	Armadillo repeat
aSyn	Alpha-Synuclein
BBB	Blood Brain Barrier
BCA	Bicinchoninic acid
BD	Bipolar disorder
BMDM	Bone marrow-derived macrophage
CBD	Corticobasal degeneration
CC3	Cleaved caspase-3
CD	Crohn's disease
CFU	Colony forming unit
CNS	Central Nervous System
COR	C-terminal of Roc domain
CSF	Cerebrospinal fluid
DA	Dopamine
DLB	Dementia with Lewy bodies
DPI	Days post inoculation
EOPD	Early onset Parkinson's disease
GCase	Glucocerebrosidase
GCS	Glucosylceramide synthase
GD	Gaucher disease
GI	Gastrointestinal
GlcCer	Glucosylceramide
GlcSph	Glucosylsphingosine
GWAS	Genome-Wide Association Studies
HA	Hemagglutinin
HET	Heterozygous
IAV	Influenza A virus
Iba1	Ionized calcium binding adaptor molecule 1
IFN	Interferon
IL	Interleukin
kDA	Kilodalton
KI	Knock-in
KO	Knockout

L-dopa	Levodopa
LB	Lewy body
LD_{50}	Lethal dose 50%
LN	Lewy neurite
LPS	Lipopolysaccharide
LRR	Leucine rich repeat
LRRK2	Leucine rich repeat kinase 2
M-CSF	Macrophage colony-stimulating factor
MHV	Mouse hepatitis virus
MPTP	1-methyl-4-phenyl-1,2,3,6-tetrahydropyridine
MSA	Multiple system atrophy
NfL	Neurofilament light chain
NSAID	Nonsteroidal anti-inflammatory drug
OB	Olfactory bulb
p-Tau	Phosphorylated tau
P0	Post natal day 0
P1	Post natal day 1
PBS	Phosphate-buffered saline
PD	Parkinson's disease
PFU	Plaque forming unit
pLrrk2	Phosphorylated Lrrk2
poly I:C	Polyinosinic:polycytidylic acid
PSP	Progressive supranuclear palsy
REM	Rapid eye movement
REO	Respiratory enteric orphan
RES	Reactive electrophilic species
RNS	Reactive nitrogen species
ROC	Ras of complex proteins domain
ROS	Reactive oxygen species
SDS	Sodium dodecyl sulfate
SEM	Standard error of the mean
Ser	Serine
SLE	Systemic lupus erythematosus
SNP	Single nucleotide polymorphism
SNpc	Substantia nigra *pars compacta*
snRNA-seq	Single nucleus RNA sequencing
SPI	Salmonella pathogenicity island
ST	*Salmonella typhimurium*
T1L	Type 1 Lang
T1R	Type 1 reaction

T2J	Type 2 Jones
T3D	Type 3 Dearing
TGF	Transforming growth factor
Thr	Threonine
TLR	Toll-like receptor
TNF	Tumor necrosis factor
TXS	Triton-X extraction buffer
V:V	Volume: Volume
VSV	Vesicular Stomatitis Virus
VTA	Ventral Tegmental Area
W:V	Weight: Volume
WEEV	Western equine encephalitis virus
WPI	Weeks post inoculation
WT	Wild-type

List of Figures

- **Chapter 1**:
  - **Fig. 1.1**: Schematic Diagram of LRRK2's Structure, Inflammatory Disease-Associated Mutations, and Phosphorylation Sites.
- **Chapter 2**:
  - **Fig. 2.1**: Expression of the Parkinson's Disease-Linked Lrrk2 p.G2019S Variant Does Not Alter Outcomes of Acute Reovirus T3D-Induced Encephalitis When Inoculated Intracerebrally.
  - **Fig. 2.2**: Expression of the Lrrk2 Kinase-Dead p.D1994S Mutant Does Not Alter Outcomes of Acute Reovirus T3D-Induced Encephalitis When Inoculated Intracerebrally.
  - **Fig. 2.3**: Phospho-Tau Levels, But Not Total Tau or α-Synuclein Abundance, Are Significantly Increased After Intracerebral Reovirus T3D Infection in Lrrk2 p.G2019S Mice.
  - **Fig. 2.4**: Expression Of Murine *Snca* Gene Does Not Alter Outcomes of an Acute, Intracerebral Infection by Reovirus-Induced Encephalitis.
  - **Supplemental Fig. 2.1**: α-Synuclein and Total Tau Protein Abundance Are Both Correlated to Reovirus Viral Titres in the Brains of Nasally Inoculated Mice.
  - **Supplemental Fig. 2.2**: Inoculation At Post-Natal Day 3 Does Not Uncover Genotypic Differences in Time-To-Death Between Wild-Type, Heterozygous, or Homozygous Lrrk2 p.D1994S Mutant Mice.
- **Chapter 3**:
  - **Fig. 3.1**: Homozygous Female Lrrk2 p.G2019S Knock-in Mice Lose Sex-Specific Survival Benefit from Encephalitis Following Nasal Inoculation with Vesicular Stomatitis Virus.
  - **Fig. 3.2**: Expression of *Lrrk2* p.G2019S Knock-in Alleles Does Not Alter Survival, Weight Change, or Viral Titres in the Lungs of Mice Nasally Inoculated with Influenza Virus, H1N1.
  - **Fig. 3.3**: Mice Expressing Kinase-Dead *Lrrk2* p.D1994S-Knock-in Alleles Show the Same Survival Rates as Wild-type Mice After Nasal Inoculation with VSV or H1N1.

- **Fig. 3.4**: Lrrk2 p.G2019S Knock-In Allele-Expressing Mice Do Not Show Altered Cytokine Signalling in the Brain or Serum or Detectable Neurofilament Difference in the Serum When Compared to Wild-type Mice Following VSV Infection.
- **Fig. 3.5**: Microscopic Analyses of Microglial Response in Olfactory Bulbs from Mock- and VSV-Infected Wild-type and Homozygous Lrrk2 p.G2019S Knock-in Mice.
- **Fig. 3.6**: Quantitative Analysis of Microglial Density and Morphology in Mock- and VSV- Infected Olfactory Bulbs of Wild-type and Homozygous Lrrk2 p.G2019S Knock-in Mice.
- **Fig. 3.7**: Quantitative Analysis of Microglial Density and Morphology in Mock- and VSV-Infected Brain Regions Other Than the Olfactory Bulb of Wild-type and Homozygous Lrrk2 p.G2019S Knock-in Mice.
- **Fig. 3.8**: Microscopic Analyses of Cleaved Caspase-3 Reactivity in Olfactory Bulbs from Mock- and VSV-Infected Wild-type and Homozygous Lrrk2 p.G2019S Knock-in Mice.
- **Fig. 3.9**: Adult Mice that Survived a VSV or H1N1 Infection Show Changes in Oxidative Stress Markers and α-Synuclein Abundance at 6 Weeks Post Inoculation.
- **Fig. 3.10**: Abundance of Phosphorylated Tau is Increased in the Brains of Adult Mice Infected by VSV or H1N1-Virus Without a Detectable Lrrk2 Mutation Effect.
- **Supplemental Fig. 3.1**: Additional Results for Cytokine and Chemokine Analyses in Hemibrain Homogenates from Wild-Type and Lrrk2 p.G2019S Mutant Mice Following VSV Infection.
- **Supplemental Fig. 3.2**: Additional Results for Cytokine and Chemokine Analyses in Sera from Wild-Type and Lrrk2 p.G2019S Mutant Mice Following VSV Infection.

- **Chapter 4**:
  - **Fig. 4.1**: *Gba1* p.D409V Alleles Do Not Alter Survival or Weight Loss in Mice Following Inoculation with Influenza A Virus.
  - **Fig. 4.2**: *Gba1* p.D409V Alleles Do Not Alter *Salmonella Typhimurium* Bacterial Load in Mice With or Without Preceding Influenza A Virus H1N1 Infection.

- **Fig. 4.3**: Female Sex and *Gba1* p.D409V Knock-in Alleles Confer Survival Benefits in Mice During Infection by Vesicular Stomatitis Virus.
- **Fig. 4.4**: Organ Tropism, Sex and *Gba1* Genotype Determine Viral Loads in Adult Mice During Acute Infection with Vesicular Stomatitis Virus.
- **Fig. 4.5**: GCase Activity Measured *In Vitro* is Altered in Gba1 p.D409V Knock-in Mice in a Sex-and Organ-Specific Manner During Acute Infection with Vesicular Stomatitis Virus.
- **Fig. 4.6**: *Gba1* p.D409V Knock-in Alleles Modify Select Cytokines/Chemokines in an Infection- and Sex-Dependent Manner Following Inoculation with Vesicular Stomatitis Virus.
- **Fig. 4.7**: Total α-Synuclein, p-Tau, and Lrrk2 Levels are Unchanged During Acute Vesicular Stomatitis Virus Infection in Gba1 p.D409V Mutant Mice.
- **Supplemental Fig. 4.1**: Additional Results for Cytokine and Chemokine Analyses in Gba1 p.D409V Mutant Mice Following VSV Infection.

- **Chapter 5**:
  - **Fig. 5.1**: Summary of Biochemical Changes Observed Following VSV or H1N1 Infection in Wild-Type, Lrrk2 p.G2019S, and Lrrk2 p.D1994S Mice at 6 Weeks Post Inoculation.

List of Tables

- **Chapter 4**:
  - **Supplemental Table 4.1**: GCase Activity in Mock- and VSV-Infected Olfactory Bulbs, Brains Without Olfactory Bulbs, and Lungs from Wild-Type (WT/WT), Heterozygous (WT/D409V), And Homozygous (D409V/D409V) Gba1 p.D409V Knock-In Mice At 2dpi.

Chapter 1: General Introduction

1. Parkinson's Disease

Parkinson's disease (PD) is a highly prevalent motor and neurodegenerative disorder. PD was first described by James Parkinson in 1817, but the exact etiology and mechanisms for disease progression remain to be elucidated (Parkinson, 1817). Typical PD presents with Lewy pathology characterized as the intracellular accumulation of fibrillar α-synuclein; however, PD exhibits a high level of heterogeneity (Outeiro et al., 2023; Wüllner et al., 2023). Presently, one in 500 Canadians are affected by PD and approximately 6,600 new cases of PD are diagnosed each year (UCB Canada Inc., 2022). Pathologically, PD manifests due to the death of vulnerable dopaminergic neurons in the Substantia nigra *pars compacta* (SNpc), which is involved in basal ganglia circuitry and leads to impairment of integration and execution of motoric tasks.

2. Clinical Manifestations

Clinically, parkinsonism is characterized by the presence of four cardinal motor symptoms: tremor, rigidity, brady-/akinesia, and postural instability. Diagnosis of PD requires at least two of these hallmark sign/symptoms, as well as evidence of progression and responsiveness to treatment, *e.g.*, levodopa (L-dopa) (Grimes et al., 2019). These signs/symptoms present heterogeneously in PD patients, with some symptoms onsetting sooner or more dramatically in some. Importantly, the motor signs of PD are only a fraction of the disease signs and symptoms that present. A large portion of PD changes are non-motor and can appear up to 20 years before motor signs present; however, diagnosis often only occurs at the time of overt motor sign presentation (Kalia and Lang, 2015). This period, prior to motor sign onset but in the presence of non-motor symptoms, is referred to as the prodromal period. Many of these non-motor symptoms present during the prodromal phase but persist for the entire duration of disease.

As high as 80% of PD patients present with depression as a co-morbidity, and it is estimated that PD patients have a six times higher risk of developing depression (Blonder and Slevin, 2011). Further, common non-motor signs and symptoms include: constipation and other gastrointestinal (GI) disturbances; sleep disorders including insomnia and rapid-eye-movement (REM) sleep behaviour disorder; and loss of olfactory function (Kalia and Lang, 2015). Indeed, olfactory dysfunction (hypo-/anosmia) is seen in 90% of idiopathic PD cases and many familial cases of PD (Doty et al., 1988). Given this high prevalence of hyposmia in PD patients early in disease, this symptom is currently being used in clinical trials as a prodromal predictive marker of PD risk (e.g., Li et al., 2022; Schlossmacher et al., 2017). Notably, multiple of these early disease presentations occur outside of the brain, and therefore suggest that PD etiology may also initiate outside of the brain.

The highest risk factor for PD onset is advanced age (Schlossmacher et al., 2017). Majority of PD cases are diagnosed after age 55. Cases that are diagnosed earlier are considered early-onset Parkinson's disease (EOPD); specifically, before the age of 40 it is considered 'young-onset', and before the age of 20 it is considered 'juvenile onset' (Kolicheski et al., 2022). The risk for PD onset increases 10-fold from 0.4% to 4% from age 50 to age 80 years (Berg et al., 2015). It is estimated that PD is present in 5% of individuals over 85 years of age (de Lau and Breteler, 2006). Beyond this, typical PD presents with a male sex bias of ~1.5x (Berg et al., 2015); however, this male sex bias is not consistent across all genetic forms of the disease (*i.e.,* in LRRK2-linked cases of PD, discussed below) (Cilia et al., 2014; Marder et al., 2015).

3. Genetics of Parkinson's Disease

Cases of PD are either categorized as sporadic/idiopathic or familial. An estimated 85% of PD cases are sporadic, meaning that onset is due to unknown causes, likely with both genetic (*de novo* mutations and low penetrance of risk alleles) and environmental influence (Tysnes & Storstein, 2017; Willis et al., 2022). A thorough review of environmental risk factors involved in idiopathic PD onset will be discussed in section 5.

Though less common, much research has been pursued towards familial PD. With great advancements in genetic sequencing, many genes have been identified as monogenic forms of PD in the past few decades (Cherian and Divya, 2020). Genes that are both autosomal dominant and autosomal recessive have been linked to heritable PD. Further, both point mutations, deletions, and multiplication events of disease genes have been identified. Importantly, there is only a small subset of identified *causative* alleles, and even so, often these causative gene mutations present with low penetrance (*i.e., LRRK2* mutations). Genetic variants are often associated with increased susceptibility to PD onset instead of true-to-form monogenic disease initiation.

The first identified gene, discovered in 1997, carried a point mutation (p.A53T) in the *SNCA* gene which encodes α-synuclein (Polymeropoulos et al., 1997). Mutations in *SNCA* present as point mutations or multiplication (duplication or triplication) events, and are inherited autosomal dominantly (Konno et al., 2016). *SNCA* being a prominent disease gene for PD is unsurprising, as the protein encoded for by *SNCA*, α-synuclein, is the hallmark pathological protein aggregate in PD. *SNCA* triplication mutations are fully penetrant, whereas *SNCA* duplication mutations are not (Konno et al, 2016).

Further autosomal dominant PD disease genes include *LRRK2*, *VPS35*, and *RAB32*. *LRRK2* variants have been linked to rare monogenic, familial PD as well as increased genetic susceptibility

to idiopathic PD. It is estimated that mutations in *LRRK2* account for 4% of familial cases of PD and 1-2% of sporadic (Healy et al., 2008). In the Western hemisphere, the most common mutation in *LRRK2* is the p.G2019S variant in the kinase domain, which causes a two- to three-fold increase in the phosphorylation activity of the protein (Kachergus et al., 2005). The p.G2019S mutation is an autosomal dominantly inherited mutation but has a relatively low penetrance to cause PD (~28% at age 59 years) (Healy et al., 2008). The most recently identified genetic form of PD, *RAB32*, likely functions in a similar manner as *LRRK2* mutations, as the PD-associated *RAB32* p.S71R mutations leads to increased LRRK2 kinase activity (Gustavsson et al., 2024). Mutations in *VPS35* are often linked to endolyosomal disruptions, which has also been implicated in *LRRK2* pathobiology (Vilariño-Güell, et al., 2011). LRRK2 will be discussed in detail in section 7.

Three disease genes, *PRKN*, *PINK1*, and *DJ1*, are inherited autosomal recessively and lead to monogenic PD (Bonifati, 2012). Mutations in *PRKN* may account for up to ~50% of autosomal recessive cases of PD, whereas cases linked to *PINK1* and *DJ1* are much rarer. PRKN-, PINK1-, and DJ1-PD are primarily early-onset cases. PD-linked mutations in each of these three genes appear to converge at least partly on mitochondrial dysfunction (Dodson and Guo, 2007).

The commonest, known genetic risk factor for PD is mutations in *GBA1*, which encodes for the enzyme β-glucocerebrosidase (GCase) (Neudorfer et al., 1996; Sidransky et al., 2009). An estimated 9% of all PD patients harbour a *GBA1* mutation (Avenali et al., 2020). Homozygous mutations in *GBA1* invariably lead to one of three forms of the lysosomal storage disorder Gaucher disease (GD) (Mehta, 2006). It was first identified that relatives of GD patients had a higher prevalence of PD (*i.e.,* those with heterozygous *GBA1* mutations) (Neudorfer et al., 1996). Heterozygous mutation carriers have roughly a 15% increased risk of developing PD, with some

cohorts reporting up to 31% (Sidranksy et al., 2009; Aharon-Peretz et al., 2004). GBA1-PD-linked pathology and biology will be discussed in section 8.

4. Molecular Pathology of Parkinson's Disease

The cellular and molecular hallmarks of PD are the death of dopaminergic (DA) neurons and the aggregation and accumulation of the protein α-synuclein (though α-synuclein pathology is lacking in some cases, as discussed below). Strikingly, at the time of overt motor symptoms and disease diagnosis, as high as 80% of striatal dopamine has been lost and 50% of DA neurodegeneration has already occurred (Riederer and Wuketich, 1976; Ross et al., 2004). Presently, there are no treatments or pharmacological means to prevent DA cell loss or α-synuclein accumulation.

4.1. Dopaminergic Neuronal Cell Loss

All cases of PD/parkinsonism can be attributed to the selective and progressive dysfunction and/or loss of DA neurons in the SNpc, and to a lesser extent in other regions including in the ventral tegmental area (VTA). The loss of DA neurons in the SNpc results in an overall decrease in dopamine in the nigrostriatal pathway, which ultimately results in disruptions to voluntary motor control (Blandini et al., 2000). In humans, DA neurons in the SNpc also produce neuromelanin, a black-pigmented substrate, that can be used to identify the SNpc in the gross human brain (Zucca et al., 2004). In PD, the loss of neuromelanin-producing DA neurons results in the loss of the hallmark "black" appearance of the SNpc.

DA neurons in the SNpc are selectively vulnerable to neurodegeneration in the disease progression of PD though the exact cause remains elusive. The production and metabolism of

dopamine and neuromelanin produces high quantities of reactive oxygen species (ROS) and reactive electrophilic species (RES), which causes a great deal of oxidative stress even under physiological conditions (Pacelli et al., 2015; Tokarew et al., 2021), which is believed to play a factor in DA neuronal vulnerability. Further, the high arborization of DA neurons of the SNpc requires a high level of mitochondria for energy generation, which further contributes to the oxidative stress burden on DA neurons (Pacelli et al., 2015). Finally, DA neurons of the SNpc uniquely use calcium channels (as opposed to sodium channels used by DA neurons of the VTA) for regulatory functions, which can result in intracellular calcium overload with detrimental effects on mitochondrial health and cell viability (Guzman et al., 2010; Khaliq and Bean, 2010).

4.2. α-Synuclein

The shared sign of many neurodegenerative diseases is the accumulation of a specific protein. In PD, the protein aggregate hallmark is α-synuclein (aSyn), encoded by *SNCA*. As it stands, the exact cause and/or role of these protein aggregates in neurodegeneration remains unknown, though hypotheses of both pathological and protective roles have been given. aSyn is a 14kDa protein first named for its (pre-) synaptic and nuclear localization (Maroteaux et al., 1988). The aSyn protein can exist physiologically along a spectrum of a soluble, unstructured state and a membrane-bound, helical state (Burré et al., 2015). In PD, aSyn undergoes misfolding events and ultimately results in proteinaceous aggregates called Lewy bodies (LB) and Lewy neurites (LN) (Spillantini et al., 1997). LBs and LNs are the pathological hallmark of PD and are used for confirmative diagnosis of PD *post-mortem*. LBs are intracellular, cytoplasmic inclusions formed within cell bodies, mainly comprised of aggregated aSyn but have also been shown to harbour cellular components, including organelles, lipids, and phagosomes (Shahmoradian et al., 2019).

LNs are abnormal, diseased neurites harbouring misfolded, aggregated aSyn, similar to what is found in LBs.

The aSyn protein undergoes multiple post-translational modifications, many of which are believed to promote protein misfolding and aggregation. aSyn is phosphorylated on multiple tyrosines and serines (Ser), but the most well-know is p-Ser129, which is often used as a marker for disease-associated aSyn (Fujiwara et al., 2002; Koga et al., 2021). Beyond this, the aSyn protein can also be C-terminally truncated which causes the protein to be more aggregate-prone (Zhang et al., 2022).

In 2003, Braak and Del Tredici proposed a staging model for the spread of aggregated aSyn in PD disease progression, based on examining and tracing autopsy samples for immunoreactivity of aSyn (Braak et al., 2003). Braak and Del Tredici proposed that aSyn could travel in a prion-like pattern over 6 stages. Notably, the initiation of aSyn propagation in stage 1 is proposed to occur at two sites: the dorsal motor nucleus of the vagus nerve and the olfactory bulb (OB), two sites in the body that theoretically first encounter exogenous substances (from the GI tract and the nasal cavity, respectively). This hypothesis is further strengthened by PD symptomology, whereby the majority of PD patients present with both GI impairment and hyposmia prior to motor sign onset (Kalia and Lang, 2015). Of note, aSyn can be found outside of neurons and the CNS, including in the retina, gut, red blood cells, and heart (Böttner et al., 2012; Sumikura et al., 2015; Javanshiri et al., 2022; Raunio et al., 2022; Hart de Ruyter et al., 2023; Scherzer et al., 2008; Wagner et al., 2023).

There is a certain degree of variability in aSyn pathology as it relates to genetic cases of PD. Specifically, most cases of PD caused by mutations in *PRKN* (*i.e.,* EOPD) lack LBs (though some cases have been described) (Doherty and Hardy, 2013). These cases otherwise exhibit the cardinal clinical signs of PD, and pathologically have DA neurodegeneration. Moreover, LRRK2-linked

cases of PD are pleiotropic, whereby a subset of patients present with typical LB pathology, and others lack LB pathology, but instead present with tau hyperphosphorylation (*i.e.,* similar to what is found in Alzheimer's disease (AD) and progressive supranuclear palsy (PSP)), whereas other, albeit rare, cases may not show any inclusion formation (Kalia et al., 2015; Henderson et al., 2019).

Further, the presence of aSyn inclusions is not always linked to PD. Indeed, PD falls under an umbrella of diseases that feature aSyn-positive inclusions called synucleinopathies. Other diseases in this category include incidental Lewy body disease, dementia with Lewy bodies (DLB), and all variants of multiple system atrophy (MSA). Despite the convergence of synuclein deposits, these synucleinopathies are phenotypically different from PD.

5. Environmental Risk Factors for Parkinson's Disease

Numerous risk factors have been correlated to PD. These factors play an important role primarily in idiopathic PD, but likely contribute to onset of a subset of familial PD cases as well. Well-established environmental risk factors for parkinsonism include neurotoxin exposure (namely 1-methyl-4-phenyl-1,2,3,6-tetrahydropyridine [MPTP]), exposure to pesticides (namely rotenone and paraquat), rural living (*e.g.,* agriculture and farm occupations, well water drinking), usage of beta-blockers, heavy metal exposure (namely manganese), severe and/or repeated head trauma, and finally microbial exposures (Kalia and Lang, 2015; Schlossmacher et al., 2017).

MPTP was the first neurotoxin discovered as an environmental risk agent for PD (Langston et al., 1983). MPTP is directly taken up by DA neurons and disrupts mitochondrial oxidation by blocking complex I (Sian et al., 1999). MPTP leads to the selective neurodegeneration of DA neurons in the SNpc (but not the VTA) similar to PD. In humans (as seen from recreational drug

use) and in animal models, the use of MPTP leads to parkinsonism (Blanchard et al., 1994; Burns et al., 1984).

Pesticide use has long been linked to PD risk. Namely, the organic insecticide, rotenone, and the non-selective herbicide, paraquat, have both been linked to PD risk, and have been used extensively in animal studies of the disease (Rudyk et al., 2019; Dwyer et al., 2021; Semchuk et al., 1992; Ascherio et al., 2006). In both rodent and primate studies, these pesticides, at specific doses, were able to elicit PD-like pathology, including DA neurodegeneration (Ritz et al., 2016). Similar to MPTP, each of these pesticides have mechanisms which disrupt mitochondrial functions and lead to oxidative stress, which further highlights a likely pathogenic role for mitochondrial dysfunction and oxidative stress management in PD pathogenesis (Bove and Perrier, 2012).

Interestingly, there are multiple factors that have been associated with decreased risk for PD. These include actively smoking tobacco products, caffeine consumption, usage of calcium-channel blockers, and use of non-steroidal anti-inflammatory drugs (NSAIDs), foremost ibuprofen (Kalia and Lang, 2015; Schlossmacher et al., 2017). It is suggested that some of these protective factors oppose the mechanisms of a specific risk factor, *e.g.,* pathogenic exposures and ensuing inflammatory response increases PD risk, and NSAIDs decrease inflammation, and are a protective correlative factor. However, these connections remain speculative, and the use of any of these protective factors as preventative measures are not currently encouraged by medical professionals.

It is likely that it is the cumulative exposure of multiple of these risk factors that leads to the onset of disease in genetically at-risk individuals. Researchers in our lab have done extensive modelling analyses on each of these risk factors, as well as genetic factors, to produce a mathematical model that can be utilized to predict the incidence of PD (Li et al., 2022; Schlossmacher et al., 2017). This model has been tested and shown to be highly successful in

differentiating healthy controls from those that have a PD diagnosis (Li et al., 2022; Schlossmacher et al., 2017).

Building on their original aSyn staging hypothesis (Braak et al., 2003), Braak and colleagues also proposed a second hypothesis: the dual hit hypothesis of disease initiation (Hawkes et al., 2007). This hypothesis speculates that aSyn propagation is stimulated by a neurotropic pathogen (likely viral) acquired either in the nasal cavity, or orally travelling then to the stomach. The nasal and oral cavities are most in contact with exogenous substances, and the corresponding OB and GI system are the two sites named in stage 1 of aSyn staging (Braak et al., 2003). They propose that neurotropic viruses travel anterograde via cranial nerve 1 from the olfactory mucosa to the OB or retrograde from the stomach to the brain via the vagus nerve to gain access to the brain. Then, it is proposed that these neurotropic infections (and the ensuing inflammatory response) can initiate aSyn propagation and therefore disease (Hawkes et al., 2007; Hawkes et al., 2009), which we proposed necessitates genetic predisposition (Kitada et al., 2012).

This thesis was motivated by the dual-hypothesis developed by Hawkes, Del Tredici, and Braak (Hawkes et al., 2007; Hawkes et al., 2009) and informs our approach regarding the impact of an infection (specifically viral) in mice harboring a PD-linked mutation (Kitada et al., 2012). In the next section, evidence of both viral and bacterial infections as risk factors for PD will be detailed.

6. Inflammation and Parkinson's Disease

6.1. Inflammation

It is now widely accepted by the field that inflammation plays an important role in the pathogenesis of PD (as well as virtually all neurodegenerative diseases). Inflammation is a key component of the innate immune response and is the body's first response against pathogenic insult and injury. Clinically, inflammation presents as heat, redness, swelling, and pain (Punchard et al., 2004). Molecularly, inflammation is categorized by edema, increased vascular permeability to the site of injury, release of chemical mediators, and infiltration of white blood cells. The further effect of inflammation is the release of cytokines and chemokines which activate and engage the adaptive immune response, thus continuing and transitioning the immune response from innate to adaptive (Marieb and Hoehn, 2019). Under acute, physiological conditions, inflammation is a critical host response against infections to limit pathogen replication and spread, as well as to limit the amount of tissue injury and clear cellular debris. We and others posit that it is uncontrolled, sustained, chronic inflammation that is linked to PD risk and pathogenesis.

The key cells of the innate immune system are neutrophils and macrophages (but also includes dendritic cells and natural killer cells). Neutrophils are the first cells to arrive at the site of injury, in massive numbers. Neutrophils can cause destruction through phagocytosis and the release of neutrophil extracellular traps, a network mainly composed of DNA which traps pathogens. Importantly, though neutrophils arrive quickly at the site of injury, they also undergo cell death in the process of phagocytosis (Papayannopoulos, 2019). As such, macrophages arrive at the site of injury next. Though lesser in number, macrophages accomplish most phagocytosis involved in clearance. Importantly, both neutrophils and macrophages release cytokines and chemokines which aids in directing the immune response; however, macrophages are also antigen presenting cells (APCs) and therefore also present antigens to B- and T-cells to initiate the adaptive immune response (Marieb and Hoehn, 2019).

An important aspect of the innate immune response is release of reactive molecular species as pathogen defence: these include ROS and reactive nitrogen species (RNS). ROS and RNS are released by phagocytic cells during a respiratory burst (Andrés et al., 2022). The main ROS molecules are O_2^- and H_2O_2, which are highly effective at killing bacteria specifically. Neutrophils often kill bacteria by engulfing the microbe and then activating the respiratory burst intracellularly, killing the invader. Macrophages can also induce death via ROS and RNS within the phagosome. As expected, at uncontrolled levels, accumulation of ROS and RNS can be damaging to the host and therefore they must quickly be reduced and removed (Andrés et al., 2022).

Macrophages exist both peripherally in circulation and as tissue-specific macrophages. For example, alveolar macrophages reside within the alveoli of the lungs and play an important role in defence against inspired threats. The CNS's specialized macrophages are microglia. Microglia are the principle innate immune cells of the brain and primarily (but not solely) lead the inflammatory response in the brain. Structurally and functionally, they exist in two states: a quiescent/resting state, identified by their long, surveilling processes; and an active (and inflammatory) form, where the microglia appear much more ameboid and are functionally ready to respond to perceived threats (Jurga et al., 2020). These phenotypic differences between resting and active microglia are used in research to identify the inflammatory state of the tissue environment.

For decades, the brain was believed to be 'immune-privileged' because of the highly efficient blood-brain-barrier (BBB) (Louveau et al., 2015). The BBB is the complex network of tight junctions between astrocytes, pericytes, and endothelial cells that prevents the entrance of most macromolecules and cells into the CNS, whilst also carefully maintaining the composition of the extracellular fluid around signaling neurons. Despite this, it is now known that peripheral immune cells (both leukocytes and lymphocytes) can enter the CNS, and interact with microglia, neurons,

and other glial cells (Herz et al., 2017). The infiltration of peripheral myeloid cells as well as inflammatory chemicals released by these cells into the CNS has been linked to PD pathogenesis in mice and in humans (Shutinoski et al., 2019; Moehle et al., 2012). Importantly, it is known that the BBB integrity begins to markedly decline progressively in humans at the age of 60; and this may play an important role in the pathogenesis of many diseases (Shao et al., 2024).

6.2. Cytokines in Parkinson's Disease

Cytokines are critical inflammatory signaling molecules released by virtually all immune cells, as well as by other cell types including astrocytes and neurons. There is a wide array of cytokines, and each has specific functions to direct the immune response (Marieb and Hoehn, 2019). Examples of these functions include promoting cell differentiation, proliferation, adhesion, and survival or death (Ozaki and Leonard, 2002). Common cytokines include interleukins (ILs), interferons (IFNs) which are involved in viral response specifically, and tumor necrosis factors (TNFs). A subset of cytokines, called chemokines, specifically promote chemotaxis of immune cells to the site of injury. Though largely reductive, most hallmark cytokines can be categorized as either pro-inflammatory or anti-inflammatory. Canonical pro-inflammatory cytokines include IL-1β, IL-6, TNF-α, and IFN-α/β/γ, while IL-2, IL-4 and IL-10 are considered anti-inflammatory (Ozaki and Leonard, 2002).

Generally, the presence of a high abundance of pro-inflammatory cytokines has been linked to neurodegeneration. High levels of IL-6, TNF-α, and IFN-γ have each been linked to numerous neurodegenerative diseases including PD, amyotrophic lateral sclerosis (ALS), and AD (Diaz et al., 2002; Guidotti et al., 2021; Zheng et al., 2016). This increase of pro-inflammatory cytokines, as well as an increase of microglia in the active state, has been identified in *post-mortem* PD brains

as well as in cerebrospinal fluid (CSF) of PD patients (Schröder et al., 2018). Animal studies which involve genetic knockout of specific pro-inflammatory cytokines (*i.e.,* TNF-α, and IFN-γ) protected against toxin-induced nigrostriatal damage (Barcia et al., 2011). These authors conclude that the loss of these cytokines resulted in less microglial recruitment and activation, and subsequent protection from DA neurodegeneration (Barcia et al., 2011).

6.3. Epidemiological Evidence of Pathogen Exposure and Parkinson's Disease

Evidence of bacterial and viral exposure as risk factors for PD exists both epidemiologically and in animal studies. First, following the 1918 influenza pandemic caused by the influenza A virus serotype H1N1, there was an outbreak of encephalitis lethargica (also referred to as von Economo's disease) and postencephalitic parkinsonism, which suggests a potential association between the disease and the infection (Jordan, 1927). Additionally, individuals born during the 1918 outbreak have a 2-3 times higher risk of developing PD compared to those born before 1918 or after 1924 (Martyn, 1997). The likelihood of exhibiting parkinsonian symptoms increases with the number of influenza infections, indicating a strong link between virus exposure and parkinsonian behavior (Martyn, 1997). Importantly, these cases of postencephalitic parkinsonism differed from idiopathic PD because they were defined by the presence of tau pathology and a lack of Lewy pathology (Jellinger, 2009). A challenge to this hypothesis is that *post-mortem* analysis of postencephalitic patients with parkinsonism did not reveal detectable H1N1 viral RNA in their brain specimens (Lo et al., 2003). However, it is still possible that a peripheral viral infection and ensuing inflammation could have triggered the onset and/or progression of parkinsonism, while the virus itself was cleared from the system.

Most recently, in a Danish cohort study, the authors found that influenza infection was strongly correlated to PD risk, as long as 10 years after infection (Cocoros et al., 2021). Furthermore, epidemiological evidence has linked multiple other pathogens, including herpes simplex virus, hepatitis C virus, West Nile virus, and *Helicopter pylori* infections, to elevated PD risk (reviewed in: Gonzalez-Latapi and Marras, 2022).

6.4. Evidence from Mouse Models of Pathogen Exposure and Parkinson's Disease

There is growing evidence that both live pathogens and pathogenic mimics have the capacity to cause neurodegeneration-like changes in the murine brain. The bacterial mimic, lipopolysaccharide (LPS), a component of the bacterial cell wall, is often used to elicit an immune response. It has been shown that LPS administration can lead to parkinsonian behavior and death of dopaminergic cells in mouse models (Arai et. al., 2006). Dwyer et al. (2020) have shown that pre-treatment with LPS increased the level of DA neurodegeneration in mice when a secondary treatment of the pesticide paraquat was administered to the SNpc. This augmentation of DA neuronal loss was attributed to the priming and hyperactivation of the large population of microglia in the SNpc. This has also been shown with paraquat and the viral mimic polyinosinic:polycytidylic acid (poly I:C) (Bobyn et al., 2012). The possibility that DA neurodegeneration is driven by reactive microglia is supported by a study that demonstrated that LPS is not sufficient to induce neuronal death *in vitro* unless the neurons were co-cultured with microglia or macrophages (Chien et al., 2016; Suzumurua et al., 2006).

Using a live virus, specifically the highly infectious influenza A virus serotype H5N1, Jang et al. (2009) demonstrated its progression from the peripheral autonomic nervous system to the CNS, where it then induced the activation of microglia, increased phosphorylation of aggregated

aSyn, and led to degeneration of dopaminergic neurons in the SNpc even after clearance of the virus. Furthermore, it was shown that the non-neurotropic influenza A virus serotype H1N1 could also lead to robust microgliosis in the SNpc of wild-type mice, which was sustained to at least 21 days post inoculation (Sandasivan et al. 2015). In a separate study, pre-treatment with the heavy metal manganese in drinking water followed by nasal inoculation of H1N1 further exacerbated both microgliosis and astrogliosis in the brain of mice (Bantle et al., 2021).

Finally, DA neurodegeneration has also been observed following a two-hit model of SARS-CoV-2 infection followed by MPTP (neither SARS-CoV-2 nor MPTP alone caused DA cell loss this study) in SARS-CoV-2-susceptible transgenic mice (Smeyne et al., 2022); and following Western equine encephalitis virus (WEEV) in wild-type mice (Bantle et al., 2019; Bantle et al., 2021)

Therefore, multiple live viruses, bacterial and viral mimics, as well as in conjunction with other known PD risk factors (*i.e.,* pesticides and heavy metals) have been shown to cause dopaminergic cell death in wild-type mice, suggesting that these factors have the capacity to induce PD-like pathologies in mice. In the next sections, the exposure to pathogens and bacterial mimics in the context of PD genetic mouse models (*i.e.*, *Lrrk2*, *Gba1* mutants) will be discussed.

7. LRRK2

7.1. LRRK2 Structure

The *LRRK2* gene encodes for a large protein, leucine-rich repeat kinase 2 (LRRK2; also referred to as Dardarin), which is comprised of 2,527 amino acids amounting to 286 kilodaltons (kDa) in size (Kang and Marto, 2017). It contains two enzymatic domains: a GTPase domain

comprised of a Ras-of-Complex (ROC) and C-terminal-of-Roc (COR) domain; and a kinase domain. It also contains an armadillo repeat (ARM), ankyrin repeat (ANK), leucine-rich repeat (LRR) region, and WD40 domain. These domains suggest that in addition to enzymatic activity, LRRK2 functions as an important scaffolding protein (Kang and Marto, 2017). Interestingly, LRR domains have an evolutionarily conserved role in immune surveillance in many organisms, from plants to mammals (Takken and Tameling, 2009; Taxman et al., 2010).

LRRK2 has many phosphorylation sites and is known to be phosphorylated at Ser910, Ser935, Ser955, Ser973 between the ANK and LRR regions, and Ser1292 in the LRR region. Autophosphorylation occurs at Ser1292; although phosphorylation at Ser935 is often used as a readout of indirect autophosphorylation, as constitutive phosphorylation on this residue is dependent on autophosphorylation activity of LRRK2 (Sheng et al., 2012; Dzamko et al., 2010). See **Figure 1.1** for a schematic of LRRK2 structure and phosphorylation sites.

7.2. Genetics of LRRK2-PD

LRRK2 is a pleiotropic locus for PD, meaning that some mutations are causally linked to PD, and some are associated with a varying degree of increased risk. The association of *LRRK2* and PD was first identified in 2004 through multiple family analyses (Zimprich et al., 2004). Many variants (>121) have now been linked to varying degrees of PD risk through GWAS analysis (Ross et al., 2011).

There are seven known pathogenic (causal) mutations that were first identified in monogenic PD families. The most common is the p.G2019S mutation, which falls in the kinase domain of the protein (Healy et al., 2008). Also falling within the kinase domain is the p.I2020T

mutation which stabilizes the LRRK2 protein in active conformation, thereby increasing kinase activity (Ray et al., 2014).

Five mutations fall within the ROC-COR (GTPase) domain of LRRK2: p.Y1699C, p.N1437H, and p.R1441C/G/H (Shu et al., 2019). These mutations are much rarer but have a much higher penetrance rate compared to p.G2019S (Trinh et al., 2022). These mutations promote a GTP-bound state which leads to elevated kinase activity (Liao et al., 2014).

Generally, each of these pathogenic LRRK2 mutations lead to an increased kinase activity of the protein, and as such, the physiology of this activity as well as inhibiting it as a treatment option for PD have both been heavily pursued (discussed in section 7.6.) (Alessi and Sammler, 2018). See **Figure 1.1.** for a schematic of LRRK2 mutations linked to PD risk.

Evolutionarily, homologues of the *LRRK2* gene are highly conserved. However, the promoter region is variable amongst species and results in variation of protein expression and abundance in tissues across species (West et al., 2014). Interestingly, it appears that PD-linked mutations in *LRRK2* have arisen in three separate incidences throughout human history, which may speak to an evolutionarily important advantage for these mutations in specific contexts (*i.e.,* in pathogen defences) (Guenther et al., 2024).

LRRK2-PD cases exhibit pleiotropy in neuropathology. In one cohort, it was found that 30% of patients carrying a p.G2019S mutation and 70% of patients carrying another *LRRK2* mutation (*i.e.,* of the other six mentioned above) had DA neuronal degeneration but did not have Lewy bodies (Kalia et al., 2015). In another cohort, it was found that only ~60% of *LRRK2* mutation carriers had aSyn pathology whereas all cases studied had phosphorylated tau pathology, which the authors identified as a pathology found in Alzheimer's disease (Henderson et al., 2019).

Phosphorylated tau pathology resembling that found in PSP has also been identified in *LRRK2* mutation carriers (Rajput et al., 2006).

Interestingly, although PD generally has a male sex bias of ~1.5x, in LRRK2-linked cases of PD, this sex biased is lost and prevalence between the sexes seems to be even (Orr-Urtreger et al., 2007; Clark et al., 2006). Some cohorts even suggest a female sex bias in LRRK2-PD cases (Cilia et al., 2014; Marder et al., 2015).

7.3. LRRK2 Variants in Other Diseases

Aligned with tau hyperphosphorylation being observed in LRRK2-linked cases of PD, mutations in *LRRK2* have also been linked to increased risk for two classical tauopathies: progressive supranuclear palsy (PSP) and corticobasal degeneration (CBD) (Sanchez-Contreras et al., 2017). Two known PD-linked mutations, p.G2019S and p.R1441C, have both been identified in PSP patients, as well as a novel mutation, p.A1413T (Sanchez-Contreras et al., 2017). The novel p.R1707K mutation was identified in a CBD patient. However, the authors do conclude the presence of *LRRK2* mutations in their large cohort had low frequency (Sanchez-Contreras et al., 2017). In a separate family analysis, the same *LRRK2* mutation led to PD onset in one family member and PSP onset in another (Zimprich et al., 2004; Spanaki et al., 2006; Rajput et al., 2006). These findings highlight a possible connection between LRRK2 and the formation of tau tangles, which will be explored later in this thesis (Herbst et al., 2022).

Beyond this, mutations in *LRRK2* have been linked to several other diseases, each characterized by chronically sustained inflammation in their disease pathogenesis. Namely, Crohn's disease (CD), leprosy (a hyper-inflammatory variant thereof), and systemic lupus

erythematosus (SLE) have all been genetically linked to *LRRK2* (Hui et al., 2018; Fava et al., 2016; Zhang et al., 2019).

In CD, a type of inflammatory bowel disease, the polymorphism p.M2397T confers risk for the sporadic form of disease. This mutation is found in the WD40 domain of the protein and causes lowered expression of LRRK2 due to increased protein instability (Liu et al., 2011). This mutation has been seen to alter type II interferon response in human monocytes (Ikezu et al., 2020). Of note, this mutation has also been linked to leprosy (Fava et al., 2016). Next, the p.N2081D mutation within the kinase domain causes increased kinase activity and confers risk for both PD and CD (Hui et al., 2018). PD and CD also share variants in *LRRK2* that confer increased protection against disease: p.N551K and p.R1398H. The p.R1398H mutation causes the GTPase domain to be constitutively active (*i.e.,* promotes GDP binding), whereas the p.N551K mutation is proposed to affect the dimerization of the protein. Finally, in a sample set analyzed by Hui et al. (2018), all human carriers of p.N551K also carried the p.R1398H mutation, possibly indicating that both are required to confer protection.

In leprosy, mutations in *LRRK2* specifically alter the incidence rate of type 1 reactions (T1R). T1R are pathological inflammatory episodes that can cause peripheral nerve damage and can occur even years after successful antibiotic treatment of *Mycobacterium leprae*. The p.R1628P mutation (in the GTPase domain), was shown to be protective against T1R in leprosy, but is a risk factor for PD (Fava et al., 2019). This team demonstrated that microglial RAW cells carrying the p.R1628P mutation had a pro-inflammatory phenotype following live bacterial insults (Fava et al., 2019).

Lastly, through GWAS, a single-nucleotide polymorphism (SNP) in the non-coding regions of *LRRK2* was strongly associate with SLE disease susceptibility (Zhang et al., 2017).

Upon further research, Zhang et al., (2019), identified that LRRK2 is up-regulated in B-cells of SLE patients, and may thus have a pathogenic role in antibody production.

It is evident that there is a complex interplay between mutations in *LRRK2* and the diseases they confer risk for, including mutations that are associated with two or more diseases. Leprosy, CD, and SLE are all inflammatory in nature; and leprosy and CD require a xenobiotic trigger to initiate disease. It is yet to be elucidated whether mutations in *LRRK2* confer risk for each of these individual diseases (including PD) through the same mechanism or cell type. See **Figure 1.1.**for a schematic diagram of the mutation that confer risk for these distinct diseases.

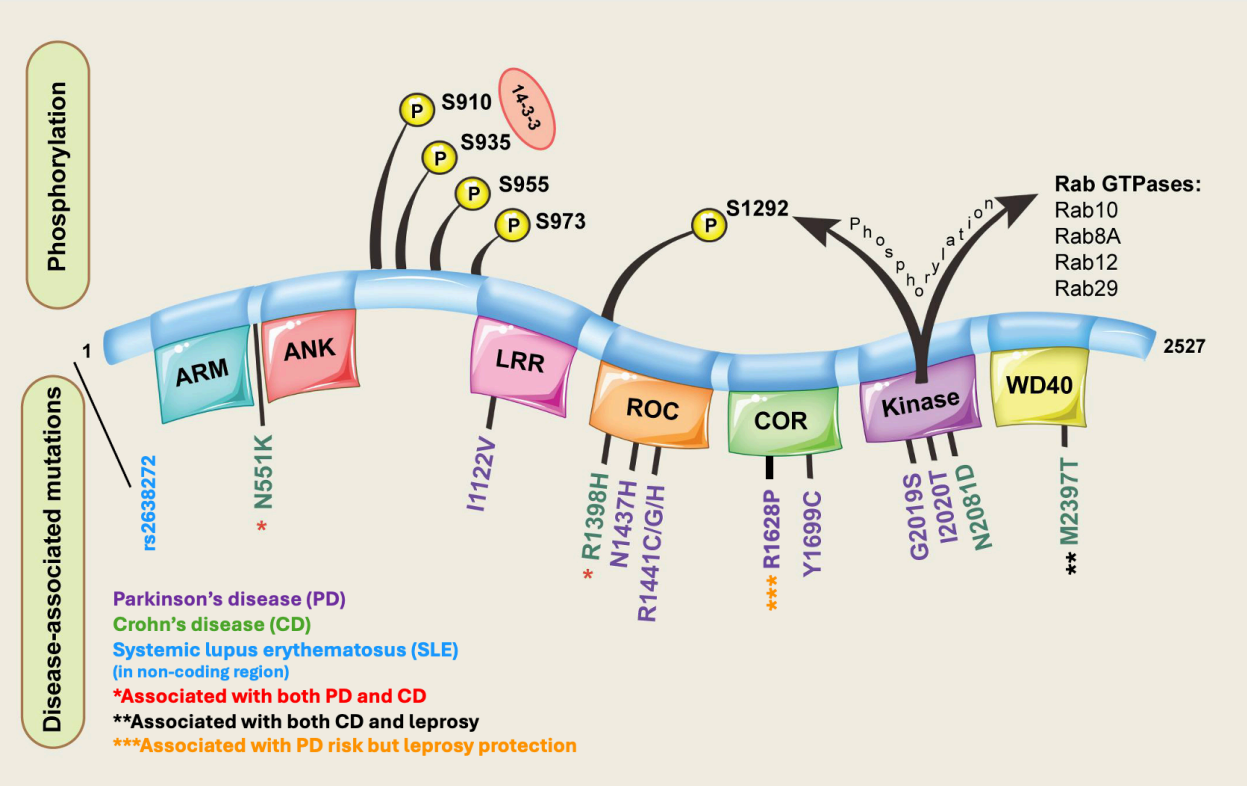


Fig. 1.1: Schematic Diagram of LRRK2's Structure, Inflammatory Disease-Associated Mutations, and Phosphorylation Sites. LRRK2's numerous domains are indicated in the image. Disease-associated mutations are labelled, including those associated with Parkinson's disease (purple), Crohn's disease (green), SLE (blue), and those associated with both PD and CD (*), CD and leprosy (**), and PD and leprosy (***). Phosphorylation sites on LRRK2 are indicated, as well as phosphorylation substrates of LRRK2 kinase, a subset of Rab GTPases and autophosphorylations on Serine 1292 (S1292). Modified from Ahmadi Rastegar and Dzamko (2020).

7.4. LRRK2 Physiological Function

The role of LRRK2 in a healthy, physiological state remains to be elucidated, though many strides have been made in the field. LRRK2 is ubiquitously expressed, but is most abundantly found in myeloid cells, the kidneys, and the lungs (Hakimi et al., 2011; Sharma et al., 2011). In the CNS, LRRK2 expression appears to be highest in the OB and the striatum in rodents, which may speak to its involvement in PD pathogenesis (Melrose et al., 2006).

A major research advancement was the identification of *bona fide* LRRK2 kinase substrates. In addition to autophosphorylation on Ser1292, it was found that LRRK2 also phosphorylates a subset of Rab GTPases in the switch-II region (Steger et al., 2016). These include: Rab8a, Rab10, Rab12, Rab29/7L1, and Rab35. Increased phosphorylation of LRRK2 Ser1292 and Rab10 have been identified in LRRK2-PD cases (Fraser et al., 2016; Wang et al., 2022). Interestingly, Rabs have also been identified upstream of LRRK2, as Rab29 and to a lesser extent Rab12, could stimulate LRRK2 kinase activity *in vitro* (Purlyte et al., 2018).

Rab proteins are key regulators of intracellular trafficking and lysosomal degradation pathways, two pathways LRRK2 is also implemented in. It has been shown that LRRK2 preferentially phosphorylates membrane-bound and GTP-bound (active-state) Rab proteins. Further, Rab29/7L1 could recruit LRRK2 to the intracellular membrane. There is evidence that LRRK2 recruitment to the intracellular membrane is increased in LRRK2-PD (Liu et al., 2018). LRRK2 has been shown to interact with Rab 8 and 10 to stimulate lysosome production and secretion following stress induction *in vitro* (Eguchi et al., 2018). Lee et al., (2020) identified that LRRK2 is required for co-recruitment of Rab proteins to late phagosomes in human IPS-derived macrophages following inoculation with TLR2- and TLR4- activating pathogens.

LRRK2 has been implicated in many cellular processes including: vesicular trafficking, autophagy and lysosomal maturation, neurite outgrowth, ciliogenesis, mitochondrial homeostasis, cytoskeletal dynamics, among others (Hur et al., 2018; Madureira et al., 2020; Winner at al., 2010; Sobu et al., 2020; Weindel et al., 2020; Civiero et al., 2018). LRRK2 is highly localized to lysosomes and endosomes in the cell (Erb and Moore, 2020; Wallings et al., 2019). Despite mounting evidence that LRRK2 plays a role in autophagy, it remains debated whether LRRK2 positively or negatively modulates autophagy (Albanese et al., 2019).

Evidence for a role of LRRK2 in autophagy and lysosomal degradation comes from the examination of Lrrk2 knockout (KO) animals (Tong et al., 2010; Herzig et al., 2011). Lrrk2 KO mice are viable and do not have any overt phenotypic or behavioural abnormalities and have a similar lifespan as wild-type mice. However, they do have identifiable pathologies in the lungs and kidneys (the two organs of highest Lrrk2 expression). Lrrk2 KO mice accumulate oxidized lipids in the kidneys, and lipid-dense lamellar body structures in type-two pneumocytes of the lungs (Herzig et al., 2011; Fuji et al., 2015). Interestingly, these phenotypes could also be observed to a certain extent in Lrrk2 kinase-dead mice (Herzig et al., 2011).

7.5. A Role for LRRK2 in the Immune System

7.5.1. LRRK2 in Innate Immunity

There is a multitude of evidence demonstrating a role for LRRK2 in the immune system (Hakimi et al., 2011). Firstly, not only is LRRK2 much more highly expressed in the periphery (*i.e.,* lung and kidney) than the brain, but LRRK2 is much more highly expressed in cells of the immune system (particularly neutrophils, monocytes, and macrophages) than neurons. Of note,

LRRK2 is also more highly expressed in innate immune cells than T- or B- cells, suggesting a primary role for LRRK2 in the innate immunity rather than adaptive (Hakimi et al., 2011; Shutinoski et al., 2019). Next, LRRK2 can be upregulated by pathogens and infectious agents, as well as inflammatory signals such as IFN-γ and NF-κB, suggesting that LRRK2 is involved in pathogen response pathways and inflammation (Gardet et al., 2010; Hakimi et al., 2011).

LRRK2 has been linked to inflammasome production, namely the NLRC4 inflammasome (Liu et al., 2017). Inflammasomes are protein complexes that result in active pro-inflammatory cytokine production. Lrrk2 phosphorylates an important residue in the NLRC4 inflammasome following *Salmonella typhimurium* infection in mice. LRRK2 and its main substrate, Rab10, are highly expressed in phagocytic cells (macrophages, dendritic cells). LRRK2 phosphorylation of Rab10 directly affects micropinocytosis in mouse and human primary macrophages (Liu et al., 2020). Herbst et al., (2020) also demonstrated the ability of LRRK2 to regulate endolyosomal homeostasis by responding to membrane damage following multiple distinct pathogens. Finally, Kim et al. (2017) have shown that LRRK2 phosphorylates WAVE2 in myeloid cells, which is a critical step for phagocytosis.

Kozina et al. (2018) have demonstrated that the combination of mutant Lrrk2 p.R1441G transgenic mice and peripheral LPS injection could lead to DA neurodegeneration. They demonstrate that this effect is due to infiltrating inflammatory molecules from the periphery (*i.e.,* cytokines, foremost IL-6) but not to overactive microglia or infiltrating peripheral myeloid cells.

The role of LRRK2 in conjunction with the effects of ageing was investigated, and it was found that peripheral immune cells from Lrrk2 p.R1441C mutant mice were prone to immune cell exhaustion (Wallings et al., 2023). These immune-exhausted macrophages from mutant mice

showed decreased antigen presentation and decreased phagocytosis. The authors demonstrated that these effects also occurred in myeloid cells from LRRK2-PD patients (Wallings et al., 2023).

7.5.2. LRRK2 in Microglia

There is interest into the relative role for LRRK2 in peripheral monocytes versus in the brain's resident immune cells, microglia, both physiologically and as it relates to PD. Although the protein expression levels of LRRK2 in microglia are much lower than those in peripheral monocytes, there is highly valuable information that has been generated regarding the role of LRRK2 in microglial-specific immune responses, some of which has been detailed in above sections. Furthermore, in murine microglia, Kim et al., (2021) demonstrated that Lrrk2 phosphorylates NFATc2, an immune transcription factor, which leads to neurodegeneration following neuronal release of aSyn. Genetically, Langston et al., (2021) demonstrated that the PD-risk SNP rs76904798 in the non-coding region of the *LRRK2* locus propagates its expression through microglia alone. Dwyer et al., (2020) have shown that microglial depletion in a two-hit infection model (LPS followed by paraquat) reduced the mortality, sickness, and behaviour phenotypes associated with these infections in mice. However, in this same study, the depletion of microglia did not prevent the neuropathology caused by LPS and paraquat, including dopaminergic cell death (Dwyer et al., 2020).

7.5.3. LRRK2 in Adaptive Immunity

Kozina et al. (2022) recently highlighted a role for LRRK2 in the adaptive immune system. Utilizing bone-marrow chimeras and Rag1 KO mice, they identified that a transgenic Lrrk2 mutant (p.R1441G) adaptive immune system was enough to stimulate dopaminergic neuronal cell loss

following an LPS insult. Replacing the adaptive immune system in a p.R1441G mutant mouse with a wild-type adaptive immune system rescued dopaminergic neuronal loss seen in p.R1441G mice alone. Using Rag1 KO and Lrrk2 p.R1441G double mutant mice confirmed that this effect was mediated by T-cells and B-cells. Furthermore, through monoclonal antibody ablation, they demonstrated that this effect was mediated by IL-6 released by lymphocytes (Kozina et al., 2022). In human studies, peripheral blood samples from PD patients were found to have an imbalance in T-helper cells, which skewed towards a pro-inflammatory disposition (Kustrimovic et al., 2018). Similarly, T-cells reactive to aSyn were found in the blood of newly diagnosed PD patients (Sulzer et al., 2017).

Fahmy et al. (2023) have recently shown that LRRK2 is involved in the antigen presentation pathway in APCs (*i.e.,* macrophages). They demonstrate that LRRK2 acts with STING upstream of the unfolded protein response pathway to regulate the transition from the innate to the adaptive immune response following TLR4 antagonism (Fahmy et al., 2023).

7.5.4. LRRK2 and Pathogen Interactions

There is a growing number of studies demonstrating interactions between Lrrk2 and live pathogens. Härtlova et al. (2018) have demonstrated, that in response to a *Mycobacterium tuberculosis* bacterial infection, Lrrk2 KO and Lrrk2 kinase-inhibited macrophages showed better control of the bacteria. Interestingly, Lrrk2 KO mice showed enhanced immune response and pathogen clearance *in vivo* in response to the same pathogen; however, this control over bacterial burden was only seen at the early stage of disease (14 days post inoculation [dpi]) and no longer seen in the later stages (56 dpi). In addition, Lrrk2 p.G2019S derived macrophages had worsened control of the *Mycobacterium* pathogen and decreased lysosomal markers (Härtlova et al., 2018).

Liu et al. (2017) employed a *Salmonella typhimurium* infection model and found that Lrrk2 KO mice had increased bacterial burden in the spleen, as well as in blood and peritoneal fluid. In Lrrk2 p.G2019S mice, they reported decreased bacterial burden in spleen, blood, and peritoneal fluid. They attribute these observed changes in bacterial burden mainly to NLRC4 inflammasome activation and downstream IL-1β production. *In vitro*, using bone marrow-derived macrophages (BMDMs), they demonstrated that Lrrk2 phosphorylated Ser533 on NLRC4, leading to activation of the NLRC4 inflammasome (Liu et al., 2017). This activation is associated with downstream signaling of pro-inflammatory cytokines such as IL-1β (Franchi et al., 2006). Consistent with this, they demonstrated *in vivo* that Lrrk2 KO mice had decreased IL-1β levels, whereas Lrrk2 p.G2019S mice had increased levels (Liu et al., 2017). In a study by Feng et al., (2020), *Porphyromonas gingivalis,* a bacterium that can commonly cause chronic periodontitis, was orally administered to wild-type and Lrrk2 p.R1441G mice, and it was found that the Lrrk2 p.R1441G mice had increased TNF-α and IL-1β in their colons compared to wild-type mice following inoculation.

Within our lab, we have previously investigated and published two distinct infection models in Lrrk2 KO and Lrrk2 p.G2019S mice: (1) a peripheral, bacterial *Salmonella typhimurium* (ST) infection causing sepsis in adult mice; and (2) a neurotropic virus, reovirus T3D, in neonatal pups causing encephalitis (Shutinoski et al., 2019).

In the context of an ST infection, Lrrk2 p.G2019S homozygous and heterozygous mice had a significantly longer time-to-death than wild-types littermates. Similarly, Lrrk2 p.G2019S mice had significantly lower bacterial titres in the spleen. Interestingly, this phenotype was associated with significantly higher concentrations of H_2O_2 in both the spleen and brain of ST-infected Lrrk2 p.G2019S mice compared to wild-type mice (which was not found at baseline). Therefore, Lrrk2

p.G2019S mutant mice appear to have a heightened immune response to ST, which corresponds to decreased bacterial titre and increased survival (Shutinoski et al., 2019). In contrast, the absence of Lrrk2 (Lrrk2 KO) did not affect the time-to-death interval of ST infection; however, the loss of Lrrk2 caused a significant increase in the bacterial titre in the spleen compared to wild-type mice (Shutinoski et al., 2019).

When monitoring survival following nasal inoculation of reovirus T3D, we found that mice lacking the Lrrk2 protein showed significantly decreased survival in response to this systemic, viral infection. Importantly, Lrrk2 p.G2019S homozygous (female) mice also had increased mortality compared to wild-type littermates, despite having decreased viral titres in both the lung and brain. Similar to what we observed following ST infection, BMDMs from Lrrk2 p.G2019S mice had higher ROS production following reovirus T3D infection *in vitro* compared to those derived from wild-type mice. Taken together, we postulate that this is due to an over-inflammatory phenotype in the Lrrk2 p.G2019S female mice, whereby these mice overshot their immune response such that they could control and eliminate the pathogen more efficiently, but that the ensuing inflammation was higher than needed and therefore damaging to the host (Shutinoski et al., 2019).

7.6. LRRK2 Kinase Inhibition as a Therapeutic Target

As generally all pathogenic mutations in LRRK2 associated with PD lead to increased kinase activity of the protein, there has been much research into the function of the kinase activity of LRRK2 as well as kinase inhibitors as a potential therapeutic target for PD (Alessi and Sammler, 2018). Many mouse models have investigated the kinase activity of LRRK2, using either genetic or pharmacological knock-down of the LRRK2 kinase activity. A popular mouse model is the

Lrrk2 p.D1994S mouse, with a point mutation within the kinase domain which renders Lrrk2 kinase-dead (Herzig et al., 2011). This model allows researchers to study the kinase effect of Lrrk2 directly. A limitation is such that in this model the Lrrk2 protein becomes relatively unstable and causes mice to have about half the Lrrk2 protein abundance compared to a wild-type mouse (Herzig et al., 2011). Many studies have demonstrated that Lrrk2 kinase-dead mice, as well as pharmacological inhibition of Lrrk2 kinase, conferred neuroprotection against multiple insults (Ilieva et al., 2024; Ho et al., 2022; Pena et al., 2024).

In light of this research, a LRRK2 kinase inhibitor, BIIB122, has already entered Phase 2b human clinical trial stage in a PD population (Denali Therapeutics & Biogen; NCT05348785). As we and others have identified a role for both wild-type and p.G2019S Lrrk2 kinase activity in response to pathogens, it is of great importance to investigate the effect of loss of Lrrk2 kinase activity in response to microbial infections. This is to ensure that LRRK2 kinase inhibitors, in an ageing PD population, will not cause patients to be immunocompromised.

8. *GBA1* in Parkinson's Disease

The most associated genetic risk factor for Parkinson's disease is those within the *GBA1* gene (Nalls et al., 2014). *GBA1* encodes the lysosomal acid hydrolase glucocerebrosidase (GCase) (Migdalska-Richards and Shapira et al., 2016). GCase is an enzyme involved in lipid metabolism. Homozygous mutations in *GBA1* lead to the lysosomal storage disorder Gaucher disease (GD), which is characterized by a severe decrease in GCase enzymatic activity (<15%), and accumulation of lipid substrates, namely glucosylceramide and glucosylsphingosine (Hugues and Pastores, 2018). The accumulation of these lipids leads to the presence of "Gaucher cells" which are lipid-laden macrophages and the hallmark of GD (Sidransky and Lopez, 2012). Disease

manifestation is varied in GD, and the level of reduction in enzymatic activity does not always correlate to disease severity uniformly in each tissue.

A link between *GBA1* and PD was first identified because some GD patients were observed to clinically develop parkinsonian symptoms (Neudorfer et al., 1996; Tayebi et al., 2001; Tayebi et al., 2003). Next, it was found that family members of GD patients (and therefore obligate carriers of *GBA1* mutations) were more likely to develop PD (Goker-Alpan 2004; Lwin et al., 2004; Aharon-Peretz et al., 2004). About 9% of all PD patients carry a mutation in *GBA1*, and 11-31% of PD patients in the Ashkenazi-Jewish population, making it the commonest genetic risk factor associated with PD (Avenali et al., 2020; Do et al., 2019). However, like LRRK2, despite the high prevalence of *GBA1* mutations, the penetrance rate is low, ranging from 10-30% (Alcalay et al., 2014). Either one or two mutant *GBA1* alleles increase the risk for PD to a similar extent (Anheim et al., 2012). GBA1-PD patients are phenotypically similar to idiopathic cases of PD, although they present with an earlier age of onset, more rapid progression, and more severe cognitive decline (Mullin et al., 2019).

More recently, mutations in *GBA1* have also been linked to risk of developing dementia with Lewy bodies (DLB), with one cohort suggesting that *GBA1* mutation carriers are eight times more likely to develop DLB (Nalls et al., 2013). Furthermore, another cohort reported as high as 28% of DLB patients carried a *GBA1* mutation (Clark et al., 2009).

8.1. Physiological Role of Glucocerebrosidase

Glucocerebrosidase (GCase) is an enzyme responsible for catalyzing the degradation of the lipid glucosylceramide (GlcCer) into glucose and ceramide (Boer et al., 2020). GCase is first made in the endoplasmic reticulum and then shuttled to the lysosome, where it exerts is catalytic function

under acidic lysosomal conditions. It requires the co-factor, Saposin C, to function (Boer et al., 2020). Beyond catalyzing the degradation of GlcCer, it also has direct catalytic activity against glucosylsphingosine (GlcSph). The accumulation of both GlcCer and GlcSph are commonly observed in GD patients. GlcSph is also found to be slightly elevated in plasma from GBA1-PD patients (Surface et al., 2020). Importantly, ceramide (a byproduct of GCase activity) is a central figure in sphingolipid metabolism, and as such, perturbations in its levels will have downstream effects (Alecu and Bennett, 2019; Ilan, 2019). Finally, it has been identified that GCase can also transglucosylate cholesterol, creating glucosylated cholesterol; as well as it can catalyze the reverse reaction creating glucose and cholesterol (which is the more common reaction under physiological conditions) (reviewed in: Boer et al., 2020).

It is not fully elucidated how mutations in *GBA1* lead to PD risk, and there is not a common consensus as to whether *GBA1* mutations in PD risk are due to gain-of-function or loss-of-function properties (Migdalska-Richards and Shapira, 2016; Sardi et al., 2012). A leading hypothesis suggests that reduced GCase activity changes the lipid composition of intracellular membranes, leading to increased aSyn aggregation and accumulation in lysosomes (Schlossmacher et al., 2005). A second hypothesis suggests that gain-of-function activity by mutant GCase alters aSyn homeostasis, leading to accumulation (Cullen et al., 2011).

There is evidence of a slight decrease in GCase enzymatic activity in both GBA1-PD and idiopathic cases (Gegg et al., 2012; Murphy et al., 2014; Rocha et al., 2015). However, this decreased activity likely does not fully capitulate the pathogenesis of GBA1-PD, as GD patients (with severely low GCase activity) do not uniformly develop PD. In addition to the accumulation of the lipid substrates, *GBA1* mutations associated with PD also lead to mis-folded GCase, which likely also contributes to disease (Cullen et al., 2011; Sardi et al., 2012). Of note, multiple studies

have identified that lowered GCase activity results in increased aSyn protein accumulation, both in human autopsy studies and *in vivo* in mice (Günder et al., 2019; Mazzulli et al., 2011).

8.2. *GBA1* in the Immune System

The low penetrance rate of *GBA1* mutations in PD may suggest that additional factors are needed to onset disease, possibly environmental in nature (Balestrino et al., 2020). Given that we have identified a role in host defences against microbial infection for two other PD-linked genes: *Snca* (Tomlinson et al., 2017) and *Lrrk2* (Chapter 2 and 3; Shutinoski et al., 2019), Chapter 4 investigates a role for GCase in host defences against infection.

Inflammation is increased in patients with GD and Gaucher cells accumulate in organs leading to tissue inflammation. Furthermore, *GBA1* is highly expressed in cells of myeloid and phagocytic lineage (Deleidi and Gasser, 2013). *Ex vivo* studies using granulocytes and macrophages from GD patients and healthy controls found that macrophages from GD patients had a lesser ability to kill *Staphylococcus aureus* (Maródi et al., 1995). It was found that HEK293 cells with *GBA1* knocked out could better limit influenza A virus (IAV) serotype H1N1 infection (Drews et al., 2019). Soudani et al. (2019) found that IAV infection led to increased ceramide in A549 cells, which also suppressed infectivity. Finally, two groups identified a role for glucosylceramide synthase (GCS), the enzyme responsible for the reverse reaction of GCase, in limiting IAV infectivity in cells, which was the same effect of GCase (Drews et al., 2020; Vitner et al., 2021). These authors posit that perturbations in sphingolipid homeostasis, in either direction, could affect viral infectivity of IAV (Drews et al., 2020).

Notably, *GBA1* is ubiquitously expressed in all human tissues, including the olfactory bulb and the gut; both sites lie at the interface of the environment and host, and both are relevant in

Hawkes, Del Tredici, and Braak's dual-hit hypothesis (Hawkes et al., 2007; Hawkes et al., 2009). Furthermore, as *GBA1* is very highly expressed in macrophages, it adds to the hypothesis that it may function in host responses in general (ProteinAtlas).

8.3. *GBA1* and *LRRK2*

A relationship between *GBA1* and *LRRK2* was highlighted when it was identified that a subset of PD patients carried both the *LRRK2* p.G2019S mutation and a PD-linked *GBA1* variant. It was first hypothesized that both mutations may have a synergistic effect on PD pathogenesis; however, upon investigation in multiple cohorts, it seems that the *LRRK2* mutations exert a dominant effect over the *GBA1* mutations, as these patients present phenotypically similar to LRRK2-PD rather than GBA1-PD (*i.e.,* the disease course of LRRK2-GBA1-PD is less severe than that of GBA1-PD) (Smith et al., 2022).

GCase and LRRK2 have been identified in similar cellular pathways, namely autophagy and lysosomal processing. However, given that both proteins have enzymatic activities, it is unknown which functions upstream of the other. Research into this remains inconclusive. In light of this, Kedariti et al. (2022) did an exhaustive investigation in multiple tissues, including in mice, continuous cell lines, human PBMCs, and patient-derived induced neurons. They demonstrate an overall positive correlation between LRRK2 kinase activity (*i.e.,* in the p.G2019S mutant) and GCase enzymatic activity; but that the level of GCase activity was not always directly linked to the amount of GCase protein present (Kedariti et al., 2022). The ability for the *LRRK2* p.G2019S mutation to increase GCase activity could possibly inform us as to why double-mutant PD patients have a milder disease course and it also suggests that LRRK2 functions upstream of GCase.

In the context of immunity, there are reports that Lrrk2 and GCase interact in inflammatory responses. Sanyal et al. (2020) demonstrated that a pharmacological Lrrk2 kinase inhibitor could rescue cytokine deficits following an LPS insult in mutant *Gba1* p.D409V astrocytes. This again suggests that Lrrk2 kinase activity is upstream of GCase activity and that they may converge on a common pathway in response to pathogenic insults.

9. Pathogen Selection

9.1. Reovirus T3D

In the context of PD-linked genes, the first virus explored in this thesis (Chapter 2) is Respiratory Enteric Orphan (Reo) virus type 3 Dearing (T3D). Reovirus T3D is a neurotropic virus that is ubiquitously expressed in the environment. Reovirus infection in humans causes no to mild symptoms, and most humans are seropositive with reovirus by the end of their lifetime (Norman and Lee, 2000). Reovirus is a non-enveloped, double-stranded RNA virus (Antar et al., 2009). There are three serotypes of reovirus: Type 1 Lang (T1L), Type 2 Jones (T2J), and the Type 3 Dearing (T3D). They are structurally similar; but importantly, in mice, infection with separate strains leads to differing pathology. For example, infection with reovirus T1L in adult mice will lead to fatal respiratory distress, whereas infection with reovirus T3D in adult mice will lead to mild sickness, that does not present with symptoms and is non-fatal (Gauvin et al., 2013).

As such, in Chapter 2, we employ a model of reovirus T3D infection in suckling pups. In newborn pups, nasal inoculation of reovirus T3D will result in fatality at specific doses (*i.e.,* LD_{50} is $2.7x10^5$ PFU in C57Bl/6J) (Gauvin et al., 2013; Shutinoski et al., 2019). When administered nasally, reovirus T3D will travel from the periphery to the brain via neuronal spreading and

hematogenous routes. The viral infection then causes encephalitis as the cause of death. When the virus is administered intracerebrally (as is done in Chapter 2), the infection is 100% lethal at any dose. Reovirus T3D enters the cell by binding of its filamentous attachment protein, σ1, to the host's junctional adhesion molecule-A and cell surface carbohydrates. This complex is then internalized via clathrin-coated endocytosis (Danthi et al., 2016). The immune response to reovirus T3D exposure is classified by classical innate viral response, namely, increased expression of type 1 interferons (IFNα/β) and interferon-stimulated genes such as IL-1β and TNFα (Schittone et al., 2012).

We have previously demonstrated that expression of both *Snca* and *Lrrk2* can perturb the course of illness (*i.e.,* survival rate and viral burden) of reovirus-T3D-induced encephalitis, when inoculated nasally. *Snca* knockout mice had decreased survival following infection, suggesting that endogenous *Snca* expression is important for host defences against reovirus T3D (Tomlinson et al., 2017). We have also shown that *Lrrk2* KO, the p.G2019S mutant, and the p.D1994S mutant could all perturb the disease outcomes of reovirus T3D, suggesting that both endogenous Lrrk2 and allelic variants of the protein play a role against reovirus-T3D-induced encephalitis (Shutinoski et al., 2019). These results are detailed further in Chapter 2.

9.2. Vesicular Stomatitis Virus

The next goal was to investigate PD-linked genes in the context of a neurotropic virus that could infect and cause lethality in adult mice. As such, we next employed vesicular stomatitis virus (VSV). VSV is an enveloped, negative sense single-stranded RNA rhabdovirus (Nair et al., 2014; Fensterl et al., 2012). VSV has two major serotypes: Indiana and New Jersey, of which the Indiana

strain is used in this thesis (Hansen et al., 1985; Drolet et al., 2005). VSV typically infects rodents, cattle, swine, and horses; and infections of humans is rare and typically asymptomatic.

Nasal inoculation of VSV in adult mice leads to encephalitis as the cause of death that is titre-dependent. Importantly, upon nasal inoculation, VSV can infect the olfactory epithelium and directly travel to the olfactory bulb via anterograde travel within axons of olfactory sensory neurons (Huneycutt et al., 1994; Forger et al., 1991). Other virions that have been inhaled go on to infect the lungs, and then travel to the brain via neuronal spreading, lymphatic circulation, and hematogenous spread (Trottier et al., 2009; Cornish et al., 2001). VSV leads to both encephalitis and severe meningitis (Mishra et al., 2020). Symptomatically, mice experience weight loss, respiratory distress, loss of mobility, and in some instances hind limb paralysis (which histologically can be tied to lesions of the spinal cord and meningitis) (Forger et al., 1991).

VSV enters the host cells via the ubiquitous LDL receptor, accounting in part for its wide cellular tropism (Finkelshtein et al., 2013). The binding of VSV is mediated by its surface glycoprotein, VSV-G. VSV is highly sensitive to the anti-viral type I interferon (IFN) response (Georgel et al., 2007). As an evolutionary adaptation of the VSV virus, the M protein of the VSV genome suppresses IFN transcription in cells; possibly by blocking host mRNA export from the nucleus (Black et al., 1993; Ferran and Lucas-Lenard, 1997). A laboratory-generated VSV mutant, VSVΔ51, has a mutation within the M protein which stops this IFN suppression, and therefore is a less-lethal, less-infectious form of the protein (Stojdl et al., 2003). As such, this mutant was developed for possible oncolytic properties but can also be used in the context of investigating VSV pathogenesis in specific mouse models.

9.3. Influenza A Virus Serotype H1N1

To assess the role of PD-linked genes also in the context of a non-neurotropic, mainly peripheral viral infection, we next employed mouse-adapted IAV serotype H1N1 (A/Fort Monmouth/1/1947). H1N1 is an enveloped, negative sense single-stranded RNA virus. IAV has multiple serotypes, all of which have varying pathogenicity. For example, the highly infectious, avian H5N1 serotype is highly neurotropic and leads to encephalitis. The H1N1 serotype used here is pneumotropic and has high tropism for the epithelial cells of the lungs (Mahmoud et al., 2016; McCormick et al., 2011).

In adult C57Bl/6J mice, H1N1 nasal infection leads to lethal, severe lung pathology (at the LD_{50}). Mice die from pneumonitis and symptomatically develop respiratory distress, weight loss, and limited mobility. IAV enters the host cell using its hemagglutinin (HA) molecules on their viral envelope. This molecule binds glyco- proteins and lipids on the host cell surface that contain sialic acid, which then triggers endocytosis of the viral complex (Dou et al., 2018). Infection with H1N1 induces an inflammatory cytokine storm in the murine lungs, specifically anti-viral type 1 IFN responses (Xu et al., 2011). Notably, infection with H1N1 often leaves hosts vulnerable to secondary bacterially-induced pneumonia, which is believed to be due to the initial IFN response subsequently down-regulating caspase proteins (Brundage and Shanks, 2008; Guarda et al., 2011).

9.4. *Salmonella typhimurium*

Finally, in Chapter 4, we employed a serial infection model of mice first infected with IAV serotype H1N1, followed by an intraperitoneal injection of ST strain SL1344. ST is a gram-negative, rod-shaped, facultative anaerobic bacterium. In adult C57Bl/6J mice, ST leads to uniform lethality within 15 days (Robinson et al., 2012; Shutinoski et al., 2019). ST in mice leads to a

systemic infection similar to typhoid fever in humans. Therefore, mice develop fatal sepsis, as well as splenomegaly and necrosis of the spleen (Wei et al., 2019).

The main virulent factor of these bacteria are their large gene cassettes called 'Salmonella pathogenicity islands' (SPIs). SPI effectors are injected into host cells which leads to endocytosis of the bacterium and therefore invasion of the cell (Lou et al., 2019). The main host immune response against ST infection is the recruitment of phagocytes and IFN-γ production, which is mainly generated by neutrophils and NK cells (Pham and McSorley, 2015). Macrophages are important phagocytes against ST; however, ST bacteria infect and induce death in macrophages as a means to increase virulence (Robinson et al., 2012).

10. Statement of Research

10.1. Rationale

Significant research has detailed numerous disease genes associated with familial PD. Furthermore, exposure to numerous environmental factors (*i.e.,* pesticides, neurotoxins) have been well-established as increasing risk for idiopathic PD. Despite this, the exact etiology of PD remains unknown. There is now growing evidence that inflammation is a component of PD pathogenesis and numerous epidemiological studies in humans (over the course of the past century) have positively correlated viral infections with a rise in PD incidence. Building on the dual-hit hypothesis originally proposed by Hawkes, Del Tredici, and Braak (2007, 2009), we posited that viral infections could initiate PD onset in genetically susceptible individuals (*i.e.,* complex disease) (Kitada et al., 2012). Herein, we have studied three PD-linked risk genes in the context of viral infections: *Snca*, *Lrrk2*, and *Gba1*.

In Chapter 2, we sought to investigate the role of *Snca* and *Lrrk2* in host response to reovirus T3D-induced encephalitis in neonatal mouse pups. Specifically, we built on our previous research, where variants in each of these genes was able to alter the survival rate following nasal inoculation of reovirus T3D. To delineate between the peripheral immune response and the CNS-specific immune response, in Chapter 2 we employed a direct-brain inoculation of the same pathogen to the same mutant mouse models. In doing so, we minimized peripheral immune involvement and aimed to examine the role of α-synuclein and Lrrk2 in the brain-specific immune response against reovirus T3D in neonatal mouse pups.

In Chapter 3, building on our published research and that of Chapter 2, we investigated the role of Lrrk2 in response to viral infections in adult mice. We first investigated whether the most common PD-linked mutation in *Lrrk2*, p.G2019S, could affect viral titre and survival following two distinct RNA viruses: neurotropic VSV and non-neurotropic, lung-directed H1N1. We next measured the downstream, long-term effects of resolved viral infection in the brains of all surviving mice from the aforementioned infections. We measured multiple neurodegeneration-linked biochemical changes (*i.e.,* levels of aSyn, oxidative stress, total tau and tau phosphorylation) in the brains of mock-, VSV-, and H1N1-infected wild-type and Lrrk2 mutant mice that had survived to six weeks post inoculation.

In Chapter 4, we investigated a third, and the commonest PD-linked gene, *Gba1*, for a role in host defences against viral infections. We employed a VSV infection, an H1N1 infection, and a serial infection model involving H1N1 infection followed by an ST infection. We also measured glucocerebrosidase enzymatic activity before and after viral infection, to investigate whether activity is changed downstream of it.

10.2. Hypothesis

Parkinson's disease-linked genes and their allelic variants, including in *Lrrk2*, *Snca*, and *Gba1*, can alter host responses to virulent infections in neonates and adult mice. Further, specific genotype-virus interactions will not only alter acute host responses but also affect brain health outcomes in surviving animals, which include common neurodegeneration-associated changes.

10.3. Objectives

Chapter 2: Do *Lrrk2* and *Snca* alter the course of illness of reovirus T3D-induced encephalitis primarily in the brain or the periphery?

> **Manuscript Title:** "*Lrrk2* variants do not alter the course of primary encephalitis due to neurotropic reovirus T3D in newborn mice but the p.G2019S mutant elevates phosphorylated tau"

Chapter 3: Do *Lrrk2* alleles alter the survival of adult mice nasally inoculated with RNA viruses? Can two distinct RNA viruses with differing tropism when administered systemically cause Parkinson's pathology-related outcomes in the brain? What is the effect of *Lrrk2* in such models?

> **Manuscript Title:** "Variable outcomes for phospho-tau, α-synuclein, and oxidative stress in adult mice including in Lrrk2 p.G2019S mutants after nasally acquired viral infections"

Chapter 4: What is the role of Parkinson's disease-linked *Gba1* in host responses against select microbial infections?

Manuscript Title: "*Gba1* p.D409V mutant alleles confer protection during acute infection by a neurotropic RNA virus following nasal inoculation"

<u>Chapter 2:</u> *Lrrk2* variants do not alter course of primary encephalitis due to neurotropic reovirus T3D in newborn mice but the p.G2019S mutant elevates phosphorylated tau

Michaela O. Lunn, Christopher Rousso, Nathalie A. Lengacher, Juan Li, Julianna J. Tomlinson, Earl G. Brown, Michael G. Schlossmacher

Statement of Author Contribution

ML, CR, JJT, EGB, and MGS conceptualized the study. **ML** maintained Lrrk2 p.G2019S and Lrrk2 p.D1994S breeding colonies and prepared all experimental cohorts; CR maintained the *Snca* knockout breeding colony and prepared *Snca* knockout experimental cohorts. **ML** performed all *in vivo* experiments involving Lrrk2 p.G2019S and Lrrk2 p.D1994S mice (**Fig. 2.1; Fig. 2.2; Fig. 2.3; Supp. Fig. 2.2**). CR performed all *in vivo* experiments involving *Snca* knockout mice (**Fig. 2.4**). NL performed the ELISA for α-synuclein quantification (**Fig. 2.3e**). JL performed correlation analyses (**Fig. 2.3d, 2.3f, Supp. Fig. 2.1**). **ML** wrote the manuscript, with input and edits from EGB, JJT, and MGS.

Lrrk2 variants do not alter the course of primary encephalitis due to neurotropic reovirus T3D in newborn mice but the p.G2019S mutant elevates phosphorylated tau

Michaela O. Lunn[1,2], Christopher Rousso[1], Nathalie A. Lengacher[1], Juan Li[1], Julianna J. Tomlinson[1#], Earl G. Brown[1,3#], Michael G. Schlossmacher[1,2,4,5#]

[1]Program in Neuroscience, Ottawa Hospital Research Institute, Ottawa, ON, Canada;

[2]Department of Cellular and Molecular Medicine, University of Ottawa, Ottawa, ON, Canada;

[3]Department of Biochemistry, Microbiology, and Immunology, University of Ottawa, Ottawa, ON, Canada;

[4]University of Ottawa Brain & Mind Research Institute, Ottawa, ON, Canada;

[5]Division of Neurology, Department of Medicine, The Ottawa Hospital, Ottawa, ON, Canada.

Abstract

Variants of the leucine-rich repeat kinase-2 (*LRRK2*) and α-synuclein (*SNCA*) genes are associated with Parkinson's disease risk. We previously demonstrated that two *Lrrk2* knock-in variants as well as *Snca* expression alter survival rates from combined pneumonitis and encephalitis following *nasal inoculation* of newborn mice with a double-stranded RNA virus: respiratory-enteric-orphan virus, serotype-3 strain Dearing (referred to as reovirus T3D). There, we had also found elevated inflammation and increased α-synuclein concentrations in the brain of infected Lrrk2 p.G2019 mice. Here, we examined whether outcomes of a *direct brain infection* by reovirus T3D, which uniformly causes lethal encephalitis within 15 days, could be modified by allelic variants in *Lrrk2* and *Snca*. We inoculated newborn mice intracerebrally with $5x10^2$ plaque-forming units of reovirus T3D. We found that when compared to wild-type littermates Lrrk2 p.G2019S mutant mice as well as kinase-dead p.D1994S animals showed the same time-to-death intervals post inoculation, revealed no sex difference, and had similar viral titres in the brain. Quantification of endogenous total α-synuclein and total tau in directly-infected mouse brain showed no difference for Lrrk2 p.G2019S mutant mice relative to wild-type littermates. However, we identified a significant rise in phosphorylated tau in murine brain that was both infection- and Lrrk2 p.G2019S-dependent. Unexpectedly, the reduction or absence of endogenous α-synuclein also did not alter the course of disease in the intracerebral inoculation model. Our results suggest that in contrast to the nasal inoculation of newborn mice, mutant Lrrk2 as well as endogenous α-synuclein do not measurably alter the course of encephalitis in a primary brain infection model caused by reovirus T3D. These findings suggest a systemic contribution by the Parkinson's disease-linked *Lrrk2* and *Snca* alleles in innate host responses in this acute infection model. Intriguingly, our results demonstrate that Lrrk2 p.G2019S promotes tau hyper-phosphorylation in response to reovirus T3D encephalitis.

Introduction

Parkinson's disease (PD) is one of the most prevalent neurodegenerative disorders, characterized by the progressive loss of dopaminergic neurons in the Substantia nigra pars compacta (SNpc), leading to a typical motor syndrome. While the exact etiology of PD remains elusive, the pathogenesis likely requires a multifaceted interplay between genetic and environmental factors. Further, initiation of PD pathology may commence outside of the brain. This is supported by the notion that the key prodromal symptoms, namely hyposmia and constipation, can manifest up to two decades prior to the clinical diagnosis of PD, and both arise in peripheral regions closely linked to the external environment (the nose and the gut, respectively) (Kalia and Lang, 2015). Indeed, these anatomical sites align with the Braak and Del Tredici-based staging model of α-synuclein (aSyn) inclusion formation and are among the first sites exposed to external environmental triggers, including microbial pathogens (Braak et al., 2003). As such, there is increasing interest in elucidating the role of environmental triggers, particularly of microbial origin, in the initiation and progression of PD pathology.

Both neural-based and systemic inflammation have been identified in the pathology of PD. Biochemical analyses have demonstrated elevated levels of pro-inflammatory cytokines in the midbrains of PD patients, including tumor necrosis factor-α (TNFα), interleukin-1β (IL-1β), and interferon-γ (IFN-γ) (Leal et al., 2013). This upregulation of pro-inflammatory cytokines is also observed in the cerebrospinal fluid of living PD patients, including increased levels of transforming growth factor-β1 (TGF-β1), IL-6, and IL-1β (Chen et al., 2018); as well as elevated TNFα, IL-6, and IL-1β in peripheral serum samples (Bu et al., 2015). This suggests that heightened inflammation may be acting both locally within the brain and systemically in PD. Similarly, midbrain SNpc samples from *post-mortem* human PD patients showed increased damage to the

blood-brain barrier, leukocyte extravasation, and microgliosis (Sanchez-Guajardo et al., 2013; Kortekaas et al., 2005). Epidemiologically, the incidence rate of prior infections with several viruses, including hepatitis C virus, herpes simplex virus, and influenza A virus are significantly correlated with Parkinson's disease risk in human populations (Leta et al., 2022). These findings collectively suggest that PD patients generally exhibit a pro-inflammatory signature in their brain, potentially attributed to present or previous exposures to viral pathogens, both within the brain and in the periphery.

Leucine-rich repeat kinase-2 (*LRRK2*) is a candidate gene for studying the influence of exogenous pathogens on PD pathogenesis. Mutations in *LRRK2* constitute the second most frequent genetic risk factor associated with PD, following *GBA1* (Zimprich et al., 2004; Nalls et al., 2014). These mutations, including the most prevalent variant located within the kinase domain, p.G2019S, confer increased risk to both familial and sporadic forms of PD. However, these mutations exhibit incomplete penetrance, with the p.G2019S variant having a penetrance rate as low as 28% at 59 years (Healy et al., 2008). This incomplete penetrance underscores the requirement for secondary factor(s), such as an environmental trigger, to initiate LRRK2-PD.

Regarding function, LRRK2 has relatively low expression in neurons but is highly expressed in immune cells, particularly those of innate lineage including neutrophils, monocytes, macrophages, and microglia (Gardet et al., 2010; Hakimi et al., 2011). LRRK2 expression is upregulated in response to pathogens, infectious agents, and inflammatory signals, such as IFN-γ and NF-κB, suggesting its involvement in pathogen response pathways and inflammation (Gardet et al., 2010; Hakimi et al., 2011). Additionally, mutations in *LRRK2* have also been associated with Crohn's disease and leprosy's type-I hypersensitivity reaction, both of which are characterized by exaggerated inflammation and require one or more xenobiotic triggers for disease

manifestation (Hui et al., 2018; Fava et al., 2016; Zhang et al., 2017). It is conceivable that LRRK2-linked PD may also necessitate a significant inflammatory and xenobiotic trigger for disease onset.

Our previous studies, along with those of other research groups, have explored the role of allelic variants of *Lrrk2* in modulating disease outcomes against various pathogens, including *Salmonella typhimurium*, *Mycobacterium tuberculosis*, and *Listeria monocytogenes (*Shutinoski et al., 2019; Härtlova et al., 2018; Liu et al., 2017; Zhang et al., 2015). Lrrk2 p.G2019S conferred a protective benefit in a sepsis model caused by *Salmonella typhimurium* inoculation, in reducing bacterial burden and prolonging time-to-death (Shutinoski et al., 2019; Liu et al., 2017). Moreover, we have reported that the hyper-kinase Lrrk2 p.G2019S mutation worsens, and the kinase-dead Lrrk2 p.D1994S mutation improves, survival outcomes following nasal inoculation of mice with reovirus T3D; this double-stranded, non-enveloped RNA virus induces pneumonitis followed by encephalitis as the cause of death in suckling mice (Gauvin et al. 2013; Shutinoski et al., 2019). We had chosen this particular pathogen given its tropism for the respiratory tract as well as for its ability to infect the brain (Gauvin et al., 2013). Driven by the fact that LRRK2 has low(er) expression in the brain compared to the peripheral organs, such as the lung and bone marrow, and that LRRK2 can modulate disease outcomes in non-CNS penetrating paradigms (Shutinoski et al., 2019; Hakimi et al., 2011), we sought to investigate the role of LRRK2 in a direct brain infection model with its attendant immune response.

In parallel to Lrrk2, we and others have previously shown that aSyn is relatively protective against select RNA virus infections, such as in the nasally acquired reovirus T3D infection model in newborn mice (Tomlinson et al., 2017) and West Nile virus in adult animals (Beatman et al., 2016). These reports have led to the interesting observation that aSyn confers anti-microbial properties *in vivo*; and further, that its protein expression could be induced by microbial exposure

in vitro and *in vivo* (Tomlinson et al., 2017; Park et al., 2016; Beatman et al., 2016; Monogue et al., 2022; Kim et al., 2016; Chen et al., 2016).

In our previous work both *Lrrk2* and *Snca*, two PD-associated genes, influenced disease outcomes following nasal inoculation with reovirus T3D, which involved a systemic infection followed by encephalitis with a female sex bias (Shutinoski et al., 2019; Tomlinson et al., 2017). Much research on Lrrk2 and aSyn has focused on their roles within the brain. To delineate the involvement of Lrrk2 and aSyn in host defenses against reovirus T3D in peripheral organ systems *vs.* brain-specific immune functions, we employed a direct-brain inoculation method using reovirus T3D; this to conduct experiments complementing our previous publications (Shutinoski et al., 2019; Tomlinson et al., 2017) by lessening the contributions of peripheral organ systems. Intriguingly, neither *Lrrk2* variants nor *Snca* expression altered acute disease outcomes, including time-to-death intervals and viral titres following direct-brain inoculation of mice with reovirus T3D.

Further, given that select LRRK2 mutants in PD patients can lead to pleomorphic outcomes at autopsy, including aSyn-positive or tau-reactive inclusion formation in surviving neurons (sometimes even within the same kindred with the same disease-causing allele), we also examined the effects of *Lrrk2* variants on tau and aSyn metabolism in our intracerebral inoculation model (Henderson et al., 2019; Kalia et al, 2015; Zimprich et al., 2004; Rajput et al., 2006). We hypothesized that intracerebral inoculation of mice would lead to mutant Lrrk2-dependent changes in aSyn and/or tau metabolism. There, we found evidence for an increase in tau phosphorylation, that was both infection- and Lrrk2 p.G2019S-mutation dependent.

Methods

Mouse Colonies

All mouse colonies were kept on a C57BL/6J background. Colonies were maintained with heterozygous breeding pairs. Animal experiments were performed under the guidelines by Canadian Councils on Animal Care and approved by the Ethics Board of the Animal Care Committee at the University of Ottawa. Experiments involving viral infections were done in a containment level 2 biohazard animal facility. Lrrk2 p.G2019S mice and Lrrk2 p.D1994S mice are described in Herzig et. al. (2011). α-Synuclein knockout (*Snca*$^{-/-}$) mice were first described by Cabin et. al. (2002) and were kindly obtained from Dr. Matthew Farrer. Both female and male mice were used in this study and are indicated within each figure.

Intracerebral Reovirus T3D Infection

From heterozygous breeding pairs, post-natal day 1 (p1) mouse pups were anesthetized under 3% isoflurane in oxygen. Using a 30-gauge 50µL fixed needle Hamilton syringe, 10µL of live, purified Respiratory Enteric Orphan Serotype 3 Dearing Virus (reovirus T3D) at a dose of $5x10^2$ PFU (in PBS) was injected into the left hemisphere of the pup brain (frontal lobe) (Passini et al., 2001) and returned to the home cage. For mock-treated controls, injection with 10 µl of PBS was used.

Intracerebral Reovirus T3D Infection Survival Assay

Infected animals were assessed for survival, measured as time-to-death. Infected mice were monitored twice daily (morning and evening) up to 14 days post inoculation (dpi). Moribund mice were sacrificed via rapid decapitation.

Viral Quantification in Tissue

A separate cohort of infected mice were euthanized at 8dpi via rapid decapitation for viral titre analyses in the brain and liver. Samples were homogenized in PBS at a 3:1 ratio (µl PBS:mg tissue) for brains, or a 5:1 ratio for livers. Samples were homogenized with metal beads using a Roche MagNA Lyser (Roche, Indianapolis, IN, USA) at maximum speed for 10 seconds. Samples underwent a freeze-thaw cycle in liquid nitrogen and were then centrifuged to collect the viral content in the supernatant for standard reovirus plaque assay analysis. Briefly, tissue homogenates were used for serial dilutions and overlaid onto L929 cells in 6-well plates at 90-100% confluency. Infected cells were overlaid with 2% purified agar and 2x199 media in a 1:1 ratio. Plaques were identified using 0.015% neutral red stain and manually counted. PFU was reported as plaques per gram of tissue.

ELISA Quantification of α-Synuclein and Tau

Protein was extracted from homogenates used for viral titre analysis. Aliquots of homogenates were treated with 1% Triton- X100, 5X protease inhibitors, and 2X phosphatase inhibitors and spun at 14,800 RPM for 30 minutes at 4°C. Lysates were measured for total α-synuclein using a sandwich ELISA, as described previously (Shutinoski et. al., 2019; Mollenhauer et al., 2008). α-Synuclein protein abundance values were normalized to total protein concentration. Total murine tau protein abundance was measured with the Tau (Total) Mouse ELISA Kit (KMB7011, Invitrogen).

Western Blotting

Protein concentrations were determined using a bicinchoninic acid (BCA) assay kit (Thermo Fisher Scientific). Protein samples (40µg) were combined with 1X NuPAGE™ LDS Sample Buffer (NP0007, Thermo Fisher Scientific), boiled for 5 minutes at 95-100°C, and then electrophoresed under reducing conditions on 4-12% gradient SDS gels in MES buffer. Gels were then transferred to a PVDF membrane using a standard semi-dry transfer in TRIS-glycine-Methanol buffer. The following antibodies were used: anti-actin (sc-81178, Santa Cruz; 1:1000 in 5% milk) and anti-phospho-tau (Ser202, Thr205) monoclonal antibody (AT8) (MN1020, Thermo Fisher Scientific, 1:500 in 5% milk). Western blots were imaged using BioRad ChemiDoc Imager. Image Lab (version 6.1.0) (2020 BioRad Labratories, Inc.) was used for densitometric analysis of Western blots.

Statistical Analysis

All statistical analyses were performed using GraphPad Prism version 8 (GraphPad Software, San Diego, CA, USA, www.graphpad.com). Difference between groups in survival assays was assessed using the log- rank (Mantel-Cox) test. Differences between groups were assessed using one-way ANOVA with Tukey's post-hoc tests. Correlation analysis of α-synuclein and tau quantification was done using R version 4.2.0, packages 'ggplot2' (Kassambara, 2023) and 'ggpubr' (Wickham, 2016). Data are demonstrated as mean ± SEM where applicable and as described in the figure legends. Data are displayed with P values represented as * $P < 0.05$.

Results

Parkinson's-linked Lrrk2 p.G2019S variant does not alter acute outcomes in a primary reovirus-T3D-induced encephalitis model.

The Lrrk2 p.G2019S variant was examined for its impact on acute outcomes in reovirus T3D-induced encephalitis following intracerebral inoculation. As Lrrk2 expression is comparatively low in the brain compared to peripheral tissue, our objective was to investigate the participation of this protein in peripheral *vs.* brain-specific immune responses. Therefore, we chose a primary brain infection model. Lrrk2 p.G2019S mouse pups at postnatal day 1 were intracerebrally injected with reovirus T3D and either monitored for time-to-death or used for tissue collection and viral titre analyses (**Fig. 2.1a**). Mice carrying the p.G2019S allele (heterozygous or homozygous) exhibited similar time-to-death patterns as wild-type mice ($n \geq 7$ mice per group) (**Fig. 2.1b, c**). Previously, we consistently observed a female sex bias with Lrrk2 in infectious-diseased states; therefore, we analyzed the data separately based on sex, but we found no difference in time-to-death between mutant and wild-type mice of either sex (**Fig. 2.1b, c**). These results contrast with our previous findings whereby female Lrrk2 p.G2019S mice showed significantly more death upon nasal inoculation of reovirus T3D (Shutinoski et al., 2019), indicating that the route of inoculation itself reveals genotypic as well as sex differences in survival.

To assess viral infectivity and its replication in the brain, we examined the corresponding viral titres at 8 days post-infection, as the latest timepoint before mice begin to succumb to the infection. Viral titres in the brain were similar among all genotypes, regardless of sex (**Fig. 2.1d**). We also investigated secondary dissemination of the pathogen from the brain by measuring viral titres in the liver at 8dpi. We observed viral spread from the brain to the periphery, as indicated by high viral titres in the liver. Again, there were no differences in viral titre between the wild-type

and Lrrk2 p.G2019S expressing mice (**Fig. 2.1e**). Collectively, these findings indicate that the Lrrk2 p.G2019S hyper-kinase mutation does not alter the course of illness following intracerebral inoculation with reovirus T3D, despite our previous results demonstrating its impact on both survival and viral titre in the nasal inoculation model with the same reovirus T3D pathogen (Shutinoski et al., 2019).

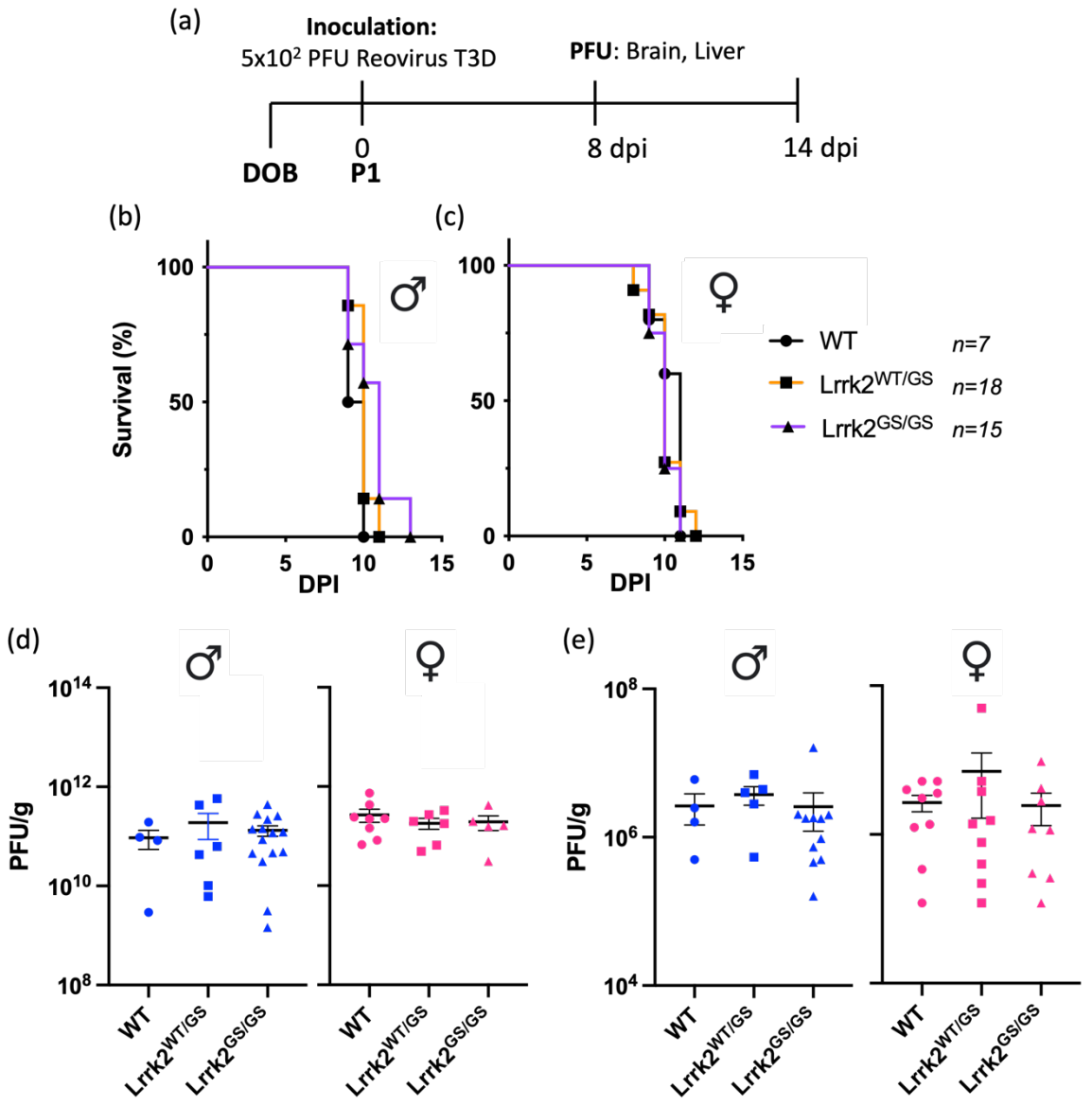


Fig. 2.1: Expression of the Parkinson's Disease-Linked Lrrk2 p.G2019S Variant Does Not Alter Outcomes of Acute Reovirus T3D-Induced Encephalitis When Inoculated Intracerebrally. Heterozygous Lrrk2 p.G2019S breeders were paired, and newborn mice were inoculated with a dose of $5x10^2$ PFU of reovirus T3D via direct brain injection into the left hemisphere and monitored for survival or sacrificed for tissue collection, as summarized in (**a**). Inoculated pups were monitored over 14 days for a pre-determined moribund state. Time-to-death is graphically displayed as percent survival against days post inoculation (DPI), separated based on sex (**b**). The *n* value indicates the sample size of sexes combined. In a second cohort, inoculated pups were sacrificed at 8dpi; brain and liver were collected and homogenized. Viral titres of the brain (**c**) and the liver (**d**) were measured via plaque assay. Data are represented in PFU/g, where each symbol represents one animal. Blue data points indicate male mice ($n \geq 4$ per group) and pink data points indicate female mice ($n \geq 5$ per group). Survival curves were statistically analyzed

using Mantel-Cox (Log-Rank) tests; viral titres were analyzed using one-way ANOVA and Tukey post-hoc tests. No significant group differences were observed.

Lrrk2 kinase-dead mice have an equal survival rate as heterozygous and wild-type mice following direct inoculation of the brain with reovirus T3D.

Given that the p.G2019S mutation of Lrrk2 confers hyper-kinase activity of the protein and due to the fact that we did not identify any genotypic differences in acute outcomes following reovirus T3D infection in newborn mice, we next investigated whether the wild-type kinase activity of Lrrk2 was required for host defence against intracerebral inoculation with reovirus T3D. Therefore, we employed this model in Lrrk2 p.D1994S knock-in mice, which renders the Lrrk2 protein kinase-dead (Herzig et al., 2011). We have previously reported that Lrrk2 p.D1994S homozygous mutant mice show increased survival compared to wild-type mice in response to nasally acquired reovirus T3D-induced encephalitis. Despite the clear survival benefit in Lrrk2 p.D1994S mice in the systemic reovirus T3D model (Shutinoski et al., 2019), we observed no differences in time-to-death following direct brain inoculation between wild-type and heterozygous and homozygous Lrrk2 p.D1994S mice ($n \geq 13$ mice per group) (**Fig. 2.2a**). As was done using the Lrrk2 p.G2019S mouse cohort, we next measured viral titres in the brain and livers of Lrrk2 p.D1994S mice. Lrrk2 p.D1994S mice exhibited similar viral titres in the brain at 8dpi compared to wild-type and heterozygous mice (**Fig. 2.2b**). We observed viral dissemination to the liver at 8dpi in the Lrrk2 p.D1994S cohort, with relatively low and comparable viral titres across the three genotypes (**Fig. 2.2c**). Collectively, these findings suggest that allelic variants in Lrrk2, both p.D1994S and p.G2019S, do not influence the course of encephalitis following direct injection of reovirus T3D into the brain. This contrasts with the significant survival differences observed with both alleles compared to wild-type mice when the same virus was administered systemically via the nasal route (Shutinoski et al., 2019).

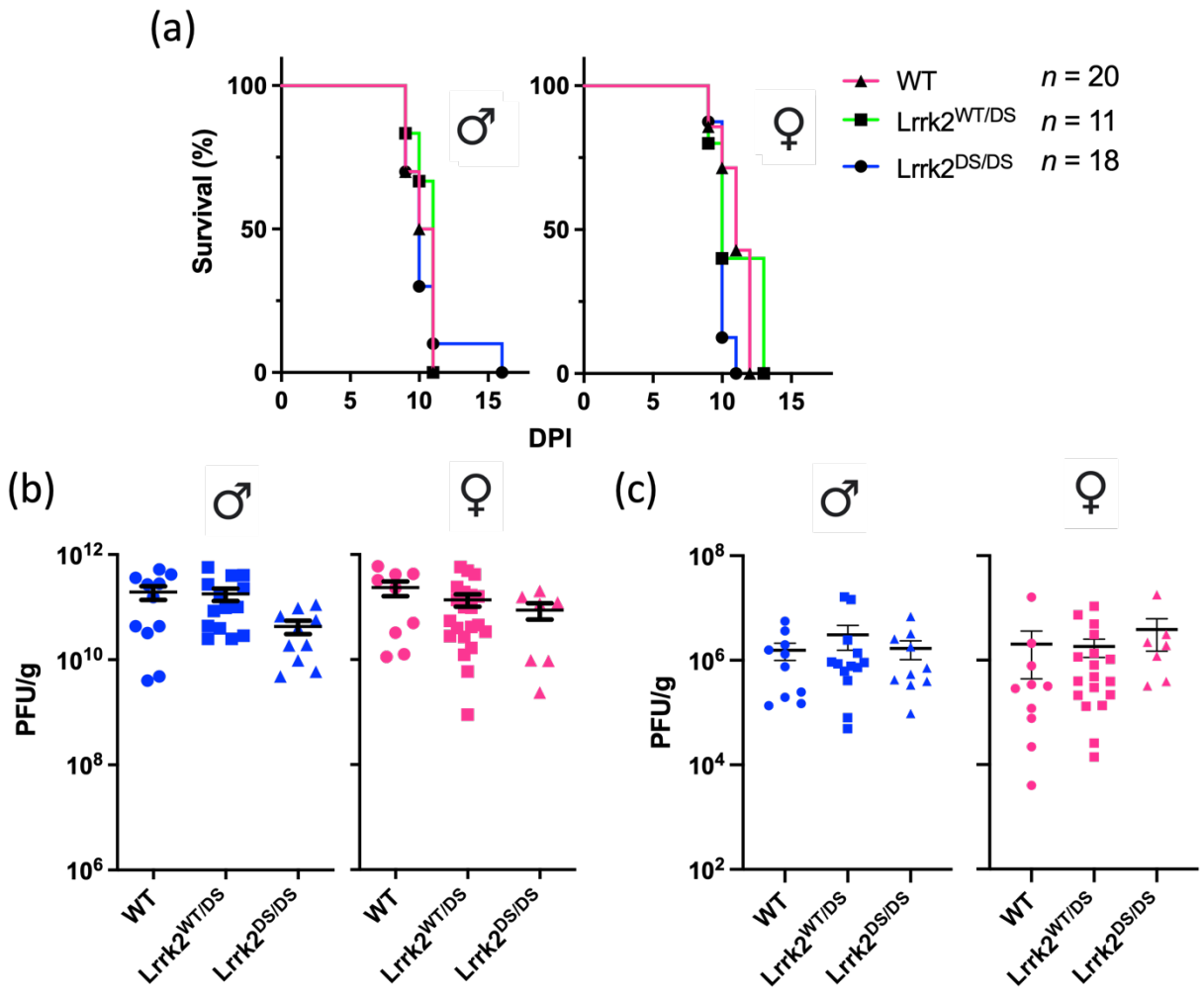


Fig. 2.2: Expression of the Lrrk2 Kinase-Dead p.D1994S Mutant Does Not Alter Outcomes of Acute Reovirus T3D-Induced Encephalitis When Inoculated Intracerebrally. Heterozygous Lrrk2 p.D1994S breeders were paired, and newborn mice were inoculated with a dose of $5x10^2$ PFU of reovirus T3D via direct brain injection into the left hemisphere. Inoculated pups were monitored over 14 days for a pre-determined moribund state. Time-to-death is graphically displayed as percent survival against days post inoculation (DPI), separated based on sex (**a**). The *n* value indicates the sample size of sexes combined. In a second cohort, inoculated pups were sacrificed at 8dpi and brain and liver were collected and homogenized. Viral titres of the brain (**b**) and liver (**c**) were measured via plaque assay. Data are represented in PFU/g, where each symbol represents one animal. Blue data points indicate male mice ($n \geq 9$ per group) and pink data points indicate female mice ($n \geq 7$ per group). Survival curves were statistically analyzed using Mantel-Cox (Log-Rank) tests and viral titre data were statistically analyzed using one-way ANOVA and Tukey post-hoc tests. No significant group differences were observed.

Intracerebral reovirus T3D infection leads to more tau phosphorylation, but not to changes in total tau or total α-synuclein protein concentrations in Lrrk2 p.G2019S mice.

We next investigated whether direct-brain reovirus T3D infection could lead to neurodegeneration-linked changes in infected mice. As human cases of LRRK2-associated PD have been described with either aSyn or tau pathology (Henderson et al., 2019; Kalia et al., 2015; Zimprich et al., 2004), we measured each of these proteins, including levels of phosphorylated tau protein. Using Western blot analyses, we identified phosphorylated-tau (p-Tau) (AT8 monoclonal antibody targeting Ser202 and Thr205) in protein extracts from intracerebrally reovirus- and mock-infected brain homogenates. Strikingly, we identified an infection-dependent rise in p-Tau that was significant in the brains of mutant mice ($P < 0.01$; **Fig. 2.3a, b**). Reovirus-infected Lrrk2 p.G2019S brain samples had significantly more p-Tau than reovirus-infected wild-type brain samples, suggesting a mutation effect on the level of tau phosphorylation following viral infection. As we have consistently observed a female sex bias with the Lrrk2 p.G2019S mutation following infection, we measured the level of p-Tau in both male and female mice and found that infection increased p-Tau abundance in Lrrk2 p.G2019S mice in both sexes (**Fig. 2.3b**). This increased abundance of tau phosphorylation was not attributed to an increase in total tau protein abundance, as levels of tau were the same across all treatment groups, genotypes, and sexes when measured via sandwich ELISA (**Fig. 2.3c**). Furthermore, total tau levels did not correlate with reovirus viral titre in the same brain (**Fig. 2.3d**).

When we measured aSyn protein abundance using a sensitive sandwich ELISA in intracerebrally inoculated reovirus T3D infected brains, we did not identify any differences between wild-type and Lrrk2 p.G2019S mock- or virus-infected brains at 8dpi (**Fig. 2.3e**), nor any correlation with reovirus viral titre in the brain (**Fig. 2.3f**). These data were surprising, as we had

previously shown that Lrrk2 p.G2019S mice had increased aSyn in the brain in response to nasally acquired reovirus T3D infection at 10dpi (Shutinoski et al., 2019); in the latter samples, we saw a significant positive correlation between viral titre and aSyn abundance in the brains of nasally inoculated mice (P=0.00035) (**Supp. Fig 2.1a**). In parallel, we also found a significant positive correlation between tau abundance and viral titre in nasally infected brains (P=0.025) (**Supp. Fig 2.1b**). Taken together, these data suggest that, in a reovirus T3D neonatal mouse model, only a viral infection that engages peripheral host response(s) appears to significantly alter aSyn and tau protein abundance in the brain, which occurs in a viral titre-dependent manner.

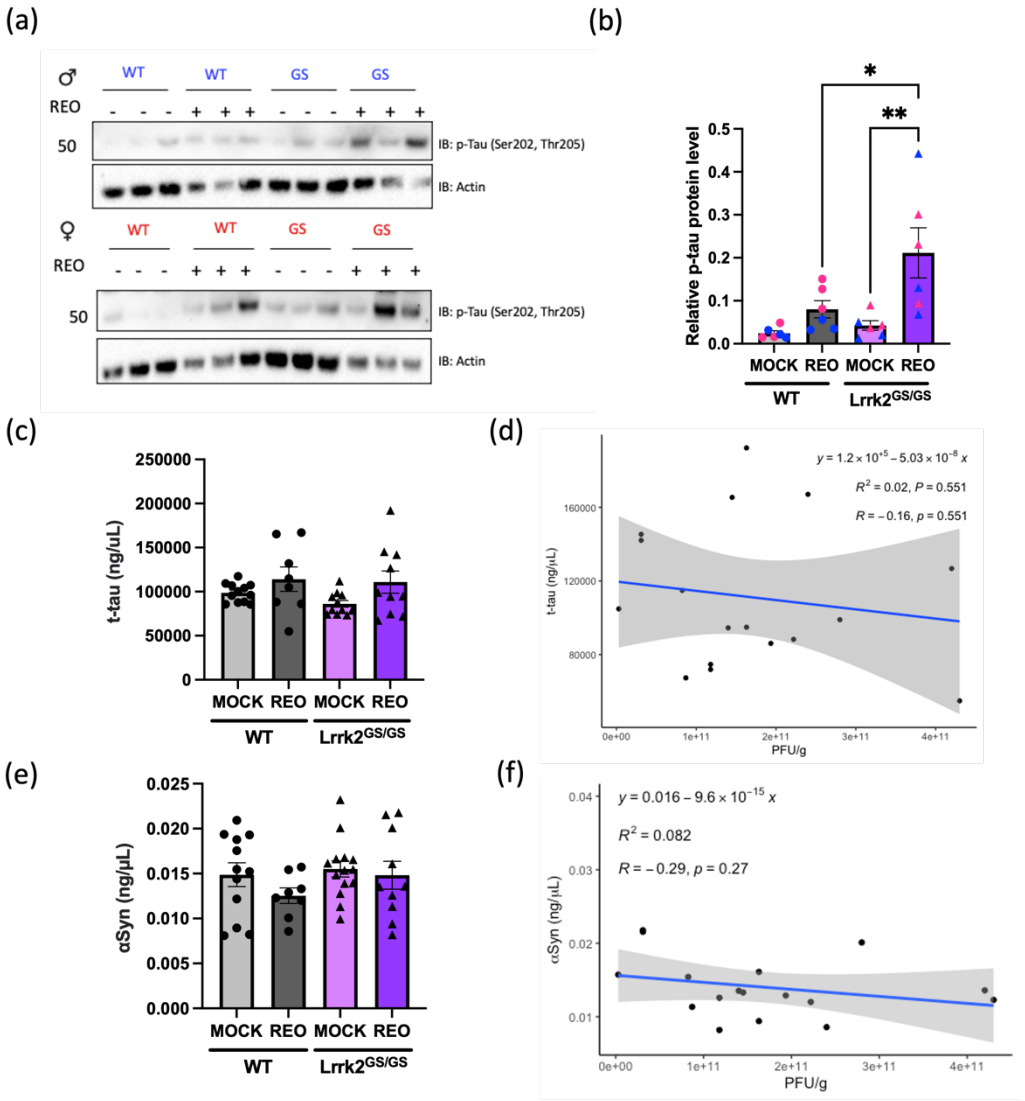


Fig. 2.3: Phospho-Tau Levels, But Not Total Tau or α-Synuclein Abundance, Are Significantly Increased After Intracerebral Reovirus T3D Infection In Lrrk2 p.G2019S Mice. Wild-type and Lrrk2 p.G2019S newborn mouse pups were intracerebrally inoculated with a dose of $5x10^2$ PFU of reovirus T3D or PBS (mock) and sacrificed at 8dpi. Brains were collected and homogenized, and phosphorylated tau protein (p-Tau) levels were measured by Western blotting, whereas total tau (t-tau) and α-synuclein (αSyn) protein concentrations were measured via sandwich ELISA. Western blot analyses of anti-p-Tau (Ser202, Thr205) (AT8) were measured in male (top panel) and female (bottom panel) mice (**a**). Densitometric analyses (measured with Image Lab) were normalized to internal blot control (not shown) and actin loading control (**b**). Pink data points represent female brains and blue data points represent male brains. Tau protein abundance is displayed for mock and reovirus-infected brains (**c**). Tau levels and viral titres did not show any correlation (Pearson R: -0.16; p-value: 0.551) (**d**). α-Synuclein protein abundance is displayed for mock and reovirus-infected brains (**e**). α-Synuclein levels and viral titres did not

show any correlation (Pearson R: -0.29; p-value: 0.27) (**f**). Statistical analysis: ANOVA with Tukey post-hoc tests, error bars represent mean ± SEM. P-value <0.05 (*), P-value <0.01 (**).

Endogenous α-synuclein does not protect against intracerebrally acquired reovirus-induced encephalitis.

Multiple viruses have been shown to induce increased expression of aSyn, but it remains unclear whether this is a protective or potentially detrimental response. The antimicrobial properties of aSyn have been demonstrated following various microbial infections (Park et al., 2016; Beatman et al., 2015). We have previously demonstrated that endogenous *Snca* expression reduced the severity of nasally acquired reovirus T3D infections (Tomlinson et al., 2017). Building on this knowledge and considering the link we established between reovirus T3D titre and aSyn protein levels, we further investigated the antiviral properties of aSyn. We performed direct-brain inoculation of reovirus T3D in $Snca^{-/-}$, $Snca^{+/-}$, and wild-type littermates. In contrast to nasal, systemic administration of reovirus T3D, direct-brain inoculation did not result in any genotypic differences in time-to-death, regardless of sex ($n \geq 10$ mice per group) (**Fig. 2.4a**). Similarly, *Snca* expression did not affect viral replication in the brain at 8dpi, regardless of sex (**Fig. 2.4b**).

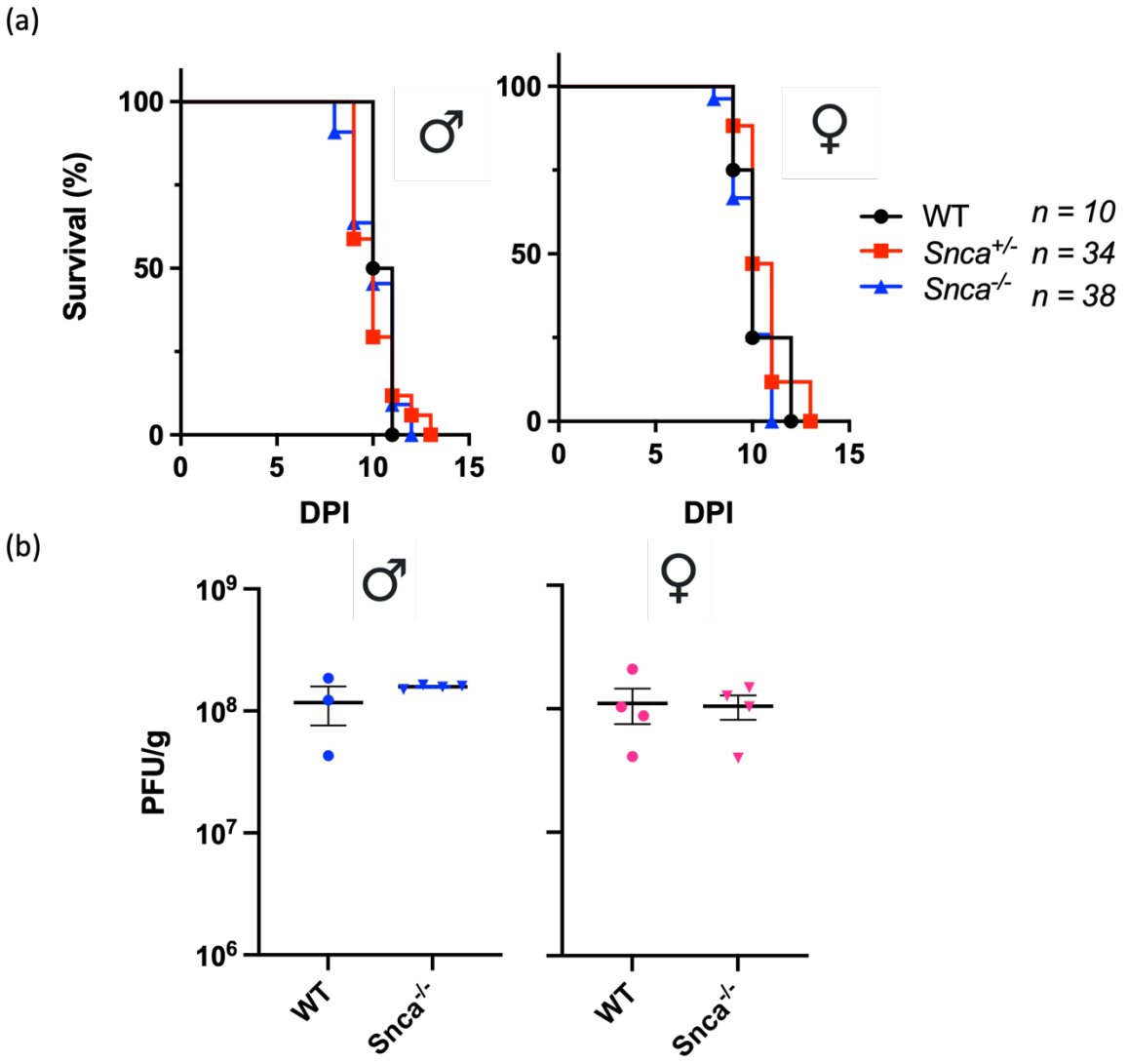


Fig. 2.4: Expression of Murine *Snca* Gene Does Not Alter Outcomes of an Acute, Intracerebral Infection by Reovirus-Induced Encephalitis. Newborn wild-type mice, *Snca* knockout (*Snca*$^{-/-}$), heterozygous (*Snca*$^{+/-}$), and wild-type (WT) pups were inoculated with a dose of 5x10^2 PFU of reovirus T3D via direct brain injection into the left hemisphere. Inoculated pups were monitored over 14 days for a pre-determined moribund state. Time-to-death is graphically displayed as percent survival against days post inoculation (DPI), separated based on sex (**a**). The *n* value indicates the sample size of sexes combined. In a second cohort, inoculated pups were sacrificed at 8dpi and brains were collected for homogenization. Viral titres of the brain were measured via plaque assay (**b**). Data are represented in PFU/g, where each symbol represents one animal. Blue data points indicate male mice ($n \geq 3$ per group) and pink data points indicate female mice ($n \geq 4$ per group). Survival curves were statistically analyzed using Mantel-Cox (Log-Rank) tests and viral titre data were statistically analyzed using one-way ANOVA and Tukey post-hoc tests. No significant group differences were observed.

Discussion

Herein, we have produced further evidence to support a role for Lrrk2 in host defences in a pathogen- and tissue-dependent manner. Specifically, we have demonstrated that even when using the same pathogen (reovirus T3D), the effect of allelic variants in *Lrrk2* (p.G2019S and p.D1994S) on acute disease outcomes depends on the inoculation site of infection, and therefore on the particular engagement of both the peripheral and the brain-specific immune response. In our previous report, we observed that nasal inoculation of reovirus T3D resulted in decreased viral load but higher mortality in female Lrrk2 p.G2019S mice relative to wild-type mice (Shutinoski et al., 2019). In the present study, viral tire and time-to-death were not detectably altered by the *Lrrk2* p.G2019S mutation following a direct-brain injection of the same virus in male or female mice. Similarly, kinase-dead Lrrk2 p.D1994S mice exhibited a survival benefit against nasally-acquired reovirus T3D encephalitis in our previous studies (Shutinoski et al., 2019); however, this allele failed to confer protection against intracerebral inoculation of reovirus T3D. These findings suggest that allelic variants in Lrrk2 modulate the response to, and therefore disease outcomes of, reovirus T3D-induced encephalitis primarily in the periphery rather than in the brain specifically, as it relates to brain health.

We have previously concluded that the *Lrrk2* p.G2019S mutation was protective against *Salmonella typhimurium*, with decreased bacterial burdens in the spleen and extended time-to-death in female Lrrk2 p.G2019S mice *(*Shutinoski et al., 2019; Liu et al., 2017). This was attributed to a pro-inflammatory phenotype exerted by the Lrrk2 p.G2019S mutant, specifically an increase of reactive oxygen species in both the spleen and brain of infected mutant mice. Neonatal mouse pups nasally infected with reovirus T3D also had decreased viral titres in the lung and brain at peak time points, which was again associated with a hyperinflammatory phenotype (increased

infiltrating myeloid cells to the brain). However, this did not translate to a survival benefit and instead these Lrrk2 p.G2019S female mice had higher mortality rate compared to wild-type littermates (Shutinoski et al., 2019). Based on this, we hypothesized that the hyperinflammatory response initiated by Lrrk2 expressed in peripheral cells worsens disease outcomes when the brain is directly implicated but is protective if/when the infection does not reach the brain (*i.e., Salmonella typhimurium*). In the context of reovirus T3D-induced encephalitis, when the inoculation method bypasses the periphery (direct-brain injection), we no longer see an effect of allelic variants in Lrrk2 on disease outcomes, again suggesting that peripheral Lrrk2 modulates disease outcomes in a viral brain infection. Notably, both nasal and intracerebral inoculation of reovirus T3D resulted in similar symptomology and illness progression, with peak lethality occurring between 6-10dpi in both models.

This concept that LRRK2 may primarily affect pathogenic disease outcomes in the periphery rather than in the brain is supported by previous literature. Kozina et al. (2018) demonstrated that lipopolysaccharide (LPS) treatment in Lrrk2 p.R1441G mice resulted in nigral neuronal loss, which was attributed to infiltrating peripheral molecules in circulation (*i.e.,* cytokines) and not monocyte recruitment to the brain or activated microglia. In a second study, they demonstrated that LPS could drive dopaminergic neuronal loss in Lrrk2 mutant mice (p.R1441G and p.G2019S), which was dependent on the presence of peripheral monocytes. Further, neutralization of peripheral IL-6 prevented this LPS-induced dopaminergic neuronal loss in Lrrk2 mutant mice (Kozina et al., 2022). This supports the hypothesis that mutations in *Lrrk2* may not directly affect the health of dopaminergic neurons but rather exert toxic effects on immune cells in the periphery, which in turn have secondary deleterious effects on dopaminergic neurons of the SNpc, thereby promoting PD pathogenesis.

While our present data do not negate the potential involvement of Lrrk2 in host-defences in the brain, they suggest that the effects of *Lrrk2* allelic variants on brain disease outcomes following reovirus-T3D-induced encephalitis require peripheral engagement of the immune response that are Lrrk2-dependent. Functional and morphological changes of microglia following direct brain inoculation were not investigated in the present study but would be informative for understanding cellular changes and potential Lrrk2 phenotypes within the brain in the absence of overt effects on acute disease outcomes, as numerous studies have highlighted a role for Lrrk2 in microglia following infections both *in vivo* and *in vitro* (Dwyer et al., 2020; Panagiotakopoulou et al., 2020; Moehle et al., 2012).

Most compellingly, we identified a rise in phosphorylated tau protein in the brain, that was both dependent on the reovirus T3D infection and on the *Lrrk2* p.G2019S mutation. In LRRK2-linked cases of Parkinson's disease, the presenting brain pathology is variable. Many patients present with the hallmark aSyn aggregates; however, many also present with tau pathology (Henderson et al., 2019). The rise of p-Tau protein abundance was independent of a rise in total tau, indicating an increase in phosphorylation of tau (or decrease in tau phosphatase activity). Tau phosphorylation is reportedly heightened during other viral infections, including SARS-CoV-2 and murine hepatitis virus, and upon treatment of the bacterial mimic, LPS (Di Primio et al., 2023; Sy et al., 2011; Bhaskar et al., 2010). Importantly, our p-Tau measurements occurred at post-natal day 9 (eight days after inoculation) and tau is known to be phosphorylated during fetal and post-natal development (Goedert et al., 1993). Neonatal tau isoform expression shifts around post-natal day 9, and post-natal tau phosphorylation begins to decrease (Tuerde et al., 2018). Therefore, the tau phosphorylation we have identified should be indicative of a viral infection effect. However, it is possible mechanistically that the viral infection is preventing phosphatase activity on tau that was

already developmentally phosphorylated as opposed to driving *de novo* tau phosphorylation. This mechanism has yet to be elucidated in our studies; however, a potential lead is presented by Sy et al. (2011), who have attributed the tau hyperphosphorylation caused by mouse hepatitis virus to increased GSK-3β activity.

Moreover, numerous studies have illustrated a potential role for Lrrk2 in promoting phosphorylation of tau (Hamm et al., 2015; Kawakami et al., 2014), with one study showing the ability of Lrrk2 to directly phosphorylate tau *in vitro* (Bailey et al., 2013). However, it is not concretely evident that Lrrk2 can phosphorylate tau *in vivo*, nor specifically in response to stressor such a viral infection; therefore, we hypothesize that Lrrk2 acts indirectly and upstream of tau phosphorylation.

Notably, the accumulation of phosphorylated tau tangles following viral infections has been well established, specifically in the case of subacute sclerosing panencephalitis induced by measles virus infection (Corselli, 1951; Malamud et al., 1950; Mandybur et al., 1977; Wisniewski et al., 1991). These patients, of all ages, present with neurofibrillary tau tangles, of which the morphology observed is similar to that found in both Alzheimer's disease and chronic traumatic encephalopathy (Mandybur et al., 1997; Qi et al., 2023). Furthermore, postencephalitic parkinsonism, a complication of encephalitis lethargic induced by influenza A viral infection that presents like PD, has been defined as a tauopathy based on the on the presence of widespread neurofibrillary tau tangles (Geddes et al., 1993). Interestingly, cases of postencephalitic parkinsonism seemingly lack aSyn pathology (Jellinger, 2009).

LRRK2 mutations have also been linked to classical tauopathies, namely progressive supranuclear palsy (PSP) and corticobasal degeneration (Sanchez-Contreras et al., 2017). Intriguingly, in some families, the same *LRRK2* mutation in one family member manifested as PD

and in another, manifested as PSP (Zimprich et al., 2004; Spanaki et al., 2006; Rajput et al., 2006). These data highlight an important link between *LRRK2* and the development of tau neurofibrillary tangles (Herbst et al., 2022).

Despite identifying a change in levels of phosphorylated tau protein, we did not identify a change in levels of total tau protein or total aSyn protein. A limitation of this study is that we did not investigate levels of phosphorylated aSyn (at Serine 129), which is pathologically linked to disease, similar to phosphorylated tau protein. Future studies will also investigate protein concentrations of phosphorylated aSyn protein.

In light of our findings with Lrrk2, and parallel studies of systemic reovirus T3D infection of *Snca* knockout mice, we also investigated the effect of endogenous *Snca* expression in this viral model. Our previous research revealed that *Snca* knockout mice exhibited decreased survival in response to nasally induced reovirus T3D-encephalitis (Tomlinson et al., 2017). In our present study, we demonstrate that the disease outcomes following direct-brain inoculation of reovirus T3D were independent of the presence of endogenous aSyn. This highlights a role for aSyn in an immune response outside of the brain. Beatman et al. (2013) demonstrated that increased expression of aSyn enhanced survival against a peripheral West Nile virus infection. Furthermore, recent work by Alam et al. (2022) demonstrated that aSyn is induced and secreted in the peritoneal cavity following intraperitoneal injection of the inflammatory inducer bacterial peptidoglycan. They show that aSyn knockout mice exhibit decreased leukocyte recruitment and reduced activation of adaptive immune cells, suggesting a role for aSyn in normal inflammatory response to pathogens (Alam et al., 2022). Our findings align with these observations and suggest that aSyn may function as an antimicrobial protein. Collectively, our results, coupled with our previous

publication, support the notion that aSyn predominantly contributes to immunity in peripheral tissues.

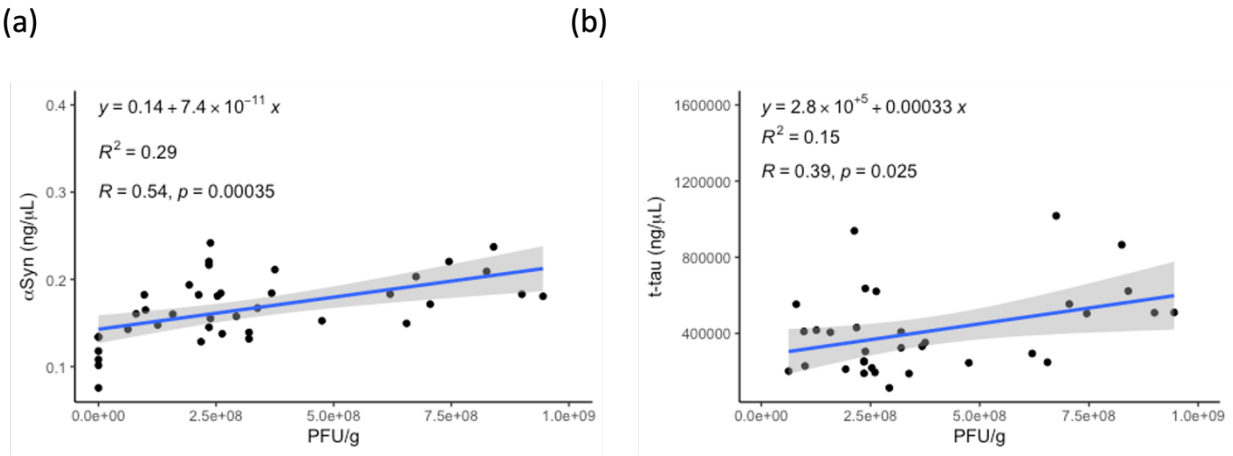
A notable limitation of our study is the severity of the intracerebral inoculation method, which may be too fulminant to reveal time-to-death differences between genotypes. This cannot be addressed by using a lower dose, as the lethal dose of reovirus T3D directly given to the brain is 10^1 PFU in the suckling mouse brain (Spriggs and Field, 1982; Virgin et al., 1988). Nonetheless, we performed a pilot assay with 50 PFU and still observed 100% lethality (data not shown). Importantly, there is no lethality in mock infected mice. This model may lack the sensitivity to detect the effect of *Lrrk2* mutations in this severe process in contrast to our prior nasal infection. However, previous literature has identified that caspase-3 knockout mice were partially rescued against the same intracerebral infection model presented here (strain and dose) in mice of the same background, indicating that this model can be sensitive enough to detect survival disparities between genotypes (Beckham et al., 2011). To further address this concern, we inoculated a separate cohort of Lrrk2 p.D1994S mice intracerebrally at 3 days post-inoculation to allow for further brain development and immune system maturation, and to investigate whether delayed development might prolong the time-to-death. Once again, the time-to-death was nearly identical to that of mice infected at postnatal day 1 and no differences between genotypes were revealed (**Supp. Fig. 2.2**).

Here, we employed the established reovirus T3D infection model (Gauvin et al., 2013) to induce an acute viral infection in neonatal pups and directly examine the innate immune response. Neonatal pups were chosen because they do not possess a fully mature adaptive immune system until four weeks of age (Landreth, 2002). Moreover, our previous research has demonstrated measurable expression of both *Lrrk2* and *Snca* in mouse brains during these early developmental

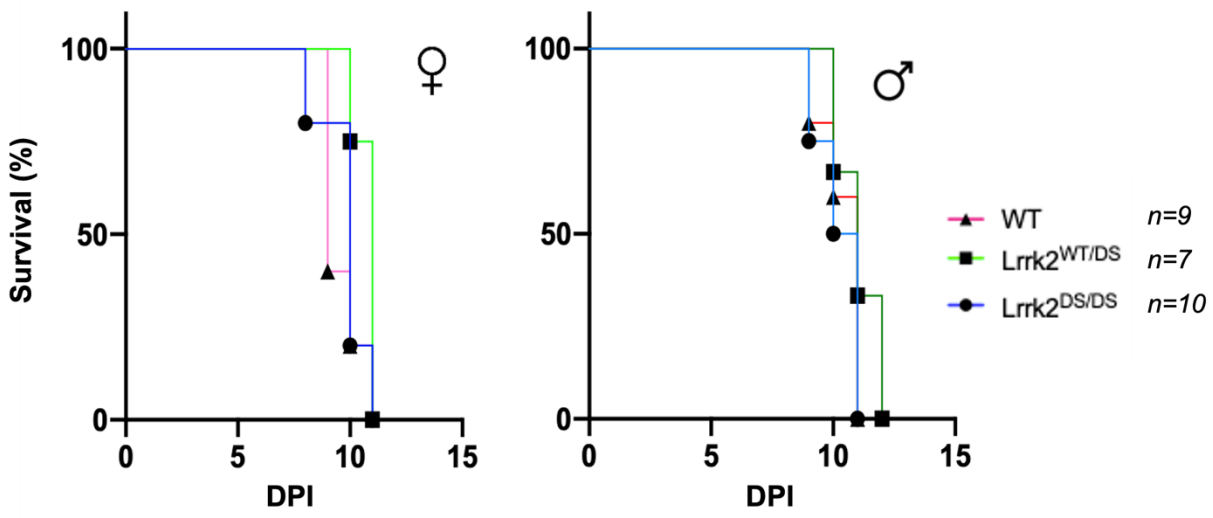
stages (Shutinoski et al., 2019; Tomlinson et al., 2017). Nonetheless, a limitation of this study is the use of neonatal pups, as they have not yet reached critical developmental stages. Assessment of Lrrk2- and α-synuclein- anti-viral properties in adult mice will allow us to investigate their role in a mature immune system and allow us to assess multiple critical factors, including age as a determinant in disease progression, development beyond puberty and the influence of sex hormones, and the maturation of the adaptive immune response. In addition to this, given the pathogen-dependent nature of the disease genes studied here, testing of different types of viruses, such as DNA *vs.* RNA (including those with double-stranded *vs.* various single-stranded genomes), in the context of *Snca* and *Lrrk2* mutants is warranted.

This study, in conjunction with our previous publications (Shutinoski et al., 2019; Tomlinson et al., 2017), suggests that two PD-associated genes, *Lrrk2* and *Snca*, play a role in host defense against reovirus T3D-induced encephalitis primarily in the periphery rather than in the brain-restricted immune response. These findings contribute to the increasing body of evidence indicating that both Lrrk2 and aSyn may have physiological roles outside of the brain. Therefore, consideration of the peripheral aspects in the initiation of PD are critical. This work highlights potential roles for both Snca and Lrrk2 in the peripheral immune response to viral infections, and the critical role of the peripheral immune system to protect the brain following infections.

Supplementary Information



Supplemental Fig. 2.1: α-Synuclein and Total Tau Protein Abundance Are Both Correlated to Reovirus Viral Titres in the Brains of Nasally Inoculated Mice. Newborn mouse pups were nasally inoculated with one LD_{50} of reovirus T3D and sacrificed at 10 or 11dpi. Brains were collected and homogenized. From the same brain lysates, viral titre (PFU/g) was measured via plaque assay, and two Parkinson disease-linked proteins, i.e., α-synuclein and total tau, were measured via sandwich ELISA (as previously published: Shutinoski et al., 2019). α-Synuclein levels and viral titres were significantly positively correlated (Pearson R: 0.54; p value: 0.00035) (**a**). Tau concentrations and viral titres were also significantly positively correlated (Pearson R: 0.39; p value: 0.025) (**b**).



Supplemental Fig. 2.2: Inoculation at Post-Natal Day 3 Does Not Uncover Genotypic Differences in Time-To-Death Between Wild-Type, Heterozygous, or Homozygous Lrrk2 p.D1994S Mutant Mice. Heterozygous Lrrk2 p.D1994S breeders were paired, and mice aged post-natal day 3 were inoculated with a dose of $5x10^2$ PFU of reovirus T3D via direct-brain injection into the left hemisphere and monitored for time-to-death. Inoculated pups were monitored over 14 days for a pre-determined moribund state. Time-to-death is graphically displayed as percent survival against days post inoculation (DPI), separated based on sex **(a)**. The *n* value indicates the sample size of sexes combined. Survival curves were statistically analyzed using Mantel-Cox (Log-Rank) tests. No significant group differences were observed.

Chapter 3: Variable outcomes for phospho-tau, α-synuclein, and oxidative stress in adult mice including in Lrrk2 p.G2019S mutants after nasally acquired viral infections

Michaela O. Lunn, Nathalie Lengacher, Karim Zahr Eddin, Quinton Hake-Volling, Earl G. Brown, Julianna J. Tomlinson, Michael G. Schlossmacher

Statement of Author Contribution

ML, QHV, NL, KZE, JJT, EGB, and MGS conceptualized the study. **ML** did all mouse breeding and colony maintenance for all Lrrk2 p.G2019 and p.D1994S mice. **ML** performed all survival analyses and viral titre analyses of VSV infected Lrrk2 p.G2019S and Lrrk2 p.D1994S mice (**Fig. 3.1**, **Fig. 3.3a-d**). **ML** and QHV performed initial cohorts of H1N1 infected Lrrk2 p.D1994S and Lrrk2 p.G2019S mice for survival analyses together; **ML** completed all subsequent cohorts for survival analyses and viral titre analyses of H1N1 infection (**Fig. 3.2**, **Fig. 3.3e-h**). **ML** inoculated mice and harvested tissue for: cyto-/chemokine analysis and NfL quantification, and all immunohistochemistry experiments. Cyto-/chemokine and NfL measurements were performed by external services (**Fig. 3.4**). KZE performed all immunohistochemistry and all computational analyses of microglial morphology, in a blinded manner. **ML** processed and analyzed the unblinded dataset and created the figures (**Fig. 3.5-3.8**). **ML** performed all Amplex® red assays to measure H_2O_2 abundance and Western blotting of protein nitrotyrosination of 6wpi samples (**Fig. 3.9a-k**). **ML** prepped all TXS and SDS samples and NL performed ELISA experiments to quantify α-synuclein of 6wpi samples (**Fig. 3.9l-q**). **ML** performed all p-Tau Westerns blotting and total tau ELISA experiments (**Fig. 3.10**). For all experiments, NL assisted **ML** with dissections and tissue harvesting. **ML** wrote the manuscript, with input and edits from EGB, JJT, and MGS.

Variable outcomes for phospho-tau, α-synuclein, and oxidative stress in adult mice including in Lrrk2 p.G2019S mutants after nasally acquired viral infections

Michaela O. Lunn[1,2], Nathalie Lengacher[1], Karim Zahr Eddin[1], Quinton Hake-Volling[1,3], Earl G. Brown[1,3], Julianna J. Tomlinson[1,2], Michael G. Schlossmacher[1,2,4]

1. Program in Neuroscience, Ottawa Hospital Research Institute, Ottawa, ON, Canada.
2. Department of Cellular and Molecular Medicine, University of Ottawa, Ottawa, ON, Canada.
3. Department of Biochemistry, Microbiology and Immunology Faculty of Medicine, and Ottawa Institute of Systems Biology, University of Ottawa, Ottawa, ON, Canada.
4. Division of Neurology, Department of Medicine, The Ottawa Hospital, Ottawa, ON, Canada.

Abstract

Mutations in the Parkinson's disease (PD)-linked *Lrrk2* gene have been shown to modulate immunological responses by mammalian hosts. We asked whether the kinase activity of Lrrk2 alters neurodegeneration-linked pathological outcomes in the brain of animals that survived a nasally acquired, viral infection. We inoculated adult mice with one of two RNA viruses: vesicular stomatitis virus (VSV), causing encephalitis; and influenza A virus (serotype H1N1), leading to pneumonitis without brain infection. We found that the *Lrrk2* p.G2019S mutation significantly decreased survival rates of homozygous female (but not male) mice following VSV infection, but not after H1N1 infection. Surprisingly, female homozygous Lrrk2 p.G2019S mice also showed less microglial activation in the brain upon VSV infection than did males. We did not observe any genotypic differences in VSV titres, or for any of 44 cytokines/chemokines screened during the acute stage of infection (i.e., 6 days post inoculation). Intriguingly, 6 weeks post inoculation the levels of H_2O_2 and protein nitrotyrosination were increased in both viral infection models. At the same time point, both viruses had led to a significant rise in phosphorylated tau protein in the brain, which appeared to be stronger in Lrrk2 p.G2019S mice compared to wild-type animals; however, total tau concentrations remained unchanged. At 6 weeks post inoculation, total α-synuclein levels in the brain were significantly lower following VSV inoculation but remained elevated after H1N1 infection. Our collective results demonstrate variable pathological outcomes in adult mice that survive nasally acquired, viral infections. They also highlight the complexity of interactions between specific environmental pathogens, cell types, allelic variants (such as in *Lrrk2*), and sex. We identify in tau hyperphosphorylation and elevated α-synuclein a shared outcome of pneumonitis by influenza A virus, which may be of relevance for the risk of late-onset disorders of the brain.

Introduction

Parkinson's disease (PD), a complex neurodegenerative motor disorder, is increasing in prevalence, yet the etiology of the disease remains elusive. It is thought that PD is caused by a complex interplay between genetics, environmental triggers, and ageing (Schlossmacher et al., 2017). Pesticide exposure, contact with neurotoxins, prior head injuries, rural living, and agricultural occupations have all been listed as environmental risk factors for PD (reviewed in: Kalia and Lang, 2015). Similarly, a multitude of genetic variants have been identified and attributed to PD, including mutations in *LRRK2*, which account for ~2% of cases with parkinsonism (Marras et al., 2016). Mutations in this gene confer risk for both familial and sporadic forms of PD, but the mechanism of disease remains elusive. Notably, there is incomplete penetrance associated with these mutations, with the most common variant, p.G2019S, having as low as 28% in penetrance rate at 59 years (Healy et al., 2008). This suggests that disease manifestation in *LRRK2*-genetically susceptible individuals may require a second, possibly environmental, trigger, which we and others have suggested may be microbial in nature (Hawkes et al., 2007; Hakimi et al., 2011). Intriguingly, LRRK2-PD exhibits pleiotropic brain pathology. Human cohorts have shown that about half of LRRK2-PD cases present with typical α-synuclein pathology; whereas another subset of LRRK2-PD patients present with tau-linked pathology, including tau hyperphosphorylation (and lack α-synuclein-positive deposits); in rare families, there can be pleomorphism even within the same pedigree (Henderson et al., 2019; Kalia et al, 2015; Zimprich et al., 2004; Rajput et al., 2006).

Notably, mutations in *LRRK2* have also been linked to Crohn's disease, a leprosy variant, and systemic lupus erythematosus (Hui et al., 2018; Fava et al., 2016; Zhang et al., 2017). Each of these diseases are characterized by chronic, dysregulated inflammation. The shared risk locus

between these four diseases raises the issue of whether an evolutionarily preserved function of LRRK2 is the regulation of immune responses. Not only is LRRK2 much more highly expressed in the periphery (*i.e.,* lung and kidney) than the brain, but LRRK2 is also more abundant in cells of the immune system, particularly neutrophils, monocytes, and macrophages, than in neurons (Hakimi et al., 2011; Galter et al., 2006). Further, Lrrk2 can be upregulated by pathogens and infectious agents as well as inflammatory signals, such as IFN-γ and NF-κB, suggesting that LRRK2 is involved in pathogen defense pathways and inflammation (Gardet et al., 2010; Hakimi et al., 2011). Recently, it has been demonstrated that Lrrk2 is involved in the STING pathway and plays a critical role in the transition from innate to adaptive immune responses under pro-inflammatory conditions (Fahmy et al., 2023).

Several studies demonstrated an effect of Lrrk2 on live bacterial pathogens, at times in opposite directions. Härtlova et al. (2018) found that Lrrk2 knockout and Lrrk2 kinase-inhibited macrophages exhibited improved control of *Mycobacterium tuberculosis* infection. However, this enhanced control was only observed in the early stage of disease. Liu et al. (2017) showed that Lrrk2 knockout mice had increased *Salmonella typhimurium* burden, while Lrrk2 p.G2019S mice had decreased burden due to NLRC4 inflammasome activation. Furthermore, our team has shown that Lrrk2 p.G2019S-expressing mice have extended survival and decreased bacterial burden following *Salmonella typhimurium* infection (Shutinoski et al., 2019). Finally, Feng et al. (2020) observed increased TNF-α and IL-1β levels in Lrrk2 p.R1441G mice following *Porphyromonas gingivalis* infection, which causes chronic periodontitis.

As the role of Lrrk2 has been studied in the context of multiple bacterial pathogens, we previously investigated the role of Lrrk2 in response to viral infections. We have previously demonstrated that disease outcomes following nasal inoculation by reovirus type 3 Dearing (T3D)

were perturbed by allelic variants of *Lrrk2* in neonatal mice (Shutinoski et al., 2019). Further, we are informed by epidemiological data, such as the 1918 influenza pandemic, which was caused by influenza A virus serotype H1N1 (herein called H1N1). Infections correlated with an increase in Economo's disease, a form of post-infectious parkinsonism (Jordan, 1927; Birkmayer and Hornykiewicz, 1961). Similarly, infants born during the 1918 pandemic had a two-to-three-fold increased risk of developing PD later in life (Martyn, 1997). More recently, a positive influenza exposure history (up to ten years prior) has been linked to an elevated incidence of PD (Cocoros et al., 2019). In mice, infection with highly pathogenic avian influenza serotype H5N1 was able to induce α-synuclein aggregation and dopaminergic neuronal cell loss in wild-type mice following a nasal inoculation paradigm (Jang et al., 2009). Overall, post-acute sequalae are being recognized as a common feature of acute infectious disease in general, including infections from SARS-CoV-2, influenza, and respiratory syncytial virus (Hirschenberger et al., 2021; Vivaldi et al., 2023; Liu et al., 2023; Ubamadu et al., 2024).

Here, we investigated the outcome of allelic variants in *Lrrk2* following viral infection of two distinct RNA viruses on disease outcomes and brain pathology in adult C57Bl/6J mice. We hypothesized that viral infections could lead to sustained alterations in the levels of multiple neurodegeneration-linked markers in the brain. Furthermore, we hypothesized that the kinase-activity of Lrrk2 could perturb disease outcomes following these viral infections. To test this, we employed two types of RNA viruses: vesicular stomatitis virus (VSV), a neurotropic virus causing encephalitis; and influenza A virus, serotype H1N1, leading to a pulmonary infection. We found that the Lrrk2 p.G2019S mutation could perturb disease outcomes after viral infection in a pathogen-specific manner with a female sex bias. Second, both viral infections led to sustained tau

hyperphosphorylation and increased oxidative stress in the brains of surviving mice as late as six weeks post inoculation.

Methods

Mouse Colonies

All mouse colonies were maintained on a C57BL/6J background. Colonies were maintained with heterozygous breeding pairs. Animal experiments were performed under Canadian Councils on Animal Care guidelines and approved by the Ethics Board of the Animal Care Committee at the University of Ottawa. Experiments involving viral infections were done in a containment level 2 biohazard animal facility. Lrrk2 p.G2019S mice and Lrrk2 p.D1994S mice are described in Herzig et. al. (2011). Both female and male mice were used in this study and are indicated within each figure.

Nasal Infection with Vesicular Stomatitis Virus

Wild-type Indiana strain Vesicular Stomatitis virus was obtained from Dr. Earl Brown (University of Ottawa) (Stojdl et al, 2003). Mice aged 8-10 weeks were anesthetized with 3% isoflurane in O_2 at 1 L/m for 1 minute and a dose of $3x10^3$ plaque forming units (PFU) VSV (Indiana strain) diluted in 50µL PBS was administered to the nostrils of anesthetized mice. Mice were observed for 14 days post inoculation (dpi) for survival studies. They were weighed from 4-14dpi and monitored twice daily. Mice were considered endpoint as a result of encephalitis, characterized by a moribund state, hind limb paralysis, and inability to walk or a loss of 30% body weight regardless of lack of other symptoms. Mice that survived the acute viral infection (evident by survival at 14dpi) were aged for four subsequent weeks (to a total of 6 weeks post inoculation [wpi]).

Nasal Infections with Mouse-Adapted Influenza A H1N1

Mouse-adapted Influenza A H1N1 (A/Fort Monmouth/1/1947) was obtained from Dr. Earl Brown (University of Ottawa) (Brown, 1990). Adult mice aged 4-7 weeks were anesthetized with 3% isoflurane in O_2 at 1L/m for 1 minute. A dose of $2x10^3$ PFU of MA-FM Influenza A H1N1 diluted in 50µL PBS was administered to the nostrils of anesthetized mice which induced severe pneumonitis in all infected animals to result in 50% lethality. Monitoring, endpoint, and timelines were exactly as described for VSV infections.

Vesicular Stomatitis Virus Plaque Assay

Mice nasally infected with $3x10^3$ PFU of VSV were sacrificed at 6dpi, perfused, and hemibrains were collected and snap frozen. For viral titre analysis, frozen hemibrains were homogenized in PBS (3:1; µl PBS:mg tissue) using metal beads and Magna Lyser machine (Roche) at maximum speed for 10 seconds. Samples were then put through one freeze-thaw cycle to further lyse the cells. L929 cells were plated in 6-well culture plates to 90% confluency. Homogenate samples were centrifuged at 5,000RPM and supernatants were serial diluted (10-fold, v:v) in serum-free DMEM media (Millipore Sigma) and 100µL was overlayed per well. Cells overlayed with viral suspensions were incubated at 37°C at 5% CO_2 for one hour, with rocking every 15 minutes to ensure even distribution among cells. After one hour, cells were overlayed with 2mL of a 1:1 mixture of 1% agarose and 2xDMEM (Gibco, Thermo Fisher Scientific) supplemented with 10% FBS. Cells were incubated at 37°C at 5% CO_2 for 24 hours. The next day, cells were stained with 1mL of Carnoy's fixative solution (methanol:acetic acid, 3:1) and incubated for one hour at room temperature. Cell overlay was removed under running tap water and cells were stained with Coomassie blue solution (0.1% Coomassie Brilliant Blue, 20% methanol, and 10% acetic acid)

and incubated for 30 minutes at room temperature with gentle rocking. Coomassie stain was removed, and plaques were counted manually. Viral titre was reported as plaque forming units (PFU) per gram of tissue.

Influenza A Virus Serotype H1N1 Plaque Assay

Mice nasally infected with $2x10^3$ PFU of Influenza A virus serotype H1N1 were sacrificed at 6dpi and hemibrains and lungs were collected and snap frozen. For viral titre analysis, frozen lungs were lysed in PBS (3:1; µl PBS:mg tissue) using metal beads and Magna Lyser machine (Roche) at a maximum speed for 10 seconds. Samples were then put through one freeze-thaw cycle to lyse the cells. MDCK cells were plated in 6-well culture plates to 90% confluency. Homogenate samples were centrifuged at 5,000RPM and supernatants were serial diluted (10-fold, v:v) in serum-free DMEM media (Millipore Sigma). MDCK cells were washed twice with PBS to remove all traces of FBS prior to viral overlay. 100µL of each dilution was overlayed per well. Cells overlayed with viral suspensions were incubated at 37ºC at 5% CO_2 for 30 minutes, with rocking at 15 minutes to ensure even distribution among cells. After one hour, cells were overlayed with 3mL of a 1:1 mixture of 1.2% agarose and 2xMEM (Gibco, Thermo Fisher Scientific) supplemented to 0.1ug/mL TPCK trypsin. Cells were incubated at 37ºC at 5% CO_2. Three days later, cells were stained with 1mL of Carnoy's fixative solution (methanol:acetic acid, 3:1) and incubated for one hour at room temperature. Cell overlay was removed under running tap water and cells were stained with Coomassie blue solution (0.1% Coomassie Brilliant Blue, 20% methanol, and 10% acetic acid) and incubated for 30 minutes at room temperature with gentle rocking. Coomassie stain was removed, and plaques were counted manually. Viral titre was reported as plaque forming units (PFU) per gram of tissue.

Protein Extraction

Protein was extracted from homogenate samples used for viral titre analyses. Aliquots of homogenates were treated with 1% Triton- X100, 2X protease inhibitors (Thermo Scientific), and 2X phosphatase inhibitors (Thermo Scientific) and centrifuged at 14,800 RPM for 30 minutes at 4°C. Protein concentrations were determined using a bicinchoninic acid (BCA) assay kit (Thermo Fisher Scientific).

Cytokine and Chemokine Measurements

Mice nasally infected with $3x10^3$ PFU of VSV were sacrificed at 6dpi and hemibrains and blood were collected. Blood was collected via cardiac puncture using an uncoated syringe. Blood was incubated at room temperature for 30 minutes and then centrifuged at 14,800 RPM for 10 minutes to collect serum. Protein extracts from hemibrain homogenates (5mg/mL) and serum were measured for cytokine and chemokine abundance using the discovery assay Mouse Cytokine Array / Chemokine Array -Plex (MD44) from EVE Technologies (Calgary, AB, Canada).

Neurofilament Light Chain Analysis

Neurofilament Light Chain (NfL) was measured in mouse serum diluted 1:8. NfL was measured using Simoa technology by Dr. Ronald Booth and the Eastern Ontario Regional Laboratory Association (EORLA) located at The Ottawa Hospital (Ottawa, ON, Canada).

Tissue Preparation: Immunohistochemistry

Mice were euthanized and perfused with PBS. Hemibrains were fixed in 10% formalin for 48 hours and then paraffin-embedded. Blocks were cut into 5μm sections starting from the midline and mounted onto slides.

Immunohistochemistry

Slides were deparaffinized in Citrisolv (Decon Labs, Inc.) and rehydrated through a series of decreasing ethanol concentrations. Endogenous peroxidase activity was quenched with 0.3% hydrogen peroxide in methanol, followed by heat-induced antigen retrieval with citrate buffer, pH 6.0. To block non-specific binding, slides were incubated in 10% goat serum (Vector Laboratories) for 30 minutes at room temperature. Sections were incubated overnight at 4°C in primary antibodies. Primary antibodies used: anti-Iba1 (1:2000) (Wako, 019-19741) and anti-cleaved caspase-3 (1:1500) (Cell Signalling, 96645). Biotinylated, secondary antibody anti-mouse or anti-rabbit IgG (H + L), made in goat (Vector Labs, BA-9200 or BA-1000) was diluted to 1:225, and sections were incubated for 90 minutes at room temperature. The signal was amplified with VECTASTAIN® Elite® ABC HRP Kit (Vector Labs) for 90 minutes at room temperature and visualized using 3'3-diaminobenzidine (Sigma). Samples were counterstained with Harris' Modified Hematoxylin stain and dehydrated through a series of increasing ethanol concentration solutions and Citrisolv. Permount Mounting Medium (Fisher Scientific) was used for mounting, and developed slides were dried before visualization.

Quantification of Microglial Morphological Parameters

Fiji (ImageJ 2) version 2.14.0 was used to analyze and quantify Z-stack images generated from scanning the stained slides utilizing an axioscanner at x20 at Louise Pelletier Histology Core. The computational protocol for analyzing microglial phenotype in brain sections can be found on protocols.io: Zahr Eddin (2024), Fiji-based quantification of glial parameters from IHC-stained mouse brain sections.

ELISA Quantification of α-Synuclein and Tau

Lysates were measured for total α-synuclein using sandwich ELISA as described previously (Shutinoski et. al., 2019; Mollenhauer et al., 2008). α-Synuclein protein concentrations were normalized to total protein concentration. Total murine tau protein abundance was measured with the Tau (Total) Mouse ELISA Kit (KMB7011, Invitrogen).

Western Blotting

Protein samples (40µg) were combined with 1X NuPAGE™ LDS Sample Buffer (NP0007, Thermo Fisher Scientific), boiled for 5 minutes at 95-100°C, and then electrophoresed under reducing (5% β-mercaptoethanol) conditions on 4-12% gradient SDS gels in MES buffer. Gels were then transferred to a PVDF membrane using a standard semi-dry transfer in TRIS-glycine-Methanol buffer. The following antibodies were used: anti-actin (sc-81178, Santa Cruz; 1:1000 in 5% milk), anti-phospho-tau (Ser202, Thr205) monoclonal antibody (AT8) (MN1020, Thermo Fisher Scientific, 1:500 in 5% milk), anti-nitrotyrosine (9691S, Cell Signalling), and anti-total tau a.a. 210-241 (MAB361, EMD Millipore). All Western blots were imaged using BioRad ChemiDoc Imager and densitometric based signal quantification was done using Image Lab (version 6.1.0)

(2020 BioRad Labratories, Inc.). For Western blotting of nitrotyrosination, 75µg protein samples were prepared and run under non-reducing conditions. These were imaged using film and densitometric analyses was done via ImageJ. Nitrotyrosine blots were normalized to Ponceau S staining for total protein.

Quantification of Reactive Oxygen Species

For H_2O_2 quantification in tissues, Amplex® red hydrogen peroxide/peroxidase assay kit (Invitrogen, A22188) was used to monitor endogenous production of H_2O_2. Hemibrain were lysed in PBS, as described above. Homogenate samples were then diluted in assay reaction buffer 1:10. A serial dilution of the H_2O_2 standard provided was prepared (20, 10, 2 and 0 µM). 50 µL of standards and samples were plated in a 96 well black plate with clear flat bottom. The reaction was started by the addition of 50µL working solution which consist of 1x reaction buffer, Amplex® red and horseradish peroxidase. The plate was incubated at room temperature for 30 minutes protected from light. A microplate reader was used to measure absorbance at 560 nm. The obtained H_2O_2 levels (µM) were normalized to the tissue weight (g).

Statistical Analyses

All statistical analyses were performed using GraphPad Prism version 8 (GraphPad Software, San Diego, CA, USA, www.graphpad.com). Differences between groups in survival assays were assessed using the log- rank (Mantel-Cox) test. Differences between groups of three or more were assessed using one-way ANOVA with Tukey's post-hoc tests. Differences between two groups were assessed using unpaired student t-test. Data are shown as mean ± SEM where applicable and

as described in the figure legends. Data are displayed with *P* values represented as $*P < 0.05$, $**P < 0.01$, $***P < 0.001$.

Results

Lrrk2 p.G2019S female mice are worse off following a neurotropic VSV infection, but not as a result of a pneumotropic H1N1 infection.

To better understand the role of Lrrk2 in host responses against viral infections, we sought to identify the effects of two distinct RNA viruses on disease outcomes in a Lrrk2 p.G2019S mouse. We first employed VSV, a neurotropic virus, which causes fatal encephalitis as the cause of death (**Fig. 3.1**). Adult mice aged 8-10 weeks were nasally infected with a previously established LD_{50} dose ($3x10^3$ PFU) in wild-type mice in a cohort of combined sexes. Survival and weight (as a proxy of disease severity) were measured daily for 14dpi, in both female (**Fig. 3.1a, b**) and male (**Fig. 3.1c, d**) mice. We identified a significant survival difference in female mice, whereby Lrrk2 p.G2019S homozygous mice had higher mortality than both heterozygous and wild-type mice ($P < 0.05$). No difference in survival rates was identified in male Lrrk2 p.G2019S mice. We observed an overall sex bias in survival following VSV infection, male wild-type mice showed a survival rate of ~50% at this dose whereas female wild-type mice showed an increased survival rate of ~80%; which is consistent with other findings in our lab (Lunn, Hake-Volling, *in prep*). Interestingly, Lrrk2 p.G2019S homozygous female mice had the same survival rate as all male mice, suggesting that at least one wild-type allele in female mice may confer protection against VSV infection.

We next measured viral titre in the brain, to identify whether the increased mortality in female Lrrk2 p.G2019S mice was linked to a higher viral burden during the timepoint of peak

sickness, 6dpi (**Fig. 3.1e**). There was no difference in viral titre between any groups, therefore suggesting that viral titre alone is not linked to the increased mortality seen in the Lrrk2 p.G2019S female mice. Next, we measured viral titre in whole brains collected from moribund mice to investigate whether the viral titre required at time of death differed between genotypes (**Fig. 3.1f**). We did not identify any significant differences between groups; however, there was increased variance in the viral titre at time of death (based on moribund state) in carriers of the Lrrk2 p.G2019S allele than in wild-type mice.

To study the role of Lrrk2 principally in the periphery, we next employed a non-neurotropic virus in Lrrk2 p.G2019S mice (**Fig. 3.2**). Influenza A virus, serotype H1N1 has lung tropism and can cause fatal pneumonitis in mice at specific doses. Notably, Lrrk2 is highly expressed in the lungs (Shutinoski et al., 2019; Herzig et al., 2011). Adult mice aged 4-6 weeks were nasally infected with a previously established LD_{50} dose ($2x10^3$ PFU), and survival and weight were measured for 14dpi in female (**Fig. 3.2a, b**) and male (**Fig 3.2c, d**) mice. In contrast to the VSV infection, we did not identify any differences between genotypes in the survival rates of these mice. However, female mice had overall higher mortality than male mice, which is consistent with previous reports for this mouse strain (Sabikunnahar et al., 2022). Similarly, there were no significant differences between genotypes in initial weight loss or subsequent weight gain across genotypes. To further probe the acute outcomes of H1N1 infection, we measured the viral titre in the lungs at the peak of viral infection, 3dpi (**Fig. 3.2e**), and saw no differences between genotypes.

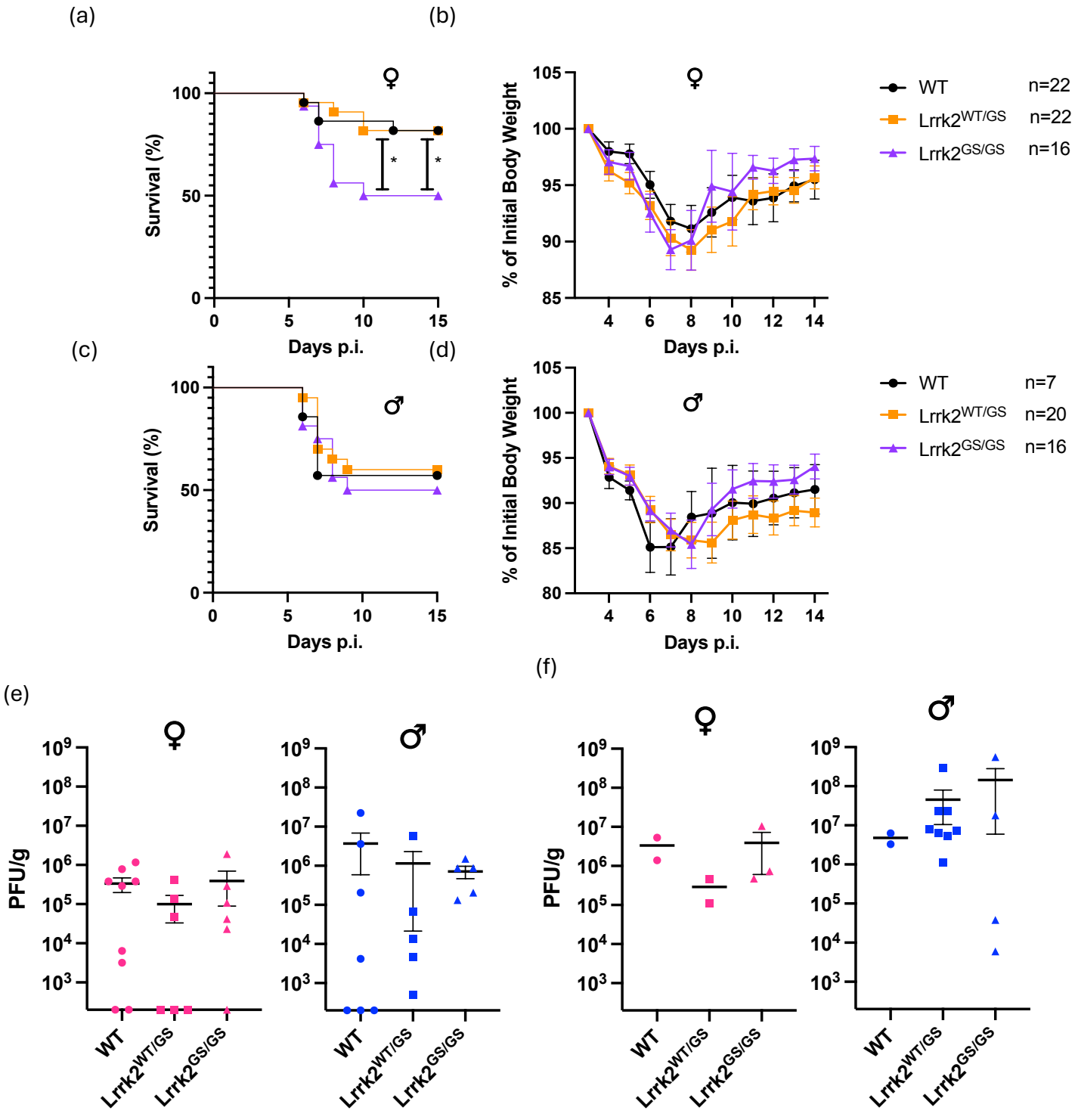


Fig. 3.1: Homozygous Female Lrrk2 p.G2019S Knock-in Mice Lose Sex-Specific Survival Benefit from Encephalitis Following Nasal Inoculation with Vesicular Stomatitis Virus. Adult mice (8-10 weeks) were nasally inoculated with a dose of $3x10^3$ PFU of vesicular stomatitis virus (VSV) and monitored daily for a predetermined moribund state to measure survival,

including weight (**a-d**) or sacrificed at 6 days post inoculation (p.i.) to measure viral titres in the brain (**e**). Survival is displayed as percent survival against days p.i. (**a, c**); weights are shown in percent of initial body weight against days p.i. (**b, d**). All data sets are separated for female mice (**a, b**) and male mice (**c, d**). Number of animals for each genotype in survival analyses is as indicated. Viral titres were measured in the brain at 3dpi (**e**) or in brains collected at time of humane endpoint (**f**) via plaque assay, where each symbol represents one animal. Error bars represent mean ± SEM. Statistical tests used: log rank (Mantel-Cox) test for survival curves; one-way ANOVA for viral titre analysis. P-value <0.05 (*).

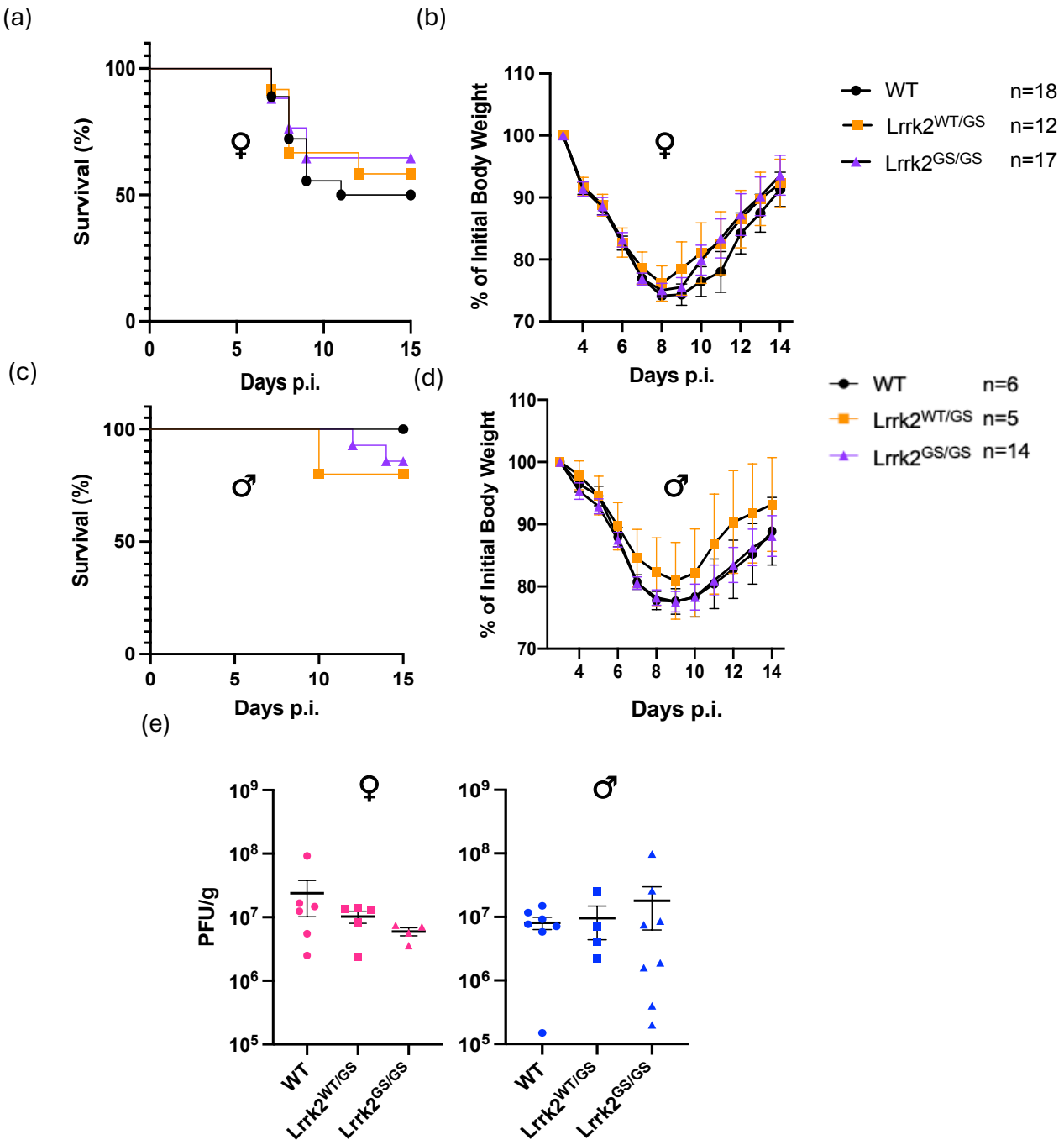


Fig. 3.2: Expression of *Lrrk2* p.G2019S Knock-in Alleles Does Not Alter Survival, Weight Change, or Viral Titres in the Lungs of Mice Nasally Inoculated with Influenza Virus, H1N1. Adult mice (5-7 weeks) were nasally inoculated with a dose of $2x10^3$ PFU of influenza A virus (serotype H1N1) and monitored for a predetermined moribund state to measure survival and weight (**a-d**) or sacrificed at 2 days post inoculation (p.i.) to measure viral titres in the lungs (**e**). Survival is graphically displayed as percent survival against days p.i. (**a, c**), and weights are shown as percent of initial body weight against days p.i. (**b, d**). All data sets are separated for female mice (**a, b**) and male mice (**c, d**). Number of animals for each genotype in survival analyses is as

indicated. Viral titres were measured in the lung (**e**) at 2dpi via plaque assay, where each symbol represents one animal. Error bars represent mean ± SEM. Statistical tests used: log rank (Mantel-Cox) test for survival curves; one-way ANOVA for viral titre. No significant differences were found.

Wild-type Lrrk2 kinase activity is not required for host defences against VSV or H1N1 infection. Given that the Lrrk2 hyper-kinase mutant, p.G2019S, caused homozygous female mice to be worse off in the context of VSV infection, we next employed this infection model in mice harboring the Lrrk2 kinase-dead mutation, p.D1994S; this, to test whether the observed phenotype was Lrrk2 kinase-specific (**Fig. 3.3**). We found that both male and female Lrrk2 p.D1994S homozygous and heterozygous mice had the same survival rate as wild-type mice following VSV infection (**Fig. 3.3a-d**). Similarly, loss of Lrrk2 kinase activity did not alter survival outcomes following H1N1 infection (**Fig. 3.3e-h**). These data suggested that wild-type Lrrk2 kinase activity was not essential in host responses against VSV or H1N1 infections and suggested a (toxic) gain-of-function role for the *Lrrk2* p.G2019S hyper-kinase mutation to underlie the lesser VSV survival response.

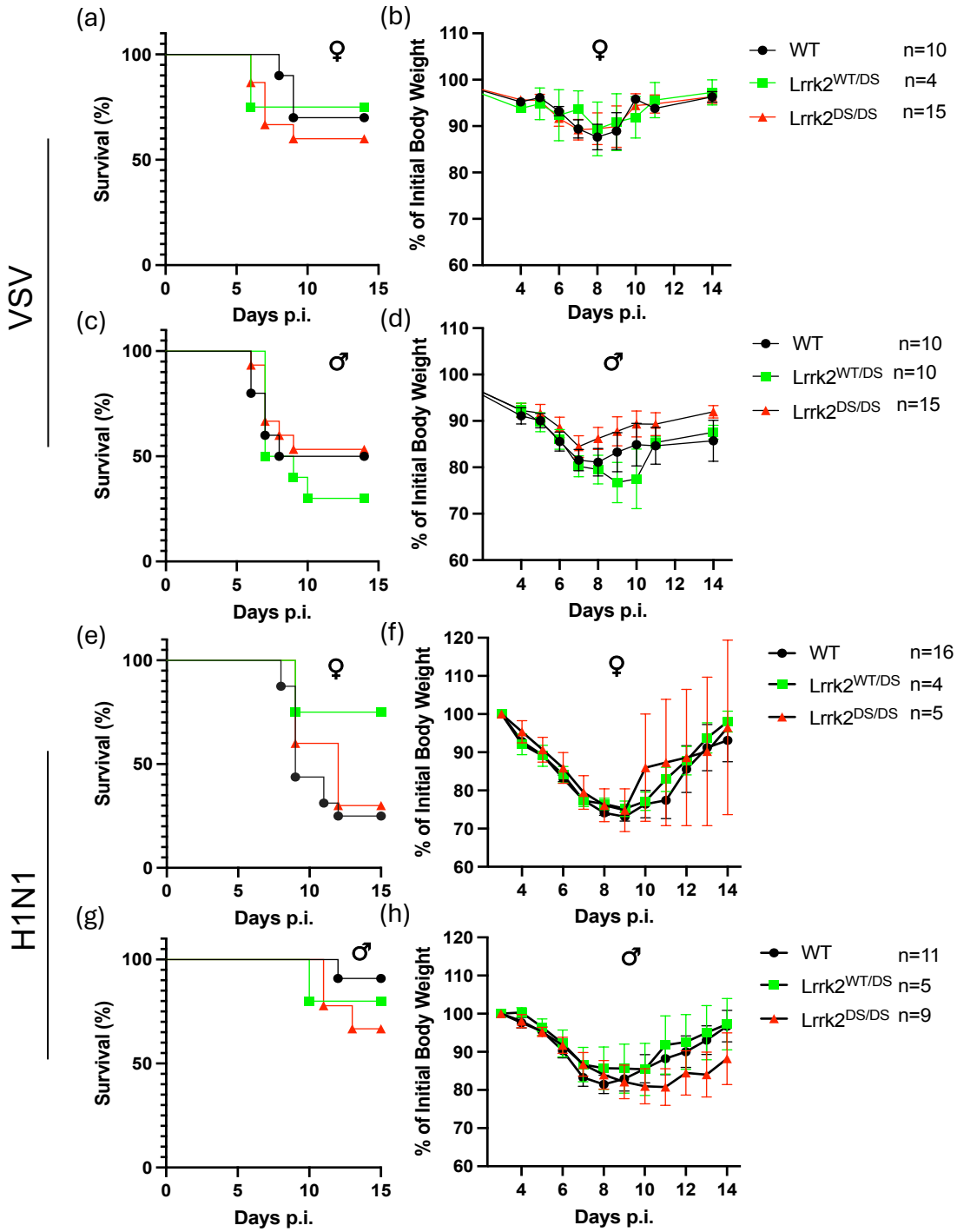


Fig. 3.3: Mice Expressing Kinase-Dead *Lrrk2* p.D1994S-Knock-in Alleles Show the Same Survival Rates as Wild-type Mice After Nasal Inoculation with VSV or H1N1. Adult mice were nasally inoculated with either a dose of $3x10^3$ PFU of VSV (**a-d**) or a dose of $2x10^3$ PFU of influenza A virus (serotype H1N1) (**e-h**), as in Figs. 1 and 2, and monitored daily for a pre-determined moribund state. Survival is graphically displayed in percent survival against days post inoculation (p.i.) with VSV (**a, c**) or with H1N1 (**e, g**); weights are displayed as percent of initial

body weight against days p.i. for VSV (**b, d**) and H1N1 (**f, h**). All data sets are separated for female mice (**a, b, e, f**) and male mice (**c, d, g, h**). Sample sizes for each genotype are as indicated. Error bars represent mean ± SEM. Statistical test used: log rank (Mantel-Cox) test for survival curves. No significant differences were found.

Lrrk2 p.G2019S mice have the same cytokine and chemokine profile as wild-type mice following VSV infection.

As we observed a significant detrimental effect of the Lrrk2 p.G2019S mutation on survival outcomes following nasal VSV infection in female mice, we next investigated several potential underlying causes. We posited that an altered inflammatory response may be contributing to the survival phenotype. Hence, we measured the abundance of 44 cytokines and chemokines using multiplex ELISA in the sera and brain homogenates of VSV-infected mice at 6dpi. Four cytokines of interest are presented in **Fig. 3.4**, constituting three pro-inflammatory cytokines (IL-6, TNF-α, IL-1β) and one anti-inflammatory cytokine (IL-10). The remainder of the analyzed cytokines can be found in **Suppl. Fig. 3.1** (data from brain homogenates) and in **Suppl. Fig. 3.2** (data from sera). In both brain homogenates (**Fig. 3.4a**) and sera (**Fig. 3.4b**), we did not identify any significant differences between wild-type and Lrrk2 p.G2019S heterozygous or homozygous mice, in male or female mice. However, we did identify a significant sex difference in IL-6, whereby male Lrrk2 p.G2019S mice had significantly higher levels of the pro-inflammatory marker in their sera than female Lrrk2 p.G2019S mice ($P = 0.0471$).

We next asked whether Lrrk2 p.G2019S female mice had more severe neuronal damage due to the CNS infection than their wild-type littermates. We therefore quantified neurofilament light chain (NfL) in the sera of mock-inoculated and VSV-infected mice at 6dpi (**Fig. 3.4c**). NfL is a cytoskeletal component that is found exclusively in the axons of neurons, and therefore, the presence of NfL in peripheral sera is an indicator of neuroaxonal damage (Dietmann et al., 2023). We did not identify any significant infection- or genotype-dependent differences, even when pooling all mock samples and all VSV-infected samples independent of genotype, indicating that NfL did not appear at detectable levels yet in sera in response to VSV infection at 6dpi (data not

shown). Taken together, these data suggested the NfL-linked neuronal damage was not a driver for the observed survival differences in VSV-induced encephalitis.

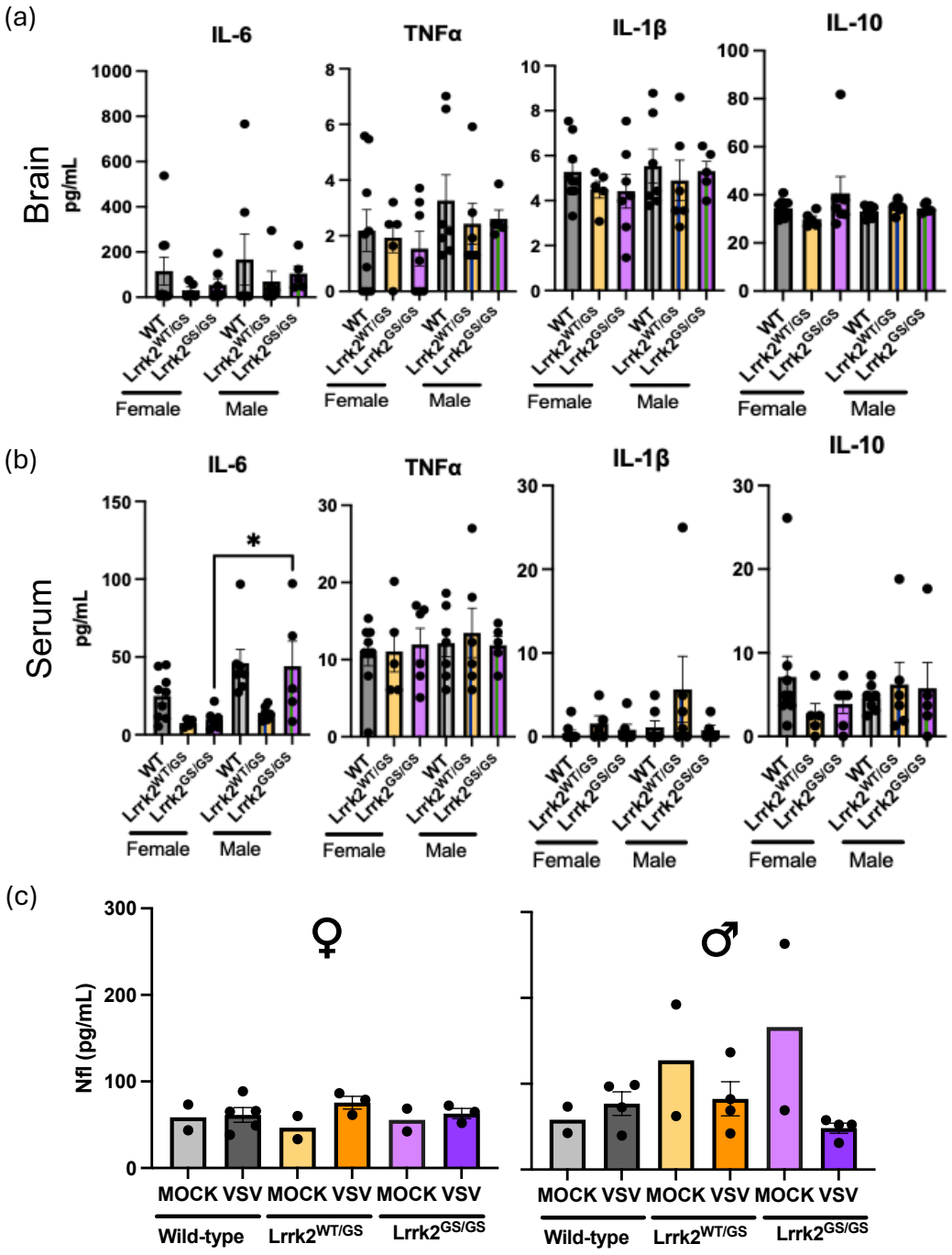


Fig. 3.4: *Lrrk2* p.G2019S Knock-In Allele-Expressing Mice Do Not Show Altered Cytokine Signalling in the Brain or Serum or Detectable Neurofilament Difference in the Serum When Compared to Wild-type Mice Following VSV Infection. Adult mice (8-10 weeks) were nasally inoculated with a dose of $3x10^3$ PFU of VSV and sacrificed at 6 days post inoculation. Multiplex ELISA was used to measure an array of cytokines and chemokines from brain homogenates (**a**) and sera (**b**). Four cytokines of interest are presented here (for other cytokine / chemokine results, see **Suppl. Data**). Neurofilament light chain (Nfl) protein abundance was measured via ELISA in

sera (**c**). Data are presented separately for female mice (♀) and male mice (♂). Each data point represents one biological replicate. Error bars represent mean ± SEM. Statistical test used: one-way ANOVA with Tukey's post hoc tests. P-value <0.05 (*).

Female Lrrk2 p.G2019S mice show reduced microglial responses to VSV infection in the olfactory bulb.

As we observed no significant changes in the previous readouts in the brains of female Lrrk2 mutant, VSV-infected mice at 6dpi, we next investigated the brains and cellular responses using immunohistochemical analyses. With a sample size of n=7-9 per genotypic group, we first measured the level of microglial activation state in these samples using the well-established microglial marker, Iba1 (**Fig. 3.5, 3.6, 3.7**). From Iba1-stained brain slides, we quantified three properties of microglial morphology across four different brain regions: their average size (**Fig. 3.6a, d**), percent area positive for Iba1 (**Fig. 3.6b, e**), and microglia perimeter (**Fig. 3.6c, f**); these parameters were measured in the olfactory bulb (OB) (**Fig. 3.5, 3.6**), the hypothalamus (**Fig. 3.7a**), the hippocampus (**Fig. 3.8b**), and the occipital lobe of the cortex (**Fig. 3c**) in each mouse. These four regions were chosen as we identified positive Iba1- and VSV-staining in these regions at this time point in our previous studies (data not shown).

Iba1 immunoreactivity was most prominent in the OB (**Fig. 3.5**); therefore, we probed the quantification dataset further for sex differences (**Fig. 3.6**). We first pooled genotypes for mock- and VSV-infected samples, where we identified a significant infection-dependent rise in microglial activation in all readouts, as expected ($P < 0.01$; **Fig. 3.6a-c**). Notably, the infection-dependent increase in all three readouts was significant in male Lrrk2 p.G2019S mice ($P < 0.05$) and trended towards increase in both male and female wild-type mice. In contrast, female Lrrk2 p.G2019S mice had the least amount of microgliosis following VSV infection in their OBs, as indicated by a lack of increase in the VSV-infected mice in each of the parameters quantified.

When quantifying Iba1 immunoreactivity in the remaining brain regions of interest, we did not identify significant differences across the genotype or treatment groups in size of the microglia,

percent area occupied of Iba1 staining, or perimeter in the hypothalamus (**Fig. 3.7a**), the hippocampus (**Fig. 3.7b**), or the occipital lobe of the cortex (**Fig. 3.7c**). However, we observed a slight trend towards an infection-dependent rise in the percent area that was positive for Iba1 signalling in all three regions.

Next, we measured cleaved caspase-3 (CC3) (**Fig. 3.8**) in the OB as a marker of programmed apoptosis and a strong indicator of cell death induction. We observed a VSV infection-dependent effect on CC3 immunoreactivity in infected samples and lack of staining in mock-treated animals, as expected (**Fig. 3.8a-h**). The percent area of positive CC3 staining was quantified and analyzed. Pooling samples based on mock- or VSV-infection independent of genotype or sex identified a significant increase in CC3 reactivity upon VSV infection ($P < 0.001$; **Fig 3.8i**). We separated the data based on genotypes into female (**Fig. 3.8j**) and male mice (**Fig. 3.8k**) and found that the VSV-dependent increase in CC3 was significantly increased in male Lrrk2 p.G2019S mutant animals, but not in female mutants ($P < 0.001$).

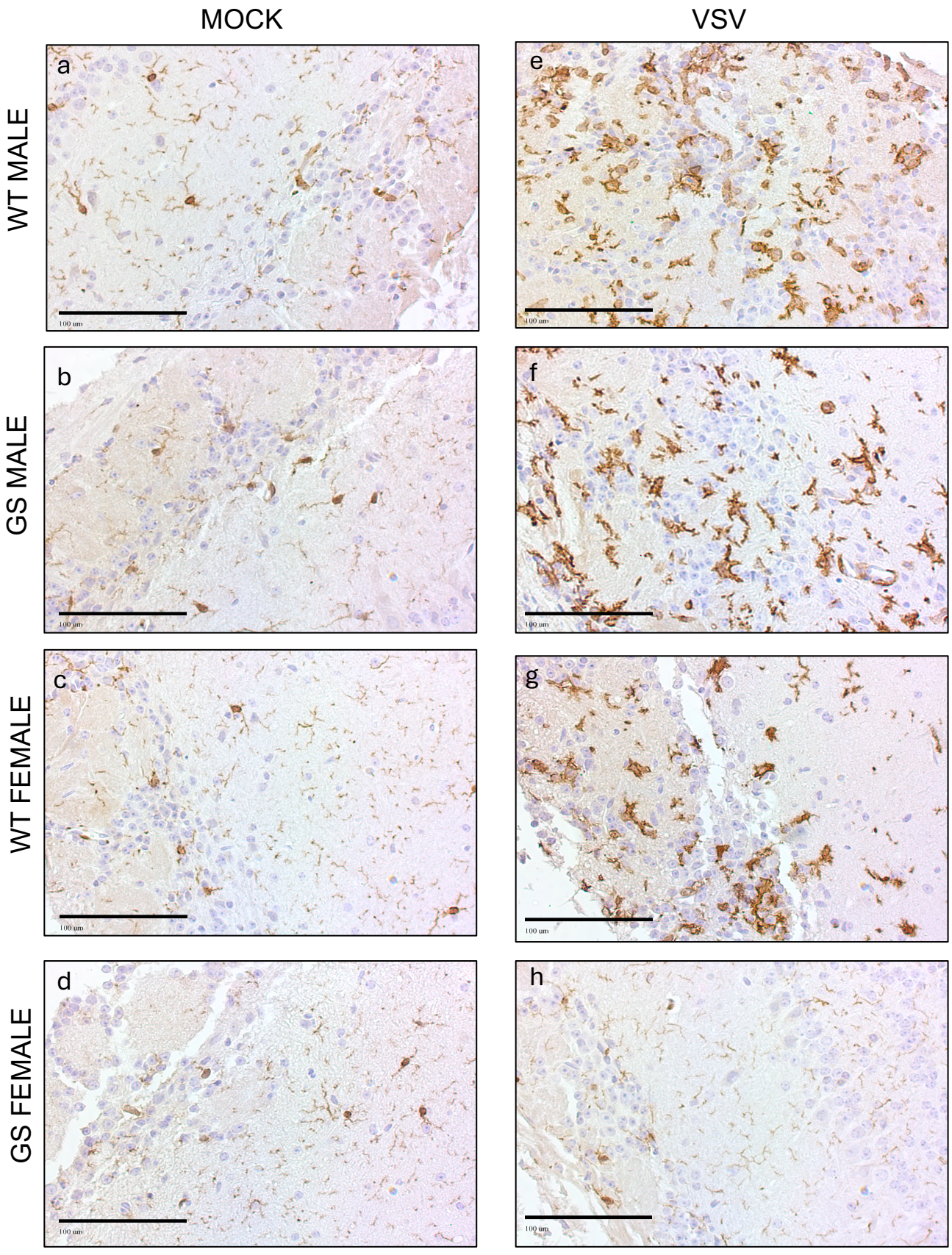

MOCK
VSV
WT MALE
GS MALE
WT FEMALE
GS FEMALE
a
b
c
d
e
f
g
h
100 um

Fig. 3.5: Microscopic Analyses of Microglial Response in Olfactory Bulbs from Mock- and VSV-Infected Wild-type and Homozygous Lrrk2 p.G2019S Knock-in Mice. Adult mice 8-10 weeks) were infected with either $3x10^3$ PFU VSV (VSV) or PBS (MOCK) nasally and sacrificed at 6 days post inoculation. Hemibrains were collected, cut along the sagittal plane, and stained for histological analyses, including with anti-Iba1 and counterstained with hematoxylin. All images shown are from the olfactory bulb at the glomerular layer at 20X magnification. Representative images from mock- (**a-d**) and VSV-infected (**e-h**) mice are shown, for both male and female animals, as indicated. Sample sizes are n=7-9 per genotypic group. Scale bars: length, 100 μm.

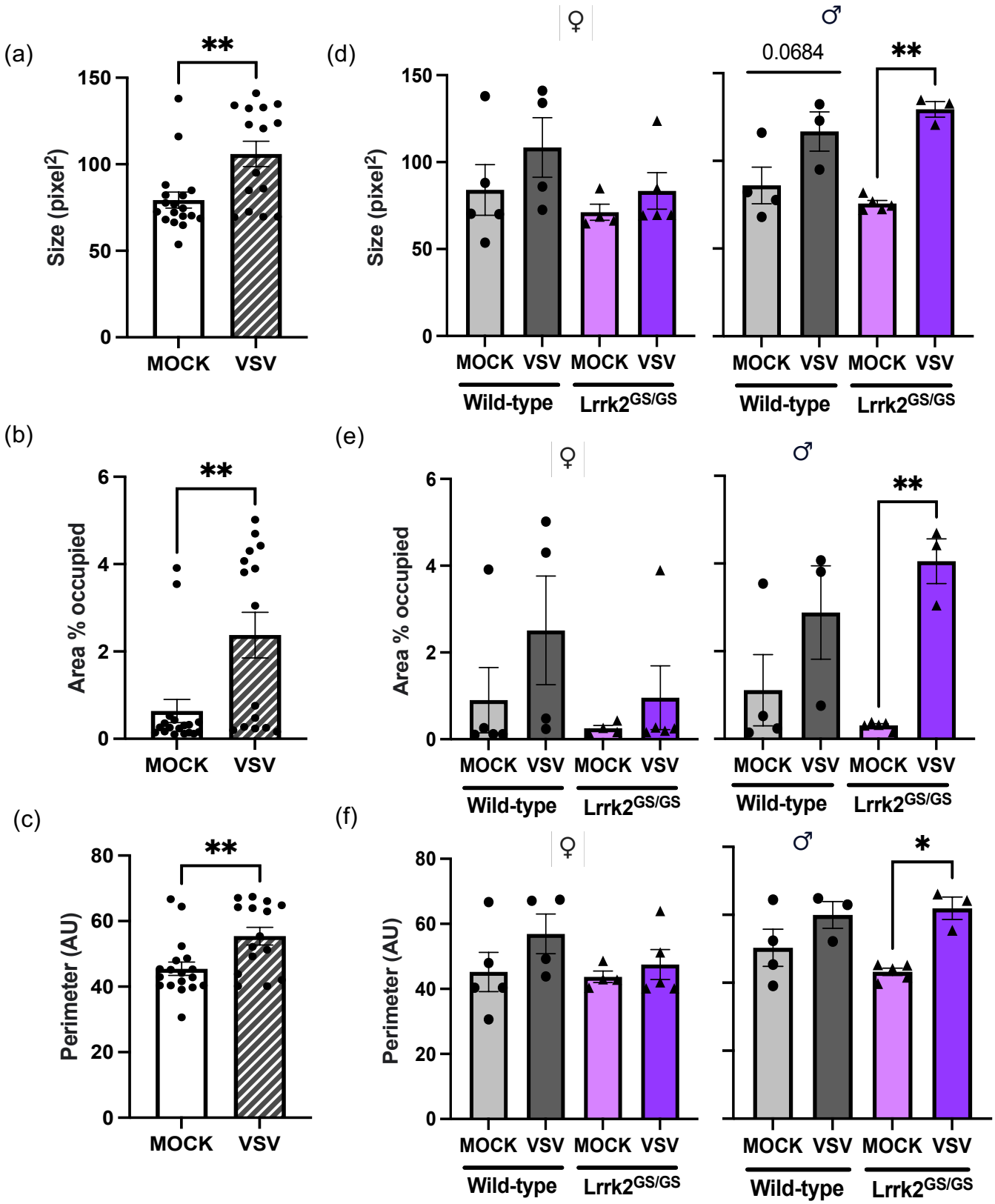

(a)
**
Size (pixel²)
150
100
50
0
MOCK
VSV
(b)
**
Area % occupied
6
4
2
0
MOCK
VSV
(c)
**
Perimeter (AU)
80
60
40
20
0
MOCK
VSV
(d)
♀
♂
0.0684
**
Size (pixel²)
150
100
50
0
MOCK VSV MOCK VSV
Wild-type
Lrrk2GS/GS
MOCK VSV MOCK VSV
Wild-type
Lrrk2GS/GS
(e)
♀
♂
**
Area % occupied
6
4
2
0
MOCK VSV MOCK VSV
Wild-type
Lrrk2GS/GS
MOCK VSV MOCK VSV
Wild-type
Lrrk2GS/GS
(f)
♀
♂
*
Perimeter (AU)
80
60
40
20
0
MOCK VSV MOCK VSV
Wild-type
Lrrk2GS/GS
MOCK VSV MOCK VSV
Wild-type
Lrrk2GS/GS

Fig. 3.6: Quantitative Analysis of Microglial Density and Morphology in Mock- and VSV-Infected Olfactory Bulbs of Wild-type and Homozygous Lrrk2 p.G2019S Knock-in Mice. Adult mice (8-10 weeks) were inoculated with either $3x10^3$ PFU VSV (VSV) or PBS (MOCK) nasally and sacrificed at 6 days post inoculation. Hemibrains were collected, serially sectioned, and stained for histology, including with anti-Iba1. Microscopic image densities of olfactory bulbs were quantified using ImageJ. Data are presented as: (**a, d**) average size of microglia expressed in pixels squared; (**b, e**) by percentage area occupied by microglia within the analyzed region; and (**c, f**) by perimeter of microglial cells measured in arbitrary units. (**a-c**) Both genotypes (wild-type and Lrrk2 p.G2019S mice) were pooled to plot infection-dependent effect. (**d-f**) Data were then separated based on genotype and presented as female samples only (♀) and male samples only (♂). Each data point represents one biological replicate. Sample sizes are n=7-9 per genotype. Statistical analyses used: unpaired student t-test (**a-c**) and ANOVA with Tukey post-hoc tests for (**d-f**). Error bars represent mean ± SEM. P-value <0.05 (*), P-value <0.01 (**).

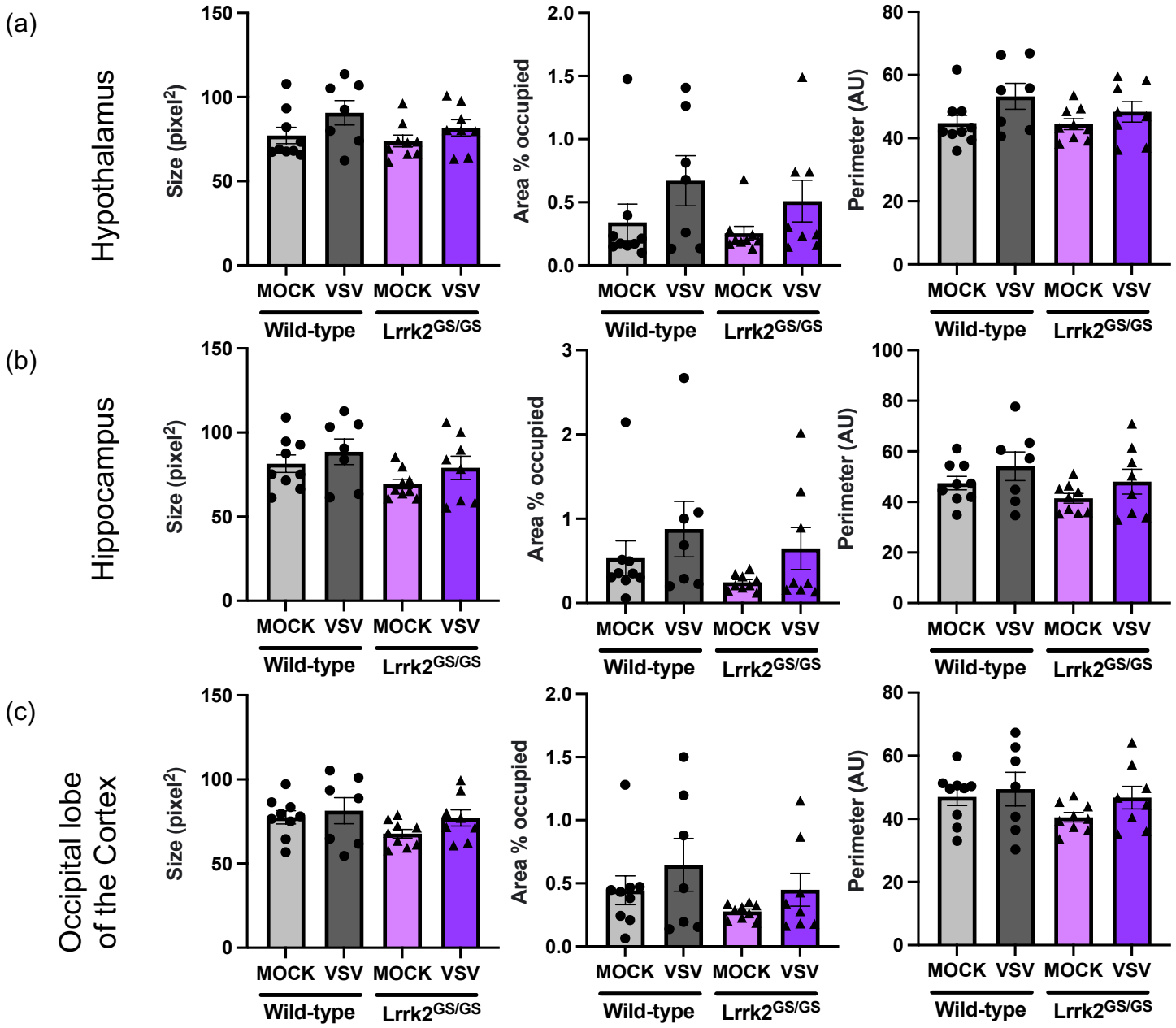


Fig. 3.7: Quantitative Analysis of Microglial Density and Morphology in Mock- and VSV-Infected Brain Regions Other Than the Olfactory Bulb of Wild-type and Homozygous Lrrk2 p.G2019S Knock-in Mice. Adult mice (8-10 weeks) were inoculated with either $3x10^3$ PFU VSV (VSV) or PBS (MOCK) nasally and sacrificed at 6 days post inoculation. Hemibrains were collected, serially sectioned, and stained for histology, including with anti-Iba1. Microscopic image densities of indicated regions were quantified using ImageJ. Quantification is demonstrated in the (**a**) hypothalamus, (**b**) hippocampus, and (**c**) the occipital lobe of the cortex. Data are presented for each as: average size of microglia expressed in pixels squared (first column), percentage area occupied by microglia within the analyzed region (second column), and the perimeter of microglia measured in arbitrary units (third column). Data presented included female and male mice combined. Each data point represents one biological replicate. Sample sizes are

n=7-9 per genotype. Statistical analysis: ANOVA with Tukey post-hoc tests. Error bars represent mean ± SEM. No statistically significant differences were identified between genotypic groups.

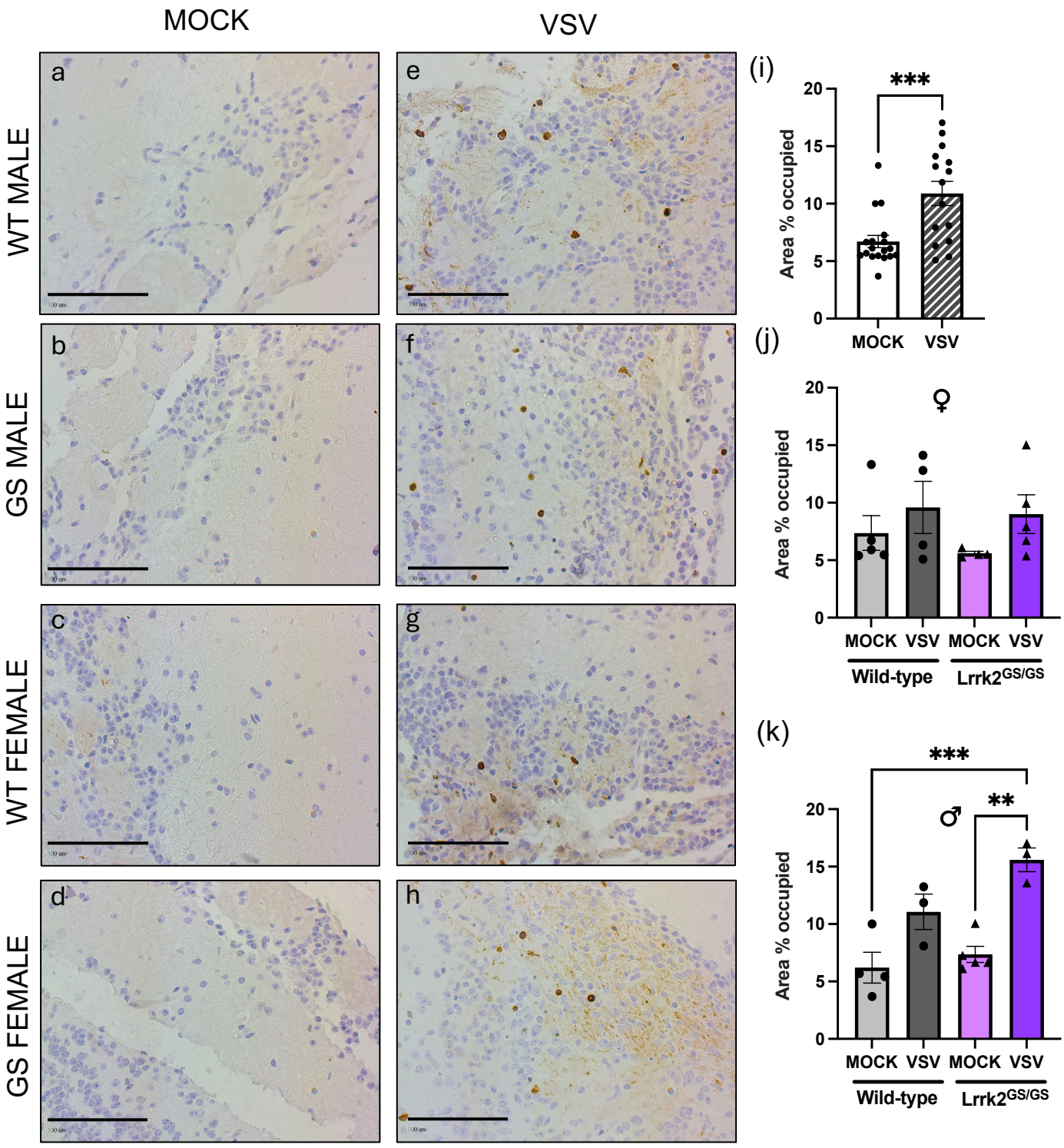


Fig. 3.8: Microscopic Analyses of Cleaved Caspase-3 Reactivity in Olfactory Bulbs from Mock- and VSV-Infected Wild-type and Homozygous Lrrk2 p.G2019S Knock-in Mice. Adult mice (8-10 weeks) were inoculated with either $3x10^3$ PFU VSV (VSV) or PBS (mock) nasally and sacrificed at 6 days post inoculation. Hemibrains were collected, serially sectioned, and stained for histology, including with anti-cleaved caspase-3. All images shown are from the glomerular layer

of the olfactory bulb at 20X magnification. Representative images from mock- (**a-d**) and VSV-infected (**e-h**) mice are presented for both sexes, as indicated. Scale bars: 100 μm. Images were quantified using ImageJ. Data are presented as percentage area occupied by positive cleaved caspase-3 staining with all genotypes pooled (**i**) and when separated based on genotype and sex in female mice (**j**) and male mice (**k**). Each data point represents one biological replicate. Sample sizes are n=7-9 per genotypic group. Statistical analyses: unpaired student t-test (**i**) and ANOVA with Tukey post-hoc tests for (**j, k**). Error bars represent mean ± SEM. P-value <0.05 (*), P-value <0.01 (**), P-value<0.001 (***).

Infections with neurotropic VSV or non-neurotropic H1N1 lead to sustained elevated oxidative stress in adult mice six weeks post inoculation.

We next explored the long-term impact of both viruses on the brains of surviving mice and any potential consequence of Lrrk2 p.G2019S mutation on chronic outcomes. To study this, all mice that survived either the VSV or H1N1 infection (survival being determined as living to 14dpi) were aged for four additional weeks, to a total of 6wpi.

We first measured the levels of oxidative stress in the brain (**Fig. 3.9a-e**). The abundance of H_2O_2 in brain homogenates from VSV- or H1N1-infected surviving mice was quantified using the Amplex® Red assay. In VSV-infected mice, there was a significant, infection-dependent increase in H_2O_2 abundance in the brain when comparing all genotypes pooled ($P < 0.05$; **Fig. 3.9a**). When we separated these data based on genotype, the Lrrk2 p.G2019S mice showed significantly higher levels than their mock-treated littermates ($P < 0.05$; **Fig. 3.9b**). Of note, when separating these data based on sex, the power for significance was lost.

Notably, when measuring H_2O_2 abundance in the brains of H1N1-infected mice, we continued to see a significant infection-dependent rise ($P < 0.001$; **Fig. 3.9c, d**), even though H1N1 does not infect the brain directly. While the increase of H_2O_2 levels following H1N1-infection was only significant in wild-type mice, a strong trend in Lrrk2 p.G2019S mice persisted ($P < 0.05$; **Fig. 3.9d**). Lastly, we measured levels of H_2O_2 in H1N1-infected Lrrk2 kinase-dead p.D1994S mice at 6wpi (**Fig. 3.9e**). Again, we found again that H_2O_2 was significantly elevated in wild-type animals following H1N1-infection, but not in Lrrk2 p.D1994S mutant mice ($P < 0.05$).

As a secondary measurement of oxidative stress, we investigated protein nitrotyrosination in protein extracts from the brains of 6wpi VSV- or H1N1-infected brains (**Fig. 3.9f-k**). In contrast to H_2O_2 abundance, which is a reversible form of oxidative stress, protein nitrotyrosination is a

measurement of irreversible oxidative stress (Bandookwala and Sengupta 2020). Using Western blotting and densitometric analyses, we first measured protein nitrotyrosination in female (**Fig. 3.9g**) and male (**Fig. 3.9h**) mice inoculated with either PBS (mock) or VSV. Surprisingly, female wild-type mice had a significant decrease in the amount of protein nitrotyrosination following infection, which was not seen in Lrrk2 p.G2019S female mice or in male mice infected with VSV ($P < 0.05$; **Fig. 3.9g, h**). Of note, we did not observe any significant difference in protein nitrotyrosination following VSV infection when pooling all genotypes (**Fig. 3.9f**). In contrast, in brain protein extracts from mice infected with H1N1, we identified a significant infection-dependent increase in protein nitrotyrosination when pooling all genotypes ($P < 0.001$; **Fig. 3.9i**). When the data were separated based on genotypes, we found the significant increase in protein nitrotyrosination occurred in male Lrrk2 p.G2019S mice specifically ($P < 0.05$; **Fig. 3.9k**); further, a strong trend for increase in protein nitrotyrosination following infection was seen in both wild-type and Lrrk2 p.G2019S mutant female mice (**Fig. 3.9j**). We concluded from these results that viral infections may have variable effects on chronic oxidative stress markers in the brain, which are influenced by the sex and genotype of the host.

α-Synuclein protein levels are decreased following VSV infection in Lrrk2 p.G2019S mice; but increased following H1N1 infection in all mice.

We next examined whether these viral infections could also alter the levels of α-synuclein in adult animals (**Fig. 3.9l-p**), as we had previously seen a Lrrk2 p.G2019S-dependent increase in α-synuclein concentration in the brains of nasally-reovirus T3D-infected, newborn mice (Shutinoski et al., 2019). Unexpectedly, we found that the concentrations of both soluble and insoluble α-synuclein proteins were significantly decreased in the brain at 6wpi following VSV-infection ($P <$

0.001; **Fig 3.9l**) *vs*. mock-treated mice, as measured in both fractions by an established sandwich ELISA (**Fig. 3.9m, n**). When these data were separated based on sex, significance remained in male mice, but not in female mice ($P < 0.05$; male data presented in **Fig. 3.9o**; non-significant female data not shown).

In contrast and unexpectedly, we detected a significant increase in total, soluble α-synuclein in the brains of mice that had survived an H1N1 infection to 6wpi, when all genotypes were pooled ($P < 0.05$; **Fig. 3.9p**). This significance was lost when we separated the data based on individual genotypes, or by sex (**Fig. 3.9q**; data not shown). These data suggested that CNS-based and peripheral infections can dynamically affect steady-states of α-synuclein in surviving animals.

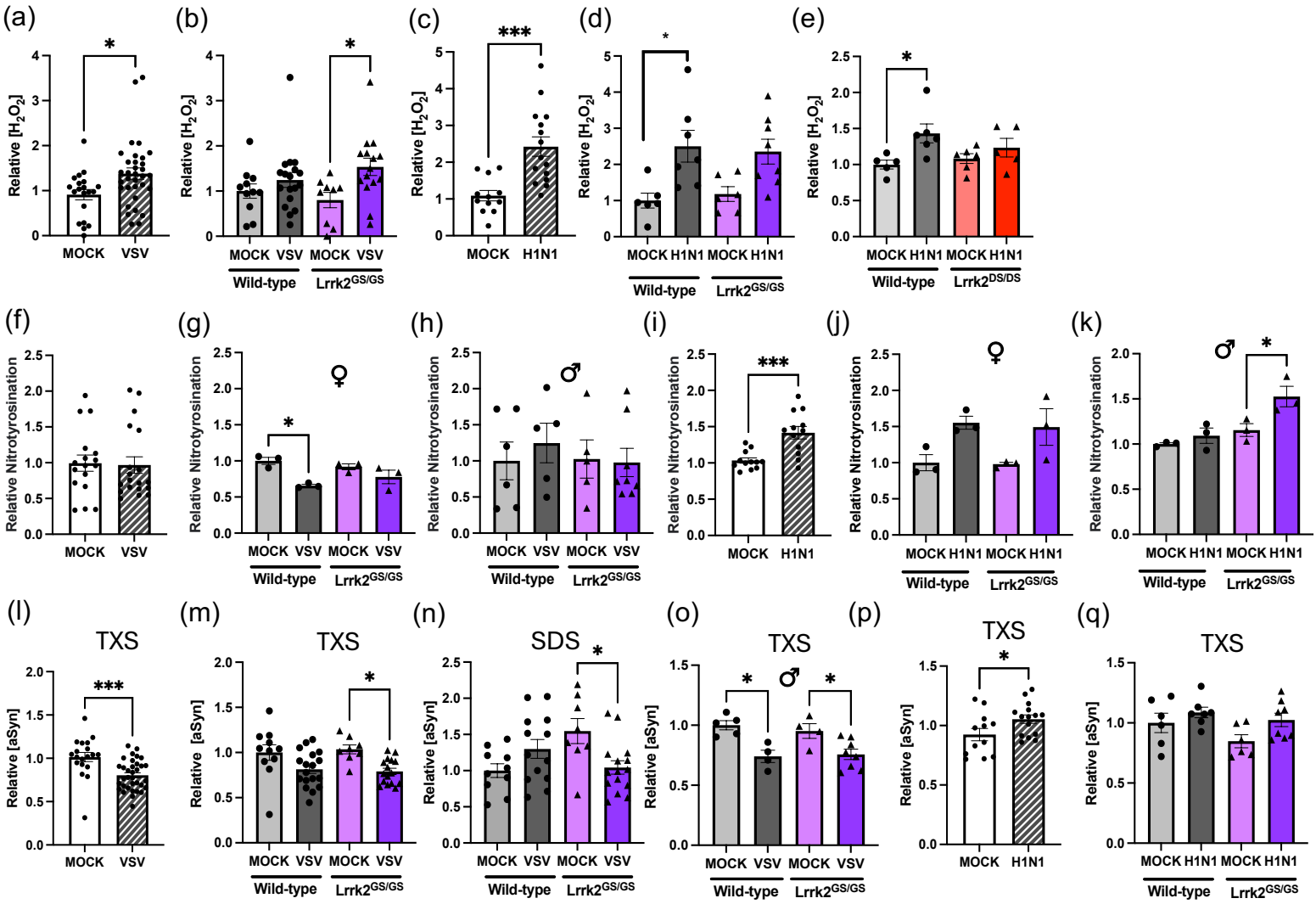


Fig. 3.9: Adult Mice that Survived a VSV or H1N1 Infection Show Changes in Oxidative Stress Markers and α-Synuclein Abundance at 6 Weeks Post Inoculation. Mice were either nasally inoculated with $3x10^3$ PFU vesicular stomatitis virus (VSV; **a, b, f-h, l-o**) or $2x10^3$ PFU of influenza A virus (serotype H1N1; **c-e, i-k, p, q**) and monitored for a predetermined moribund state. Mice that survived past 14 days post inoculation were aged for an additional 4 weeks. Brains were then collected for biochemical analyses. Brain homogenates were tested with Amplex® Red assay to measure H_2O_2 levels (**a-e**). Data are presented as a ratio of concentration of H_2O_2 to the tissue weight, where each symbol represents one animal for VSV-infected mice with genotypes pooled (**a**) or separated by genotype, i.e., WT *vs.* homozygous Lrrk2 p.G2019S knock-in mutant (**b**), H1N1-infected mice with genotypes pooled (**c**), or separated by genotype (**d**), and H1N1-infected mice that included homozygous Lrrk2 p.D1994S mutant animals (**e**). Total protein nitrotyrosination in hemibrains was measured on non-reducing Western blots and quantified by ImageJ (**f-k**). Total protein nitrotyrosination was normalized to Ponceau S and presented for VSV-infected mice with genotypes pooled (**f**) or separated by genotype and sex (**g, h**), as well as for H1N1-infected mice with genotypes pooled (**i**) or separated by genotype and sex (**j, k**). α-Synuclein protein concentrations were measured in brain samples via ELISA in 1% Triton X

extracts (**l, m, o, p, q**) and their pellets (2% SDS; **n**). Data are presented for TXS-extracted samples from VSV-infected mice with genotypes pooled (**l**) or separated based on genotype (**m**) as well as in SDS-extracted samples from VSV-infected mice separated by genotype (**n**). TXS-extracted VSV-infected samples for males only is displayed (**o**). TXS-extracted samples from H1N1-infected mice are shown with genotypes pooled (**p**) or separated by genotype (**q**). Each symbol represents one animal. Data sets are separated by female (♀) and male (♂) samples, as indicated. For every panel, all data are normalized to wild-type mock arms. Statistical analysis: ANOVA with Tukey post-hoc tests. Error bars represent mean ± SEM. P-value <0.05 (*), P-value<0.001 (***).

Viral infections with either VSV or H1N1 lead to increased tau phosphorylation in murine brain at 6 weeks post inoculation.

The observed brain pathology in Lrrk2-linked cases of Parkinson's disease is variable and includes both hallmark α-synuclein aggregates, phospho-tau-linked pathology, a paucity of inclusions, or mixed pathologies respectively (Kalia et al., 2015; Henderson et al., 2019). In this context, we next measured the abundance of total tau protein and phosphorylated tau protein (Ser202, Thr205: AT8) in murine brains of 6wpi surviving mice after either VSV or H1N1 infections (**Fig. 3.10**), using a combination of Western blotting and ELISA-based assays. There, we found that phosphorylated tau (p-Tau) protein was increased in VSV-infected brain tissue compared to mock-treated specimens ($P < 0.001$; **Fig. 3.10a, b**); this rise was significant in Lrrk2 p.G2019S mice ($P < 0.01$; **Fig. 3.10c**). A total tau ELISA was performed, which revealed no differences between treatment groups in the abundance of total tau protein; therefore, the rise in p-Tau following infection was not attributed to a rise in total tau protein (**Fig. 3.10d**). Of note, when these data (p-Tau and total tau levels) were separated based on sex, the power for significance was lost.

Compellingly, this rise in p-Tau in the brain at 6wpi was also observed in H1N1-infected animals (**Fig. 3.10e-h**), despite the influenza H1N1 virus not directly infecting the brain (Hosseinni et al., 2018). Increased levels of p-Tau protein reached significance following H1N1-infection when genotypes were pooled ($P < 0.05$; **Fig. 3.10f**), but not when data was separated by genotype (**Fig. 3.10g**). Again, we confirmed via ELISA that the levels of total tau remained consistent across genotypes and treatment groups, suggesting that the rise in p-Tau was independent of a rise in total tau protein (**Fig. 3.10h**). This H1N1 infection-induced trend appeared absent in Lrrk2 p.D1994S kinase-dead mice examined at the timepoint (**Fig. 3.10i, j**).

Given that p-Tau is highly abundant following infection at 6wpi, we next measured whether p-Tau was also abundant during the acute time point of VSV encephalitis (*i.e.,* 6 days post inoculation) *vs*. at the time of death when animals succumbed to the infection (*i.e.,* moribund mice) (**Fig. 3.10k, l**). Brain samples from moribund mice showed significantly more p-Tau than infected brains collected at 6dpi and 6wpi ($P < 0.0001$).

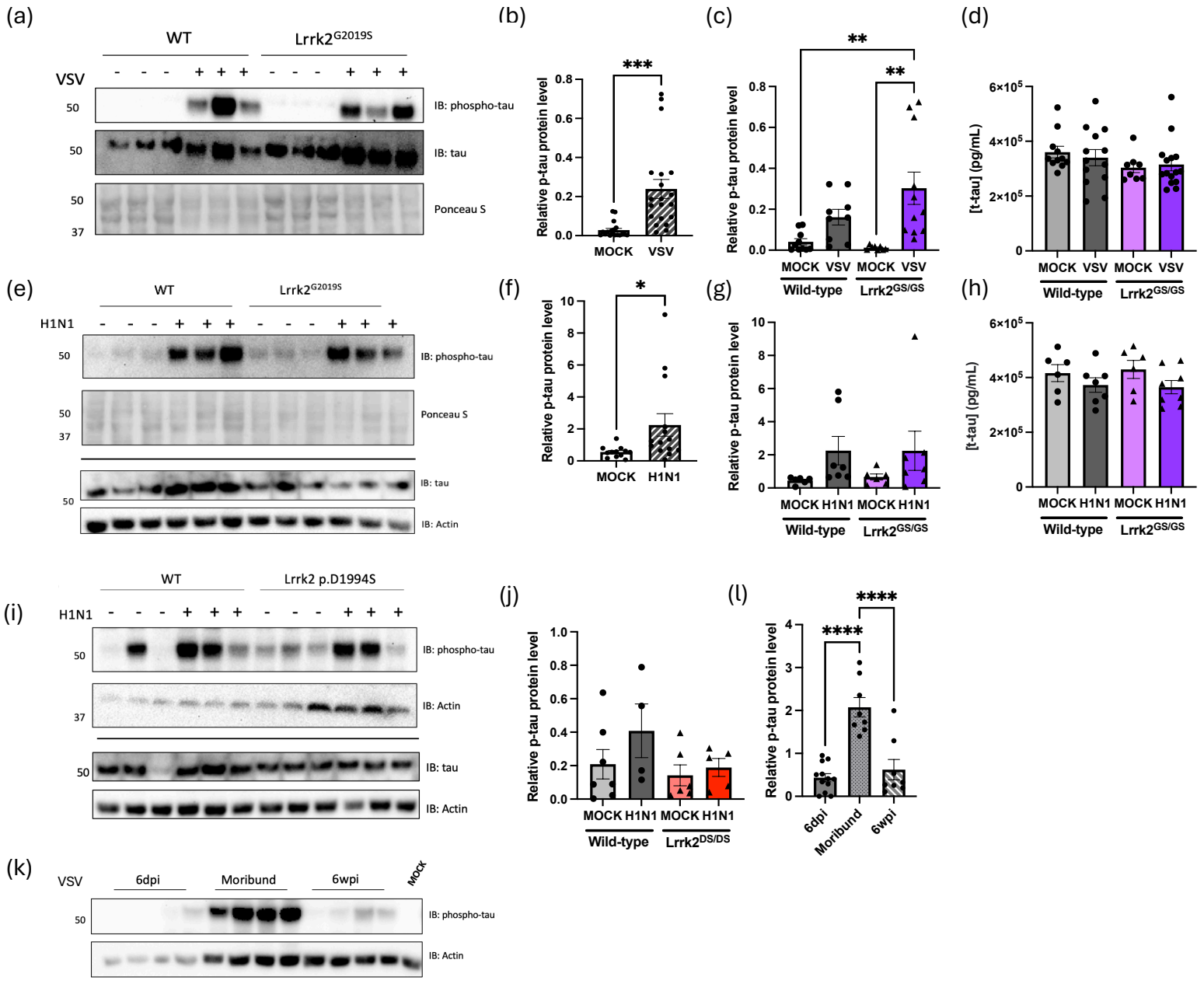


Fig. 3.10: Abundance of Phosphorylated Tau is Increased in the Brains of Adult Mice Infected by VSV or H1N1-Virus Without a Detectable Lrrk2 Mutation Effect. Mice were either nasally inoculated with $3x10^3$ PFU vesicular stomatitis virus (**a-d, k-l**) or $2x10^3$ PFU of influenza A virus (serotype H1N1; **e-h, i-j**) and monitored for a predetermined moribund state. Mice that survived past 2 weeks post inoculation (wpi) were aged for an additional 4 weeks and their brains were collected. Proteins were extracted using 1% Triton-X. Collected at 6wpi, VSV- (**a**) and H1N1-infected samples (**e**) were run on Western blots and probed for phosphorylated tau (Ser202, Thr205; antibody: AT8). Genotypes were pooled to identify VSV- (**b**) and H1N1- (**f**) dependent effects. Densitometry was measured and samples were normalized to loading control (**c, g**). Total tau protein concentration was measured by ELISA in VSV- (**d**) and H1N1-infected

samples (**h**). Brains from H1N1-infected, homozygous Lrrk2 p.D1994S mice were collected at 6wpi and phospho-tau was probed for by Western blotting (**i**) and quantified (**j**). Protein extracts from VSV-infected brains collected at either 6 days post inoculation, or at humane endpoint (moribund), or at 6wpi were probed for phosphorylated tau (**k**) and quantified densitometrically, independent of genotype (**l**). Each data point represents one animal. Data sets are presented as sexes pooled. Statistical analyses: ANOVA with Tukey post-hoc tests, $p < 0.05$. Error bars represent mean ± SEM. P-value <0.05 (*), P-value <0.01 (**), P-value <0.001 (***), P-value <0.0001 (****).

Discussion

In the present study, we have shown that resolved viral infections in adult mice could lead to sustained neuropathology-linked changes in the brain. Namely, two distinct viruses, neurotropic VSV and pneumotropic H1N1, both led to significantly increased oxidative stress, altered α-synuclein protein concentrations, and tau hyperphosphorylation in the adult brain, six weeks post inoculation, *i.e.*, at a timepoint when all mice were phenotypically healthy. Furthermore, the common Lrrk2 hyper-kinase mutation, p.G2019S, perturbed the course of illness in a pathogen-, organ-, and sex-dependent manner. Female Lrrk2 p.G2019S mice showed decreased survival rates from VSV infection, but not H1N1 infection.

Our data demonstrate that the Lrrk2 p.G2019S mutation did not confer a benefit or a risk against a peripheral, viral H1N1 infection, but did confer risk against a viral, encephalitic infection, specifically in female mice. In previous studies, Lrrk2 p.G2019S was protective against a bacterial, peripheral *Salmonella typhimurium* infection (Shutinoski et al., 2019; Liu et al., 2017) but worse off against an encephalitic reovirus T3D viral infection (Shutinoski et al., 2019). These data could support the concept that the Lrrk2 p.G2019S mutation confers increased protection against infections outside the brain, but that it confers greater risk when an infection reaches the brain.

In this study, in the context of both VSV and H1N1 infections, wild-type Lrrk2 function was not kinase-dependent, as kinase-dead Lrrk2 p.D1994S mice had no risk or benefit against either of these viral infections, though an increased sample size may uncover slight differences. These data suggest that the risk following VSV infection conferred in female Lrrk2 p.G2019S mutants is possibly caused by (toxic) gain-of-function kinase activity.

We had hypothesized that the Lrrk2 p.G2019S female mice may have a pro-inflammatory cytokine profile in sera and/or brain tissue, which has been previously reported (reviewed in: Yao

et al., 2024), although here, we did not identify major differences between groups. Importantly, cytokines from sera and whole brain homogenates were measured only at 6dpi (the time of peak weight loss and sickness from VSV); therefore, further regional- and time-dependent changes in cytokines may not have been captured in this study. However, we did identify a significant difference in IL-6, whereby male Lrrk2 p.G2019S mice had significantly more IL-6 in the serum than female Lrrk2 p.G2019S mice. This is of interest, as IL-6 has been linked to Lrrk2 p.G2019S in multiple reports (Pons-Espinal et al., 2024; Kim et al., 2012). Of great interest, Kozina et al. (2022) recently identified that LPS could induce dopaminergic neuron degeneration in Lrrk2 mutant mice, which was prevented when peripheral IL-6 was neutralized via specific antibodies. Our data supports a link between mutant Lrrk2 and IL-6 levels following infection, specifically with a possible Lrrk2 sex bias, which we consistently observed.

Intriguingly and unexpectedly, we observed decreased microgliosis specifically in Lrrk2 p.G2019S female mice following VSV infection, as measured with Iba1 staining in the olfactory bulb. This was evident in all parameters measured: average size, which indicates the cellular body of the microglia, with larger and more amoeboid-shaped microglia being indicative of an activated state; percent area occupied indicating an increase in infiltration of microglia and possibly macrophages; and perimeter, which is defined as the length of a geometric line including the cell body and its processes. Female Lrrk2 p.G2019S mice had almost absent induction of microglial recruitment (percent area) and activation (size), contrary to Lrrk2 p.G2019S male mice, where we identified a significant increase in microglial activation and infiltration. The lack of microgliosis (and likely decreased phagocytosis) observed in the female Lrrk2 p.G2019S mice following infection did not correspond with an increase in viral titre. However, importantly, microgliosis was

measured in the olfactory bulb and viral titre was measured in whole hemibrain homogenates, and therefore regional specificities may not be represented.

The present results were surprising, as many previous reports suggested that the Lrrk2 p.G2019S mutation confers a pro-inflammatory phenotype in microglia (Zhang et al., 2022; Pajarillo et al., 2023). To probe this further, we also investigated the apoptotic marker, cleaved caspase-3 (CC3). Herein, we did not identify a deficit in CC3 abundance in Lrrk2 p.G2019S female mice specifically; although, similar to Iba1 staining, a significant induction of CC3 staining was only found in Lrrk2 p.G2019S male mice. It is well-described that VSV infection leads to caspase-3 activation and is likely an important apoptotic host response to VSV infection (Hobbs et al., 2003; Lin et al., 2022). Research into the relationship between Lrrk2 p.G2019S and caspase-3 signalling indicates that this mutation consistently leads to increased caspase-3 expression, as was seen in the present study, when comparing male wild-type mice to male mutant mice (Iaccarino et al., 2007; Chen et al., 2012; Kim et al., 2019; Morrison et al., 2023).

This present study did not fully elucidate the reason behind the risk conferred by Lrrk2 p.G2019S mutation in female mice against VSV infection. The decreased microgliosis did not translate to increased viral titre; however, it is possible that Lrrk2 p.G2019S female mice had increased infiltration of peripheral myeloid cells (which contribute to viral control). This is supported by our previous data whereby Lrrk2 p.G2019S mice also had decreased Iba1 reactivity in the brain following reovirus T3D-induced encephalitis but was coupled with increased peripheral myeloid cell infiltration to the brain (Shutinoski et al., 2019). We are currently performing single nucleus RNA-sequencing (snRNA-seq) on olfactory bulbs collected from VSV-infected mice. These data will provide critical insights on sex- and genotype-dependent changes following VSV infection at the transcriptional and cellular level. This will include a non-biased

validation of the decreased microgliosis in female Lrrk2 p.G2019S mice, as well as detail which other cell populations are present in the bulb at this time (including infiltrating peripheral immune cells).

Our overarching theory is that PD is a complex disease, requiring both genetic predisposition and environmental exposure (which we posit are inflammatory/infectious in nature) to onset disease. To investigate the effects of both viral infections and the Lrrk2 p.G2019S variant on brain health, we measured multiple neurodegeneration-linked biochemical changes in the brains of these mice following nasal, viral exposures. Importantly, we measured these changes in surviving mice six weeks after initial infection; therefore, we selected for the subset of mice that overcame the initial infection. In this way we aimed to model whether non-fatal viral infections and post-acute illness can increase the risk of Parkinson's disease onset.

Oxidative stress is a common component of the pathogenesis of PD. The vulnerable dopaminergic neurons are highly susceptible to oxidative stress, which has been implicated in their death (reviewed in: He et al., 2020). Herein, we report a significant infection-dependent increase in H_2O_2 abundance in the brain following both VSV and H1N1 infection. Because H1N1 does not directly infect the brain, this leads us to hypothesize that the inflammatory response initiated in the periphery is reaching and affecting the brain, which remains to be tested.

Perplexingly, we identified a decrease in α-synuclein protein abundance in the brain of VSV-infected mice in both TXS- (soluble) and SDS- (insoluble) extracted proteins samples. Importantly, when measuring the degree of change between mock to VSV-infected state within genotypes, only Lrrk2 p.G2019S brains had a significant decrease of α-synuclein in both soluble and insoluble protein extracts, suggesting a Lrrk2 p.G2019S-dependent effect on α-synuclein concentration following viral infection. Notably, we did not identify a significant difference

between wild-type and Lrrk2 p.G2019S brains at baseline or in the infected state. The VSV-related data contrast what we have previously reported, whereby the encephalitis-causing virus, reovirus T3D, led to a significant increase in α-synuclein at the peak time of viral replication in neonatal mouse pups (Shutinoski et al., 2019). Whether these changes (both the increase or decrease following infection) occur at the transcriptional, translational, and/or post-translational levels remains to be determined. Answers towards this will be gained from the snRNA-seq dataset.

Remarkably, we identified a consistent and strong infection-dependent increase in tau phosphorylation at least six weeks post viral inoculation and four weeks from any signs of disease. Tau hyperphosphorylation was significantly increased in the brain following neurotropic VSV infection and non-neurotropic H1N1 infection, which does not directly penetrate the brain. Notably, tau phosphorylation has been reported in mice following multiple viral infections including SARS-CoV-2 (Di Primio et al., 2023), herpes simplex virus (Powell-Doherty et al., 2020), and mouse hepatitis virus (MHV) (Sy et al., 2011). Moreover, in humans, it is well established that phosphorylated tau tangles accumulate in subacute sclerosing panencephalitis induced by measles virus infection (Corselli, 1951; Malamud et al., 1950; Mandybur et al., 1977; Wisniewski et al., 1991). Herein, phosphorylated tau was absent in almost all mock-infected samples, and relatively low during the acute phase of disease, 6dpi, compared to 6wpi. The highest abundance of p-Tau was in the brains of moribund mice collected at humane endpoint. It remains unclear whether this phosphorylation is a physiological host response against the stress (similar to what is observed following hypothermia and hibernation) (Bretteville et al., 2012; Su et al., 2008), or whether this is a detrimental consequence of the infection. These data warrant further investigation, importantly: how long this phosphorylation of tau persists beyond 6 weeks post inoculation; and whether the high abundance of p-Tau in the brains of the surviving mice is linked

to any neurobehavioural phenotypes or any degree of neurodegeneration, and if these potential phenotypes are genotype-dependent.

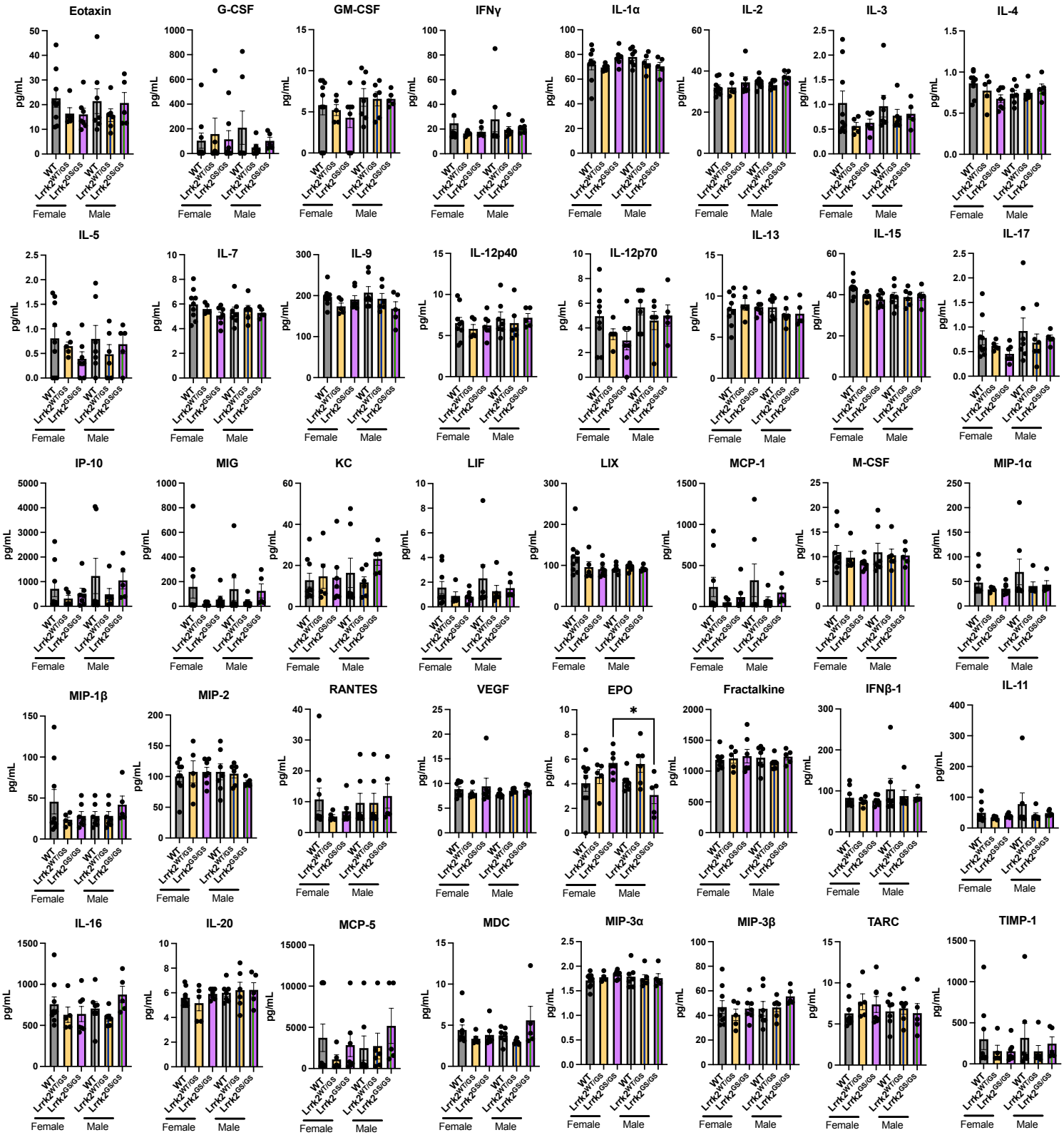
In human LRRK2-linked Parkinson's disease patients, disease neuropathology at autopsy is variable. Specifically, the p.G2019S mutation and the p.R1441C/G mutations have been linked to tau misprocessing in the brain, in addition to synucleinopathy in other cases (reviewed in Kawakami and Ichikawa, 2015). Specifically following the neurotropic VSV infection, we identified a possible Lrrk2 p.G2019S effect in exacerbating the induction of tau hyperphosphorylation, as the increase in tau phosphorylation between the mock- and VSV-infected brains of Lrrk2 p.G2019S mice was higher than the same increase measured in wild-type mice. Physiologically, numerous *in vitro* studies have illustrated a potential role for Lrrk2 in promoting phosphorylation of tau (Hamm et al., 2015; Kawakami et al., 2014), with one study showing the ability of Lrrk2 to phosphorylate tau directly *in vitro* (Bailey et al., 2013). Castro-Sanchez et al. (2020) have previously demonstrated that treatment with a Lrrk2 inhibitor could decrease tau hyperphosphorylation, further supporting a role for Lrrk2 kinase in this process. Notably, in the present study we also observed a lesser degree of tau phosphorylation in Lrrk2 kinase-dead p.D1994S mice following H1N1 infection, compared to wild-type and Lrrk2 p.G2019S mice.

Overall, changes in tau phosphorylation could result from increased activity of tau-specific kinases, decreased activity of tau-specific phosphatases, or decreased autophagic processing of hyperphosphorylated tau aggregates. Notably, Sy et al. (2011) attributed increased tau phosphorylation following MHV infection in mice to increased GSK3-β activity. Future studies will address the mechanism behind virally induced tau phosphorylation in our studies, and how this may be modulated by Lrrk2 p.G2019S *in vivo*.

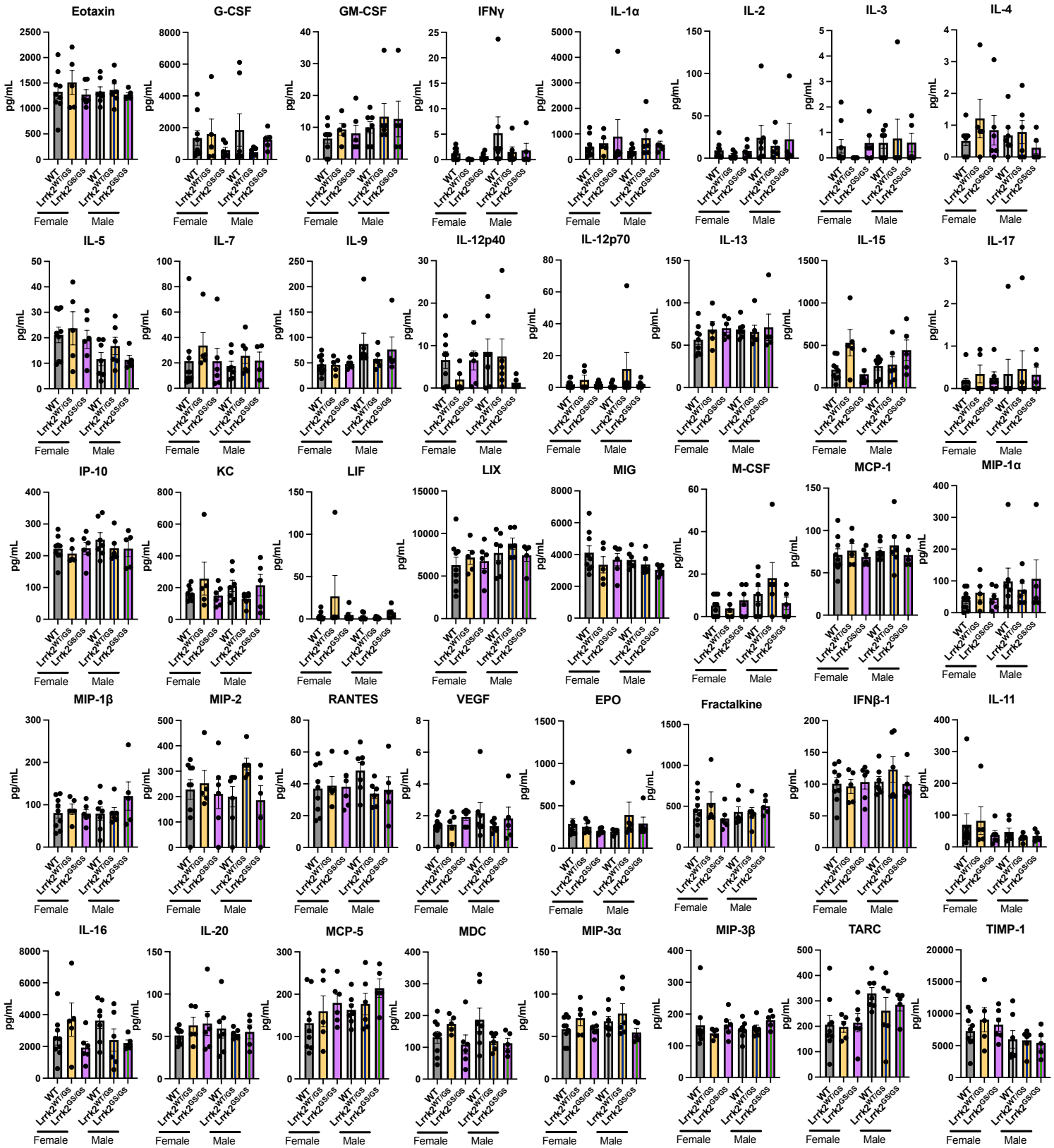
It is an important consideration in the present study that we did not identify a prominent effect of the Lrrk2 p.G2019S variant over the wild-type genotype for the parameters measured here (*i.e.,* oxidative stress, α-synuclein, or p-Tau protein) at baseline or in the infected state. The most prominent and strongest effects were infection-dependent (both VSV and H1N1) and were evident in both wild-type and Lrrk2 p.G2019S mice. These results suggest that the effect sizes are relatively small and with respect to the development of PD in humans may only become more prominent when combined with the factors of ageing, other allelic variants, or subsequent exposure to additional (or recurrent) environmental exposures.

Taken together, our results implicate a role for Lrrk2 in immune response(s), demonstrating its ability to modulate disease outcomes following viral infections in adult mice in both the periphery and the brain, and doing so with a female sex bias. Viral infections, even those that are not neurotropic, can affect the levels of phosphorylated tau, oxidative stress, and total α-synuclein in the brain as late as six weeks after the acute infection. Our findings in adult mice raised under controlled environmental conditions unequivocally demonstrate a link between nasally acquired RNA viruses and brain pathologies that are associated with LRRK2-PD and may point to a role for infections (even those occurring peripherally) in subsequent brain health, and thus, as potential risk factors for a host of neurodegenerative disorders.

Supplementary Materials



Supplemental Fig. 3.1: Additional Results for Cytokine and Chemokine Analyses in Hemibrain Homogenates from Wild-Type and Lrrk2 p.G2019S Mutant Mice Following VSV Infection. Adult mice aged 8-10 weeks were nasally inoculated with a dose of $3x10^3$ PFU of vesicular stomatitis virus (VSV), sacrificed at 6dpi, and hemibrains were collected and homogenized in PBS. Multiplex ELISA was used to measure an array of cytokines and chemokines in each animal. One point represents one biological replicate. Error bars represent mean ± SEM. Statistical tests used: one-way ANOVA with Tukey's post-hoc tests. P-value <0.05 (*).


Eotaxin
G-CSF
GM-CSF
IFNγ
IL-1α
IL-2
IL-3
IL-4
IL-5
IL-7
IL-9
IL-12p40
IL-12p70
IL-13
IL-15
IL-17
IP-10
KC
LIF
LIX
MIG
M-CSF
MCP-1
MIP-1α
MIP-1β
MIP-2
RANTES
VEGF
EPO
Fractalkine
IFNβ-1
IL-11
IL-16
IL-20
MCP-5
MDC
MIP-3α
MIP-3β
TARC
TIMP-1
pg/mL
WT
Lrrk2WT/GS
Lrrk2GS/GS
Female
Male

Supplemental Fig. 3.2: Additional Results for Cytokine and Chemokine Analyses in Sera from Wild-Type and Lrrk2 p.G2019S Mutant Mice Following VSV Infection. Adult mice aged 8-10 weeks were nasally inoculated with a dose of $3x10^3$ PFU of vesicular stomatitis virus (VSV), sacrificed at 6dpi, and sera were collected by cardiac puncture. Multiplex ELISA was used to measure an array of serum cytokines and chemokines in each animal. One point represents one biological replicate. Error bars represent mean ± SEM. Statistical tests used: one-way ANOVA with Tukey's post-hoc tests. No significant differences were found.

<u>Chapter 4:</u> *Gba1* p.D409V Mutant Alleles Confer Protection During Acute Infection by a Neurotropic RNA Virus Following Nasal Inoculation

Michaela O. Lunn*, Quinton Hake-Volling*, Nathalie Lengacher, Qiubo Jiang, Earl G. Brown, Julianna J. Tomlinson, Michael G. Schlossmacher

* Authors contributed equally

Statement of Author Contribution

ML, QHV, JJT, EGB, and MGS conceptualized the study. QHV and QJ maintained the breeding colony of Gba1 p.D409V mice and prepared cohorts. QHV and **ML** performed initial cohorts of survival of H1N1 infections together (**Fig. 4.1**). QHV performed all studies involving *Salmonella typhimurium* (**Fig. 4.2**). QHV performed all survival analyses of VSV infection (**Fig. 4.3**). QHV performed VSV viral titre analyses of brain and lung; **ML** performed viral titre analyses of olfactory bulbs (**Fig. 4.4**). QHV performed all *in vitro* GCase activity analysis (**Fig. 4.5**). QHV inoculated and harvested tissue from mock- and VSV-infected mice for cyto-/chemokine analyses; **ML** processed and organized all tissue for measurements and analyzed all data. An external service measured all cyto-/chemokine abundances (**Fig. 4.6**). QHV collected mock- and VSV-infected tissue for protein analyses. NL measured α-synuclein abundance via ELISA. **ML** processed all tissue for protein analyses, completed the Western blotting, and performed densitometry (**Fig. 4.7**). QHV and **ML** analyzed the datasets and prepared figures. **ML** wrote the manuscript, with input and edits from EGB, JJT, and MGS.

Gba1 p.D409V Mutant Alleles Confer Protection During Acute Infection by a Neurotropic RNA Virus Following Nasal Inoculation

Michaela O. Lunn[1,2]*, Quinton Hake-Volling[2,3]*, Nathalie Lengacher[1], Qiubo Jiang[1], Earl G. Brown[1,3], Julianna J. Tomlinson[1], Michael G. Schlossmacher[1,2,4]

* Authors contributed equally

1. Program in Neuroscience, Ottawa Hospital Research Institute, Ottawa, ON, Canada.
2. Department of Cellular and Molecular Medicine, University of Ottawa, Ottawa, ON, Canada.
3. Department of Biochemistry, Microbiology and Immunology Faculty of Medicine, and Ottawa Institute of Systems Biology, University of Ottawa, Ottawa, ON, Canada.
4. Division of Neurology, Department of Medicine, The Ottawa Hospital, Ottawa, ON, Canada.

Abstract

Typical, late-onset Parkinson's disease (PD) is a complex disorder arising from interactions between genetic risk, environmental exposure(s), and lasting effects from their interactions; these are modified by biological sex and ageing. We previously published that *Lrrk2* and *Snca* alleles play roles in host responses to microbial infections. Mutations in the *GBA1* gene, which encodes the lysosomal enzyme glucocerebrosidase (GCase), represent the commonest risk factor for the development of PD and dementia with Lewy bodies. Here, we explored the role of murine GCase in host responses to select viruses and bacteria. We tested this in four specific models: mice carrying one or two *Gba1* p.D409V knock-in alleles did not show an altered course of illness in response to nasal inoculation by Influenza A virus (serotype H1N1); intravenous inoculation to the bacterium *Salmonella typhimurium* (subtype SL13344); or serial infection by these two pathogens. In response to nasal inoculation with vesicular stomatitis virus (VSV; Indiana strain), which causes pneumonitis followed by encephalitis, Gba1 p.D409V-expressing male mice survived infection at a significantly higher rate than wild-type animals. Intriguingly, female heterozygous -but not homozygous- Gba1 p.D409V mice also had lower viral titres in their lungs after VSV infection. Select cytokine responses and GCase activities measured *in vitro* were found to be altered in VSV-infected Gba1 p.D409V mice in a sex-and organ-dependent manner, revealing at times opposing trends between one *vs.* two mutant alleles. In the early stages of VSV infection, the levels of α-synuclein, tau, phospho-tau, and Lrrk2 were not altered in the brain. Taken together, our results identify a modulatory role for GCase in host survival during one of four infection models tested. Further, in the context of *GBA1*-focused studies our findings highlight a complex interplay of biological sex and organ-specific responses when exploring the impact of environmental pathogens.

Introduction

Parkinson's disease (PD) is a neurodegenerative disorder with heterogenous symptoms, signs, and disease progression. Braak and Del Tredici have proposed a "dual-hit hypothesis" for PD initiation, based on their finding that disease pathology begins in the gastrointestinal tract and/or the olfactory system. Building on this, we and others have hypothesized that this was in response to an environmental trigger in genetically susceptible individuals (Hawkes et al., 2007; Kitada et al., 2012). In this context, teams including ours have investigated the roles of multiple PD-linked disease genes in the context of a dual-hit, complex disease model, employing genetic models against multiple environmental triggers.

Mutations in *GBA1* are the commonest genetic risk factor for PD (Sidransky et al., 2009). Homozygous *GBA1* mutations cause Gaucher disease (GD), a lipid storage disorder. It was then identified that obligate carriers of *GBA1* mutations among relatives of GD patients had a higher incidence rate of PD (Goker-Alpan 2004; Lwin et al., 2004; Aharon-Peretz et al., 2004). It is now estimated that up to 9% of the general PD population carry a mutation in *GBA1* (Avenali et al., 2020). Symptomatically, *GBA1*-linked cases are phenotypically similar to idiopathic PD, although with a more severe disease course and earlier onset (Mullin et al., 2019; Thaler et al., 2017). Furthermore, mutations in the same gene have also been strongly linked to another 'synucleinopathy', dementia with Lewy bodies (DLB); as high as 28% of DLB patients carried a *GBA1* mutation in one cohort (Clark et al., 2009). Like PD, *GBA1* carriers present with a more malignant form of DLB, with earlier age of onset and more severe cognitive and motor deficits (Gaubert et al., 2022).

The *GBA1* gene encodes the lysosomal acid hydrolase glucocerebrosidase (GCase), which is responsible for hydrolyzing the sphingolipid glucosylceramide (GlcCer) into glucose and

ceramide (Migdalska-Richards and Shapira et al., 2016). GlcCer is then converted to glucosylsphingosine (GlcSph) by acid ceramidase (Boer et al., 2020). As such, in cases of defective GCase, higher accumulation of both GlcCer and GlcSph is observed (Rocha et al., 2015). Furthermore, GCase has been shown to catalyze the glucosylation of cholesterol (Boer et al., 2020). In GD, the GCase enzymatic activity is markedly reduced (less than 15%) (Hugues and Pastores, 2018). Decreased GCase activity has been identified in both GBA1-PD and idiopathic PD, though to a much lesser extent than in GD (Gegg et al., 2012; Rocha et al., 2015). These decreased levels of GCase activity have been associated with an identified rise in GlcCer and GlcSph in human GBA1-PD patients (Marano et al., 2024). In the context of PD pathogenesis, the role of lipid metabolism and network interactions remains understudied, despite the substantial effect lipids play in cellular homeostasis (Alecu and Bennett, 2019).

We hypothesize that gene-environment interactions play a critical role in the development of PD. Specifically, that PD-associated genes modulate host responses to environmental insults, leading to subsequent pathological outcomes (Schlossmacher et al., 2017). GBA1-PD lends itself well to this hypothesis, as mutations in *GBA1* have relatively low penetrance rate, despite the high prevalence of mutations (Alcalay et al., 2014). This may highlight a need for an environmental trigger to onset disease in *GBA1*-susceptible individuals. It has been established that another PD-linked disease gene, *LRRK2*, also with a low penetrance rate, can alter disease outcomes following multiple inflammatory triggers, including those pathogenic (*e.g.,* LPS, viral infections) and chemical (*e.g.*, pesticides, MPTP) in nature (Shutinoski et al., 2019; Ahmadi Rastegar et al., 2022; Rudyk et al., 2019; Arbez et al., 2020; Lunn et al., *in prep*;).

As such, we hypothesized that the most common PD risk gene, *GBA1*, may also play a role in host defences against pathogenic insults. Importantly, *GBA1* is highly expressed in cells of the

mononuclear phagocyte lineage (Deleidi and Gasser, 2013). Further, GD patients show altered inflammation, likely in large part due to the pathological hallmark of GD, the accumulation of lipid-laden macrophages (Sidransky and Lopez 2012). Moreover, granulocytes and mononuclear phagocytes from GD patients were found to have lesser control of *Staphylococcus aureus* growth *ex vivo* (Maródi et al., 1995). Contrarily, GBA1 knockout HEK293 cells were able to inhibit infection of Influenza H1N1 (PR8 strain) (Drews et al., 2019). These studies highlight a capacity for GCase activity in pathogen response.

To investigate a role for GCase in host responses against infections with live pathogens, we tested a range of microbial pathogens in adult Gba1 p.D409V mutant mice. Though not a mutation found in human PD cases, this is a highly characterized mouse model and exhibits a loss of GCase activity in both the heterozygous and homozygous states (Xu et al., 2003; Clarke et al., 2019; Polinski et al., 2021). We hypothesized that disease-relevant mutations in *Gba1* would lead to altered disease outcomes (as measured by survival rate and/or viral/bacterial titres) following a nasal, microbial infection. We utilized infections of: neurotropic vesicular stomatitis virus (VSV); non-neurotropic lung-directed influenza A virus serotype H1N1 (herein referred to as H1N1); peripherally restricted bacterial *Salmonella typhimurium* (ST); as well as a serial infection of the latter two, to investigate either anti-microbial properties or higher pathogen susceptibility in mutant Gba1 mice. Herein, we show that Gba1 p.D409V mice were protected against VSV infection with a sex bias, but not against H1N1 or ST infection. Further, GCase activity was altered in VSV-infected Gba1 p.D409V mice in a sex-and organ-dependent manner. Taken together, this study identifies a possible role for GCase in host response to an acute neurotropic infection and highlights the importance of exploring sex-dependent outcomes in *Gba1*-focused studies.

Methods

Mouse Colonies

Mice with a knock-in *Gba1* p.D409V mutation were initially obtained by Dr. Gregory Grabowski and are described in Xu et al. (2003). They were backcrossed and subsequently maintained on a C57BL/6J background. Colonies were maintained with heterozygous breeding pairs. Animal experiments were performed under the guidelines by Canadian Councils on Animal Care and approved by the Ethics Board of the Animal Care Committee at the University of Ottawa. Experiments involving pathogenic infections were done in a containment level 2 biohazard animal facility. Both female and male mice were used in this study and are indicated within each figure.

Nasal Infection with Mouse-Adapted Influenza A H1N1

Mouse-adapted Influenza A H1N1 (A/Fort Monmouth/1/1947) was obtained from Dr. Earl Brown (University of Ottawa) (Brown, 1990). Adult mice aged 6-9 weeks were anesthetized with 3% isoflurane in O_2 at 1L/m for 1 minute. $2x10^3$ plaque forming units (PFU) of Influenza A H1N1 diluted in 50µL PBS were administered to the nostrils of anesthetized mice. Mice were observed twice daily and monitored for weight loss, sickness, and survival from 4 to 14 days post inoculation (dpi). Mice were considered endpoint upon respiratory distress or a loss of 30% body weight, even in absence of other symptoms.

Intraperitoneal Infection with *Salmonella typhimurium* and Measurement of CFUs

Salmonella typhimurium strain SL1344 was used for bacterial inoculations. Wild-type, heterozygous, and homozygous Gba1 p.D409V littermates were intraperitoneally inoculated with 200 colony forming units (CFUs) of ST in 100µL of PBS. Mice were euthanized 5dpi and spleens

were collected in 10mL of RPMI serum-free media (Gibco). Spleens were homogenized and serially diluted (10-fold, v:v). 100µL of homogenate was spread on sterile agar culture plates. Plates were incubated at 37°C for 24 hours. Colonies were counted and bacterial load was measured as colonies per spleen.

Serial Infection with *Salmonella typhimurium* in H1N1 Survivors

Survivors of the H1N1 infection that had regained 100% of their starting weight were infected with *Salmonella typhimurium* 4 weeks after the initial H1N1 infection (two weeks after the end of the 14-day H1N1 infection course) (see **Fig. 4.2a**). 200 CFU of ST diluted in 100µL of PBS were administered intraperitoneally. Mice were euthanized and spleens were harvested 5 days after ST infection.

Nasal Infection with Vesicular Stomatitis Virus

Wild-type Indiana strain Vesicular Stomatitis virus was obtained from Dr. Earl Brown (University of Ottawa) (Stojdl et al, 2003). Mice aged 6-10 weeks were anesthetized with 3% isoflurane in O_2 at 1 L/m for 1 minute and $3x10^3$ PFU VSV (Indiana strain) diluted in 50µL PBS were administered to the nostrils of anesthetized mice. Mice were observed for 14 days post inoculation for survival studies. Mice were weighed from 4-14 dpi and monitored twice daily. Mice were considered endpoint as a result of encephalitis, characterized by moribund state, hind limb paralysis, and inability to walk or a loss of 30% body weight regardless of lack of other symptoms.

Vesicular Stomatitis Virus Plaque Assay

Mice nasally infected with $3x10^3$ PFU of VSV were sacrificed at 2dpi and hemibrains, olfactory bulbs, and lungs were dissected and snap frozen. For viral titre analysis, frozen hemibrains were lysed in PBS (3:1, µl PBS:mg tissue), lungs (3:1), and olfactory bulbs (6:1) using metal beads and Magna Lyser machine (Roche) at maximum speed for 10 seconds. Samples were then put through one freeze-thaw cycle to lyse the cells. Vero cells were plated in 12-well culture plates to 90% confluency. Homogenate samples were centrifuged at 5,000RPM and supernatants were serial diluted (10-fold, v:v) in serum-free DMEM media (Millipore Sigma) and 250µL was overlayed per well. Cells overlayed with viral suspensions were incubated at 37ºC at 5% CO_2 for one hour, with rocking every 15 minutes to ensure even distribution among cells. After one hour, cells were overlayed with 2mL of a 1:1 mixture of 1% agarose and 2xDMEM (Gibco, Thermo Fisher Scientific) supplemented with 10% FBS. Cells were incubated at 37ºC at 5% CO_2 for 24 hours. The next day, cells were stained with 1mL of fixative Carnoy's reagent (methanol:acetic acid 3:1) and incubated for one hour at room temperature. Cell overlay was removed by gentle lifting and cells were stained with Coomassie blue solution (0.1% Coomassie Brilliant Blue, 20% methanol, and 10% acetic acid) and incubated for 30 minutes at room temperature with gentle rocking. Coomassie stain was removed, and plaques were counted manually. Viral titre was reported as plaque forming units (PFU) per gram of tissue.

Measuring Lysosomal GCase Activity from Mouse Tissue *In Vitro*

Snap frozen tissue was lysed in citric acid buffer containing 176mM K_2HPO_4, 50mM citric acid, 10mM sodium taurocholate, and 0.01% Tween-20 at pH 5.9 as previously published (Fishbein et al., 2014). Tissues were homogenized using metal beads and Magna Lyser (Roche) at maximum

speed for 10 seconds. Homogenized tissue was centrifuged at 14,000 rpm for 10 minutes at 4°C and supernatant was collected and frozen. Tissue lysates were measured for concentration using Pierce bicinchoninic acid (BCA) assay (Thermo Fisher Scientific) and all samples were diluted to a final concentration of 0.625mg/ml. Samples were assayed in black flat-bottom 96-well plates. Forty µL of tissue lysate was measured in duplicate with or without the presence of 5µl of 20mM CBE (Millipore Sigma), a selective GCase inhibitor for 30 minutes at 37°C. Samples were then incubated with 40µL of 10mM 4-Methylumbelliferyl β-D-glucopyranoside substrate (Millipore Sigma) for one hour at 37°C. Standard curve using 4-methylumbelliferone (Millipore Sigma) was run in parallel. After one hour, 40µL of glycine stop solution (1M glycine, 1M NaOH, pH 10.6) was added. Samples were subsequently measured for fluorescence at excitation and emission wavelengths of 365nm and 450nm, respectively. Relative fluorescent units were converted to pmol of substrate using the standard curve.

Cytokine and Chemokine Measurements

Mice nasally infected with $3x10^3$ PFU of VSV (or 50µL of PBS for mock infection) were sacrificed at 2dpi and blood was collected via cardiac puncture using an uncoated syringe. Blood was incubated at room temperature for 30 minutes and then centrifuged at 14,800 RPM for 10 minutes to collect serum. Serum was measured for cytokine and chemokine abundance using the discovery assay Mouse Cytokine Array / Chemokine Array -Plex (MD32) from EVE Technologies (Calgary, AB, Canada).

Protein Extraction

Hemibrains were homogenized in PBS as described above and used for protein extraction.

Aliquots of homogenates were treated with 1% Triton- X100, 2X protease inhibitors, and 2X phosphatase inhibitors and centrifuged at 14,800 RPM for 30 minutes at 4°C. Protein concentrations were determined using a BCA assay kit (Thermo Fisher Scientific).

ELISA Quantification of α-Synuclein

Lysates were measured for total α-synuclein using sandwich ELISA as described previously (Shutinoski et. al., 2019; Mollenhauer et al., 2008). Protein concentration was quantified by Bradford protein assay (Bio-Rad) and standardized at a concentration of 5mg/mL.

Western Blotting

Protein samples (40μg) were combined with 1X NuPAGE™ LDS Sample Buffer (NP0007, Thermo Fisher Scientific), boiled for 5 minutes at 95-100°C, and then electrophoresed under reducing (5% β-mercaptoethanol) conditions on 4-12% gradient SDS gels in MES buffer. Gels were then transferred to a PVDF membrane using a standard semi-dry transfer in TRIS-glycine-Methanol buffer. The following antibodies were used: anti-actin (sc-81178, Santa Cruz; 1:500 in 5% milk), anti-phospho-tau (Ser202, Thr205) monoclonal antibody (AT8) (MN1020, Thermo Fisher Scientific, 1:500 in 5% milk), anti-total tau a.a. 210-241 (MAB361 EMD Millipore, 1:1000 in 5% milk), anti-LRRK2 (MJFF2 c41-2, ab133474, AbCam, 1:1000 in 5% BSA), and anti-p-LRRK2-S935 (UDD2 10(12), ab133450, AbCam, 1:1000 in 5% BSA). All Western blots were imaged using BioRad ChemiDoc Imager. Image Lab (version 6.1.0) (2020 BioRad Laboratories, Inc.) was used for densitometric analysis of Western blots.

Statistical Analyses

All statistical analyses were performed using GraphPad Prism version 9 (GraphPad Software, San Diego, CA, USA, www.graphpad.com). Differences between groups in survival assays was assessed using the log- rank (Mantel-Cox) test. Differences between groups of three or more was assessed using one-way ANOVA with Tukey's post-hoc tests (unless otherwise stated in figure legend). Differences between two groups was assessed using unpaired student t-test. Data are demonstrated as mean ± SEM where applicable and as described in the figure legends. Data are displayed with *P* values represented as $*P < 0.05$, $**P< 0.01$, $***P< 0.001$.

Results

The p.D409V Gba1 *mutation does not alter survival outcomes of H1N1 infection in nasally inoculated adult mice.*

To first probe for any role in host defences for wild-type *Gba1* or the p.D409V mutant, we nasally inoculated wild-type, heterozygous, and homozygous mutant mice with influenza A virus serotype H1N1. It has previously been shown that *GBA1* knockout cells could alter the response to Influenza A virus infection *in vitro* (Drews et al., 2019). Herein, adult mice, aged 6-9 weeks were nasally inoculated with a dose of $2x10^3$ PFU of H1N1 virus. Mice were monitored and weighed up to 14dpi. As we have observed a strong sex bias in our viral infection studies involving the PD-linked gene, *Lrrk2*, we consistently analyzed the present data in both sexes (Shutinoski et al., 2019; Lunn et al. *in prep*).

When analyzing the data for female mice alone (**Fig. 4.1a, b**), and male mice alone (**Fig. 4.1c, d**), no differences in survival rates were identified across groups. Indeed, there was a very low mortality rate across the groups in response to the H1N1 infection. Mice did become sick, as

indicated by their drop in weight (**Fig. 4.1b, d**), but using weight as a sickness score, there was no difference across genotypes.

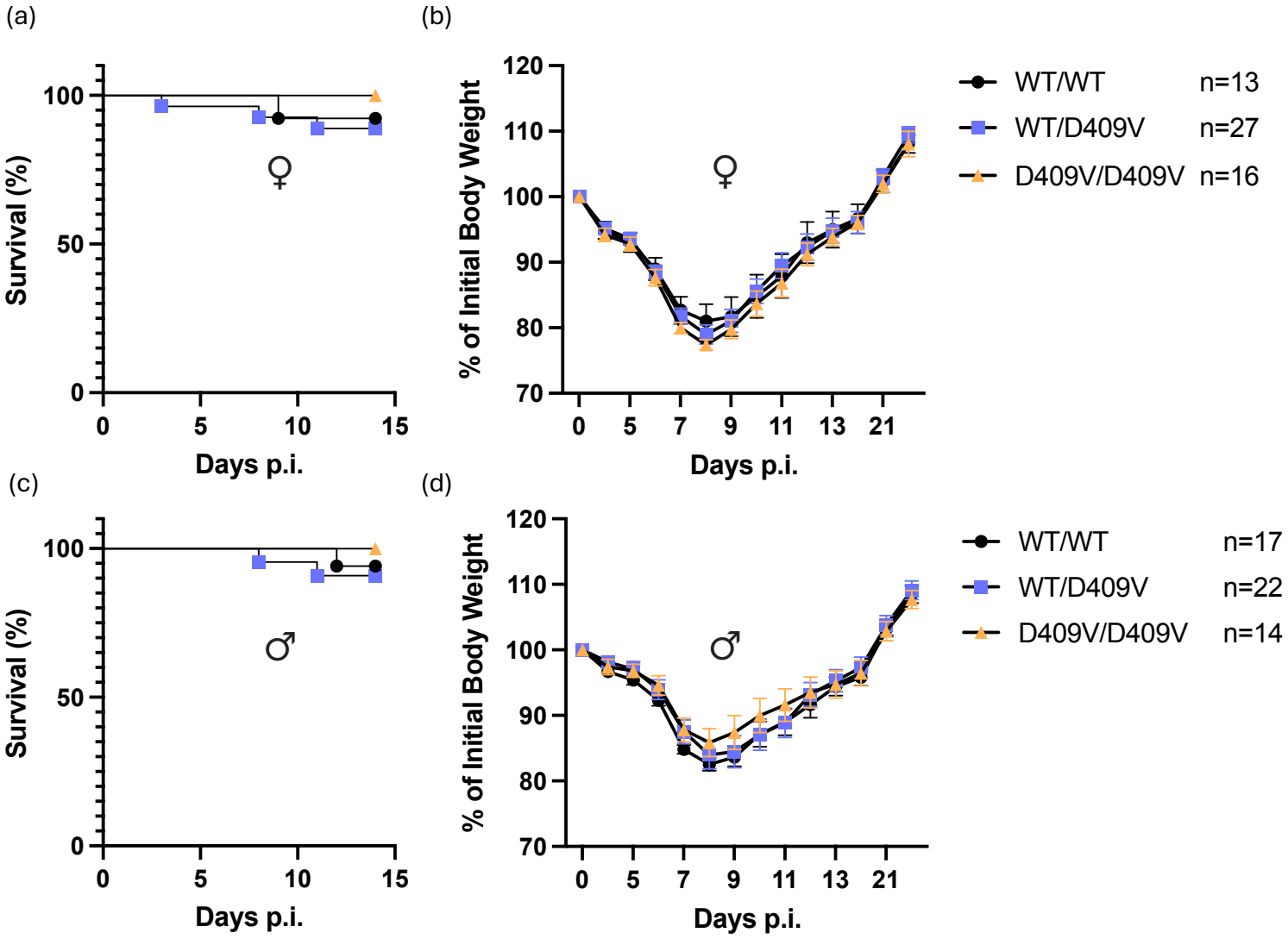


Fig. 4.1: *Gba1* p.D409V Alleles Do Not Alter Survival or Weight Loss in Mice Following Inoculation with Influenza A Virus. Wild-type (WT/WT), heterozygous (WT/D409V), and homozygous (D409V/D409V) Gba1 p.D409V knock-in littermates were inoculated at 6-9 weeks of age with a dose of $2x10^3$ PFU of influenza A virus (serotype H1N1) and monitored for a predetermined moribund state to measure survival (**a, c**) and their daily weight (**b, d**) for 14 days. Data are presented as female mice only (♀) (**a, b**), and as male mice only (♂) (**c, d**). Survival is graphically displayed as percent survival against days post inoculation, and weights are displayed as percent of initial body weight against days pays post inoculation. Sample sizes for each genotype are as indicated in the legends. Error bars represent mean ± SEM. Statistical test used: log rank (Mantel-Cox) test for survival rates. One-Way ANOVA with Tukey post hoc-test was used between genotypes on each individual day for weight changes. No statistically significant differences were observed.

H1N1 infection-surviving Gba1 p.D409V mice have the same* Salmonella typhimurium *bacterial burden in the spleen as wild-type mice in a serial infection paradigm.

As we observed a high survival rate in all mice in our H1N1-infected cohort, we employed a serial infection model. A second, bacterial exposure was added to examine whether a pre-existing viral infection could alter the response to a super-infection in Gba1 p.D409V mice. Two-weeks following the completion of the 14-day experimental period of H1N1, mice were infected with ST by intraperitoneal injection (**Fig. 4.2a**). Spleens were collected at 5dpi following ST inoculation, and bacterial burden via CFU analysis was measured. No significant differences were found across genotypes in female (**Fig. 4.2b**) or male mice (**Fig. 4.2c**). Importantly, in a separate cohort of mice, wild-type, heterozygous, and homozygous Gba1 p.D409V mice were infected with ST only and bacterial burden in the spleens were measured at 5dpi. As seen in the serial infection paradigm, there were no differences in the ST bacterial burden-only scenario between genotypes in female (**Fig. 4.2d**) or male mice (**Fig. 4.2e**).

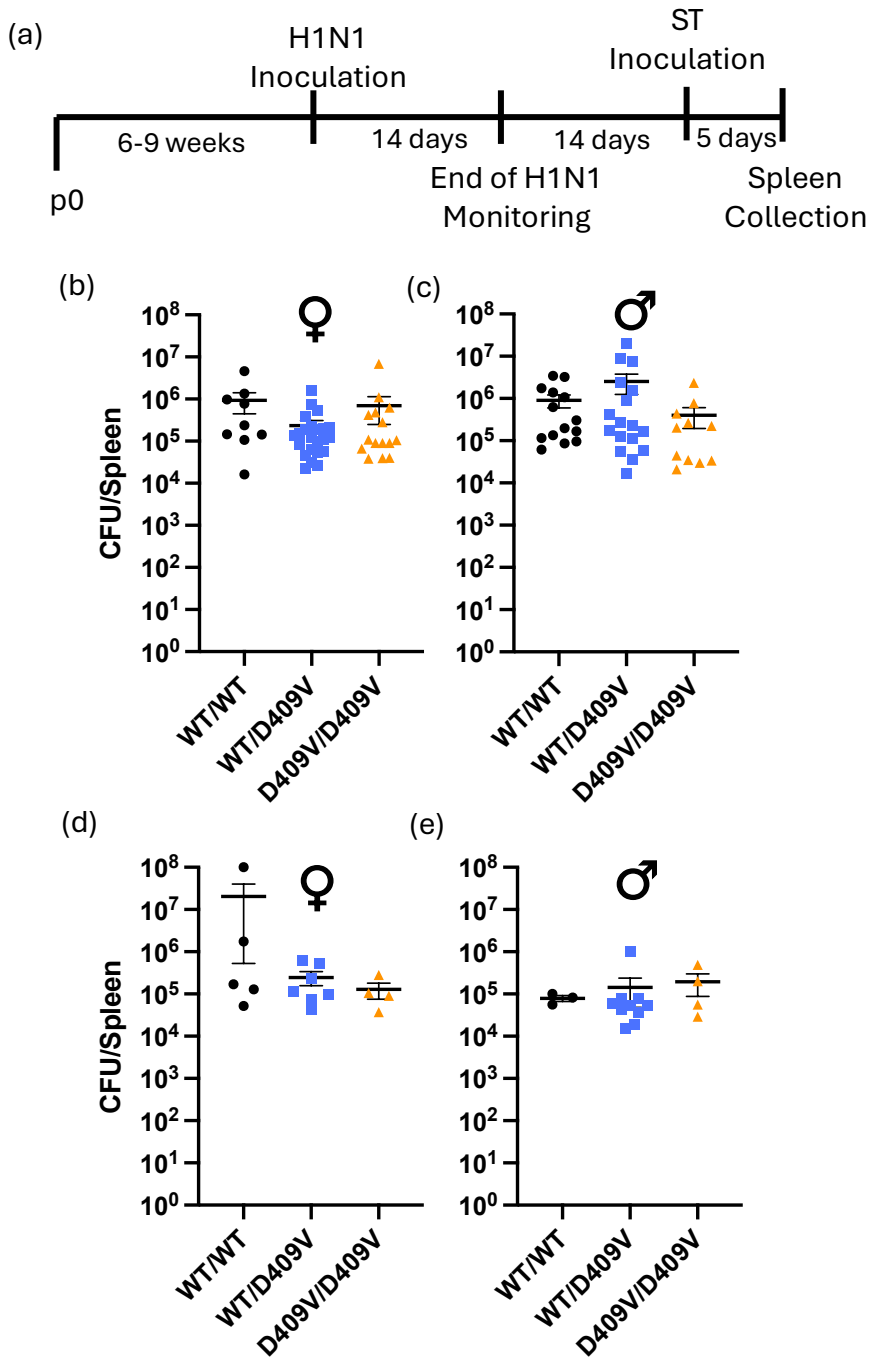


Fig. 4.2: *Gba1* p.D409V Alleles Do Not Alter *Salmonella Typhimurium* Bacterial Load in Mice With or Without Preceding Influenza A Virus H1N1 Infection. (**a-c**) Mice that regained a minimum of 100% of original body weight 4 weeks after initial H1N1 infection (as in Fig. 4.1) were inoculated intraperitoneally with 200 colony forming units (CFU) of *Salmonella typhimurium* (subtype SL1344) as outlined in (**a**). Bacterial load at 5 days post inoculation is shown as CFU per spleen in female mice (♀) (**b**), and in male mice (♂) (**c**). Each data point represents one biological replicate. (**d, e**) Adult mice without preceeding viral infection were infected intraperitoneally with 200 CFU of *Salmonella typhimurium* SL1344 at 6 months of age. Animals were euthanized on 5

days post inoculation and processed as above. Bacterial load is compared in female mice (♀) (**d**), and in male mice (♂) (**e**). Error bars represent mean ± SEM. Data were tested with One-Way ANOVA with Tukey post-hoc tests. No statistically significant differences were observed.

Male, but not female, Gba1 p.D409V mutant mice are relatively protected against vesicular stomatitis virus nasal infection.

The low lethality in the pneumotropic H1N1 viral infection model led us to test a second viral infection model. Also an RNA viral pathogen, VSV is neurotropic and causes encephalitis as the cause of death at lethal doses. Adult mice aged 6-10 weeks were nasally inoculated with a dose of $3x10^3$ PFU of VSV and monitored to 14dpi (what we consider 'survival' in this experimental model). Male mice overall had significantly higher mortality in response to VSV infection than female mice which has been previously reported (Barna et al., 1996; Lunn et al., *in prep*). When examining the survival rate of both sexes combined, wild-type mice had a significantly lower survival rate than both homozygous and heterozygous mice ($P < 0.05$; **Fig. 4.3a**). Curiously, when analyzing the data separated by sex, we observed a trend in female mice to suggest that heterozygous Gba1 p.D409V mice had a survival advantage over both wild-type and homozygous littermates (**Fig. 4.3c**); but male homozygous Gba1 p.D409V mice had a significantly higher survival rate compared to wild-type littermates, and a higher, though not statistically significant, survival rate than heterozygous littermates ($P < 0.05$; **Fig. 4.3e**). Body weight was measured throughout the survival assay (**Fig. 4.3b, d, f**) as a proxy measurement of illness. All mice lost weight over the course of the study, indicative of sickness, although there were no significant differences between genotypes; however, in general male mice showed more weight loss than female mice, consistent with their differences in survival rate.

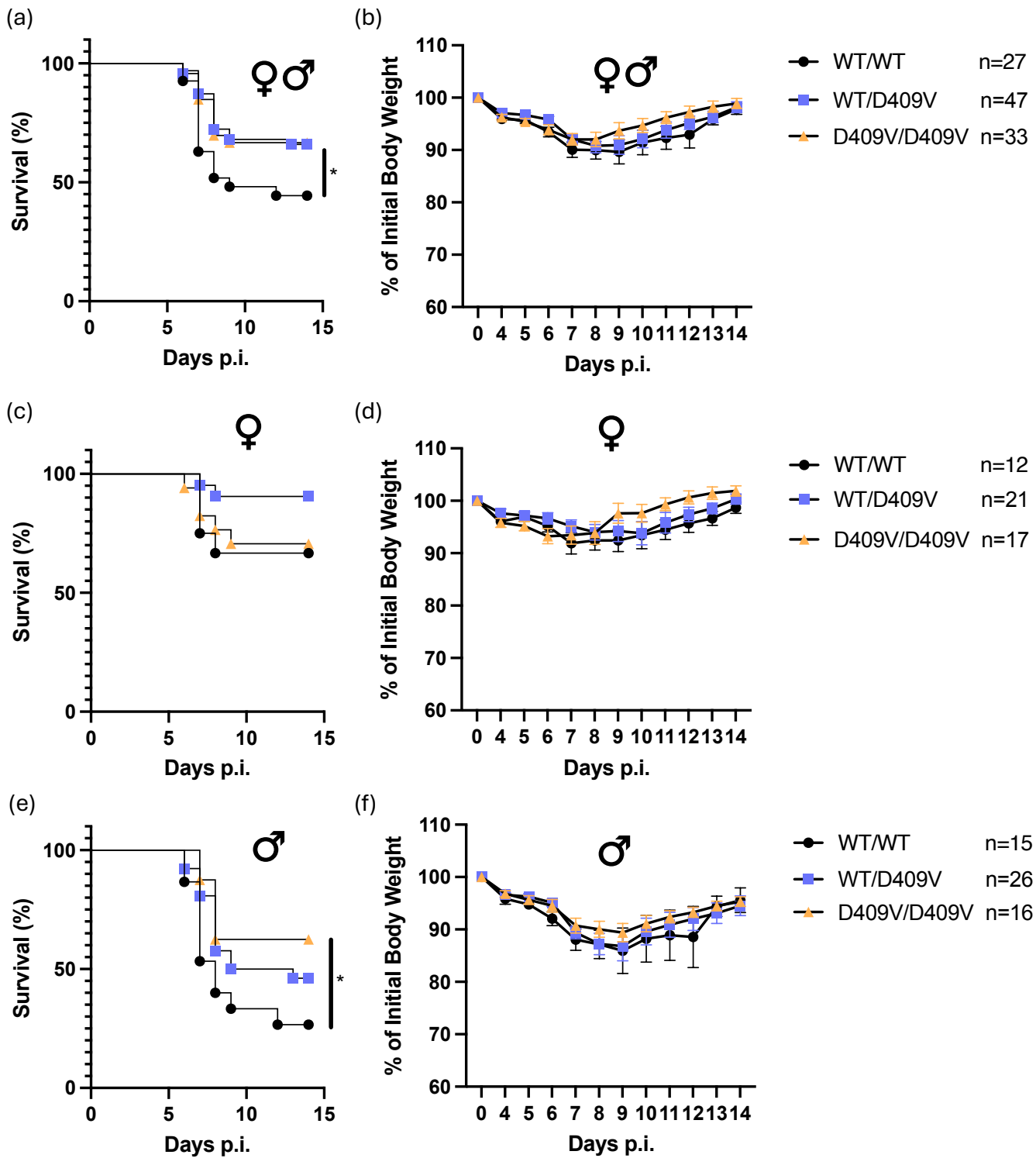

(a)
♀♂
Survival (%)
Days p.i.
*
(b)
♀♂
% of Initial Body Weight
Days p.i.
WT/WT n=27
WT/D409V n=47
D409V/D409V n=33
(c)
♀
Survival (%)
Days p.i.
(d)
♀
% of Initial Body Weight
Days p.i.
WT/WT n=12
WT/D409V n=21
D409V/D409V n=17
(e)
♂
Survival (%)
Days p.i.
*
(f)
♂
% of Initial Body Weight
Days p.i.
WT/WT n=15
WT/D409V n=26
D409V/D409V n=16

Fig. 4.3: Female Sex and *Gba1* p.D409V Knock-in Alleles Confer Survival Benefits in Mice During Infection by Vesicular Stomatitis Virus. Wild-type (WT/WT), heterozygous (WT/D409V), and homozygous (D409V/D409V) Gba1 p.D409V knock-in littermates aged 6-10 weeks were nasally inoculated with a dose of $3x10^3$ PFU of vesicular stomatitis virus (VSV) and monitored for a pre-determined moribund state and their daily weight for 14 days post inoculation. Data are presented as sexes pooled (♀♂) (**a, b**), female mice only (♀) (**c, d**), and as male mice only (♂) (**e, f**). Survival is graphically displayed as percent survival against days post inoculation (**a, c, e**), and weights are displayed as percent of initial body weight against days pays post inoculation (**b, d, f**). Statistical methods used: log-rank (Mantel-Cox) test was used to analyze survival rates. One-Way ANOVA with Tukey post hoc-test was used between genotypes on each individual day for weight changes. P-value <0.05 (*).

VSV viral load is decreased in the lungs of female heterozygous Gba1 p.D409V mice.

To investigate the significant protection observed in survival following VSV infection in male Gba1 p.D409V mice, we measured titres of VSV in the olfactory bulb (OB) (**Fig. 4.4a**), the brain without the OB (**Fig. 4.4b**), and the lungs (**Fig. 4.4c**) at 2dpi in female and male mice. Each of these tissues have been shown to have viral titres of VSV at this time point (Nair et al., 2014). Furthermore, the OB is the first site of infection upon nasal inoculation, and the brain and lungs are the main sites of the disease process (*i.e.,* encephalitis and pneumonitis, respectively). Examining these tissues from male mice, we did not observe any differences in viral titres between genotypes that could be linked to the heightened survival in homozygous Gba1 p.D409V male mice (**Fig. 4.3a-c**; ♂ graphs). Surprisingly, we did identify a significant difference in viral titre in the lungs (but not OB or brain) of female mice ($P < 0.05$; **Fig. 4.4a-c**; ♀ graphs), where female heterozygous mice had significantly lower VSV titres in the lungs than did homozygous and wild-type female mice. This is consistent with the trend observed of female Gba1 p.D409V heterozygous mice having increased survival (**Fig. 4.3a**).

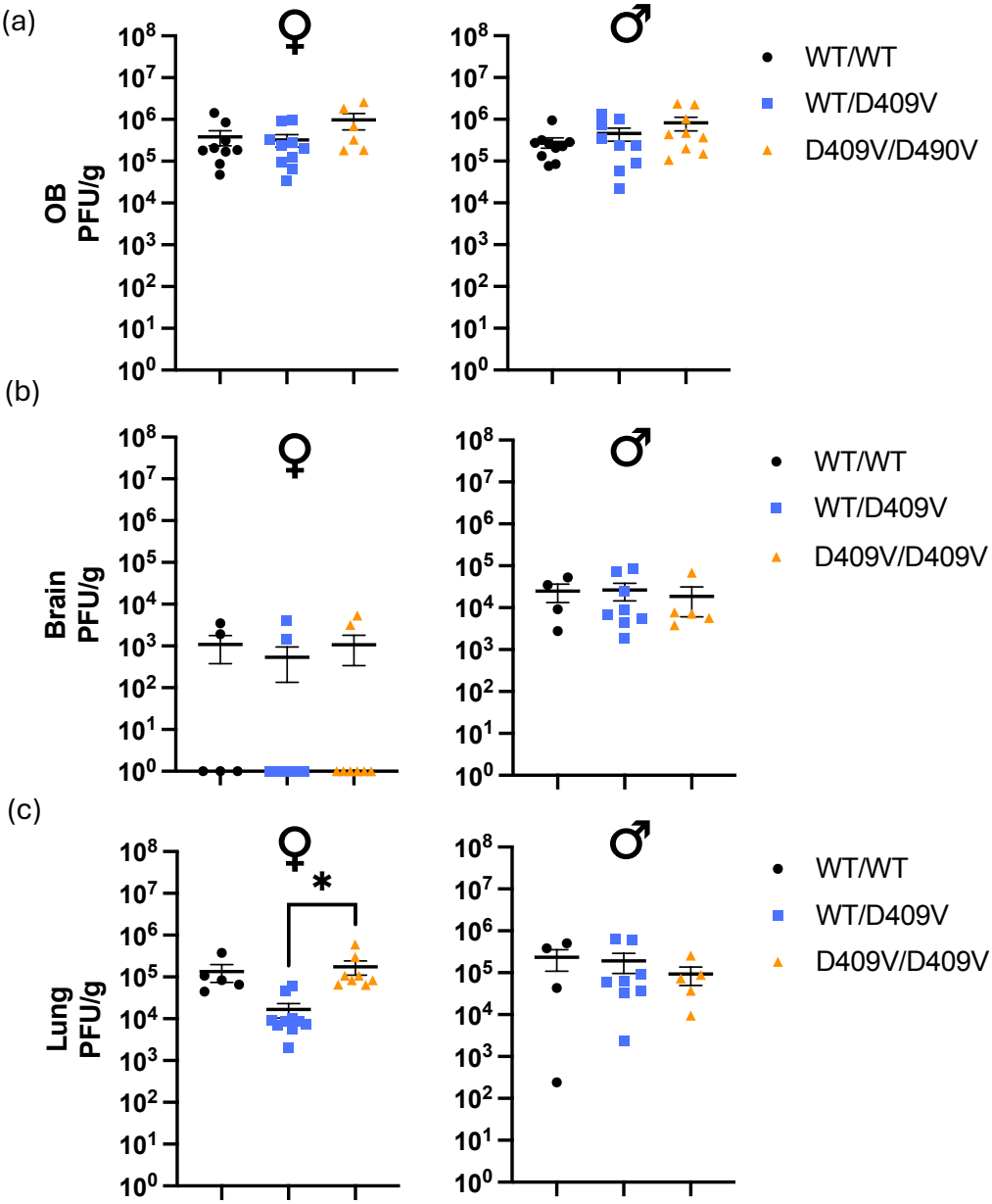


Fig. 4.4: Organ Tropism, Sex and *Gba1* Genotype Determine Viral Loads in Adult Mice During Acute Infection with Vesicular Stomatitis Virus. Adult wild-type (WT/WT), heterozygous (WT/D409V), and homozygous (D409V/D409V) Gba1 p.D409V knock-in mutant littermates were nasally inoculated with a dose of $3x10^3$ PFU of vesicular stomatitis virus (VSV; as in Fig. 4.3) and sacrificed at 2 days post inoculation. Titres are shown as PFU/g of tissue. Olfactory bulbs (OB) in isolation (**a**), brains without olfactory bulbs (**b**), and lungs (**c**) were examined. Genotypes are compared for female mice alone (left panels, ♀), and male mice alone (right panels, ♂). Each point represents one animal. Error bars represent mean ± SEM. Statistical analysis included one-Way ANOVA with Tukey post-hoc tests. P-value <0.05 (*).

In vitro *glucocerebrosidase activity is altered following VSV infection in a sex- and organ-dependent manner.*

The changes in viral responses (observed as survival and titres) in mice carrying a mutation in *Gba1* next led to us ask what impact the infection itself had on GCase activity across the three genotypes. We measured GCase activity in the OB, the brain without the OB, and the lungs in both mock- and VSV-infected animals at 2dpi (**Fig. 4.5**). The levels of GCase activity in mock- and VSV-infected animals are displayed for female and male mice of wild-type, heterozygous, and homozygous genotypes in the OB (**Fig. 4.5a**), the brain without the OB (**Fig. 4.5d**), and the lungs (**Fig. 4.5g**). An unpaired student t-test was performed to identify any significance in the change from mock- to infected-state within pairs of the same sex and genotype. A significant difference was only identified in the OB of female homozygous Gba1 p.D409V mice, where GCase activity was significantly decreased following VSV infection ($P < 0.01$). As expected, GCase activities were markedly decreased in all homozygous Gba1 p.D409V tissues, and also decreased in heterozygous p.D409V tissues, to a lesser extent. These data can be found compiled in **Supplemental Table 4.1**.

To probe for further, possibly subtle genotypic effects in GCase activity in response to VSV infection, GCase activity data are further plotted as a ratio of activity in infected tissue relative to mock-infected tissue and then normalized to this ratio in wild-type mice. These data represent GCase activity changes in response to infection within each genotype, compared to the change observed in wild-type mice (**Fig. 4.5b, c, e, f, h, i**). In female mice, there were no genotypic differences in GCase activity from mock-to-infection in the brain (**Fig. 4.5e**); however, female wild-type mice had a significantly higher mock-to-infection increase in GCase activity than female homozygous Gba1 p.D409V mice in both the OB and the lungs ($P < 0.05$; **Fig. 4.5b, h**). In male

mice, there were no genotypic differences in GCase activity following infection in the OB or the lungs (**Fig. 4.5c, i**); however, in the brain, heterozygous Gba1 D.409V male mice had significantly higher GCase activity following infection than wild-type mice ($P < 0.01$; **Fig. 4.5f**).

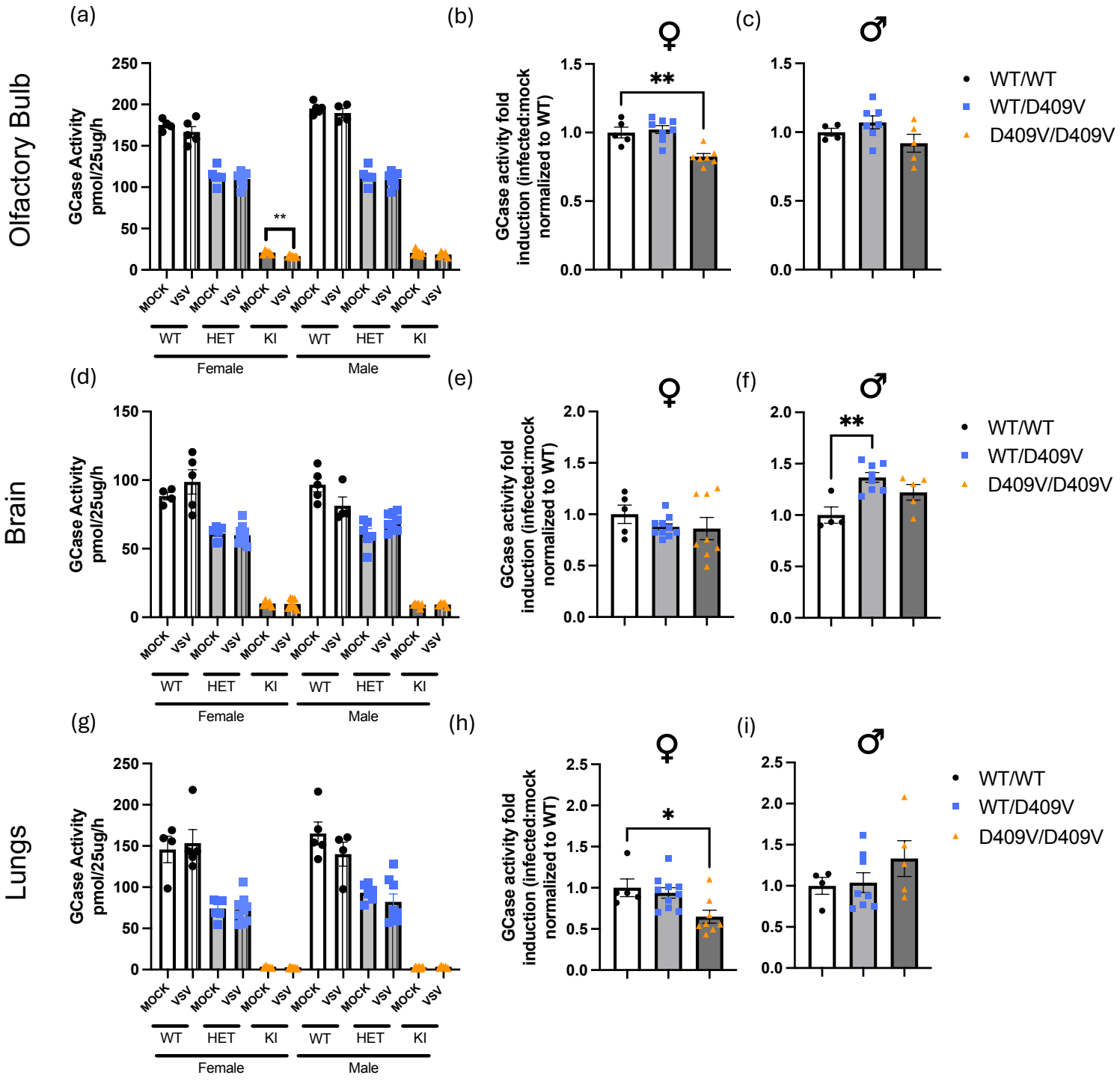


Fig. 4.5: GCase Activity Measured *In Vitro* is Altered in Gba1 p.D409V Knock-in Mice in a Sex-and Organ-Specific Manner During Acute Infection with Vesicular Stomatitis Virus. Wild-type (WT/WT), heterozygous (HET; WT/D409V), and homozygous (KI; D409V/D409V) Gba1 p.D409V knock-in littermates were nasally inoculated with 50 µL of PBS (mock) or a dose of $3x10^3$ PFU of vesicular stomatitis virus (VSV) (as in Fig. 4.3). GCase activity was measured in organs collected at 2dpi via standardized *in vitro* GCase assay. Activity values from the three genotypes, male and female mice, and mock- and VSV-infected mice is displayed from olfactory bulbs in isolation (**a**), brains without the olfactory bulb (**d**), and the lungs (**g**). Data are also shown as a ratio of VSV-inoculated *vs.* mock-treated samples and normalized to wild-type (WT/WT) (*i.e.,* [value at infection] / [average value at mock] with WT/WT normalized to = 1.0) for olfactory bulbs

(**b**), brains (**e**), and the lungs (**h**) in both female mice (♀) and male mice (♂). Error bars represent mean ± SEM. Statistical significance was determined in (**a, d, g**) only between mock- and infected-within the same sex and genotype using unpaired t-test. Statistical significance was determined in (**b, e, h**) using one-way ANOVA with Dunnett post-comparison. P-value <0.05 (*), P-value <0.01 (**).

Gba1 ***p.D409V heterozygous and homozygous mutations alter cytokine and chemokine levels following VSV infection in a sex-dependent manner.***

To further investigate the response to VSV infection and a possible reason for the increased survival rate seen in homozygous Gba1 p.D409V males, we next measured the protein abundance of an array of cytokines and chemokines in the serum of 2dpi mock- and VSV-infected mice. Of the 32 cytokines and chemokines analyzed, Fig. 4.6 shows six cytokines/chemokines of interest in sera from female (**Fig. 4.6a-f**) and male (**Fig. 4.6g-l**) mice. These six cytokines/chemokines were chosen because their levels have either been linked to GD in humans (Michelakakis et al., 1996; Allen et al., 1997) or, we have previously identified changes in these markers associated with a neurotropic infection *in vitro* (Shutinoski et al., 2019; Sanyal et al., 2020). For each cytokine/chemokine, only comparisons within genotypes between mock- and infected-levels (shown in black) and between genotypes of the same treatment groups (shown in red) were made. The remainder of the analyzed cyto-/chemokines can be found in **Supplemental Fig. 4.1.** For female mice, each group had n=4-6 animals, and for male mice each group had n=3-9 animals.

In both male and female mice, all infected mice had a significant induction of IL-6 from mock to VSV infection, as expected ($P < 0.001$; **Fig. 4.6a, g**). However, interestingly, female VSV-infected homozygous Gba1 p.D409V mice had significantly more IL-6 than infected heterozygous littermates ($P < 0.001$; **Fig. 4.6a**).

For TNFα, in female mice, only infected Gba1 p.D409V heterozygous mice differed significantly from their mock-infected counterparts, though the other genotypes trended strongly ($P < 0.01$; **Fig. 4.6b**). All infected male mice had significantly more TNFα than each of the mock-infected mice, except Gba1 homozygous males, which had generally lower levels of TNFα after infection ($P < 0.001$; **Fig. 4.6h**).

The chemokine RANTES was significantly higher in infected samples than in mock samples for all male mice, but not in female mice ($P < 0.001$; **Fig. 4.6c, i**). There is also an infection effect on the macrophage growth factor, M-CSF, in male and female mice, but this was strongest and only significant in female Gba1 p.D409V heterozygous mice ($P < 0.05$; **Fig. 4.6d, j**). The chemokine IP-10 was significantly higher in all VSV-infected samples than mock samples in both male and female samples ($P < 0.001$; **Fig. 4.6e, k**).

Finally, in measurements of the chemokine KC, both wild-type and homozygous Gba1 p.D409V female VSV-infected samples were significantly higher than all mock samples; however, heterozygous Gba1 p.D409V female infected samples were not significantly higher than any mock-infected samples ($P < 0.001$; **Fig. 4.6f**). Indeed, KC abundance was significantly higher in homozygous mutant infected female mice than in their heterozygous infected littermates ($P < 0.05$; **Fig. 4.6f**). In males, Gba1 p.D409V heterozygous infected mice had significantly higher KC levels than their mock-infected counterparts ($P < 0.01$; **Fig. 4.6l**).

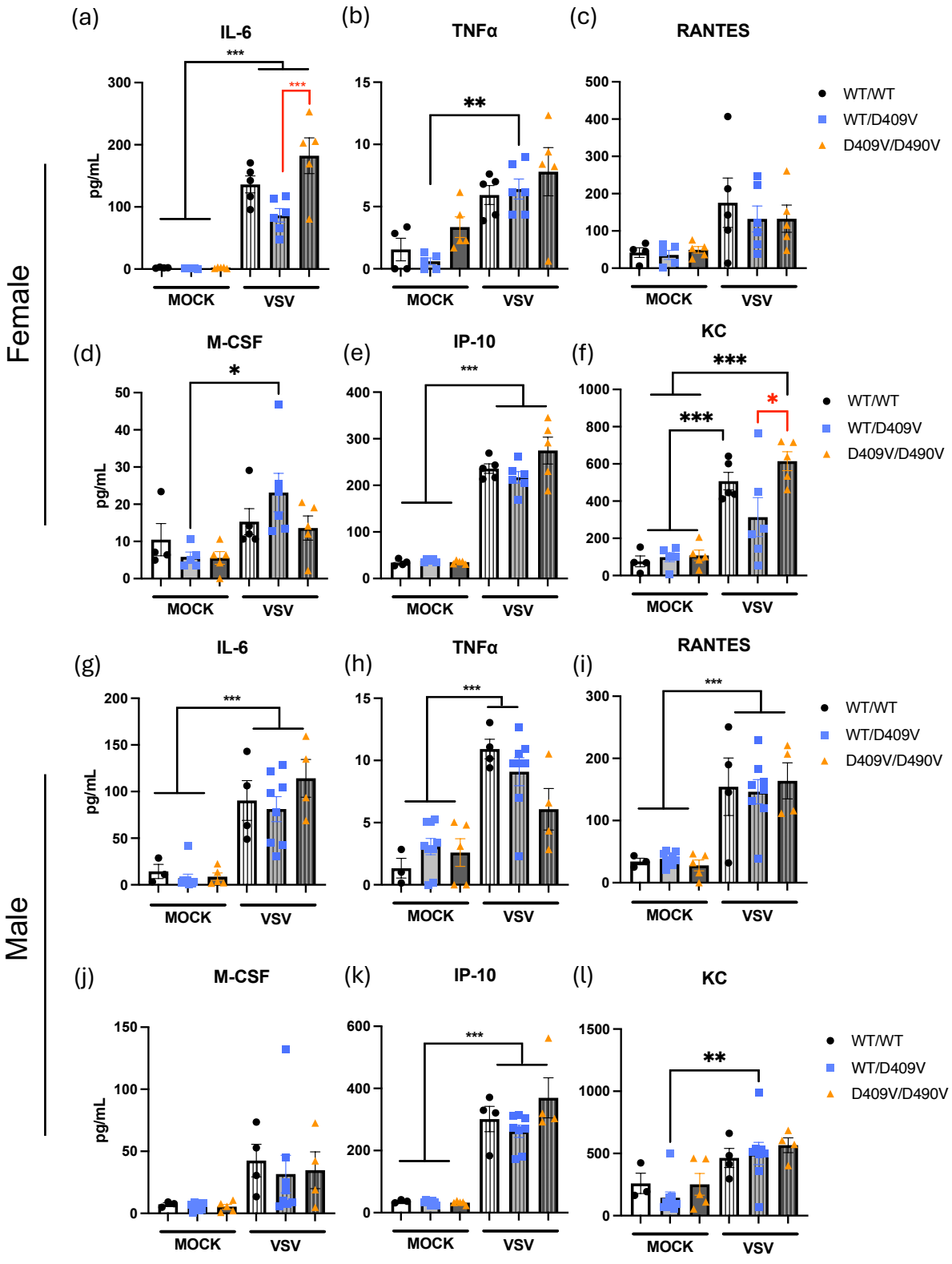

Female
Male
(a)
IL-6
(b)
TNFα
(c)
RANTES
(d)
M-CSF
(e)
IP-10
(f)
KC
(g)
IL-6
(h)
TNFα
(i)
RANTES
(j)
M-CSF
(k)
IP-10
(l)
KC
pg/mL
MOCK
VSV
WT/WT
WT/D409V
D409V/D490V

Fig. 4.6: *Gba1* p.D409V Knock-in Alleles Modify Select Cytokines/Chemokines in an Infection- and Sex-Dependent Manner Following Inoculation with Vesicular Stomatitis Virus. Adult wild-type (WT/WT), heterozygous (WT/D409V), and homozygous (D409V/D409V) mice aged 11-13 weeks were nasally inoculated with 50 μL of PBS (mock) or a dose of $3x10^3$ PFU of vesicular stomatitis virus (VSV), sacrificed at 2dpi, and sera were collected by cardiac puncture. Multiplex ELISA was used to measure an array of serum cytokines and chemokines in each animal. Six cytokines and chemokines are presented here: IL-6 (**a, g**), TNFα (**b, h**), RANTES (**c, i**), M-CSF (**d, j**), IP-10 (**e, k**), and KC (**f, l**). For remainder, see **Suppl. Fig. 4.1**. Data are separated into graphs for female mice (**a-f**) and male mice (**g-l**). Statistical bars in black identify those values that are significantly different as a result of infection; bars in red denote those that differ significantly due to genotype within a treatment group. Error bars represent mean ± SEM. Statistical tests used: one-way ANOVA with Tukey's post-hoc tests. P-value <0.05 (*), P-value <0.01 (**), P-value <0.001 (***).

α-Synuclein, phosphorylated tau protein, and Lrrk2 levels are unchanged following VSV-infection in Gba1 p.D409V mice at 2dpi.

We have previously identified a role for two other PD-linked genes in host defence: *Snca* (encoding α-synuclein) (Tomlinson et al., 2017) and *Lrrk2* (Shutinoski et al., 2019, Lunn et al., *in prep*) and we and others have shown increased protein levels of both α-synuclein and Lrrk2, as well as increased tau phosphorylation in response to infections *in vivo* (Tomlinson et al., 2017; Alam et al., 2022; Beatman et al., 2016; Shutinoski et al., 2019; Gardet et al., 2010; Hakimi et al., 2011; Sy et al., 2011; Lunn et al., *in prep*). We therefore next investigated whether abundances of these proteins were altered in the infected OBs of *Gba1* mutant mice at 2dpi, which is the timepoint of highest viral load in this tissue. α-Synuclein protein concentration was measured via sandwich ELISA in both mock- and VSV-infected olfactory bulbs at 2dpi, and we saw no infection- or genotype-dependent differences at this timepoint (**Fig. 4.7a-c**).

Next, we assayed the neuropathology-associated protein, phosphorylated tau (p-Tau; Ser202, Thr205; AT8). We have previously found a strong, significant infection-dependent increase in p-Tau following VSV infection at 6 weeks post infection in wild-type mice, and to a lesser degree at 6dpi (Lunn et al., *in prep*). Therefore, we measured p-Tau by Western blot in hemibrain (+OB) protein extracts. While total tau was present in all samples, p-Tau was undetectable at 2dpi in the OB, including mock and infected tissues (**Fig. 4.7d**); as such densitometry-based quantification was not possible. Male and female mice were both used for analyses of p-Tau and total tau, as indicated on the blot, and no differences were observed between sexes.

Lastly, we measured pSer935-Lrrk2 (pLrrk2) and total Lrrk2 protein abundance via Western blotting (**Fig. 4.7e-g**). Phosphorylation at this site depends on autophosphorylation and

thus routinely used as an indirect measure of Lrrk2 kinase activity (Steger et al., 2016). We did not uncover any differences across genotypes or treatments (mock *vs.* VSV) in pLrrk2 or Lrrk2 protein abundance following densitometric analysis (n=4 per group, per sex) (**Fig. 4.7f, g**). We also did not observe any significant differences between sexes regarding pLrrk2 or Lrrk2 protein abundance.

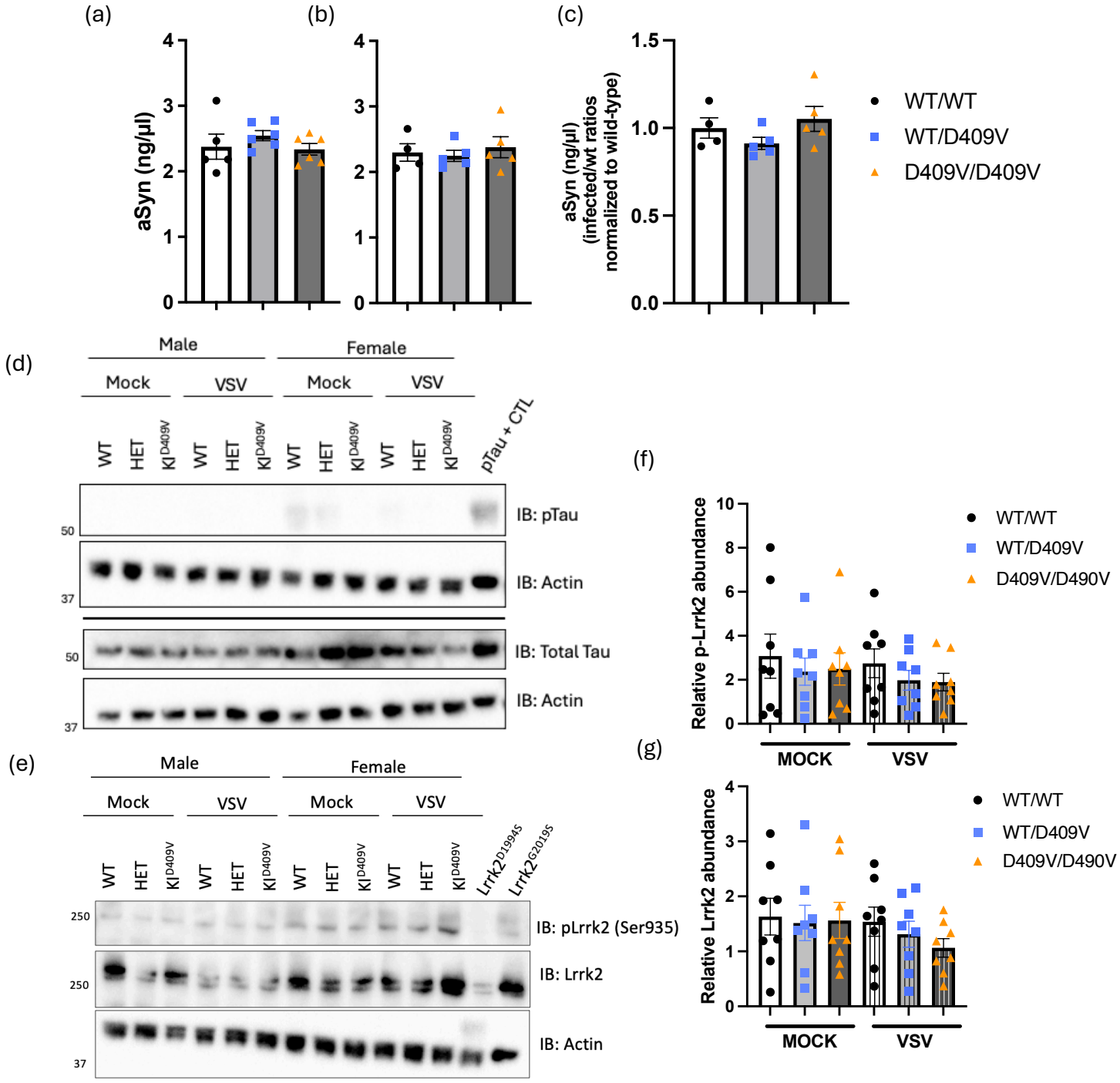


Fig. 4.7: Total α-Synuclein, p-Tau, and Lrrk2 Levels are Unchanged During Acute Vesicular Stomatitis Virus Infection in Gba1 p.D409V Mutant Mice. Adult (11-13 week-old) wild-type (WT/WT), heterozygous (HET; WT/D409V), and homozygous (KI^{D409V}; D409V/D409V) Gba1 p.D409V knock-in littermates were nasally inoculated with 50 µL of PBS (mock) or a dose of $3x10^3$ PFU of vesicular stomatitis virus (VSV) and sacrificed at 2dpi. Brain extracts were prepared by using 1% Triton-X-containing buffer. α-Synuclein was measured by sandwich ELISA (**a, b, c**). Samples from mock- (**a**) and VSV- (**b**) inoculated samples are shown as α-synuclein concentration in ng/µl. Ratios for VSV:mock values, normalized to wild-type (WT/WT) are shown in (**c**). Each

point represents one animal. Brain extracts were also used to measure phosphorylated tau (pTau; at Ser202, Thr205) and total tau by Western blotting and representative blots for pTau and tau are shown (the same samples were run for each). [The positive pTau control is a VSV-infected Lrrk2 p.G2019S mutant brain sample at 6 weeks post inoculation] (**d**). (**e-g**) Brain proteome was also used to measure phosphophorylated Lrrk2 (Ser935) and total Lrrk2 by Western blotting and a representative blot is displayed (**e**). Individual protein abundances were measured via densitometry (n=4 per group per sex). All samples were normalized to actin loading control, and to an internal blot control (Lrrk2 p.G2019S) to combine samples from multiple Western blots. A Lrrk2 p.D1994S sample is used as a negative control for pLrrk2. Quantification shows data sets for sexes combined (**f, g**). Error bars represent mean ± SEM. Statistical methods included one-way ANOVA with Tukey post-hoc comparison. No statistically significant differences were found.

Discussion

Herein, we have demonstrated that the p.D409V knock-in mutation of *Gba1*, which causes decreased GCase enzymatic activity, confers a degree of protection against nasally acquired, VSV-induced encephalitis in adult mice with a male sex bias. Furthermore, we identified a heterozygous *Gba1* p.D409V allele-dependent effect on viral titres in the lungs of female mice and a VSV exposure-dependent effect on GCase activity for homozygous mice in the tissues that are first infected, namely the olfactory bulb and lungs, also in a female sex-dependent manner. Interestingly, we did not identify any significant, *Gba1* p.D409V-mediated effects on H1N1- or ST-induced disease outcomes, suggesting that the *Gba1* p.D409V variant may exhibit anti-microbial effects in a pathogen- and organ-dependent manner. These results suggest a role for the PD-linked gene *GBA1* in host defences against an acute, neurotropic, RNA virus-based infection. These findings, together with a role for *Lrrk2* and *Snca* also protecting mice against neurotropic viral infections (Shutinoski et al., 2019; Tomlinson et al., 2017; Lunn et al., *in prep*), support a model in which dysregulated or altered immune response to microbial insults, either during an isolated event or encountered over a lifetime could contribute to disease risk and onset in PD. Potential mediators of lasting effects could entail reactive oxygen species-based molecules, as we have observed in *Lrrk2* studies, and chronically dysregulated pro-inflammatory lipids, which will be addressed in future studies (Shutinoski et al., 2019).

We studied three pathogens with target organs where GCase activity is relatively high in wild-type mice: the lungs (H1N1), the spleen (ST), and the brain (VSV) (Liou et al., 2019). When measuring GCase activity levels *in vitro* in each of these organs in the Gba1 p.D409V mouse model, we observed that homozygous Gba1 p.D409V mice had ~1% of wild-type GCase activity in the lung, ~2% in the spleen, and ~15% in the brain. Heterozygous Gba1 p.D409V mice had

~50% of wild-type GCase activity in both the lung and the spleen, and ~75% in the brain (data not shown). First, we employed the lung-directed H1N1 infection in adult mice. Importantly, Braak and Del Tredici posit that a critical point of initiation for the aggregation of misfolded α-synuclein is the olfactory system, and as such each of our viruses were administered via nasal inoculation to primarily infect the nasal cavity and olfactory epithelium.

In the H1N1 paradigm, we did not find any differences in survival between wild-type and Gba1 p.D409V mutant mice, which was surprising, given that *GBA1* knockout, as well as knockout of the opposing enzyme to GCase, glucosylceramide synthase, was shown to limit H1N1 infection *in vitro* (Drews et al., 2019, Soudani et al., 2019; Vitner et al., 2021; Drews et al., 2020). The authors of the latter study concluded that any disturbance in GCase-related lipid homeostasis, in either direction, may impact viral infectivity (Drews et al., 2020). Our present data suggest that at the whole organism level, perturbations in GCase (as a result of the *Gba1* p.D409V mutation) did not translate to altered survival outcomes following nasal H1N1 infection. We have not yet assessed what impact this mutation has on lipid homeostasis in these mice. Of note, we recorded over 90% survival in all mice following H1N1 infection and therefore, this may also reflect a lack of sensitivity in this assay.

This high survival rate following a viral H1N1 infection model lent itself to a serial infection paradigm, specifically with a bacterial pathogen exposure as a second hit. This serial infection model is well-established, as the engagement of the interferon response in the primary viral infection renders organisms more highly susceptible to a secondary bacterial infection (reviewed in: Rynda-Apple et al., 2015). We hypothesized that the Gba1 mutant mice may have an altered immune and inflammatory response during the first viral infection, which could lead to altered health outcomes following a subsequent infection with ST. However, in this case, H1N1 pre-

infection was insufficient in eliciting genotypic differences in splenic bacterial load, which may in part be due to the extended period (four weeks) between the two infections. Consistent with this, we saw no *Gba1*-dependent difference in outcomes following an isolated ST infection. Of note, ST infection is uniformly lethal, hence why we chose to collect spleens for bacterial burden analysis at 5dpi. However, a time-to-death experiment may have uncovered differences in time-to-death intervals between genotypes, especially given the extremely high expression of *Gba1* in the spleen, which is highly targeted during ST-induced sepsis.

We next investigated the outcomes of a virus with direct effects on brain health. As such, we employed a neurotropic virus (VSV) that first infects olfactory sensory neurons of which axons project to glomeruli in the olfactory bulb (Nair et al., 2014). We found that heterozygous and homozygous Gba1 p.D409V mice survived significantly better than wild-type mice. When separating these data based on sex, we found that heterozygous female mice had a non-significant survival advantage, whereas male homozygous mice had a significant survival advantage against VSV compared to wild-type mice. These data suggest that that at least one *Gba1* p.D409V knock-in allele may confer a protective function in response to VSV infection. Given the established role for lipid species in host defences, it is conceivable that GCase (and mutations within) could influence host defences against viral infections (Mazzon and Mercer, 2014; Heaton and Randall, 2011). The observed survival benefit conferred by the Gba1 p.D409V variant against neurotropic VSV-induced encephalitis but not against two peripherally restricted infections (H1N1 and ST) likely speaks to pathogen- and organ-specificity in a role for GCase-linked activity in pathogen response.

The lack of differences in viral load in the brains of these mice did not correlate with the trends observed in survival rates. This suggests that *Gba1* mutations might not affect the control

of viral spread and replication but may instead be involved in mechanisms that reduce neuronal cell death in response to VSV infection, which is similar to what has been reported in a GD mouse model following neurotropic Sindbis infection (Melamed et al., 2020). Heterozygous female mice exhibited lower viral loads in the lungs in our infection model using VSV, which was consistent with the observed survival trends.

We hypothesized that the survival benefit against VSV-induced encephalitis in Gba1 p.D409V male mice may be due to an alteration in the number of peripheral inflammatory mediators that enter the brain. As such, we measured cytokine and chemokine abundance in sera from venous blood. Although we did find alterations in cytokine signalling that were both sex- and infection-, as well as genotype-dependent, we did not find a definitive perturbation in these circulating inflammatory mediators that could have explained the survival benefit observed. Of note, IL-6, TNFα, and M-CSF have all be linked to GD in human serum, at increased levels (Michelakakis et al., 1996; Allen et al., 1997). Contrarily, a recent study demonstrated that both homozygous and heterozygous Gba1 p.D409V knock-in astrocytes had markedly decreased IL-6, TNFα, and IP-10 than wild-type mice in naïve and LPS-induced states (Sanyal et al., 2020).

Not only did the *Gba1* p.D409V variant affect disease outcomes of VSV infection, but we also found altered GCase activity downstream of VSV infection. To assess genotype-dependent differences in GCase activity after infection, a ratio of infected-to-mock activity change was calculated and subsequently normalized to wild-type activity, as a measure of relative increases or decreases in mutant mice following infection compared to changes in wild-type mice. In the brain without the OB, the ratio of infected-to-mock of GCase activity was significantly higher in male heterozygous animals, with male homozygous mice following a similar, yet insignificant, trend compared to male wild-type animals. Female wild-type mice had a significantly higher ratio of

GCase activity from infected-to-mock than female homozygous Gba1 p.D409V mice in both the lungs and the OB (but not the whole brain). Importantly, when considering raw values, only the olfactory bulbs of homozygous mutant female mice had a significantly different GCase activity in infected samples compared to mock samples. These changes likely affect downstream lipid metabolism which is currently being pursued.

Our team and others have highlighted a role for both α-synuclein (*Snca*) and Lrrk2 in host defences against encephalitic viral infections (Tomlinson et al., 2017; Shutinoski et al., 2019; Lunn et al., *in prep*) and have now demonstrated a role for *Gba1*. To probe for connections between these three PD-linked genes, we investigated levels of both α-synuclein and Lrrk2 following VSV infection in the Gba1 mutant mice. We did not identify any changes in Lrrk2 abundance or level of auto-phosphorylation (indicative of its kinase activity) dependent on VSV infection nor dependent on the *Gba1* p.D409V variant. There are reports that Lrrk2 and GCase interact in inflammatory responses. Sanyal et al. (2020) demonstrated that a pharmacological Lrrk2 kinase inhibitor could rescue cytokine deficits following LPS insult in mutant Gba1 p.D409V astrocytes. Our results suggest that mutant GCase does not affect levels of Lrrk2 or pLrrk2 following a VSV infection at 2dpi, which supports that instead Lrrk2 activity is likely upstream of GCase (Kedariti et al., 2022; Sanyal et al., 2020). Similarly, levels of α-synuclein were not changed at this timepoint, despite a demonstrated link between GCase dysfunction and α-synuclein misprocessing and reports of an age-associated change in α-synuclein in Gba1 p.D409V mice (Mazzulli et al., 2011, Cullen et al., 2011; Sardi et al., 2011; Clarke et al., 2019). It is possible that the long half-life of α-synuclein (over one week) meant that the interval between infection and tissue collection (48 hours) was too short to measure detectable changes in α-synuclein (in either direction) (Mollenhauer et al., 2008).

In parallel work, we have shown that VSV infection can lead to sustained tau hyperphosphorylation (Lunn et al., *in prep*). In the present study, we did not detect p-Tau at 2dpi in VSV-infected mice. Together with the aforementioned study, in which p-Tau was detectable at low levels at 6dpi and significantly increased at 6 weeks post-VSV infection, these data suggest that tau phosphorylation may not be part of an acute response to VSV invasion and replication, but may occur secondary to cell injury and potentially persist well beyond the acute replication phase of the virus (Lunn et al., *in prep*). Similar to α-synuclein, tau protein has a very long half-life in the brain, and therefore the short time interval between infection and tissue collection may not have yet unmasked changes in the protein (Hier et al., 2022).

Important future steps of this project will be to understand the mechanistic and downstream effects of the *Gba1* p.D409V variant on lipid metabolism following VSV infection. As such, we have collected plasma from VSV-infected mice at 2dpi for lipid species analysis. This will allow us to examine whether the lipidome is altered and/or involved in the initial immune response during the acute time of infection, and if the *Gba1* p.D409V genotype has an impact. This may inform indirect anti-viral properties of GCase, namely its involvement in cholesterol metabolism, as infectivity of both influenza A virus and VSV are impacted by modulations in cholesterol (Li et al., 2022; Wang et al., 2009). Secondly, future studies will investigate cellular mechanisms using primary cell cultures *i.e.*, isolation of resident macrophages from the lung and brain to understand how GCase activity changes in response to infection and how manipulation of GCase activity and protein folding (*e.g.*, through pharmacological agents) can affect VSV replication and cell death.

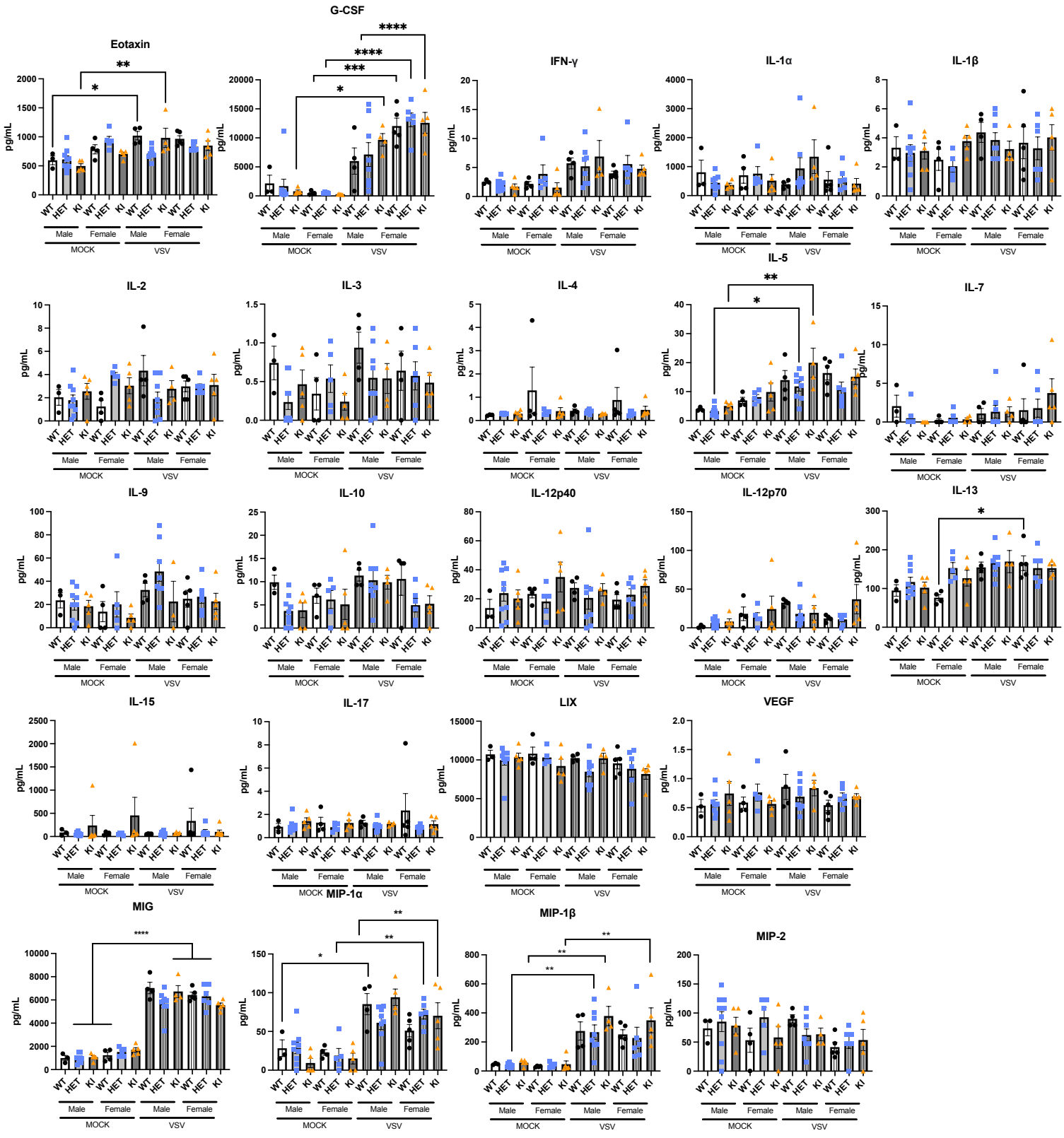
The study presented here has highlighted a potential role for GCase in host response to neurotropic infections. In mice, mutations in *Gba1* perturbed the course of illness in an acute VSV infection model. Additionally, *in vitro* levels of GCase activity, cytokine and chemokine response,

and viral titre all had sex-dependent outcomes following VSV infection in mutant Gba1 mice. This work now demonstrates the ability of another PD-linked gene (*Gba1*) to affect disease outcomes following a neurotropic virus, adding to our previously published work on *Snca* and *Lrrk2* (Tomlinson et al., 2017; Shutinoski et al., 2019; Lunn et al., *in prep*). Together, these data highlight a possible relationship between PD risk genes (*i.e.*, *Gba1*) and altered immune responses to viral infections, which may contribute to disease risk.

Supplementary Materials

Supplemental Table 4.1: GCase Activity in Mock- and VSV-Infected Olfactory Bulbs, Brains Without Olfactory Bulbs, and Lungs from Wild-Type (WT/WT), Heterozygous (WT/D409V), And Homozygous (D409V/D409V) Gba1 p.D409V Knock-In Mice At 2dpi. Data corresponds to that presented in **Fig. 4.5** (**a, d, g**). Statistical significance was determined only between mock- and infected-samples of the same sex and genotype using unpaired t-test, where P-value <0.05 (*), P-value <0.01 (**). SEM: standard error of the mean.

Organ	Sample	Treatment	Mean	SEM	Sample Size (n)	Significance Between Groups
Olfactory Bulb	Female WT/WT	Mock	175.2	3.434	4	n.s.
		VSV	166.7	6.516	5	
	Male WT/WT	Mock	195.2	3.146	5	n.s.
		VSV	189.7	5.33	4	
	Female WT/D409V	Mock	113.2	4.084	6	n.s.
		VSV	110	3.097	8	
	Male WT/D409V	Mock	132.2	3.678	5	n.s.
		VSV	137.7	5.999	7	
	Female D409V/D409V	Mock	21.02	0.9741	5	**
		VSV	16.49	0.4557	7	
	Male D409V/D409V	Mock	20.81	1.361	6	n.s.
		VSV	18.6	1.313	5	
Brain	Female WT/WT	Mock	88.31	2.726	4	n.s.
		VSV	98.66	8.868	5	
	Male WT/WT	Mock	96.6591	5.178	5	n.s.
		VSV	81.259	6.459	4	
	Female WT/D409V	Mock	61.11	2.189	6	n.s.
		VSV	59.86	2.102	10	
	Male WT/D409V	Mock	60.59	4.065	6	n.s.
		VSV	69.58	2.414	8	
	Female D409V/D409V	Mock	10.1	0.8371	5	n.s.
		VSV	9.717	1.219	8	
	Male D409V/D409V	Mock	9.103	0.5611	6	n.s.
		VSV	9.347	0.5776	5	
Lungs	Female WT/WT	Mock	145.7	16	4	n.s.
		VSV	153.4	16.5	5	
	Male WT/WT	Mock	165.2	13.93	5	n.s.
		VSV	140.2	14.57	4	
	Female WT/D409V	Mock	73.98	4.93	6	n.s.
		VSV	73.08	4.935	10	
	Male WT/D409V	Mock	93.29	4.268	6	n.s.
		VSV	82.19	9.556	8	
	Female D409V/D409V	Mock	3.099	0.4738	5	n.s.
		VSV	2.118	0.2564	8	
	Male D409V/D409V	Mock	2.757	0.4789	6	n.s.
		VSV	3.116	0.5094	5	


Eotaxin
G-CSF
IFN-γ
IL-1α
IL-1β
IL-2
IL-3
IL-4
IL-5
IL-7
IL-9
IL-10
IL-12p40
IL-12p70
IL-13
IL-15
IL-17
LIX
VEGF
MIG
MIP-1α
MIP-1β
MIP-2
pg/mL
WT HET KI WT HET KI WT HET KI WT HET KI
Male Female Male Female
MOCK VSV

Supplemental Fig. 4.1: Additional Results for Cytokine and Chemokine Analyses in Gba1 p.D409V Mutant Mice Following VSV Infection. Adult wild-type (WT/WT), heterozygous (WT/D409V), and homozygous (D409V/D409V) mice aged 11-13 weeks were nasally inoculated with 50 μL of PBS (mock) or a dose of $3x10^3$ PFU of vesicular stomatitis virus (VSV), sacrificed at 2dpi, and sera were collected by cardiac puncture. Multiplex ELISA was used to measure an array of serum cytokines and chemokines in each animal. Error bars represent mean ± SEM. Statistical tests used: one-way ANOVA with Tukey's post-hoc tests. P-value <0.05 (*), P-value <0.01 (**), P-value <0.001 (***).

Chapter 5: General Discussion

1. Summary

Parkinson's disease is a complex disease, with heterogenous symptomatology and disease presentation. The disease can be subdivided into familial (*i.e.,* genetic) and idiopathic (*i.e.,* sporadic) forms. Many disease genes have been linked to PD causality and/or risk and many environmental risk factors have been positively correlated to PD (Schlossmacher et al., 2017; Li et al., 2022). Hawkes, Braak, and Del Tredici proposed a dual-hit model of PD initiation, whereby an environmental factor can trigger PD onset α-synuclein propagation in two sites: the olfactory bulb and the gastrointestinal tract, two sites that interface with the external environment (Braak et al., 2003; Hawkes et al., 2007; Hawkes et al., 2009). In light of this, we posited that environmental triggers (possibly microbial in nature) could onset PD in a genetically susceptible individual (Kitada et al., 2012).

In epidemiological studies, viral exposures have been linked to PD risk in multiple cohorts (reviewed in: Smeyne et al., 2021; Leta et al., 2022). Furthermore, many pathogens (*i.e.,* bacterial, viral, fungi, mimics) have been employed in multiple genetic mouse models of PD and these pathogens were able to illicit PD-linked genotype-specific outcomes following infection including dopaminergic neurodegeneration in some instances (Dwyer et al., 2020; Bobyn et al., 2012; Jang et al., 2009; Smeyne et al., 2022; Bantle et al., 2019; Bantle et al., 2021; Pisa et al., 2020).

This thesis was motivated largely by this dual-hit hypothesis and the possibility of viral exposures as risk factors for PD (Hakwes et al., 2007; Hawkes et al., 2009; Kitada et al., 2012). To investigate PD as a complex disease requiring genetic susceptibility and environmental trigger(s) to onset disease, we employed three mouse models linked to three PD-linked genes: *Snca*, *Lrrk2*, and *Gba1*. Herein, we have employed three different viruses as well a serial viral and bacterial infection paradigm to model pathogenic environmental triggers.

We have previously shown that *Snca* knockout and two variants of *Lrrk2* in neonatal mice could perturb the course of illness of nasally acquired reovirus T3D-induced encephalitis (Tomlinson et al., 2017; Shutinoski et al., 2019). Specifically, *Snca* knockout mice had higher mortality against the infection, suggesting that endogenous α-synuclein expression plays a role in host defences against reovirus T3D-induced encephalitis in pups (Tomlinson et al., 2017). Further, the PD-linked hyper-kinase mutation of *Lrrk2*, p.G2019S, led to better control of the virus in both the brain and lung, but higher mortality specifically in female mice. Kinase-dead Lrrk2 p.D1994S mutant mice had increased survival against reovirus-T3D induced encephalitis in pups (Shutinoski et al., 2019). Altogether, these data suggest that both endogenous *Snca* expression and allelic variants of *Lrrk2* play a role in host defences against reovirus T3D-induced encephalitis as measured by survival rate and viral titres in target organs. Importantly, nasal inoculation was used in this model, meaning that the virus first infected the olfactory epithelium within the nasal cavity, and the lungs, before viral titres peak in the brain leading to encephalitis. This model involves full engagement of peripheral innate immunity prior to peak involvement of the CNS-specific immune system.

Given that much research has studied both α-synuclein and Lrrk2 in CNS-specific roles, we wished to delineate the role of each of these proteins in the peripheral- *vs.* brain-specific immune response in response to reovirus T3D. To do this, we employed the same viral strain in the same mouse models mentioned above instead now using a direct-brain, intracerebral inoculation model. In doing so, we aimed to minimize (though cannot complete exclude) the role of the peripheral immune system and its effects on the brain and aimed to target the CNS-specific immune response. By performing parallel experiments in Chapter 2 as was done in Tomlinson et al. (2017) and Shutinoski et al. (2019), and comparing the outcomes of the parallel paradigms, we

have begun to parse the relative contribution of both α-synuclein and Lrrk2 in the periphery *vs.* in the brain as it relates to the host defence against reovirus T3D infection and death due to encephalitis.

As we have established a role for Lrrk2 in host response against a neurotropic virus in Chapter 2 and in Shutinoski et al. (2019) in neonatal mouse pups, we next wished to investigate the role of allelic variants in *Lrrk2* against viral infections in adult mice. As such, we employed two distinct types of single-stranded RNA viruses. We first employed vesicular stomatitis virus (VSV) which has neurotropism and causes meningoencephalitis in adult mice. Next, we employed the non-neurotropic, pneumotropic influenza A virus, serotype H1N1, which causes pneumonitis. We chose these two viruses for their differing tropism (*i.e.,* periphery- *vs.* brain-directed). VSV models a second neurotropic, encephalitic virus, akin to reovirus T3D; but, in adult mice. Furthermore, influenza infections have been epidemiologically linked to PD in numerous reports and is therefore a PD-relevant virus (Jordan, 1927; Martyn, 1997; Cocoros et al., 2021). We studied both the hyper-kinase *Lrrk2* p.G2019S and the kinase-dead *Lrrk2* p.D1994S mutations in response to each of these pathogens.

Beyond a role for Lrrk2 in perturbing the course of illness following viral infections acutely, we also wished to investigate the downstream outcomes and long-term sequelae of viral infections on brain health. As such, we measured multiple neurodegeneration-linked biochemical markers in the brains of mice that survived the original infections. We aged these mice to a total of six weeks post inoculation (wpi), a timepoint when all mice were phenotypically healthy. We measured three main markers that are linked to neurodegeneration: α-synuclein protein concentration, levels of oxidative stress, and phosphorylated tau protein abundance. By looking at the effect of viral infections on brain health in surviving mice (both wild-type and mutant), we

began to investigate whether, and if so, how viral infections may act as risk factors to promote neurodegeneration over the course of one's lifetime and over the culmination of multiple exposures.

Finally, in Chapter 4, we investigated the role of a third PD risk gene, *Gba1* (encoding GCase), in response to both VSV and H1N1. *GBA1* is the commonest genetic risk factor for PD and therefore insights into the physiology of *GBA1* will greatly inform PD pathogenesis. Unlike Lrrk2, research into the role of GCase in host response to pathogens has been limited. We were motivated by our positive results showing that both α-synuclein and Lrrk2 could perturb disease outcomes following multiple pathogens, and that GCase is highly expressed in macrophages suggesting a potential role in immune function(s). Furthermore, there are reports that GCase can affect viral infectivity *in vitro* (Maródi et al., 1995; Drews et al., 2019, Soudani et al., 2019; Vitner et al., 2021; Drews et al., 2020; Sanyal et al., 2020). We employed four pathogenic infection models in mutant Gba1 mice: neurotropic VSV, non-neurotropic H1N1, bacterial *Salmonella typhimurium*, and a serial infection of the latter two. We investigated disease outcomes (survival rate and/or pathogenic titre) in wild-type, heterozygous, and homozygous Gba1 p.D409V mice in each of these models. Importantly, homozygous mutations in *GBA1* in humans cause Gaucher disease, whereas both heterozygous and homozygous *GBA1* mutations confer risk for PD at a mean penetrance rate of 33% (Anheim et al., 2012). As such, both heterozygous and homozygous mice are biologically relevant in this study. We also investigated GCase enzymatic activity downstream of infection in each genotype.

This thesis aimed to further implicate viral infections (and the ensuing inflammation) as a risk factor for PD and to further demonstrate an ability for multiple PD-linked genes to alter the course of illness following multiple viral infections in mice. In uncovering the chronic effects of

viral infections on brain health, we aimed to highlight that viral infections (even those that do not directly infect the brain, *i.e.,* non-neurotropic H1N1) can lead to pathology-associated changes in the brain in mice that survive the infection. By extension, this may highlight the importance of regular vaccinations against viral infections and possibly anti-inflammatory medications as preventative measures for PD risk (likely in genetically susceptible individuals) (Gao et al., 2011).

In demonstrating a role for PD-linked genes in host defences against infections, we will further uncover both the physiology and pathophysiology of these proteins. By understanding these functions, we can begin to parse the disease mechanisms behind these proteins, which will allow an avenue for cause-directed therapeutics in these disease pathways.

2. Principal Findings

In this thesis, together with our previous publications, we have shown that variants of three PD-linked genes, *Snca*, *Lrrk2*, and *Gba1*, could all perturb the course of illness (*i.e.,* survival rate) in response to a neurotropic, encephalitic virus (*Snca*: reovirus T3D; *Lrrk2*: reovirus T3D and VSV; *Gba1*: VSV). Furthermore, both neurotropic VSV and non-neurotropic H1N1 could lead to changes in multiple neurodegeneration-linked biochemical markers in the brains of surviving wild-type and *Lrrk2* mutant mice, as late as six weeks after inoculation. These data demonstrate a reciprocal relationship of viruses and PD disease genes/pathologies: PD-linked genes can function upstream of infections to alter the course of illness, and downstream effects of viral infections include lasting and marked changes in neurodegenerative disease hallmarks, including α-synuclein protein concentration and tau hyperphosphorylation, in the brains of otherwise healthy mice who survived a viral infection.

In **Chapter 2**, we sought to understand the peripheral- *vs.* CNS-specific contribution of *Lrrk2* and *Snca* in response to reovirus T3D-induced encephalitis. When we administered the virus in neonatal mouse pups via a direct-brain intracerebral injection, we found that Lrrk2 p.G2019S mice had the same time-to-death interval as wild-type mice. This, even though when the same virus was administered nasally (and therefore fully engaged the periphery), these same mice had a decreased survival rate compared to wild-type littermates (Shutinoski et al., 2019). Similarly, kinase-dead Lrrk2 p.D1994S mutant pups were relatively protected against a nasal inoculation of reovirus T3D compared to wild-type littermates but had the same time-to-death as wild-type mice when the virus was administered intracerebrally. Importantly, our previous work held a consistent female sex bias when regarding reovirus T3D and *Lrrk2* variants, and as such we separated all data based on sex but did not uncover any further differences in the intracerebral delivery model. Taken together with Shutinoski et al. (2019), these data suggest that in the context of reovirus-T3D-induced encephalitis, allelic variants of *Lrrk2* contribute to the host response primarily in peripheral tissues to protect the brain, rather than specifically in the CNS. It remains to be tested which cells are driving this phenotype in the periphery, but our previous data suggest it may be driven by macrophages and neutrophils (Shutinoski et al., 2019). How they then alter brain-related outcomes in this model requires further investigation; however, as shown in Chapter 3 and as published in Shutinoski et al., (2019), infections in the periphery can lead to increased ROS production in the brain and this is exacerbated by the Lrrk2 p.G2019S genotype.

We also investigated the levels of two LRRK2-PD-linked disease proteins: α-synuclein and phosphorylated-tau protein. This was motivated by our findings that nasal inoculation of reovirus T3D could lead to an increase in α-synuclein in Lrrk2 p.G2019S mice, as well as parallel studies in Chapter 3 demonstrating that viral infection consistently led to increased tau phosphorylation.

We did not find a difference in α-synuclein concentration following intracerebral infection of reovirus T3D. Strikingly, we found a significant increase in phosphorylated tau protein at 8 days post inoculation (dpi) that was both infection- and Lrrk2 p.G2019S-dependent, which we observed in both male and female mice. These data present a relationship between the *Lrrk2* p.G2019S mutation, an encephalitic viral infection, and the level of tau phosphorylation at an acute time point of disease in neonatal mouse pups.

Finally, we did not observe any differences in the time-to-death interval of *Snca* knockout mice following intracerebral inoculation of reovirus T3D, despite finding that these mice had higher mortality following nasal inoculation of reovirus T3D (Tomlinson et al., 2017). This suggests that endogenous α-synuclein protects against reovirus T3D-induced encephalitis primarily in the periphery rather than the CNS. Importantly, in both inoculation methods of reovirus T3D, the time-to-death (*i.e.,* 5-10dpi) and disease presentation was the same.

In **Chapter 3**, we investigated the role of variants in *Lrrk2* in adult mice in response to two distinct viruses: neurotropic VSV and non-neurotropic, lung-directed H1N1. In Chapter 3, both viruses were administered nasally and therefore represented systemic infections with both peripheral and CNS-specific immune involvement in their respective disease courses. By administering viruses with two different tropisms, we hoped to further investigate the pathogen- and organ-specific roles of Lrrk2.

We found that homozygous Lrrk2 p.G2019S female -but not male- mice had a decreased survival rate compared to both wild-type and heterozygous mice against VSV-induced encephalitis. This female sex bias is consistent with our previous studies involving pathogenic infections and the *Lrrk2* p.G2019S mutation. Interestingly, this phenotype was not found in response to the lung-directed H1N1 infection. In this case, all female mice and all male mice had

similar survival rates to their respective genotypes. These data further suggest the pathogen- and organ-specificity of Lrrk2, and beyond this suggest that the *Lrrk2* p.G2019S mutation may worsen disease outcomes (*i.e.,* survival rate) in the context of a brain-based pathological process (and related inflammation) but does not worse disease outcomes in infections that are restricted to the periphery in their disease course. This is supported by previous data that demonstrated that Lrrk2 p.G2019S mice were protected against a peripheral *Salmonella typhimurium* infection (Shutinoski et al., 2019; Liu et al., 2017).

We investigated, but did not find, the mechanisms behind the decreased survival rate found in Lrrk2 p.G2019S female mice. However, using immunohistochemical analyses, we did identify that Lrrk2 p.G2019S female, but not male, mice had decreased microgliosis following VSV infection in the olfactory bulb at 6dpi. Female wild-type, male wild-type, and male Lrrk2 p.G2019S mice all had a clear increase of microglial size and quantity after VSV infection that was not evident in female Lrrk2 p.G2019S mice, possibly indicating that they did not mount a sufficient immune response. An important aspect of the disease induced by VSV is severe meningitis (together with encephalitis) which we have not histologically captured with brain slides. In ongoing parallel work investigating the effects of VSV in wild-type mice, we have employed whole skull mounts to investigate immune cell infiltration and inflammation in the meninges (Tomlinson et al., 2017; Zahr Eddin et al., *unpublished*). The degree of meningitis could underlie the higher death rates observed in female Lrrk2 p.G2019S mice, which is support by an observed trend of more hind limb paralysis in female Lrrk2 p.G2019S mice specifically. Future data will employ histological analysis of whole skull mounts in this model.

As a secondary objective of Chapter 3, we explored the effects of viral infections on brain health in mice that survived the infection. In both models (VSV and H1N1) all mice that survived

the initial infection were aged to a total of six weeks post inoculation and the brains were collected. We found that α-synuclein concentration, levels of oxidative stress and phosphorylated tau protein in the brain were all altered by both viral infections – meaning that even H1N1, which does not directly infect the brain and causes a peripheral disease course, could lead to measurable changes in neurodegeneration-linked proteins in the brain six weeks from infection. Importantly, each of these findings were found in both wild-type and Lrrk2 p.G2019S mice, meaning that a neurodegenerative disease gene is not required for these changes to occur post-viral infection.

Specifically, we found that both viruses led to changes in two oxidative markers: concentrations of reversible H_2O_2 and levels of irreversible protein nitrotyrosination (a post-translational protein modification that occurs secondary to oxidative stress). Surprisingly, we found an opposite effect of the two viruses on α-synuclein concentration: VSV led to a significant decrease in the protein, and H1N1 led to a trend towards increase of the protein in the brain. These data show that two distinct viral infections could both lead to changes in the levels of two PD-linked hallmarks in healthy mice who survived a viral infection.

Most excitingly, we found a consistent and marked increase in the level of phosphorylated-tau (p-Tau) protein in response to both viral infections at six weeks post infection in adult animals; p-Tau was absent in almost all mock-infected samples, but notably and reproducibly identified at six weeks post inoculation following both VSV and H1N1 infection. Of note, p-Tau has also been identified in mice following SARS-CoV-2 (Di Primio et al., 2023), herpes simplex virus (Powell-Doherty et al., 2020), and mouse hepatitis virus (MHV) (Sy et al., 2011). We found markedly less p-Tau in mice all sacrificed at six *days* post inoculation of VSV infection (compared to at 6wpi), suggesting that p-Tau may be a consequence of lingering infection rather than an immediate

response. Remarkably, the highest abundance of p-Tau protein was identified in brains collected from moribund (humane endpoint) mice of VSV infection.

We did not observe a Lrrk2 p.G2019S-dependent effect on tau phosphorylation at 6wpi, though in the context of VSV infection we did see a stronger induction between mock- and infected samples in Lrrk2 p.G2019S brains than in wild-type brains, possibly suggesting an ability for Lrrk2 p.G2019S to exacerbate (but not drive) this phenotype. Interestingly, it has been shown that Lrrk2 kinase inhibitors could limit tau hyperphosphorylation in an AD mouse model (Castro-Sanchez et al., 2020) and herein, we observed that Lrrk2 kinase-dead p.D1994S mice had a lower level of p-Tau protein abundance after H1N1 infection compared to wild-type and Lrrk2 p.G2019S mice, which requires further validation, but may support these data.

Although we observed increased tau phosphorylation following resolved viral infections, we cannot conclude that these also include and/or will lead to neurofibrillary tau tangles. Tau tangles are the hallmark of numerous tauopathies, including Alzheimer's disease (AD), progressive supranuclear palsy (PSP), and corticobasal degeneration (CBD). In humans, the presence of tau phosphorylation can appear long before the presence of tau tangles. Therefore, it remains to be examined whether these infections can also lead to misfolded neurofibrillary tau tangles in mice.

A graphic summary of all results measured at 6 weeks post inoculation of both VSV or H1N1 can be found below (**Fig. 5.1**).

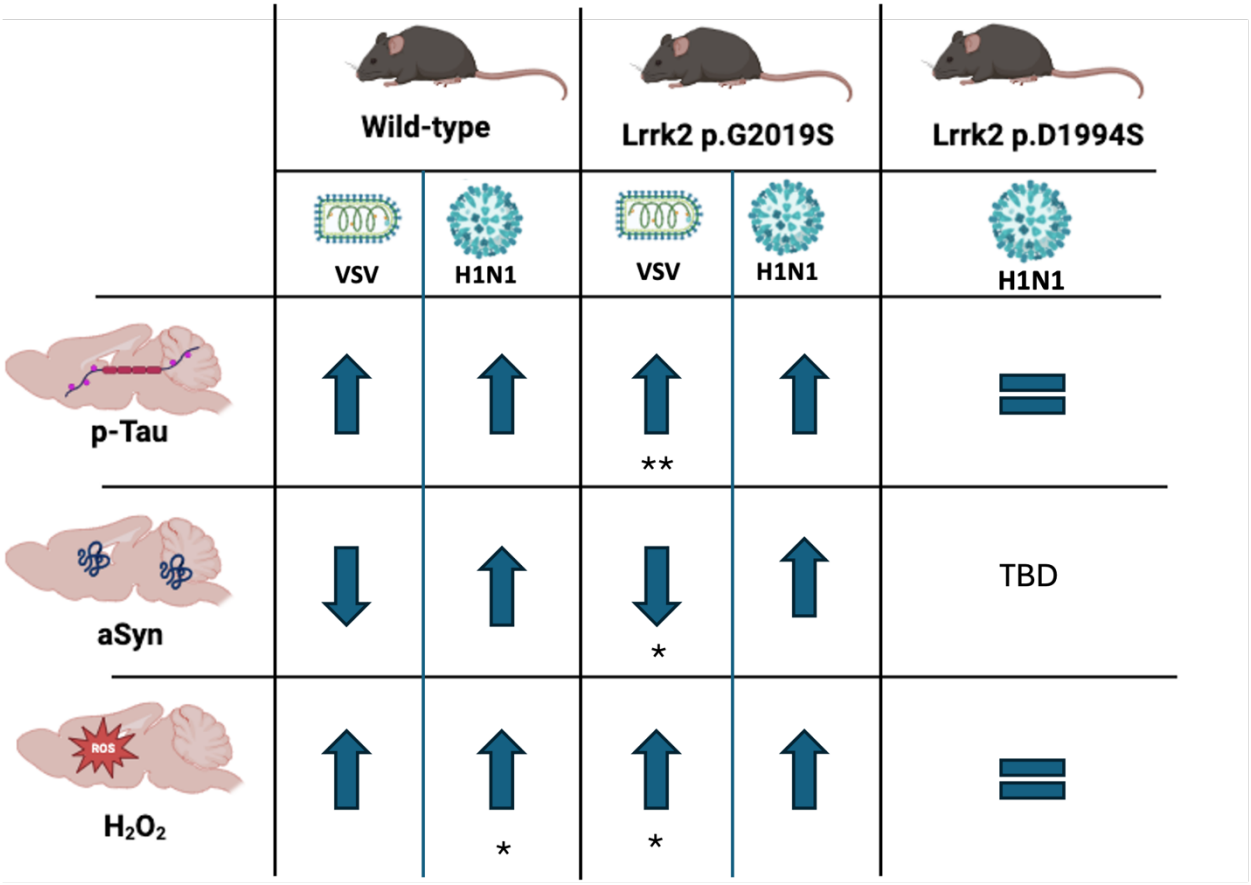


Fig. 5.1: Summary of Biochemical Changes Observed Following VSV or H1N1 Infection in Wild-Type, Lrrk2 p.G2019S, And Lrrk2 p.D1994S Mice at 6 Weeks Post Inoculation. Adult mice were inoculated with a dose of $3x10^3$ PFU of VSV or a dose of $2x10^3$ PFU of H1N1, and any mice that survived the infection were aged to a total of 6 weeks post inoculation. In the brains of sacrificed mice, three parameters were then measured: levels of phosphorylated tau protein (p-Tau) via Western blot; concentrations of α-synuclein (aSyn) via sandwich ELISA; and concentration of H_2O_2 via Amplex® Red assay. Arrows and equal signs within each box refer to comparisons between mock- and virus-infected samples within one genotype, with sexes pooled. Stars denote significance between groups as measured by ANOVA with Tukey post-hoc tests. P-value <0.05 (*), P-value <0.01 (**). TBD (to be determined) indicates an experiment that was not completed.

In **Chapter 4**, we investigated a possible role for a third PD-linked gene, *Gba1*, in host defences against pathogenic infections. We used the Gba1 p.D409V mouse model, in which the homozygous genotype leads to a marked decrease in GCase activity, and a partial reduction in the heterozygous genotype (Xu et al., 2003; Clarke et al., 2019; Polinski et al., 2021). Indeed, GCase levels are as low as 1% of wild-type activity in the lungs and spleen of Gba1 p.D409V homozygous mice, and ~15% in the brain. In heterozygous Gba1 p.D409V mice, GCase activity is ~50% of wild-type activity in the lungs and spleen, and ~75% in the brain. We did not find an effect of these genotypes on survival outcomes of H1N1-induced pneumonitis, *Salmonella typhimurium*-induced sepsis, or a serial infection model of the two.

Interestingly, we did observe a Gba1 p.D409V effect on VSV survival rates. When we pooled the sexes, both homozygous and heterozygous Gba1 p.D409V mice had significantly higher survival rates than wild-type mice. When we separated these data based on sex (motivated by the Lrrk2-dependent sex bias observed in Chapter 3), we found that homozygous Gba1 p.D409V male mice were significantly protected against VSV infection, and we observed a trend in female mice whereby heterozygous, but not homozygous, mice were protected against VSV compared to wild-type mice. In female mice, this survival trend was associated with a significant decrease in viral titre in the lungs at 2dpi.

We also measured GCase enzymatic activity at 2dpi to examine the downstream effects of VSV viral infection on GCase enzymatic activity. When comparing levels at baseline (mock) compared to in VSV-infected tissue within the same genotype and sex, GCase activity was only significantly altered in female homozygous Gba1 p.D409V mice, in the olfactory bulb. It is possible that subtle changes were only uncovered in samples with overall low levels of GCase

activity. These data suggest that viral infections could affect GCase activity levels, but in a tissue-, sex-, and genotype-specific manner.

Finally, building on our data from Chapter 3, we measured p-Tau protein abundance in our VSV tissue collected at 2dpi. Unlike at 6wpi, p-Tau was completely absent in all tissues at 2dpi. Taken together with our investigations into p-Tau in this thesis, these data suggest that phosphorylation of tau following viral infections is a long-term effect (possibly a consequence) in healthy, surviving mice and not an immediate response to infection during the initial phase of disease. However, as moribund mice had the highest levels of p-Tau compared to all other timepoints measured, these data also suggest that tau becomes heavily phosphorylated when sickness becomes so severe that it causes fatality.

Altogether, Chapter 4 demonstrated an effect for variants in *Gba1* on disease outcomes stemming from VSV-induced encephalitis, but not H1N1 or ST infection, these results suggest that, akin to Lrrk2, GCase is involved in host response(s) to infection in a pathogen- and organ-specific manner. These data also demonstrate in multiple assays (*i.e.,* survival outcomes, cytokine signalling, GCase activity) the importance of considering sex as factor in *Gba1* studies.

3. Future Directions

This thesis has begun to illustrate a role for three key Parkinson's disease-linked genes in perturbing the course of illness of multiple viral infections. Furthermore, it has demonstrated that viruses can lead to biochemical neurodegeneration-linked changes in the brains of healthy mice who survived a viral infection. However, much remains to be elucidated and there are many avenues of research to continue regarding the present thesis.

One, we did not succinctly elucidate the mechanism behind Lrrk2 p.G2019S female mice having decreased survival rates against nasal VSV infection; this will be pursued in future studies. During the period of this thesis, olfactory bulbs were collected from a full cohort of mock- and VSV-infected wild-type and Lrrk2 p.G2019S mice at 2dpi for single nuclei RNA-sequencing, the analysis of which is ongoing. The olfactory bulb was chosen as the tissue of interest given our interest in the OB as a potential first site of aSyn pathology initiation, motivated by the high incidence of hyposmia in the prodromal phase of PD (*i.e.,* Braak et al., 2003; Hawkes et al., 2007; Li et al., 2022). Upon nasal inoculation, the OB can become directly infected (*i.e.,* bypass the periphery) by virions entering the CNS via aSyn-rich olfactory sensory neurons. Therefore, we believe the OB to be relevant in PD pathogenesis and as such differences in the transcriptome between wild-type and Lrrk2 p.G2019S mutant mice following VSV infection may be uncovered here. Furthermore, VSV viral titres peak in the olfactory bulb at 2dpi. This study will provide insights into transcriptional changes between genotypes, sexes, and treatment groups during the acute phase of VSV infection. This experiment will be an unbiased approach at uncovering mechanistic changes between groups at the transcriptional level.

Furthermore, this data set will validate and inform our perplexing finding gained by immunohistochemical analyses that Lrrk2 p.G2019S female mice appear to have less microgliosis in the olfactory bulb upon infection compared to all other mice. Specifically, the snRNA-seq dataset will uncover microglia-specific transcripts which will inform microglial activation state and heterogeneity of the microglia cell populations in the olfactory bulb between groups.

Moreover, akin to these findings, we have previously observed a decreased survival rate in Lrrk2 p.G2019S female mice following the encephalitic virus, reovirus T3D, in neonatal mouse pups (Shutinoski et al., 2019). In those studies, we found this phenotype was associated with

increased peripheral myeloid cell infiltration to the brain, as measured by flow cytometry. By using snRNA-seq in our present dataset, we can identify cell populations in the olfactory bulb at this time of infection, and therefore we can address whether there is also an increase of infiltrating myeloid cells in Lrrk2 p.G2019S mice following VSV infection.

More extensive mechanistic and cellular studies into the observed phenotype of decreased survival rate in Lrrk2 p.G2019S mice, which we have now shown in the context of two encephalitic viruses, must be done in order to fully inform Lrrk2 biology. This can be done further by employing *in vitro* studies for comprehensive pathway analysis with primary cell cultures including bone marrow-derived macrophages, or continuous cell lines such as RAW macrophages or BV-2 microglia (given Lrrk2's high expression in phagocytes).

Two, as detailed below, further infection paradigms should be performed to inform: 1) the antiviral capacities of these PD-linked genes (namely *Lrrk2*), and 2) whether a combination of viruses and/or varying time(s) of inoculation can further exacerbate the neurodegeneration-linked changes we identified following VSV/H1N1; and moreover, whether there is dopaminergic neurodegeneration in the SNpc of these mice.

Firstly, in our present study we did not investigate whether our observed biochemical changes (*i.e.,* oxidative stress, α-synuclein concentration, and p-Tau levels) persisted beyond 6 weeks post inoculation, which should be investigated, including histological based analyses of these parameters (*i.e.,* α-synuclein, p-Tau) to identify site-specific localization. Furthermore, it it should be investigated histologically whether there is any dopaminergic neuronal death in the SNpc. If the death of dopaminergic neurons is identified, it remains conceptually debated in the field whether neurodegeneration stems from cell-to-cell transmission of pathogenic components (such as seeds, *i.e.,* prion hypothesis); or from signalling mediators (possibly from the periphery)

that eventually reach cell populations that are innately vulnerable (*i.e.,* dopaminergic neurons). The data presented herein, namely the identification of increased quantities of ROS, α-synuclein, and p-Tau in the brain at 6wpi following a non-neurotropic, peripheral H1N1 infection course may provide evidence for the latter, though we have yet to identify neurodegeneration in these samples. Importantly, in complex human disease it is likely a mixture of both factors that leads to neurodegeneration.

Beyond this, a chronic viral model which is non-fatal but where the virus persists in the host for a longer period would investigate whether a chronic (*vs.* acute) infection could exacerbate (or diminish) the pathology-linked phenotypes we have observed herein. A possible model for this would be the chronic lymphocytic choriomeningitis virus infection model. This is a well-established chronic viral murine model, where infections via peripheral inoculation (*i.e.,* intraperitoneal) are often non-lethal but the virus remains in the host for a chronic period (Bocharov et al., 2015).

Next, we employed a serial infection model of H1N1 and *Salmonella typhimurium* in Chapter 4 but did not investigate these brains at an aged time point for the same biochemical changes as in Chapter 3. It is of high interest to employ a serial infection model, even in wild-type mice, such as in a pilot study, to measure the impact of multiple infections on the biochemical changes we measured herein (p-Tau protein abundance, α-synuclein concentration, and oxidative stress levels) but also to investigate the cell health of dopaminergic neurons in the SNpc in the brain of recovered mice. A potentially attractive model would be to use pneumonitis-causing H1N1 followed by a pneumonia-inducing bacteria, as this type of superinfection is commonly seen in humans and would highly engage the immune system. In our studies, we have not yet investigated whether a bacterial infection can also induce tau hyperphosphorylation; though previous studies

have shown an ability of LPS treatment (bacterial mimic) to do so (Kitazawa et al., 2005; Sy et al., 2011).

Herein, we have investigated three RNA viruses in the context of PD-linked genes, but we have yet to investigate the effects of a DNA virus. It will be highly informative to employ DNA viruses in these paradigms and investigate the effects of *Lrrk2*, *Snca*, and *Gba1* following a range of distinct viral types. DNA viruses including herpes zoster virus, hepatitis B virus, and Epstein-Barr virus have been well linked to PD risk (Carmacho-Soto et al., 2020; Lai et al., 2017; Choi et al., 2020; Pakpoor et al., 2017; Hseih et al., 2022; Zhang et al., 2021; Tiwari et al., 2022).

Finally, in Chapter 2, a major limitation of the study is the possibility that intracerebral inoculation of reovirus T3D is too severe and fulminant to uncover differences in time-to-death between genotypes. Although we performed some preliminary studies to address this, and other researchers have successfully used this model to identify genotype-dependent outcomes on survival (specifically, knockout of the caspase-3-encoding gene) (Beckham et al., 2011), we must validate our interpretation of these findings using a less severe infection paradigm. Specifically, by employing VSV intracerebrally in adult mice to mirror what we have already completed with nasal inoculation in Chapter 3, we may validate our findings in Chapter 2. This would allow us to conclude on the relative contribution of Lrrk2 in the peripheral- *vs.* brain-specific immune response to an encephalitic virus, this time in adult mice. Furthermore, both CNS-penetrant and CNS-impenetrable (*i.e.,* cannot readily pass the BBB) Lrrk2 kinase inhibitors are readily available, and could be used as an alternative approach to investigate the role of Lrrk2 kinase activity (*i.e.,* in the wild-type and Lrrk2 p.G2019S hyper-kinase state) restricted to the periphery *vs.* with full CNS inhibition.

Three, much remains to be investigated regarding the mechanisms behind the high level of tau phosphorylation in the brain following viral infections.

Firstly, how long does tau remain phosphorylated after VSV or H1N1 infection? The furthest we have investigated is 6wpi. It would be informative to measure p-Tau levels at 2wpi (what we consider the end of the 'survival' experimental period), at three months post inoculation, and even a year from initial inoculation. Is this a permanent effect or transient? If transient, how long does it last? Does it progress to tau tangle pathologies and possible neurodegeneration?

Importantly, it remains to be concluded whether the phosphorylation of tau during these acute infection models is protective or detrimental. It is possible that tau phosphorylation plays a role as a stress response protein against the infection (akin to hypothermia and hibernation) (Bretteville et al., 2012; Su et al., 2008). It has been reported that phosphorylation of tau may be a physiological response to stressors which facilitates neuronal healing and neuroplasticity (reviewed in Rissman, 2010); furthermore, it has been found that neurons expressing hyperphosphorylated tau were resistant to apoptosis *in vitro* (Zhang et al., 2009). Conversely, it may be that tau phosphorylation is a detrimental, and possibly lethal, side effect of viral infection.

Firstly, it should be investigated whether there are any phenotypic, neurobehavioural effects of this high level of tau phosphorylation on these mice. Future studies will involve performing cognitive and motor behavioural tests of surviving mice aged to (at least) 6wpi, to investigate whether this level of tau phosphorylation manifests as a detectable phenotype and how this might progress over time.

Next, mechanistic studies will inform the (patho-) physiology of this tau phosphorylation. There are multiple potential underlying mechanisms: a downregulation of tau phosphatases; an upregulation of tau kinases; or a decrease in autophagic clearance of phosphorylated tau. Notably,

Sy et al. (2011) have attributed their observed increase in p-Tau protein following mouse hepatitis virus specifically to GSK-3β activity. In our future studies, we could utilize the GSK-3β inhibitor, lithium, to investigate if tau phosphorylation occurring in our studies is GSK-3β-dependent. Importantly, this should be implemented in both the adult (*i.e.,* H1N1/VSV) and neonatal mouse pup (*i.e.,* reovirus T3D) model, as it is possible that the mechanisms in each are not the same, as tau is heavily phosphorylated during the neonatal period and therefore reovirus T3D infection may be perturbing an alternate mechanism.

If a link between this tau phosphorylation and GSK-3β is identified, the effects of lithium treatment on survival rates, as well as on the neurobehavioural phenotype of surviving mice, following VSV or H1N1 infection would be revealing as to whether this tau phosphorylation leads to neuroprotection (*i.e.,* physiological) or neuronal vulnerability (*i.e.,* pathogenic). If mice that receive lithium treatment have a higher survival rate following viral infection, this would imply that the tau phosphorylation was contributing negatively to the mouse's health during infection; conversely, if lithium treatment leads to more mortality in these mice, it would imply that tau phosphorylation was an important, protective infection response of the host. Further, measuring the level of neurodegeneration in aged, surviving mice with or without lithium treatment would inform whether tau phosphorylation following infection is protective or harmful to neuronal health, long-term.

Interestingly, epidemiologically, patients with bipolar disorder (BD), who have used lithium as a treatment for many years, are at lower risk of developing dementia (Mauer et al., 2014; Moon et al., 2022). Another study showed that lithium treatment in human patients with mild cognitive impairment had lower concentrations of p-Tau in their CSF compared to those who were untreated (Forlenza et al., 2011).

Though we did not find a Lrrk2-specific effect on tau phosphorylation following VSV or H1N1 infection, we did identify a Lrrk2 p.G2019S-specific effect following reovirus T3D. Therefore, both wild-type and Lrrk2 p.G2019S mice should continue to be included in future studies.

Four, in the present thesis we utilized the kinase-dead Lrrk2 p.D1994S mutant to investigate which phenotypes were dependent on the wild-type kinase activity of Lrrk2. Much research has been done on a protective effect of inhibiting Lrrk2 kinase activity on multiple phenotypes, including under inflammatory conditions (Mutti et al., 2023; Ilieva et al., 2024; Rocha et al., 2020; Bu et al., 2023). Future studies building on Chapter 3 should investigate whether Lrrk2 kinase inhibition, both genetic and pharmacological, can prevent the observed biochemical changes in the brain associated with viral infections. For example, we have preliminary (yet inconclusive) data presented in Chapter 3 suggesting that the kinase-dead Lrrk2 mutant mice may have less tau hyperphosphorylation. This should be pursued further to determine if there may be a rescue effect, as has been suggested by other authors (Castro-Sanchez et al., 2020; Lubben et al., 2023). In these studies, both the kinase-dead genetic mouse model and readily available pharmacological Lrrk2 kinase inhibitors (which are biologically relevant to what is currently in clinical trials as use for PD patients) should be used.

Five, in Chapter 4, we have initiated studies into a role for GCase in host defenses against the neurotropic virus VSV. However, it is imperative to investigate the downstream effects of viral infections on lipidomic homeostasis, and whether this can be perturbed by the *Gba1* p.D409V mutation. As such, we have collected plasma at 2dpi from mock- and VSV-infected wild-type, Gba1 p.D409V heterozygous, and homozygous male and female mice. This will investigate what changes occur in the lipidome during the acute phase of VSV viral infection. Furthermore: how

does the lipidome differ between genotypes in the mock *vs.* the infected state? Could this inform the observed survival benefit in Gba1 p.D409V homozygous male mice? By extension then: does the lipidome play an active role in immune response against VSV viral infection at this time point? Importantly, both H1N1 and VSV utilize cholesterol, a direct substrate of GCase, in their infectivity. It is therefore conceivable that perturbations in GCase activity-linked cholesterol metabolism could be contributing to the relative protection observed with the *Gba1* p.D409V allele in VSV infection. As it stands, this research is being actively pursued by us together with our lipidomics colleagues.

4. Conclusion

The results of this thesis provide insight into the effects of viral infections on multiple markers linked to neurodegenerative disease. Furthermore, three PD-linked genes, *Snca*, *Lrrk2*, and *Gba1*, each could alter survival rates of encephalitic viral infections. These data firstly contribute to the growing evidence that viral infections are likely risk factors for neurodegenerative diseases, including PD. Secondly, by demonstrating a relationship between PD-disease genes and viral infections, it supports the original dual-hit hypothesis that PD onset in genetically susceptibly individuals requires an environmental (possibly viral) trigger (Hawkes et al., 2007; Hawkes et al., 2009; Kitada et al., 2012).

This is supported by our key finding that resolved viral infection in adult mice led to varied biochemical changes in the brain, in a virus-dependent manner. The measured changes represent numerous distinct neuropathological hallmarks which are linked to multiple distinct neurodegenerative proteinopathies including PD, DLB, AD, PSP, and CBD. This model further

raises the importance of environmental triggers meeting genetic susceptibility in onset of neurodegenerative diseases (Schlossmacher et al., 2017).

These data highlight the importance of regular vaccinations, including annually against influenza virus and those in unique scenarios such as during the SARS-CoV-2 pandemic, not only as preventative measures against viral infections; but also, to protect the brain from potential, long-term effects that may predispose adults to the development of a sporadic, neurodegenerative disease. Moreover, further mechanistic studies into the relationship between viral infections and *Snca*, *Lrrk2*, and *Gba1* will inform the pathobiology of mutant allele-encoded proteins, and ideally inform therapeutics for numerous diseases associated with these genes.

References Cited

Aharon-Peretz, J., Rosenbaum, H., & Gershoni-Baruch, R. (2004). Mutations in the Glucocerebrosidase Gene and Parkinson's Disease in Ashkenazi Jews. *New England Journal of Medicine*, *351*(19), 1972–1977. https://doi.org/10.1056/NEJMoa033277

Ahmadi Rastegar, D., & Dzamko, N. (2020). Leucine Rich Repeat Kinase 2 and Innate Immunity. *Frontiers in Neuroscience*, *14*, 193. https://doi.org/10.3389/fnins.2020.00193

Ahmadi Rastegar, D., Hughes, L. P., Perera, G., Keshiya, S., Zhong, S., Gao, J., Halliday, G. M., Schüle, B., & Dzamko, N. (2022). Effect of LRRK2 protein and activity on stimulated cytokines in human monocytes and macrophages. *Npj Parkinson's Disease*, *8*(1), 34. https://doi.org/10.1038/s41531-022-00297-9

Alam, M. M., Yang, D., Li, X.-Q., Liu, J., Back, T. C., Trivett, A., Karim, B., Barbut, D., Zasloff, M., & Oppenheim, J. J. (2022). Alpha synuclein, the culprit in Parkinson disease, is required for normal immune function. *Cell Reports*, *38*(2), 110090. https://doi.org/10.1016/j.celrep.2021.110090

Albanese, F., Novello, S., & Morari, M. (2019). Autophagy and LRRK2 in the Aging Brain. *Frontiers in Neuroscience*, *13*, 1352. https://doi.org/10.3389/fnins.2019.01352

Alcalay, R. N., Dinur, T., Quinn, T., Sakanaka, K., Levy, O., Waters, C., Fahn, S., Dorovski, T., Chung, W. K., Pauciulo, M., Nichols, W., Rana, H. Q., Balwani, M., Bier, L., Elstein, D., & Zimran, A. (2014). Comparison of Parkinson Risk in Ashkenazi Jewish Patients With Gaucher Disease and *GBA* Heterozygotes. *JAMA Neurology*, *71*(6), 752. https://doi.org/10.1001/jamaneurol.2014.313

Alecu, I., & Bennett, S. A. L. (2019). Dysregulated Lipid Metabolism and Its Role in α-Synucleinopathy in Parkinson's Disease. *Frontiers in Neuroscience*, *13*, 328. https://doi.org/10.3389/fnins.2019.00328

Alessi, D. R., & Sammler, E. (2018). LRRK2 kinase in Parkinson's disease. *Science*, *360*(6384), 36–37. https://doi.org/10.1126/science.aar5683

Allen, M. J., Myer, B. J., Khokher, A. M., Rushton, N., & Cox, T. M. (1997). Pro-inflammatory cytokines and the pathogenesis of Gaucher's disease: Increased release of interleukin-6 and interleukin-10. *QJM*, *90*(1), 19–25. https://doi.org/10.1093/qjmed/90.1.19

Andrés, C., Pérez De La Lastra, J., Juan, C., Plou, F., & Pérez-Lebeña, E. (2022). The Role of Reactive Species on Innate Immunity. *Vaccines*, *10*(10), 1735. https://doi.org/10.3390/vaccines10101735

Anheim, M., Elbaz, A., Lesage, S., Durr, A., Condroyer, C., Viallet, F., Pollak, P., Bonaiti, B., Bonaiti-Pellie, C., & Brice, A. (2012). Penetrance of Parkinson disease in glucocerebrosidase gene mutation carriers. *Neurology*, *78*(6), 417–420. https://doi.org/10.1212/WNL.0b013e318245f476

Antar, A. A. R., Konopka, J. L., Campbell, J. A., Henry, R. A., Perdigoto, A. L., Carter, B. D., Pozzi, A., Abel, T. W., & Dermody, T. S. (2009). Junctional Adhesion Molecule-A Is Required for Hematogenous Dissemination of Reovirus. *Cell Host & Microbe*, *5*(1), 59–71. https://doi.org/10.1016/j.chom.2008.12.001

Arbez, N., He, X., Huang, Y., Ren, M., Liang, Y., Nucifora, F. C., Wang, X., Pei, Z., Tessarolo, L., Smith, W. W., & Ross, C. A. (2020). G2019S-LRRK2 mutation enhances MPTP-linked Parkinsonism in mice. *Human Molecular Genetics*, *29*(4), 580–590. https://doi.org/10.1093/hmg/ddz271

Ascherio, A., Chen, H., Weisskopf, M. G., O'Reilly, E., McCullough, M. L., Calle, E. E., Schwarzschild, M. A., & Thun, M. J. (2006). Pesticide exposure and risk for Parkinson's disease. *Annals of Neurology*, *60*(2), 197–203. https://doi.org/10.1002/ana.20904

Avenali, M., Blandini, F., & Cerri, S. (2020). Glucocerebrosidase Defects as a Major Risk Factor for Parkinson's Disease. *Frontiers in Aging Neuroscience*, *12*, 97. https://doi.org/10.3389/fnagi.2020.00097

Bailey, R. M., Covy, J. P., Melrose, H. L., Rousseau, L., Watkinson, R., Knight, J., Miles, S., Farrer, M. J., Dickson, D. W., Giasson, B. I., & Lewis, J. (2013). LRRK2 phosphorylates novel tau epitopes and promotes tauopathy. *Acta Neuropathologica*, *126*(6), 809–827. https://doi.org/10.1007/s00401-013-1188-4

Balestrino, R., Tunesi, S., Tesei, S., Lopiano, L., Zecchinelli, A. L., & Goldwurm, S. (2020). Penetrance of Glucocerebrosidase (*GBA*) Mutations in Parkinson's Disease: A Kin Cohort Study. *Movement Disorders*, *35*(11), 2111–2114. https://doi.org/10.1002/mds.28200

Bandookwala, M., & Sengupta, P. (2020). 3-Nitrotyrosine: A versatile oxidative stress biomarker for major neurodegenerative diseases. *International Journal of Neuroscience*, *130*(10), 1047–1062. https://doi.org/10.1080/00207454.2020.1713776

Bantle, C. M., Phillips, A. T., Smeyne, R. J., Rocha, S. M., Olson, K. E., & Tjalkens, R. B. (2019). Infection with mosquito-borne alphavirus induces selective loss of dopaminergic neurons, neuroinflammation and widespread protein aggregation. *Npj Parkinson's Disease*, *5*(1), 20. https://doi.org/10.1038/s41531-019-0090-8

Bantle, C. M., Rocha, S. M., French, C. T., Phillips, A. T., Tran, K., Olson, K. E., Bass, T. A., Aboellail, T., Smeyne, R. J., & Tjalkens, R. B. (2021). Astrocyte inflammatory signaling mediates α-synuclein aggregation and dopaminergic neuronal loss following viral encephalitis. *Experimental Neurology*, *346*, 113845. https://doi.org/10.1016/j.expneurol.2021.113845

Barcia, C., Ros, C. M., Annese, V., Gómez, A., Ros-Bernal, F., Aguado-Llera, D., Martínez-Pagán, M. E., De Pablos, V., Fernandez-Villalba, E., & Herrero, M. T. (2011). IFN-γ signaling, with the synergistic contribution of TNF-α, mediates cell specific microglial and astroglial activation in experimental models of Parkinson's disease. *Cell Death & Disease*, *2*(4), e142–e142. https://doi.org/10.1038/cddis.2011.17

Barna, M., Komatsu, T., Bi, Z., & Reiss, C. S. (1996). Sex differences in susceptibility to viral infection of the central nervous system. *Journal of Neuroimmunology*, *67*(1), 31–39. https://doi.org/10.1016/0165-5728(96)00022-7

Beatman, E. L., Massey, A., Shives, K. D., Burrack, K. S., Chamanian, M., Morrison, T. E., & Beckham, J. D. (2016). Alpha-Synuclein Expression Restricts RNA Viral Infections in the Brain. *Journal of Virology*, *90*(6), 2767–2782. https://doi.org/10.1128/JVI.02949-15

Beckham, J. D., Tuttle, K. D., & Tyler, K. L. (2010). Caspase-3 activation is required for reovirus-induced encephalitis in vivo. *Journal of Neurovirology*, *16*(4), 306–317. https://doi.org/10.3109/13550284.2010.499890

Berg, D., Postuma, R. B., Adler, C. H., Bloem, B. R., Chan, P., Dubois, B., Gasser, T., Goetz, C. G., Halliday, G., Joseph, L., Lang, A. E., Liepelt-Scarfone, I., Litvan, I., Marek, K., Obeso, J., Oertel, W., Olanow, C. W., Poewe, W., Stern, M., & Deuschl, G. (2015). MDS research criteria for prodromal Parkinson's disease: MDS Criteria for Prodromal PD. *Movement Disorders*, *30*(12), 1600–1611. https://doi.org/10.1002/mds.26431

Bhaskar, K., Konerth, M., Kokiko-Cochran, O. N., Cardona, A., Ransohoff, R. M., & Lamb, B. T. (2010). Regulation of Tau Pathology by the Microglial Fractalkine Receptor. *Neuron*, *68*(1), 19–31. https://doi.org/10.1016/j.neuron.2010.08.023

Birkmayer, W., & Hornykiewicz, O. (1961). [The L-3,4-dioxyphenylalanine (DOPA)-effect in Parkinson-akinesia]. *Wiener Klinische Wochenschrift*, *73*, 787–788.

Black, B. L., Rhodes, R. B., McKenzie, M., & Lyles, D. S. (1993). The role of vesicular stomatitis virus matrix protein in inhibition of host-directed gene expression is genetically separable from its function in virus assembly. *Journal of Virology*, *67*(8), 4814–4821. https://doi.org/10.1128/jvi.67.8.4814-4821.1993

Blanchard, V., Raisman-Vozari, R., Vyas, S., Michel, P. P., Javoy-Agid, F., Uhl, G., & Agid, Y. (1994). Differential expression of tyrosine hydroxylase and membrane dopamine transporter genes in subpopulations of dopaminergic neurons of the rat mesencephalon. *Molecular Brain Research*, *22*(1–4), 29–38. https://doi.org/10.1016/0169-328X(94)90029-9

Blandini, F., Nappi, G., Tassorelli, C., & Martignoni, E. (2000). Functional changes of the basal ganglia circuitry in Parkinson's disease. *Progress in Neurobiology*, *62*(1), 63–88. https://doi.org/10.1016/S0301-0082(99)00067-2

Blonder, L. X., & Slevin, J. T. (2011). Emotional Dysfunction in Parkinson's Disease. *Behavioural Neurology*, *24*(3), 201–217. https://doi.org/10.1155/2011/143857

Bobyn, J., Mangano, E. N., Gandhi, A., Nelson, E., Moloney, K., Clarke, M., & Hayley, S. (2012). Viral-toxin interactions and Parkinson's disease: Poly(I:C) priming enhanced the neurodegenerative effects of paraquat. *Journal of Neuroinflammation*, *9*(1), 86. https://doi.org/10.1186/1742-2094-9-86

Bocharov, G., Argilaguet, J., & Meyerhans, A. (2015). Understanding Experimental LCMV Infection of Mice: The Role of Mathematical Models. *Journal of Immunology Research*, *2015*, 1–10. https://doi.org/10.1155/2015/739706

Boer, D. E. C., van Smeden, J., Bouwstra, J. A., & Aerts, J. M. F. G. (2020). Glucocerebrosidase: Functions in and Beyond the Lysosome. *Journal of Clinical Medicine*, *9*(3), 736. https://doi.org/10.3390/jcm9030736

Bonifati, V. (2012). Autosomal recessive parkinsonism. *Parkinsonism & Related Disorders*, *18*, S4–S6. https://doi.org/10.1016/S1353-8020(11)70004-9

Böttner, M., Zorenkov, D., Hellwig, I., Barrenschee, M., Harde, J., Fricke, T., Deuschl, G., Egberts, J.-H., Becker, T., Fritscher-Ravens, A., Arlt, A., & Wedel, T. (2012). Expression pattern and localization of alpha-synuclein in the human enteric nervous system. *Neurobiology of Disease*, *48*(3), 474–480. https://doi.org/10.1016/j.nbd.2012.07.018

Bové, J., & Perier, C. (2012). Neurotoxin-based models of Parkinson's disease. *Neuroscience*, *211*, 51–76. https://doi.org/10.1016/j.neuroscience.2011.10.057

Braak, H., Tredici, K. D., Rüb, U., de Vos, R. A. I., Jansen Steur, E. N. H., & Braak, E. (2003). Staging of brain pathology related to sporadic Parkinson's disease. *Neurobiology of Aging*, *24*(2), 197–211. https://doi.org/10.1016/S0197-4580(02)00065-9

Bretteville, A., Marcouiller, F., Julien, C., Mouginot, D., Levesque, G., Hébert, S., & Planel, E. (2012). P3-001: Hypothermia-induced hyperphosphorylation: A new model to study tau kinase inhibitors. *Alzheimer's & Dementia*, *8*(4S_Part_12). https://doi.org/10.1016/j.jalz.2012.05.1219

Brown, E. G. (1990). Increased virulence of a mouse-adapted variant of influenza A/FM/1/47 virus is controlled by mutations in genome segments 4, 5, 7, and 8. *Journal of Virology*, *64*(9), 4523–4533. https://doi.org/10.1128/jvi.64.9.4523-4533.1990

Brundage, J. F., & Shanks, G. D. (2008). Deaths from Bacterial Pneumonia during 1918–19 Influenza Pandemic. *Emerging Infectious Diseases*, *14*(8), 1193–1199. https://doi.org/10.3201/eid1408.071313

Bu, M., Follett, J., Deng, I., Tatarnikov, I., Wall, S., Guenther, D., Maczis, M., Wimsatt, G., Milnerwood, A., Moehle, M. S., Khoshbouei, H., & Farrer, M. J. (2023). Inhibition of LRRK2 kinase activity rescues deficits in striatal dopamine physiology in VPS35 p.D620N knock-in mice. *Npj Parkinson's Disease*, *9*(1), 167. https://doi.org/10.1038/s41531-023-00609-7

Bu, X.-L., Wang, X., Xiang, Y., Shen, L.-L., Wang, Q.-H., Liu, Y.-H., Jiao, S.-S., Wang, Y.-R., Cao, H.-Y., Yi, X., Liu, C.-H., Deng, B., Yao, X.-Q., Xu, Z.-Q., Zhou, H.-D., & Wang, Y.-J. (2015). The association between infectious burden and Parkinson's disease: A case-control study. *Parkinsonism & Related Disorders*, *21*(8), 877–881. https://doi.org/10.1016/j.parkreldis.2015.05.015

Burns, R. S., Markey, S. P., Phillips, J. M., & Chiueh, C. C. (1984). The Neurotoxicity of 1-Methyl-4-phenyl-1, 2, 3, 6-tetrahydropyridine in the Monkey and Man. *Canadian Journal of Neurological Sciences / Journal Canadien Des Sciences Neurologiques*, *11*(S1), 166–168. https://doi.org/10.1017/S0317167100046345

Burré, J. (2015). The Synaptic Function of α-Synuclein. *Journal of Parkinson's Disease*, *5*(4), 699–713. https://doi.org/10.3233/JPD-150642

Camacho-Soto, A., Faust, I., Racette, B. A., Clifford, D. B., Checkoway, H., & Searles Nielsen, S. (2020). Herpesvirus Infections and Risk of Parkinson's Disease. *Neurodegenerative Diseases*, *20*(2–3), 97–103. https://doi.org/10.1159/000512874

Castro-Sánchez, S., Zaldivar-Diez, J., Luengo, E., López, M. G., Gil, C., Martínez, A., & Lastres-Becker, I. (2020). Cognitive enhancement, TAU phosphorylation reduction, and neuronal protection by the treatment of an LRRK2 inhibitor in a tauopathy mouse model. *Neurobiology of Aging*, *96*, 148–154. https://doi.org/10.1016/j.neurobiolaging.2020.09.006

Chen, C.-Y., Weng, Y.-H., Chien, K.-Y., Lin, K.-J., Yeh, T.-H., Cheng, Y.-P., Lu, C.-S., & Wang, H.-L. (2012). (G2019S) LRRK2 activates MKK4-JNK pathway and causes degeneration of SN dopaminergic neurons in a transgenic mouse model of PD. *Cell Death & Differentiation*, *19*(10), 1623–1633. https://doi.org/10.1038/cdd.2012.42

Chen, S. G., Stribinskis, V., Rane, M. J., Demuth, D. R., Gozal, E., Roberts, A. M., Jagadapillai, R., Liu, R., Choe, K., Shivakumar, B., Son, F., Jin, S., Kerber, R., Adame, A., Masliah, E., & Friedland, R. P. (2016). Exposure to the Functional Bacterial Amyloid Protein Curli Enhances Alpha-Synuclein Aggregation in Aged Fischer 344 Rats and Caenorhabditis elegans. *Scientific Reports*, *6*(1), 34477. https://doi.org/10.1038/srep34477

Chen, X., Hu, Y., Cao, Z., Liu, Q., & Cheng, Y. (2018). Cerebrospinal Fluid Inflammatory Cytokine Aberrations in Alzheimer's Disease, Parkinson's Disease and Amyotrophic Lateral Sclerosis: A Systematic Review and Meta-Analysis. *Frontiers in Immunology*, *9*. https://doi.org/10.3389/fimmu.2018.02122

Cherian, A., & Divya, K. P. (2020). Genetics of Parkinson's disease. *Acta Neurologica Belgica*, *120*(6), 1297–1305. https://doi.org/10.1007/s13760-020-01473-5

Chien, C.-H., Lee, M.-J., Liou, H.-C., Liou, H.-H., & Fu, W.-M. (2016). Microglia-Derived Cytokines/Chemokines Are Involved in the Enhancement of LPS-Induced Loss of Nigrostriatal Dopaminergic Neurons in DJ-1 Knockout Mice. *PLOS ONE*, *11*(3), e0151569. https://doi.org/10.1371/journal.pone.0151569

Choi, H., Mai, T. H., Kim, K., Cho, H., & Ki, M. (2020). Association between viral hepatitis infection and Parkinson's disease: A population-based prospective study. *Journal of Viral Hepatitis*, *27*(11), 1171–1178. https://doi.org/10.1111/jvh.13346

Cilia, R., Siri, C., Rusconi, D., Allegra, R., Ghiglietti, A., Sacilotto, G., Zini, M., Zecchinelli, A. L., Asselta, R., Duga, S., Paganoni, A. M., Pezzoli, G., Seia, M., & Goldwurm, S. (2014). LRRK2 mutations in Parkinson's disease: Confirmation of a gender effect in the Italian population. *Parkinsonism & Related Disorders*, *20*(8), 911–914. https://doi.org/10.1016/j.parkreldis.2014.04.016

Civiero, L., Cogo, S., Biosa, A., & Greggio, E. (2018). The role of LRRK2 in cytoskeletal dynamics. *Biochemical Society Transactions*, *46*(6), 1653–1663. https://doi.org/10.1042/BST20180469

Clark, L. N., Kartsaklis, L. A., Wolf Gilbert, R., Dorado, B., Ross, B. M., Kisselev, S., Verbitsky, M., Mejia-Santana, H., Cote, L. J., Andrews, H., Vonsattel, J.-P., Fahn, S., Mayeux, R., Honig, L. S., & Marder, K. (2009). Association of Glucocerebrosidase Mutations With Dementia With Lewy Bodies. *Archives of Neurology*, *66*(5). https://doi.org/10.1001/archneurol.2009.54

Clark, L. N., Wang, Y., Karlins, E., Saito, L., Mejia-Santana, H., Harris, J., Louis, E. D., Cote, L. J., Andrews, H., Fahn, S., Waters, C., Ford, B., Frucht, S., Ottman, R., & Marder, K. (2006). Frequency of *LRRK2* mutations in early- and late-onset Parkinson disease. *Neurology*, *67*(10), 1786–1791. https://doi.org/10.1212/01.wnl.0000244345.49809.36

Clarke, E., Jantrachotechatchawan, C., Buhidma, Y., Broadstock, M., Yu, L., Howlett, D., Aarsland, D., Ballard, C., & Francis, P. T. (2019). Age-related neurochemical and behavioural changes in D409V/WT GBA1 mouse: Relevance to lewy body dementia. *Neurochemistry International*, *129*, 104502. https://doi.org/10.1016/j.neuint.2019.104502

Cocoros, N. M., Svensson, E., Szépligeti, S. K., Vestergaard, S. V., Szentkúti, P., Thomsen, R. W., Borghammer, P., Sørensen, H. T., & Henderson, V. W. (2021). Long-term Risk of Parkinson Disease Following Influenza and Other Infections. *JAMA Neurology*, *78*(12), 1461. https://doi.org/10.1001/jamaneurol.2021.3895

Cornish, T. E., Stallknecht, D. E., Brown, C. C., Seal, B. S., & Howerth, E. W. (2001). Pathogenesis of Experimental Vesicular Stomatitis Virus (New Jersey Serotype) Infection in the Deer Mouse (*Peromyscus maniculatus*). *Veterinary Pathology*, *38*(4), 396–406. https://doi.org/10.1354/vp.38-4-396

Correia Guedes, L., Ferreira, J. J., Rosa, M. M., Coelho, M., Bonifati, V., & Sampaio, C. (2010). Worldwide frequency of G2019S LRRK2 mutation in Parkinson's disease: A systematic review. *Parkinsonism & Related Disorders*, *16*(4), 237–242. https://doi.org/10.1016/j.parkreldis.2009.11.004

Corsellis, J. A. N. (1951). Sub-Acute Sclerosing Leuco-Encephalitis: A Clinical and Pathological Report of Two Cases. *Journal of Mental Science*, *97*(408), 570–583. https://doi.org/10.1192/bjp.97.408.570

Cullen, V., Sardi, S. P., Ng, J., Xu, Y., Sun, Y., Tomlinson, J. J., Kolodziej, P., Kahn, I., Saftig, P., Woulfe, J., Rochet, J., Glicksman, M. A., Cheng, S. H., Grabowski, G. A., Shihabuddin, L. S., & Schlossmacher, M. G. (2011). Acid β-glucosidase mutants linked

to gaucher disease, parkinson disease, and lewy body dementia alter α-synuclein processing. *Annals of Neurology*, *69*(6), 940–953. https://doi.org/10.1002/ana.22400

Danthi, P., Holm, G. H., Stehle, T., & Dermody, T. S. (2013). Reovirus Receptors, Cell Entry, and Proapoptotic Signaling. In S. Pöhlmann & G. Simmons (Eds.), *Viral Entry into Host Cells* (Vol. 790, pp. 42–71). Springer New York. https://doi.org/10.1007/978-1-4614-7651-1_3

De Lau, L. M., & Breteler, M. M. (2006). Epidemiology of Parkinson's disease. *The Lancet Neurology*, *5*(6), 525–535. https://doi.org/10.1016/S1474-4422(06)70471-9

Deleidi, M., & Gasser, T. (2013). The role of inflammation in sporadic and familial Parkinson's disease. *Cellular and Molecular Life Sciences*, *70*(22), 4259–4273. https://doi.org/10.1007/s00018-013-1352-y

Di Primio, C., Quaranta, P., Mignanelli, M., Siano, G., Bimbati, M., Scarlatti, A., Piazza, C. R., Spezia, P. G., Perrera, P., Basolo, F., Poma, A. M., Costa, M., Pistello, M., & Cattaneo, A. (2023). Severe acute respiratory syndrome coronavirus 2 infection leads to Tau pathological signature in neurons. *PNAS Nexus*, *2*(9). https://doi.org/10.1093/pnasnexus/pgad282

Diaz, K., Kohut, M. L., Russell, D. W., & Stegemöller, E. L. (2022). Peripheral inflammatory cytokines and motor symptoms in persons with Parkinson's disease. *Brain, Behavior, & Immunity - Health*, *21*, 100442. https://doi.org/10.1016/j.bbih.2022.100442

Dietmann, A.-S., Kruse, N., Stork, L., Gloth, M., Brück, W., & Metz, I. (2023). Neurofilament light chains in serum as biomarkers of axonal damage in early MS lesions: A histological–serological correlative study. *Journal of Neurology*, *270*(3), 1416–1429. https://doi.org/10.1007/s00415-022-11468-2

Do, J., McKinney, C., Sharma, P., & Sidransky, E. (2019). Glucocerebrosidase and its relevance to Parkinson disease. *Molecular Neurodegeneration*, *14*(1), 36. https://doi.org/10.1186/s13024-019-0336-2

Dodson, M. W., & Guo, M. (2007). Pink1, Parkin, DJ-1 and mitochondrial dysfunction in Parkinson's disease. *Current Opinion in Neurobiology*, *17*(3), 331–337. https://doi.org/10.1016/j.conb.2007.04.010

Doherty, K. M., & Hardy, J. (2013). Parkin disease and the Lewy body conundrum. *Movement Disorders*, *28*(6), 702–704. https://doi.org/10.1002/mds.25486

Doty, R. L., Deems, D. A., & Stellar, S. (1988). Olfactory dysfunction in parkinsonism: A general deficit unrelated to neurologic signs, disease stage, or disease duration. *Neurology*, *38*(8), 1237–1237. https://doi.org/10.1212/WNL.38.8.1237

Dou, D., Revol, R., Östbye, H., Wang, H., & Daniels, R. (2018). Influenza A Virus Cell Entry, Replication, Virion Assembly and Movement. *Frontiers in Immunology*, *9*, 1581. https://doi.org/10.3389/fimmu.2018.01581

Drews, K., Calgi, M. P., Harrison, W. C., Drews, C. M., Costa-Pinheiro, P., Shaw, J. J. P., Jobe, K. A., Han, J. D., Fox, T. E., White, J. M., & Kester, M. (2020). Glucosylceramide synthase maintains influenza virus entry and infection. *PLOS ONE*, *15*(2), e0228735. https://doi.org/10.1371/journal.pone.0228735

Drews, K., Calgi, M. P., Harrison, W. C., Drews, C. M., Costa-Pinheiro, P., Shaw, J. J. P., Jobe, K. A., Nelson, E. A., Han, J. D., Fox, T., White, J. M., & Kester, M. (2019). Glucosylceramidase Maintains Influenza Virus Infection by Regulating Endocytosis. *Journal of Virology*, *93*(12), e00017-19. https://doi.org/10.1128/JVI.00017-19

Drolet, B. S., Campbell, C. L., Stuart, M. A., & Wilson, W. C. (2005). Vector Competence of <I>Culicoides sonorensis</I> (Diptera: Ceratopogonidae) for Vesicular Stomatitis Virus. *Journal of Medical Entomology*, *42*(3), 409–418. https://doi.org/10.1603/0022-2585(2005)042[0409:VCOCSD]2.0.CO;2

Dwyer, Z., Rudyk, C., Farmer, K., Beauchamp, S., Shail, P., Derksen, A., Fortin, T., Ventura, K., Torres, C., Ayoub, K., & Hayley, S. (2021). Characterizing the protracted neurobiological and neuroanatomical effects of paraquat in a murine model of Parkinson's disease. *Neurobiology of Aging*, *100*, 11–21. https://doi.org/10.1016/j.neurobiolaging.2020.11.013

Dwyer, Z., Rudyk, C., Thompson, A., Farmer, K., Fenner, B., Fortin, T., Derksen, A., Sun, H., & Hayley, S. (2020). Leucine-rich repeat kinase-2 (LRRK2) modulates microglial phenotype and dopaminergic neurodegeneration. *Neurobiology of Aging*, *91*, 45–55. https://doi.org/10.1016/j.neurobiolaging.2020.02.017

Dzamko, N., Deak, M., Hentati, F., Reith, A. D., Prescott, A. R., Alessi, D. R., & Nichols, R. J. (2010). Inhibition of LRRK2 kinase activity leads to dephosphorylation of Ser910/Ser935, disruption of 14-3-3 binding and altered cytoplasmic localization. *Biochemical Journal*, *430*(3), 405–413. https://doi.org/10.1042/BJ20100784

Eguchi, T., Kuwahara, T., Sakurai, M., Komori, T., Fujimoto, T., Ito, G., Yoshimura, S., Harada, A., Fukuda, M., Koike, M., & Iwatsubo, T. (2018). LRRK2 and its substrate Rab GTPases are sequentially targeted onto stressed lysosomes and maintain their homeostasis. *Proceedings of the National Academy of Sciences*, *115*(39). https://doi.org/10.1073/pnas.1812196115

Erb, M. L., & Moore, D. J. (2020). LRRK2 and the Endolysosomal System in Parkinson's Disease. *Journal of Parkinson's Disease*, *10*(4), 1271–1291. https://doi.org/10.3233/JPD-202138

Fahmy, A. M., Cannon, T., Paredes, C. H., Ahmadi, A., Xu, Y. Z., Barette, B., Ibrahim, M., Lanoix, J., Arango-Duque, G., Schurr, E., Chevet, E., Thibault, P., Gruenheid, S., McBride, H., & Desjardins, M. (2023). *LRRK2 regulates the activation of the unfolded protein response and antigen presentation in macrophages during inflammation*. https://doi.org/10.1101/2023.06.14.545012

Fava, V. M., Manry, J., Cobat, A., Orlova, M., Van Thuc, N., Ba, N. N., Thai, V. H., Abel, L., Alcaïs, A., & Schurr, E. (2016). A Missense LRRK2 Variant Is a Risk Factor for Excessive Inflammatory Responses in Leprosy. *PLOS Neglected Tropical Diseases*, *10*(2), e0004412. https://doi.org/10.1371/journal.pntd.0004412

Fava, V. M., Xu, Y. Z., Lettre, G., Van Thuc, N., Orlova, M., Thai, V. H., Tao, S., Croteau, N., Eldeeb, M. A., MacDougall, E. J., Cambri, G., Lahiri, R., Adams, L., Fon, E. A., Trempe, J.-F., Cobat, A., Alcaïs, A., Abel, L., & Schurr, E. (2019). Pleiotropic effects for Parkin and LRRK2 in leprosy type-1 reactions and Parkinson's disease. *Proceedings of the National Academy of Sciences*, *116*(31), 15616–15624. https://doi.org/10.1073/pnas.1901805116

Feng, Y.-K., Wu, Q.-L., Peng, Y.-W., Liang, F.-Y., You, H.-J., Feng, Y.-W., Li, G., Li, X.-J., Liu, S.-H., Li, Y.-C., Zhang, Y., & Pei, Z. (2020). Oral P. gingivalis impairs gut permeability and mediates immune responses associated with neurodegeneration in LRRK2 R1441G mice. *Journal of Neuroinflammation*, *17*(1), 347. https://doi.org/10.1186/s12974-020-02027-5

Fensterl, V., Wetzel, J. L., Ramachandran, S., Ogino, T., Stohlman, S. A., Bergmann, C. C., Diamond, M. S., Virgin, H. W., & Sen, G. C. (2012). Interferon-Induced Ifit2/ISG54 Protects Mice from Lethal VSV Neuropathogenesis. *PLoS Pathogens*, *8*(5), e1002712. https://doi.org/10.1371/journal.ppat.1002712

Ferran, M. C., & Lucas-Lenard, J. M. (1997). The vesicular stomatitis virus matrix protein inhibits transcription from the human beta interferon promoter. *Journal of Virology*, *71*(1), 371–377. https://doi.org/10.1128/jvi.71.1.371-377.1997

Finkelshtein, D., Werman, A., Novick, D., Barak, S., & Rubinstein, M. (2013). LDL receptor and its family members serve as the cellular receptors for vesicular stomatitis virus. *Proceedings of the National Academy of Sciences*, *110*(18), 7306–7311. https://doi.org/10.1073/pnas.1214441110

Fishbein, I., Kuo, Y.-M., Giasson, B. I., & Nussbaum, R. L. (2014). Augmentation of phenotype in a transgenic Parkinson mouse heterozygous for a Gaucher mutation. *Brain*, *137*(12), 3235–3247. https://doi.org/10.1093/brain/awu291

Forger, J. M., Bronson, R. T., Huang, A. S., & Reiss, C. S. (1991). Murine infection by vesicular stomatitis virus: Initial characterization of the H-2d system. *Journal of Virology*, *65*(9), 4950–4958. https://doi.org/10.1128/jvi.65.9.4950-4958.1991

Forlenza, O. V., Diniz, B. S., Radanovic, M., Santos, F. S., Talib, L. L., & Gattaz, W. F. (2011). Disease-modifying properties of long-term lithium treatment for amnestic mild cognitive impairment: Randomised controlled trial. *British Journal of Psychiatry*, *198*(5), 351–356. https://doi.org/10.1192/bjp.bp.110.080044

Franchi, L., Amer, A., Body-Malapel, M., Kanneganti, T.-D., Özören, N., Jagirdar, R., Inohara, N., Vandenabeele, P., Bertin, J., Coyle, A., Grant, E. P., & Núñez, G. (2006). Cytosolic flagellin requires Ipaf for activation of caspase-1 and interleukin 1β in salmonella-infected macrophages. *Nature Immunology*, *7*(6), 576–582. https://doi.org/10.1038/ni1346

Fraser, K. B., Rawlins, A. B., Clark, R. G., Alcalay, R. N., Standaert, D. G., Liu, N., Parkinson's Disease Biomarker Program Consortium, & West, A. B. (2016). Ser(P)-1292 LRRK2 in urinary exosomes is elevated in idiopathic Parkinson's disease. *Movement Disorders*, *31*(10), 1543–1550. https://doi.org/10.1002/mds.26686

Fuji, R. N., Flagella, M., Baca, M., S. Baptista, M. A., Brodbeck, J., Chan, B. K., Fiske, B. K., Honigberg, L., Jubb, A. M., Katavolos, P., Lee, D. W., Lewin-Koh, S.-C., Lin, T., Liu, X., Liu, S., Lyssikatos, J. P., O'Mahony, J., Reichelt, M., Roose-Girma, M., … Watts, R. J. (2015). Effect of selective LRRK2 kinase inhibition on nonhuman primate lung. *Science Translational Medicine*, *7*(273). https://doi.org/10.1126/scitranslmed.aaa3634

Fujiwara, H., Hasegawa, M., Dohmae, N., Kawashima, A., Masliah, E., Goldberg, M. S., Shen, J., Takio, K., & Iwatsubo, T. (2002). α-Synuclein is phosphorylated in synucleinopathy lesions. *Nature Cell Biology*, *4*(2), 160–164. https://doi.org/10.1038/ncb748

Galter, D., Westerlund, M., Carmine, A., Lindqvist, E., Sydow, O., & Olson, L. (2006). LRRK2 expression linked to dopamine-innervated areas. *Annals of Neurology*, *59*(4), 714–719. https://doi.org/10.1002/ana.20808

Gao, X., Chen, H., Schwarzschild, M. A., & Ascherio, A. (2011). Use of ibuprofen and risk of Parkinson disease. *Neurology*, *76*(10), 863–869. https://doi.org/10.1212/WNL.0b013e31820f2d79

Gardet, A., Benita, Y., Li, C., Sands, B. E., Ballester, I., Stevens, C., Korzenik, J. R., Rioux, J. D., Daly, M. J., Xavier, R. J., & Podolsky, D. K. (2010). LRRK2 Is Involved in the IFN-γ Response and Host Response to Pathogens. *The Journal of Immunology*, *185*(9), 5577–5585. https://doi.org/10.4049/jimmunol.1000548

Gaubert, S., Hourregue, C., Mouton-Liger, F., Millot, P., Franco, M., Amar-Bouaziz, E., Aarsland, D., Hugon, J., & Paquet, C. (2022). Exploring the link between GBA1 mutations and Dementia with Lewy bodies, A mini-review. *Neuroscience & Biobehavioral Reviews*, *141*, 104856. https://doi.org/10.1016/j.neubiorev.2022.104856

Gauvin, L., Bennett, S., Liu, H., Hakimi, M., Schlossmacher, M., Majithia, J., & Brown, E. G. (2013). Respiratory infection of mice with mammalian reoviruses causes systemic infection with age and strain dependent pneumonia and encephalitis. *Virology Journal*, *10*(1), 67. https://doi.org/10.1186/1743-422X-10-67

Geddes, J. F., Hughes, A. J., Lees, A. J., & Daniel, S. E. (1993). Pathological overlap in cases of parkinsonism associated with neurofibrillary tangles: A study of recent cases of postencephalitic parkinsonism and comparison with progressive supranuclear palsy and Guamanian parkinsonism-dementia complex. *Brain*, *116*(1), 281–302. https://doi.org/10.1093/brain/116.1.281

Gegg, M. E., Burke, D., Heales, S. J. R., Cooper, J. M., Hardy, J., Wood, N. W., & Schapira, A. H. V. (2012). Glucocerebrosidase deficiency in substantia nigra of parkinson disease brains. *Annals of Neurology*, *72*(3), 455–463. https://doi.org/10.1002/ana.23614

Georgel, P., Jiang, Z., Kunz, S., Janssen, E., Mols, J., Hoebe, K., Bahram, S., Oldstone, M. B. A., & Beutler, B. (2007). Vesicular stomatitis virus glycoprotein G activates a specific antiviral Toll-like receptor 4-dependent pathway. *Virology*, *362*(2), 304–313. https://doi.org/10.1016/j.virol.2006.12.032

Goedert, M., Jakes, R., Crowther, R. A., Six, J., Lübke, U., Vandermeeren, M., Cras, P., Trojanowski, J. Q., & Lee, V. M. (1993). The abnormal phosphorylation of tau protein at Ser-202 in Alzheimer disease recapitulates phosphorylation during development. *Proceedings of the National Academy of Sciences*, *90*(11), 5066–5070. https://doi.org/10.1073/pnas.90.11.5066

Goker-Alpan, O. (2004). Parkinsonism among Gaucher disease carriers. *Journal of Medical Genetics*, *41*(12), 937–940. https://doi.org/10.1136/jmg.2004.024455

Gonzalez-Latapi, P., & Marras, C. (2022). Epidemiological Evidence for an Immune Component of Parkinson's Disease. *Journal of Parkinson's Disease*, *12*(s1), S29–S43. https://doi.org/10.3233/JPD-223180

Grimes, D., Fitzpatrick, M., Gordon, J., Miyasaki, J., Fon, E. A., Schlossmacher, M., Suchowersky, O., Rajput, A., Lafontaine, A. L., Mestre, T., Appel-Cresswell, S., Kalia, S. K., Schoffer, K., Zurowski, M., Postuma, R. B., Udow, S., Fox, S., Barbeau, P., & Hutton, B. (2019). Canadian guideline for Parkinson disease. *Canadian Medical Association Journal*, *191*(36), E989–E1004. https://doi.org/10.1503/cmaj.181504

Guarda, G., Braun, M., Staehli, F., Tardivel, A., Mattmann, C., Förster, I., Farlik, M., Decker, T., Du Pasquier, R. A., Romero, P., & Tschopp, J. (2011). Type I Interferon Inhibits Interleukin-1 Production and Inflammasome Activation. *Immunity*, *34*(2), 213–223. https://doi.org/10.1016/j.immuni.2011.02.006

Guenther, D. T., Follett, J., Amouri, R., Sassi, S. B., Hentati, F., & Farrer, M. J. (2024). The Evolution of Genetic Variability at the LRRK2 Locus. *Genes*, *15*(7), 878. https://doi.org/10.3390/genes15070878

Guidotti, G., Scarlata, C., Brambilla, L., & Rossi, D. (2021). Tumor Necrosis Factor Alpha in Amyotrophic Lateral Sclerosis: Friend or Foe? *Cells*, *10*(3), 518. https://doi.org/10.3390/cells10030518

Gündner, A. L., Duran-Pacheco, G., Zimmermann, S., Ruf, I., Moors, T., Baumann, K., Jagasia, R., Van De Berg, W. D. J., & Kremer, T. (2019). Path mediation analysis reveals GBA impacts Lewy body disease status by increasing α-synuclein levels. *Neurobiology of Disease*, *121*, 205–213. https://doi.org/10.1016/j.nbd.2018.09.015

Gustavsson, E. K., Follett, J., Trinh, J., Barodia, S. K., Real, R., Liu, Z., Grant-Peters, M., Fox, J. D., Appel-Cresswell, S., Stoessl, A. J., Rajput, A., Rajput, A. H., Auer, R., Tilney, R., Sturm, M., Haack, T. B., Lesage, S., Tesson, C., Brice, A., … Farrer, M. J. (2024). *A pathogenic variant in RAB32 causes autosomal dominant Parkinson's disease and* activates LRRK2 kinase. https://doi.org/10.1101/2024.01.17.24300927

Guzman, J. N., Sanchez-Padilla, J., Wokosin, D., Kondapalli, J., Ilijic, E., Schumacker, P. T., & Surmeier, D. J. (2010). Oxidant stress evoked by pacemaking in dopaminergic neurons is attenuated by DJ-1. *Nature*, *468*(7324), 696–700. https://doi.org/10.1038/nature09536

Hakimi, M., Selvanantham, T., Swinton, E., Padmore, R. F., Tong, Y., Kabbach, G., Venderova, K., Girardin, S. E., Bulman, D. E., Scherzer, C. R., LaVoie, M. J., Gris, D., Park, D. S., Angel, J. B., Shen, J., Philpott, D. J., & Schlossmacher, M. G. (2011). Parkinson's disease-linked LRRK2 is expressed in circulating and tissue immune cells and upregulated following recognition of microbial structures. *Journal of Neural Transmission*, *118*(5), 795–808. https://doi.org/10.1007/s00702-011-0653-2

Hamm, M., Bailey, R., Shaw, G., Yen, S., Lewis, J., & Giasson, B. I. (2015). Physiologically relevant factors influence tau phosphorylation by leucine-rich repeat kinase 2. *Journal of Neuroscience Research*, *93*(10), 1567–1580. https://doi.org/10.1002/jnr.23614

Hansen, D. E., Thurmond, M. C., & Thorburn, M. (1985). Factors associated with the spread of clinical vesicular stomatitis in California dairy cattle. *American Journal of Veterinary Research*, *46*(4), 789–795.

Hart De Ruyter, F. J., Morrema, T. H. J., Den Haan, J., Gase, G., Twisk, J. W. R., De Boer, J. F., Scheltens, P., Bouwman, F. H., Verbraak, F. D., Rozemuller, A. J. M., & Hoozemans, J. J. M. (2023). α-Synuclein pathology in post-mortem retina and optic nerve is specific for α-synucleinopathies. *Npj Parkinson's Disease*, *9*(1), 124. https://doi.org/10.1038/s41531-023-00570-5

Härtlova, A., Herbst, S., Peltier, J., Rodgers, A., Bilkei-Gorzo, O., Fearns, A., Dill, B. D., Lee, H., Flynn, R., Cowley, S. A., Davies, P., Lewis, P. A., Ganley, I. G., Martinez, J., Alessi, D. R., Reith, A. D., Trost, M., & Gutierrez, M. G. (2018). LRRK2 is a negative regulator of Mycobacterium tuberculosis phagosome maturation in macrophages. *The EMBO Journal*, *37*(12). https://doi.org/10.15252/embj.201798694

Hawkes, C. H., Del Tredici, K., & Braak, H. (2007). Parkinson's disease: A dual-hit hypothesis. *Neuropathology and Applied Neurobiology*, *33*(6), 599–614. https://doi.org/10.1111/j.1365-2990.2007.00874.x

Hawkes, C. H., Del Tredici, K., & Braak, H. (2009). Parkinson's Disease: The Dual Hit Theory Revisited. *Annals of the New York Academy of Sciences*, *1170*(1), 615–622. https://doi.org/10.1111/j.1749-6632.2009.04365.x

He, J., Zhu, G., Wang, G., & Zhang, F. (2020). Oxidative Stress and Neuroinflammation Potentiate Each Other to Promote Progression of Dopamine Neurodegeneration.

Oxidative Medicine and Cellular Longevity, *2020*, 1–12. https://doi.org/10.1155/2020/6137521

Healy, D. G., Falchi, M., O'Sullivan, S. S., Bonifati, V., Durr, A., Bressman, S., Brice, A., Aasly, J., Zabetian, C. P., Goldwurm, S., Ferreira, J. J., Tolosa, E., Kay, D. M., Klein, C., Williams, D. R., Marras, C., Lang, A. E., Wszolek, Z. K., Berciano, J., … Wood, N. W. (2008). Phenotype, genotype, and worldwide genetic penetrance of LRRK2-associated Parkinson's disease: A case-control study. *The Lancet Neurology*, *7*(7), 583–590. https://doi.org/10.1016/S1474-4422(08)70117-0

Heaton, N. S., & Randall, G. (2011). Multifaceted roles for lipids in viral infection. *Trends in Microbiology*, *19*(7), 368–375. https://doi.org/10.1016/j.tim.2011.03.007

Henderson, M. X., Sengupta, M., Trojanowski, J. Q., & Lee, V. M. Y. (2019). Alzheimer's disease tau is a prominent pathology in LRRK2 Parkinson's disease. *Acta Neuropathologica Communications*, *7*(1), 183. https://doi.org/10.1186/s40478-019-0836-x

Herbst, S., Campbell, P., Harvey, J., Bernard, E. M., Papayannopoulos, V., Wood, N. W., Morris, H. R., & Gutierrez, M. G. (2020). LRRK 2 activation controls the repair of damaged endomembranes in macrophages. *The EMBO Journal*, *39*(18), e104494. https://doi.org/10.15252/embj.2020104494

Herbst, S., Lewis, P. A., & Morris, H. R. (2022). The emerging role of LRRK2 in tauopathies. *Clinical Science*, *136*(13), 1071–1079. https://doi.org/10.1042/CS20220067

Herz, J., Filiano, A. J., Wiltbank, A. T., Yogev, N., & Kipnis, J. (2017). Myeloid Cells in the Central Nervous System. *Immunity*, *46*(6), 943–956. https://doi.org/10.1016/j.immuni.2017.06.007

Herzig, M. C., Kolly, C., Persohn, E., Theil, D., Schweizer, T., Hafner, T., Stemmelen, C., Troxler, T. J., Schmid, P., Danner, S., Schnell, C. R., Mueller, M., Kinzel, B., Grevot, A., Bolognani, F., Stirn, M., Kuhn, R. R., Kaupmann, K., Van Der Putten, P. H., … Shimshek, D. R. (2011). LRRK2 protein levels are determined by kinase function and are crucial for kidney and lung homeostasis in mice. *Human Molecular Genetics*, *20*(21), 4209–4223. https://doi.org/10.1093/hmg/ddr348

Hier, D. B., Azizi, S., Thimgan, M. S., & Wunsch, D. C. (2022). Tau kinetics in Alzheimer's disease. *Frontiers in Aging Neuroscience*, *14*, 1055170. https://doi.org/10.3389/fnagi.2022.1055170

Hirschenberger, M., Hunszinger, V., & Sparrer, K. M. J. (2021). Implications of Innate Immunity in Post-Acute Sequelae of Non-Persistent Viral Infections. *Cells*, *10*(8), 2134. https://doi.org/10.3390/cells10082134

Ho, P. W.-L., Chang, E. E.-S., Leung, C.-T., Liu, H., Malki, Y., Pang, S. Y.-Y., Choi, Z. Y.-K., Liang, Y., Lai, W. S., Ruan, Y., Leung, K. M.-Y., Yung, S., Mak, J. C.-W., Kung, M. H.-W., Ramsden, D. B., & Ho, S.-L. (2022). Long-term inhibition of mutant LRRK2 hyper-kinase activity reduced mouse brain α-synuclein oligomers without adverse effects. *Npj Parkinson's Disease*, *8*(1), 115. https://doi.org/10.1038/s41531-022-00386-9

Hobbs, J. A., Hommel-Berrey, G., & Brahmi, Z. (2003). Requirement of caspase-3 for efficient apoptosis induction and caspase-7 activation but not viral replication or cell rounding in cells infected with vesicular stomatitis virus. *Human Immunology*, *64*(1), 82–92. https://doi.org/10.1016/S0198-8859(02)00702-4

Hosseini, S., Wilk, E., Michaelsen-Preusse, K., Gerhauser, I., Baumgärtner, W., Geffers, R., Schughart, K., & Korte, M. (2018). Long-Term Neuroinflammation Induced by Influenza

A Virus Infection and the Impact on Hippocampal Neuron Morphology and Function. *The Journal of Neuroscience*, *38*(12), 3060–3080. https://doi.org/10.1523/JNEUROSCI.1740-17.2018

Hsieh, J.-C. (2002). Parkinson-like syndrome as the major presenting symptom of Epstein-Barr virus encephalitis. *Archives of Disease in Childhood*, *87*(4), 358–358. https://doi.org/10.1136/adc.87.4.358

Hughes, D. A., & Pastores, G. M. (1993). Gaucher Disease. In M. P. Adam, J. Feldman, G. M. Mirzaa, R. A. Pagon, S. E. Wallace, L. J. Bean, K. W. Gripp, & A. Amemiya (Eds.), *GeneReviews®*. University of Washington, Seattle. http://www.ncbi.nlm.nih.gov/books/NBK1269/

Hui, K. Y., Fernandez-Hernandez, H., Hu, J., Schaffner, A., Pankratz, N., Hsu, N.-Y., Chuang, L.-S., Carmi, S., Villaverde, N., Li, X., Rivas, M., Levine, A. P., Bao, X., Labrias, P. R., Haritunians, T., Ruane, D., Gettler, K., Chen, E., Li, D., … Peter, I. (2018). Functional variants in the LRRK2 gene confer shared effects on risk for Crohn's disease and Parkinson's disease. *Science Translational Medicine*, *10*(423). https://doi.org/10.1126/scitranslmed.aai7795

Huneycutt, B. S., Plakhov, I. V., Shusterman, Z., Bartido, S. M., Huang, A., Reiss, C. S., & Aoki, C. (1994). Distribution of vesicular stomatitis virus proteins in the brain of BALB/c mice following intranasal inoculation: An immunohistochemical analysis. *Brain Research*, *635*(1–2), 81–95. https://doi.org/10.1016/0006-8993(94)91426-5

Hur, E.-M., Jang, E.-H., Jeong, G. R., & Lee, B. D. (2019). LRRK2 and membrane trafficking: Nexus of Parkinson's disease. *BMB Reports*, *52*(9), 533–539. https://doi.org/10.5483/BMBRep.2019.52.9.186

Iaccarino, C., Crosio, C., Vitale, C., Sanna, G., Carrì, M. T., & Barone, P. (2007). Apoptotic mechanisms in mutant LRRK2-mediated cell death. *Human Molecular Genetics*, *16*(11), 1319–1326. https://doi.org/10.1093/hmg/ddm080

Ikezu, T., Koro, L., Wolozin, B., Farraye, F. A., Strongosky, A. J., & Wszolek, Z. K. (2020). Crohn's and Parkinson's Disease-Associated LRRK2 Mutations Alter Type II Interferon Responses in Human CD14+ Blood Monocytes Ex Vivo. *Journal of Neuroimmune Pharmacology*, *15*(4), 794–800. https://doi.org/10.1007/s11481-020-09909-8

Ilan, Y. (2019). β-Glycosphingolipids as Mediators of Both Inflammation and Immune Tolerance: A Manifestation of Randomness in Biological Systems. *Frontiers in Immunology*, *10*, 1143. https://doi.org/10.3389/fimmu.2019.01143

Ilieva, N. M., Hoffman, E. K., Ghalib, M. A., Greenamyre, J. T., & De Miranda, B. R. (2024). LRRK2 kinase inhibition protects against Parkinson's disease-associated environmental toxicants. *Neurobiology of Disease*, *196*, 106522. https://doi.org/10.1016/j.nbd.2024.106522

Inflammation and infection in Parkinson's disease. (2006). *Histology and Histopathology*, *21*, 673–678. https://doi.org/10.14670/HH-21.673

Jang, H., Boltz, D., Sturm-Ramirez, K., Shepherd, K. R., Jiao, Y., Webster, R., & Smeyne, R. J. (2009). Highly pathogenic H5N1 influenza virus can enter the central nervous system and induce neuroinflammation and neurodegeneration. *Proceedings of the National Academy of Sciences*, *106*(33), 14063–14068. https://doi.org/10.1073/pnas.0900096106

Javanshiri, K., Drakenberg, T., Haglund, M., & Englund, E. (2022). Cardiac Alpha-Synuclein Is Present in Alpha-Synucleinopathies. *Journal of Parkinson's Disease*, *12*(4), 1125–1131. https://doi.org/10.3233/JPD-223161

Jellinger, K. A. (2009). Absence of α-synuclein pathology in postencephalitic parkinsonism. *Acta Neuropathologica*, *118*(3), 371–379. https://doi.org/10.1007/s00401-009-0537-9
Jordan, E. (1927). Epidemic influenza: A survey. *Chicago: American Medical Association*.
Jurga, A. M., Paleczna, M., & Kuter, K. Z. (2020). Overview of General and Discriminating Markers of Differential Microglia Phenotypes. *Frontiers in Cellular Neuroscience*, *14*, 198. https://doi.org/10.3389/fncel.2020.00198
Kachergus, J., Mata, I. F., Hulihan, M., Taylor, J. P., Lincoln, S., Aasly, J., Gibson, J. M., Ross, O. A., Lynch, T., Wiley, J., Payami, H., Nutt, J., Maraganore, D. M., Czyzewski, K., Styczynska, M., Wszolek, Z. K., Farrer, M. J., & Toft, M. (2005). Identification of a Novel LRRK2 Mutation Linked to Autosomal Dominant Parkinsonism: Evidence of a Common Founder across European Populations. *The American Journal of Human Genetics*, *76*(4), 672–680. https://doi.org/10.1086/429256
Kalia, L. V., & Lang, A. E. (2015). Parkinson's disease. *The Lancet*, *386*(9996), 896–912. https://doi.org/10.1016/S0140-6736(14)61393-3
Kalia, L. V., Lang, A. E., Hazrati, L.-N., Fujioka, S., Wszolek, Z. K., Dickson, D. W., Ross, O. A., Van Deerlin, V. M., Trojanowski, J. Q., Hurtig, H. I., Alcalay, R. N., Marder, K. S., Clark, L. N., Gaig, C., Tolosa, E., Ruiz-Martínez, J., Marti-Masso, J. F., Ferrer, I., López De Munain, A., … Marras, C. (2015). Clinical Correlations With Lewy Body Pathology in *LRRK2* -Related Parkinson Disease. *JAMA Neurology*, *72*(1), 100. https://doi.org/10.1001/jamaneurol.2014.2704
Kang, U., & Marto, J. A. (2017). Leucine-rich repeat kinase 2 and Parkinson's disease. *PROTEOMICS*, *17*(1–2), 1600092. https://doi.org/10.1002/pmic.201600092
Kassambara A (2023). *ggpubr: 'ggplot2' Based Publication Ready Plots*. R package version 0.6.0, https://rpkgs.datanovia.com/ggpubr/
Kawakami, F., & Ichikawa, T. (2015). The Role of *α* -Synuclein and LRRK2 in Tau Phosphorylation. *Parkinson's Disease*, *2015*, 1–10. https://doi.org/10.1155/2015/734746
Kawakami, F., Shimada, N., Ohta, E., Kagiya, G., Kawashima, R., Maekawa, T., Maruyama, H., & Ichikawa, T. (2014). Leucine-rich repeat kinase 2 regulates tau phosphorylation through direct activation of glycogen synthase kinase-3β. *The FEBS Journal*, *281*(1), 3–13. https://doi.org/10.1111/febs.12579
Kedariti, M., Frattini, E., Baden, P., Cogo, S., Civiero, L., Ziviani, E., Zilio, G., Bertoli, F., Aureli, M., Kaganovich, A., Cookson, M. R., Stefanis, L., Surface, M., Deleidi, M., Di Fonzo, A., Alcalay, R. N., Rideout, H., Greggio, E., & Plotegher, N. (2022). LRRK2 kinase activity regulates GCase level and enzymatic activity differently depending on cell type in Parkinson's disease. *Npj Parkinson's Disease*, *8*(1), 92. https://doi.org/10.1038/s41531-022-00354-3
Khaliq, Z. M., & Bean, B. P. (2010). Pacemaking in Dopaminergic Ventral Tegmental Area Neurons: Depolarizing Drive from Background and Voltage-Dependent Sodium Conductances. *The Journal of Neuroscience*, *30*(21), 7401–7413. https://doi.org/10.1523/JNEUROSCI.0143-10.2010
Kim, B., Yang, M.-S., Choi, D., Kim, J.-H., Kim, H.-S., Seol, W., Choi, S., Jou, I., Kim, E.-Y., & Joe, E. (2012). Impaired Inflammatory Responses in Murine Lrrk2-Knockdown Brain Microglia. *PLoS ONE*, *7*(4), e34693. https://doi.org/10.1371/journal.pone.0034693
Kim, C., Beilina, A., Smith, N., Li, Y., Kim, M., Kumaran, R., Kaganovich, A., Mamais, A., Adame, A., Iba, M., Kwon, S., Lee, W.-J., Shin, S.-J., Rissman, R. A., You, S., Lee, S.-J., Singleton, A. B., Cookson, M. R., & Masliah, E. (2020). LRRK2 mediates microglial

neurotoxicity via NFATc2 in rodent models of synucleinopathies. *Science Translational Medicine*, *12*(565). https://doi.org/10.1126/scitranslmed.aay0399

Kim, C., Lv, G., Lee, J. S., Jung, B. C., Masuda-Suzukake, M., Hong, C.-S., Valera, E., Lee, H.-J., Paik, S. R., Hasegawa, M., Masliah, E., Eliezer, D., & Lee, S.-J. (2016). Exposure to bacterial endotoxin generates a distinct strain of α-synuclein fibril. *Scientific Reports*, *6*(1), 30891. https://doi.org/10.1038/srep30891

Kim, H., Park, H. J., Choi, H., Chang, Y., Park, H., Shin, J., Kim, J., Lengner, C. J., Lee, Y. K., & Kim, J. (2019). Modeling G2019S-LRRK2 Sporadic Parkinson's Disease in 3D Midbrain Organoids. *Stem Cell Reports*, *12*(3), 518–531. https://doi.org/10.1016/j.stemcr.2019.01.020

Kim, K. S., Marcogliese, P. C., Yang, J., Callaghan, S. M., Resende, V., Abdel-Messih, E., Marras, C., Visanji, N. P., Huang, J., Schlossmacher, M. G., Trinkle-Mulcahy, L., Slack, R. S., Lang, A. E., Canadian Lrrk2 in Inflammation Team (CLINT), Park, D. S., Brown, E., Gibbings, D., Hayley, S., Park, D., … Schurr, E. (2018). Regulation of myeloid cell phagocytosis by LRRK2 via WAVE2 complex stabilization is altered in Parkinson's disease. *Proceedings of the National Academy of Sciences*, *115*(22). https://doi.org/10.1073/pnas.1718946115

Kitada, T., Tomlinson, J. J., Ao, H. S., Grimes, D. A., & Schlossmacher, M. G. (2012). Considerations Regarding the Etiology and Future Treatment of Autosomal Recessive Versus Idiopathic Parkinson Disease. *Current Treatment Options in Neurology*, *14*(3), 230–240. https://doi.org/10.1007/s11940-012-0175-8

Kitazawa, M., Oddo, S., Yamasaki, T. R., Green, K. N., & LaFerla, F. M. (2005). Lipopolysaccharide-Induced Inflammation Exacerbates Tau Pathology by a Cyclin-Dependent Kinase 5-Mediated Pathway in a Transgenic Model of Alzheimer's Disease. *The Journal of Neuroscience*, *25*(39), 8843–8853. https://doi.org/10.1523/JNEUROSCI.2868-05.2005

Koga, S., Sekiya, H., Kondru, N., Ross, O. A., & Dickson, D. W. (2021). Neuropathology and molecular diagnosis of Synucleinopathies. *Molecular Neurodegeneration*, *16*(1), 83. https://doi.org/10.1186/s13024-021-00501-z

Kolicheski, A., Turcano, P., Tamvaka, N., McLean, P. J., Springer, W., Savica, R., & Ross, O. A. (2022). Early-Onset Parkinson's Disease: Creating the Right Environment for a Genetic Disorder. *Journal of Parkinson's Disease*, *12*(8), 2353–2367. https://doi.org/10.3233/JPD-223380

Konno, T., Ross, O. A., Puschmann, A., Dickson, D. W., & Wszolek, Z. K. (2016). Autosomal dominant Parkinson's disease caused by SNCA duplications. *Parkinsonism & Related Disorders*, *22*, S1–S6. https://doi.org/10.1016/j.parkreldis.2015.09.007

Kortekaas, R., Leenders, K. L., van Oostrom, J. C. H., Vaalburg, W., Bart, J., Willemsen, A. T. M., & Hendrikse, N. H. (2005). Blood–brain barrier dysfunction in parkinsonian midbrain in vivo. *Annals of Neurology*, *57*(2), 176–179. https://doi.org/10.1002/ana.20369

Kozina, E., Byrne, M., & Smeyne, R. J. (2022). Mutant LRRK2 in lymphocytes regulates neurodegeneration via IL-6 in an inflammatory model of Parkinson's disease. *Npj Parkinson's Disease*, *8*(1), 24. https://doi.org/10.1038/s41531-022-00289-9

Kozina, E., Sadasivan, S., Jiao, Y., Dou, Y., Ma, Z., Tan, H., Kodali, K., Shaw, T., Peng, J., & Smeyne, R. J. (2018). Mutant LRRK2 mediates peripheral and central immune responses

leading to neurodegeneration in vivo. *Brain*, *141*(6), 1753–1769. https://doi.org/10.1093/brain/awy077

Kustrimovic, N., Comi, C., Magistrelli, L., Rasini, E., Legnaro, M., Bombelli, R., Aleksic, I., Blandini, F., Minafra, B., Riboldazzi, G., Sturchio, A., Mauri, M., Bono, G., Marino, F., & Cosentino, M. (2018). Parkinson's disease patients have a complex phenotypic and functional Th1 bias: Cross-sectional studies of CD4+ Th1/Th2/T17 and Treg in drug-naïve and drug-treated patients. *Journal of Neuroinflammation*, *15*(1), 205. https://doi.org/10.1186/s12974-018-1248-8

Lai, S.-W., Lin, C.-H., Lin, H.-F., Lin, C.-L., Lin, C.-C., & Liao, K.-F. (2017). Herpes zoster correlates with increased risk of Parkinson's disease in older people: A population-based cohort study in Taiwan. *Medicine*, *96*(7), e6075. https://doi.org/10.1097/MD.0000000000006075

Langston, J. W., Ballard, P., Tetrud, J. W., & Irwin, I. (1983). Chronic Parkinsonism in Humans Due to a Product of Meperidine-Analog Synthesis. *Science*, *219*(4587), 979–980. https://doi.org/10.1126/science.6823561

Langston, R., Beilina, A., Reed, X., Singleton, A., Blauwendraat, C., Gibbs, J., & Cookson, M. (2021). Association of a Common Genetic Variant with Parkinson's Disease is Propagated through Microglia. *bioRxiv Preprint*. https://doi.org/: https://doi.org/10.1101/2021.01.15.426824

Leal, M. C., Casabona, J. C., Puntel, M., & Pitossi, F. J. (2013). Interleukin-1β and tumor necrosis factor-α: Reliable targets for protective therapies in Parkinson's Disease? *Frontiers in Cellular Neuroscience*, *7*. https://doi.org/10.3389/fncel.2013.00053

Lee, H., Flynn, R., Sharma, I., Haberman, E., Carling, P. J., Nicholls, F. J., Stegmann, M., Vowles, J., Haenseler, W., Wade-Martins, R., James, W. S., & Cowley, S. A. (2020). LRRK2 Is Recruited to Phagosomes and Co-recruits RAB8 and RAB10 in Human Pluripotent Stem Cell-Derived Macrophages. *Stem Cell Reports*, *14*(5), 940–955. https://doi.org/10.1016/j.stemcr.2020.04.001

Leta, V., Urso, D., Batzu, L., Lau, Y. H., Mathew, D., Boura, I., Raeder, V., Falup-Pecurariu, C., van Wamelen, D., & Ray Chaudhuri, K. (2022). Viruses, parkinsonism and Parkinson's disease: The past, present and future. *Journal of Neural Transmission*, *129*(9), 1119–1132. https://doi.org/10.1007/s00702-022-02536-y

Li, J., Mestre, T. A., Mollenhauer, B., Frasier, M., Tomlinson, J. J., Trenkwalder, C., Ramsay, T., Manuel, D., & Schlossmacher, M. G. (2022). Evaluation of the PREDIGT score's performance in identifying newly diagnosed Parkinson's patients without motor examination. *Npj Parkinson's Disease*, *8*(1), 94. https://doi.org/10.1038/s41531-022-00360-5

Li, Y.-J., Chen, C.-Y., Yang, J.-H., & Chiu, Y.-F. (2022). Modulating cholesterol-rich lipid rafts to disrupt influenza A virus infection. *Frontiers in Immunology*, *13*, 982264. https://doi.org/10.3389/fimmu.2022.982264

Liao, J., Wu, C.-X., Burlak, C., Zhang, S., Sahm, H., Wang, M., Zhang, Z.-Y., Vogel, K. W., Federici, M., Riddle, S. M., Nichols, R. J., Liu, D., Cookson, M. R., Stone, T. A., & Hoang, Q. Q. (2014). Parkinson disease-associated mutation R1441H in LRRK2 prolongs the "active state" of its GTPase domain. *Proceedings of the National Academy of Sciences*, *111*(11), 4055–4060. https://doi.org/10.1073/pnas.1323285111

Lill, C. M. (2016). Genetics of Parkinson's disease. *Molecular and Cellular Probes*, *30*(6), 386–396. https://doi.org/10.1016/j.mcp.2016.11.001

Lin, J., Liu, F., Gao, F., Chen, Y., Wang, R., Wang, X., Li, Y., Li, Q., Sun, S., Li, Z., Lan, Y., Lu, H., Guo, W., Du, L., Gao, F., Song, D., Zhao, K., Guan, J., & He, W. (2022). Vesicular stomatitis virus sensitizes immunologically cold tumors to checkpoint blockade by inducing pyroptosis. *Biochimica et Biophysica Acta (BBA) - Molecular Basis of Disease*, *1868*(12), 166538. https://doi.org/10.1016/j.bbadis.2022.166538

Liou, B., Zhang, W., Fannin, V., Quinn, B., Ran, H., Xu, K., Setchell, K. D. R., Witte, D., Grabowski, G. A., & Sun, Y. (2019). Combination of acid β-glucosidase mutation and Saposin C deficiency in mice reveals Gba1 mutation dependent and tissue-specific disease phenotype. *Scientific Reports*, *9*(1), 5571. https://doi.org/10.1038/s41598-019-41914-7

Liu, T.-H., Huang, P.-Y., Wu, J.-Y., Chuang, M.-H., Hsu, W.-H., Tsai, Y.-W., & Lai, C.-C. (2023). Comparison of post-acute sequelae following hospitalization for COVID-19 and influenza. *BMC Medicine*, *21*(1), 480. https://doi.org/10.1186/s12916-023-03200-2

Liu, W., Liu, X., Li, Y., Zhao, J., Liu, Z., Hu, Z., Wang, Y., Yao, Y., Miller, A. W., Su, B., Cookson, M. R., Li, X., & Kang, Z. (2017). LRRK2 promotes the activation of NLRC4 inflammasome during Salmonella Typhimurium infection. *Journal of Experimental Medicine*, *214*(10), 3051–3066. https://doi.org/10.1084/jem.20170014

Liu, Z., Bryant, N., Kumaran, R., Beilina, A., Abeliovich, A., Cookson, M. R., & West, A. B. (2018). LRRK2 phosphorylates membrane-bound Rabs and is activated by GTP-bound Rab7L1 to promote recruitment to the trans-Golgi network. *Human Molecular Genetics*, *27*(2), 385–395. https://doi.org/10.1093/hmg/ddx410

Liu, Z., Lee, J., Krummey, S., Lu, W., Cai, H., & Lenardo, M. J. (2011). The kinase LRRK2 is a regulator of the transcription factor NFAT that modulates the severity of inflammatory bowel disease. *Nature Immunology*, *12*(11), 1063–1070. https://doi.org/10.1038/ni.2113

Lo, K. C., Geddes, J. F., Daniels, R. S., & Oxford, J. S. (2003). Lack of detection of influenza genes in archived formalin-fixed, paraffin wax-embedded brain samples of encephalitis lethargica patients from 1916 to 1920. *Virchows Archiv*, *442*(6), 591–596. https://doi.org/10.1007/s00428-003-0795-1

Lou, L., Zhang, P., Piao, R., & Wang, Y. (2019). Salmonella Pathogenicity Island 1 (SPI-1) and Its Complex Regulatory Network. *Frontiers in Cellular and Infection Microbiology*, *9*, 270. https://doi.org/10.3389/fcimb.2019.00270

Louveau, A., Harris, T. H., & Kipnis, J. (2015). Revisiting the Mechanisms of CNS Immune Privilege. *Trends in Immunology*, *36*(10), 569–577. https://doi.org/10.1016/j.it.2015.08.006

Lubben, N., Brynildsen, J. K., Webb, C. M., Li, H. L., Leyns, C. E. G., Changolkar, L., Zhang, B., Meymand, E. S., O'Reilly, M., Madaj, Z., DeWeerd, D., Fell, M. J., Lee, V. M. Y., Bassett, D. S., & Henderson, M. X. (2023). *LRRK2 kinase inhibition reverses G2019S mutation-dependent effects on tau pathology spread*. https://doi.org/10.1101/2023.10.06.561190

Lwin, A. (2004). Glucocerebrosidase mutations in subjects with parkinsonism. *Molecular Genetics and Metabolism*, *81*(1), 70–73. https://doi.org/10.1016/j.ymgme.2003.11.004

Madureira, M., Connor-Robson, N., & Wade-Martins, R. (2020). "LRRK2: Autophagy and Lysosomal Activity." *Frontiers in Neuroscience*, *14*, 498. https://doi.org/10.3389/fnins.2020.00498

Mahmoud, A. B., Tu, M. M., Wight, A., Zein, H. S., Rahim, M. M. A., Lee, S.-H., Sekhon, H. S., Brown, E. G., & Makrigiannis, A. P. (2016). Influenza Virus Targets Class I MHC-

Educated NK Cells for Immunoevasion. *PLOS Pathogens*, *12*(2), e1005446. https://doi.org/10.1371/journal.ppat.1005446

Malamud, N., Haymaker, W., & Pinkerton, H. (1950). Inclusion encephalitis; with a clinicopathologic report of three cases. *The American Journal of Pathology*, *26*(1), 133–153, incl 5 pl.

Mandybur, T. I., Nagpaul, A. S., Pappas, Z., & Niklowitz, W. J. (1977). Alzheimer neurofibrillary change in subacute sclerosing panencephalitis. *Annals of Neurology*, *1*(1), 103–107. https://doi.org/10.1002/ana.410010112

Marano, M., Zizzo, C., Malaguti, M. C., Bacchin, R., Cavallieri, F., De Micco, R., Spagnolo, F., Bentivoglio, A. R., Schirinzi, T., Bovenzi, R., Ramat, S., Erro, R., Sorrentino, C., Sucapane, P., Pilotto, A., Lupini, A., Magliozzi, A., Di Vico, I., Carecchio, M., … Di Fonzo, A. (2024). Increased glucosylsphingosine levels and Gaucher disease in GBA1-associated Parkinson's disease. *Parkinsonism & Related Disorders*, *124*, 107023. https://doi.org/10.1016/j.parkreldis.2024.107023

Marder, K., Wang, Y., Alcalay, R. N., Mejia-Santana, H., Tang, M.-X., Lee, A., Raymond, D., Mirelman, A., Saunders-Pullman, R., Clark, L., Ozelius, L., Orr-Urtreger, A., Giladi, N., Bressman, S., For the LRRK2 Ashkenazi Jewish Consortium, Alcalay, R. N., Tang, M.-X., Santana, H. M., Roos, E., … Bressman, S. (2015). Age-specific penetrance of *LRRK2* G2019S in the Michael J. Fox Ashkenazi Jewish LRRK2 Consortium. *Neurology*, *85*(1), 89–95. https://doi.org/10.1212/WNL.0000000000001708

Marieb, E., & Hoehn, K. (2019). *Human Anatomy and Physiology* (7th ed.). Pearson.

Marodi, L., Kaposzta, R., Toth, J., & Laszlo, A. (1995). Impaired microbicidal capacity of mononuclear phagocytes from patients with type I Gaucher disease: Partial correction by enzyme replacement therapy. *Blood*, *86*(12), 4645–4649. https://doi.org/10.1182/blood.V86.12.4645.bloodjournal86124645

Maroteaux, L., Campanelli, J., & Scheller, R. (1988). Synuclein: A neuron-specific protein localized to the nucleus and presynaptic nerve terminal. *The Journal of Neuroscience*, *8*(8), 2804–2815. https://doi.org/10.1523/JNEUROSCI.08-08-02804.1988

Marras, C., Alcalay, R. N., Caspell-Garcia, C., Coffey, C., Chan, P., Duda, J. E., Facheris, M. F., Fernández-Santiago, R., Ruíz-Martínez, J., Mestre, T., Saunders-Pullman, R., Pont-Sunyer, C., Tolosa, E., & Waro, B. (2016). Motor and nonmotor heterogeneity of LRRK2 -related and idiopathic Parkinson's disease. *Movement Disorders*, *31*(8), 1192–1202. https://doi.org/10.1002/mds.26614

Martyn, C. N. (1997). Infection in childhood and neurological diseases in adult life. *British Medical Bulletin*, *53*(1), 24–39. https://doi.org/10.1093/oxfordjournals.bmb.a011603

Mauer, S., Vergne, D., & Ghaemi, S. N. (2014). Standard and trace-dose lithium: A systematic review of dementia prevention and other behavioral benefits. *Australian & New Zealand Journal of Psychiatry*, *48*(9), 809–818. https://doi.org/10.1177/0004867414536932

Mazzon, M., & Mercer, J. (2014). Lipid interactions during virus entry and infection: Lipids and Viruses. *Cellular Microbiology*, *16*(10), 1493–1502. https://doi.org/10.1111/cmi.12340

Mazzulli, J. R., Xu, Y.-H., Sun, Y., Knight, A. L., McLean, P. J., Caldwell, G. A., Sidransky, E., Grabowski, G. A., & Krainc, D. (2011). Gaucher Disease Glucocerebrosidase and α-Synuclein Form a Bidirectional Pathogenic Loop in Synucleinopathies. *Cell*, *146*(1), 37–52. https://doi.org/10.1016/j.cell.2011.06.001

McCormick, S., Shaler, C. R., Small, C.-L., Horvath, C., Damjanovic, D., Brown, E. G., Aoki, N., Takai, T., & Xing, Z. (2011). Control of Pathogenic CD4 T Cells and Lethal Immunopathology by Signaling Immunoadaptor DAP12 during Influenza Infection. *The Journal of Immunology*, *187*(8), 4280–4292. https://doi.org/10.4049/jimmunol.1101050

Mehta, A. (2006). Epidemiology and natural history of Gaucher's disease. *European Journal of Internal Medicine*, *17*, S2–S5. https://doi.org/10.1016/j.ejim.2006.07.005

Melamed, S., Avraham, R., Rothbard, D. E., Erez, N., Israely, T., Klausner, Z., Futerman, A. H., Paran, N., & Vitner, E. B. (2020). Innate immune response in neuronopathic forms of Gaucher disease confers resistance against viral-induced encephalitis. *Acta Neuropathologica Communications*, *8*(1), 144. https://doi.org/10.1186/s40478-020-01020-6

Melrose, H., Lincoln, S., Tyndall, G., Dickson, D., & Farrer, M. (2006). Anatomical localization of leucine-rich repeat kinase 2 in mouse brain. *Neuroscience*, *139*(3), 791–794. https://doi.org/10.1016/j.neuroscience.2006.01.017

Michelakakis, H., Spanou, C., Kondyli, A., Dimitriou, E., Van Weely, S., Hollak, C. E. M., Van Oers, M. H. J., & Aerts, J. M. F. G. (1996). Plasma tumor necrosis factor-a (TNF-a) levels in Gaucher disease. *Biochimica et Biophysica Acta (BBA) - Molecular Basis of Disease*, *1317*(3), 219–222. https://doi.org/10.1016/S0925-4439(96)00056-7

Migdalska-Richards, A., & Schapira, A. H. V. (2016). The relationship between glucocerebrosidase mutations and Parkinson disease. *Journal of Neurochemistry*, *139*(S1), 77–90. https://doi.org/10.1111/jnc.13385

Miklossy, J., Arai, T., Guo, J.-P., Klegeris, A., Yu, S., McGeer, E. G., & McGeer, P. L. (2006). LRRK2 Expression in Normal and Pathologic Human Brain and in Human Cell Lines. *Journal of Neuropathology and Experimental Neurology*, *65*(10), 953–963. https://doi.org/10.1097/01.jnen.0000235121.98052.54

Mishra, A. R., Byrareddy, S. N., & Nayak, D. (2020). IFN-I Independent Antiviral Immune Response to Vesicular Stomatitis Virus Challenge in Mouse Brain. *Vaccines*, *8*(2), 326. https://doi.org/10.3390/vaccines8020326

Moehle, M. S., Webber, P. J., Tse, T., Sukar, N., Standaert, D. G., DeSilva, T. M., Cowell, R. M., & West, A. B. (2012). LRRK2 Inhibition Attenuates Microglial Inflammatory Responses. *The Journal of Neuroscience*, *32*(5), 1602–1611. https://doi.org/10.1523/JNEUROSCI.5601-11.2012

Mollenhauer, B., Cullen, V., Kahn, I., Krastins, B., Outeiro, T. F., Pepivani, I., Ng, J., Schulz-Schaeffer, W., Kretzschmar, H. A., McLean, P. J., Trenkwalder, C., Sarracino, D. A., VonSattel, J.-P., Locascio, J. J., El-Agnaf, O. M. A., & Schlossmacher, M. G. (2008). Direct quantification of CSF α-synuclein by ELISA and first cross-sectional study in patients with neurodegeneration. *Experimental Neurology*, *213*(2), 315–325. https://doi.org/10.1016/j.expneurol.2008.06.004

Monogue, B., Chen, Y., Sparks, H., Behbehani, R., Chai, A., Rajic, A. J., Massey, A., Kleinschmidt-Demasters, B. K., Vermeren, M., Kunath, T., & Beckham, J. D. (2022). Alpha-synuclein supports type 1 interferon signalling in neurons and brain tissue. *Brain*, *145*(10), 3622–3636. https://doi.org/10.1093/brain/awac192

Moon, W., Ji, E., Shin, J., Kwon, J. S., & Kim, K. W. (2022). Effect of valproate and lithium on dementia onset risk in bipolar disorder patients. *Scientific Reports*, *12*(1), 14142. https://doi.org/10.1038/s41598-022-18350-1

Morrison, R., Mihaylov, S. R., Luk, C. H., Rodgers, A., Athanasiadi, N., Morris, H. R., Pellegrino, E., Ultanir, S., & Gutierrez, M. G. (2023). *LRRK2 kinase dependent and independent function on endolysosomal repair promotes macrophage cell death*. https://doi.org/10.1101/2023.09.27.559807

Mullin, S., Beavan, M., Bestwick, J., McNeill, A., Proukakis, C., Cox, T., Hughes, D., Mehta, A., Zetterberg, H., & Schapira, A. H. V. (2019). Evolution and clustering of prodromal parkinsonian features in *GBA1* carriers. *Movement Disorders*, *34*(9), 1365–1373. https://doi.org/10.1002/mds.27775

Murphy, K. E., Gysbers, A. M., Abbott, S. K., Tayebi, N., Kim, W. S., Sidransky, E., Cooper, A., Garner, B., & Halliday, G. M. (2014). Reduced glucocerebrosidase is associated with increased α-synuclein in sporadic Parkinson's disease. *Brain*, *137*(3), 834–848. https://doi.org/10.1093/brain/awt367

Mutti, V., Carini, G., Filippini, A., Castrezzati, S., Giugno, L., Gennarelli, M., & Russo, I. (2023). LRRK2 Kinase Inhibition Attenuates Neuroinflammation and Cytotoxicity in Animal Models of Alzheimer's and Parkinson's Disease-Related Neuroinflammation. *Cells*, *12*(13), 1799. https://doi.org/10.3390/cells12131799

Nair, S., Michaelsen-Preusse, K., Finsterbusch, K., Stegemann-Koniszewski, S., Bruder, D., Grashoff, M., Korte, M., Köster, M., Kalinke, U., Hauser, H., & Kröger, A. (2014). Interferon Regulatory Factor-1 Protects from Fatal Neurotropic Infection with Vesicular Stomatitis Virus by Specific Inhibition of Viral Replication in Neurons. *PLoS Pathogens*, *10*(3), e1003999. https://doi.org/10.1371/journal.ppat.1003999

Nalls, M. A., Duran, R., Lopez, G., Kurzawa-Akanbi, M., McKeith, I. G., Chinnery, P. F., Morris, C. M., Theuns, J., Crosiers, D., Cras, P., Engelborghs, S., De Deyn, P. P., Van Broeckhoven, C., Mann, D. M. A., Snowden, J., Pickering-Brown, S., Halliwell, N., Davidson, Y., Gibbons, L., … Sidransky, E. (2013). A Multicenter Study of Glucocerebrosidase Mutations in Dementia With Lewy Bodies. *JAMA Neurology*, *70*(6), 727. https://doi.org/10.1001/jamaneurol.2013.1925

Nalls, M. A., Pankratz, N., Lill, C. M., Do, C. B., Hernandez, D. G., Saad, M., DeStefano, A. L., Kara, E., Bras, J., Sharma, M., Schulte, C., Keller, M. F., Arepalli, S., Letson, C., Edsall, C., Stefansson, H., Liu, X., Pliner, H., Lee, J. H., … Singleton, A. B. (2014). Large-scale meta-analysis of genome-wide association data identifies six new risk loci for Parkinson's disease. *Nature Genetics*, *46*(9), 989–993. https://doi.org/10.1038/ng.3043

Neudorfer, O., Giladi, N., Elstein, D., Abrahamov, A., Turezkite, T., Aghai, E., Reches, A., Bembi, B., & Zimran, A. (1996). Occurrence of Parkinson's syndrome in type 1 Gaucher disease. *QJM*, *89*(9), 691–694. https://doi.org/10.1093/qjmed/89.9.691

Norman, K. L., & Lee, P. W. K. (2000). Reovirus as a novel oncolytic agent. *Journal of Clinical Investigation*, *105*(8), 1035–1038. https://doi.org/10.1172/JCI9871

Orr-Urtreger, A., Shifrin, C., Rozovski, U., Rosner, S., Bercovich, D., Gurevich, T., Yagev-More, H., Bar-Shira, A., & Giladi, N. (2007). The *LRRK2* G2019S mutation in Ashkenazi Jews with Parkinson disease: Is there a gender effect? *Neurology*, *69*(16), 1595–1602. https://doi.org/10.1212/01.wnl.0000277637.33328.d8

Outeiro, T. F., Alcalay, R. N., Antonini, A., Attems, J., Bonifati, V., Cardoso, F., Chesselet, M., Hardy, J., Madeo, G., McKeith, I., Mollenhauer, B., Moore, D. J., Rascol, O., Schlossmacher, M. G., Soreq, H., Stefanis, L., & Ferreira, J. J. (2023). Defining the Riddle in Order to Solve It: There Is More Than One "Parkinson's Disease." *Movement Disorders*, *38*(7), 1127–1142. https://doi.org/10.1002/mds.29419

Ozaki, K., & Leonard, W. J. (2002). Cytokine and Cytokine Receptor Pleiotropy and Redundancy. *Journal of Biological Chemistry*, *277*(33), 29355–29358. https://doi.org/10.1074/jbc.R200003200

Pacelli, C., Giguère, N., Bourque, M.-J., Lévesque, M., Slack, R. S., & Trudeau, L.-É. (2015). Elevated Mitochondrial Bioenergetics and Axonal Arborization Size Are Key Contributors to the Vulnerability of Dopamine Neurons. *Current Biology*, *25*(18), 2349–2360. https://doi.org/10.1016/j.cub.2015.07.050

Pajarillo, E., Kim, S., Digman, A., Dutton, M., Son, D.-S., Aschner, M., & Lee, E. (2023). The role of microglial LRRK2 kinase in manganese-induced inflammatory neurotoxicity via NLRP3 inflammasome and RAB10-mediated autophagy dysfunction. *Journal of Biological Chemistry*, *299*(7), 104879. https://doi.org/10.1016/j.jbc.2023.104879

Pakpoor, J., Noyce, A., Goldacre, R., Selkihova, M., Mullin, S., Schrag, A., Lees, A., & Goldacre, M. (2017). Viral hepatitis and Parkinson disease: A national record-linkage study. *Neurology*, *88*(17), 1630–1633. https://doi.org/10.1212/WNL.0000000000003848

Panagiotakopoulou, V., Ivanyuk, D., De Cicco, S., Haq, W., Arsić, A., Yu, C., Messelodi, D., Oldrati, M., Schöndorf, D. C., Perez, M.-J., Cassatella, R. P., Jakobi, M., Schneiderhan-Marra, N., Gasser, T., Nikić-Spiegel, I., & Deleidi, M. (2020). Interferon-γ signaling synergizes with LRRK2 in neurons and microglia derived from human induced pluripotent stem cells. *Nature Communications*, *11*(1), 5163. https://doi.org/10.1038/s41467-020-18755-4

Papayannopoulos, V. (2018). Neutrophil extracellular traps in immunity and disease. *Nature Reviews Immunology*, *18*(2), 134–147. https://doi.org/10.1038/nri.2017.105

Park, S.-C., Moon, J. C., Shin, S. Y., Son, H., Jung, Y. J., Kim, N.-H., Kim, Y.-M., Jang, M.-K., & Lee, J. R. (2016). Functional characterization of alpha-synuclein protein with antimicrobial activity. *Biochemical and Biophysical Research Communications*, *478*(2), 924–928. https://doi.org/10.1016/j.bbrc.2016.08.052

Parkinson, J. (1817). An Essay on the Shaking Palsy. *The Journal of Neuropsychiatry and Clinical Neurosciences*, *14*(2), 223–236. https://doi.org/10.1176/jnp.14.2.223

Parkinson's Disease. (2022). *UCB Canada*. https://www.ucb-canada.ca/en/Patients/Conditions/Parkinson-s-Disease

Passini, M. A., & Wolfe, J. H. (2001). Widespread Gene Delivery and Structure-Specific Patterns of Expression in the Brain after Intraventricular Injections of Neonatal Mice with an Adeno-Associated Virus Vector. *Journal of Virology*, *75*(24), 12382–12392. https://doi.org/10.1128/JVI.75.24.12382-12392.2001

Pena, N., Richbourg, T., Gonzalez-Hunt, C. P., Qi, R., Wren, P., Barlow, C., Shanks, N. F., Carlisle, H. J., & Sanders, L. H. (2024). G2019S selective LRRK2 kinase inhibitor abrogates mitochondrial DNA damage. *Npj Parkinson's Disease*, *10*(1), 49. https://doi.org/10.1038/s41531-024-00660-y

Pham, O. H., & McSorley, S. J. (2015). Protective Host Immune Responses to *Salmonella* Infection. *Future Microbiology*, *10*(1), 101–110. https://doi.org/10.2217/fmb.14.98

Pisa, D., Alonso, R., & Carrasco, L. (2020). Parkinson's Disease: A Comprehensive Analysis of Fungi and Bacteria in Brain Tissue. *International Journal of Biological Sciences*, *16*(7), 1135–1152. https://doi.org/10.7150/ijbs.42257

Polinski, N. K., Martinez, T. N., Gorodinsky, A., Gareus, R., Sasner, M., Herberth, M., Switzer, R., Ahmad, S. O., Cosden, M., Kandebo, M., Drolet, R. E., Buckett, P. D., Shan, W., Chen, Y., Pellegrino, L. J., Ellsworth, G. D., Dungan, L. B., Hirst, W. D., Clark, S.

W., & Dave, K. D. (2021). Decreased glucocerebrosidase activity and substrate accumulation of glycosphingolipids in a novel GBA1 D409V knock-in mouse model. *PLOS ONE*, *16*(6), e0252325. https://doi.org/10.1371/journal.pone.0252325

Polymeropoulos, M. H., Lavedan, C., Leroy, E., Ide, S. E., Dehejia, A., Dutra, A., Pike, B., Root, H., Rubenstein, J., Boyer, R., Stenroos, E. S., Chandrasekharappa, S., Athanassiadou, A., Papapetropoulos, T., Johnson, W. G., Lazzarini, A. M., Duvoisin, R. C., Di Iorio, G., Golbe, L. I., & Nussbaum, R. L. (1997). Mutation in the α-Synuclein Gene Identified in Families with Parkinson's Disease. *Science*, *276*(5321), 2045–2047. https://doi.org/10.1126/science.276.5321.2045

Pons-Espinal, M., Blasco-Agell, L., Fernandez-Carasa, I., Andrés-Benito, P., Di Domenico, A., Richaud-Patin, Y., Baruffi, V., Marruecos, L., Espinosa, L., Garrido, A., Tolosa, E., Edel, M. J., Otero, M. J., Mosquera, J. L., Ferrer, I., Raya, A., & Consiglio, A. (2024). Blocking IL-6 signaling prevents astrocyte-induced neurodegeneration in an iPSC-based model of Parkinson's disease. *JCI Insight*, *9*(3), e163359. https://doi.org/10.1172/jci.insight.163359

Powell-Doherty, R. D., Abbott, A. R. N., Nelson, L. A., & Bertke, A. S. (2020). Amyloid-β and p-Tau Anti-Threat Response to Herpes Simplex Virus 1 Infection in Primary Adult Murine Hippocampal Neurons. *Journal of Virology*, *94*(9), e01874-19. https://doi.org/10.1128/JVI.01874-19

Punchard, N. A., Whelan, C. J., & Adcock, I. (2004). The Journal of Inflammation. *Journal of Inflammation*, *1*(1), 1. https://doi.org/10.1186/1476-9255-1-1

Purlyte, E., Dhekne, H. S., Sarhan, A. R., Gomez, R., Lis, P., Wightman, M., Martinez, T. N., Tonelli, F., Pfeffer, S. R., & Alessi, D. R. (2018). Rab29 activation of the Parkinson's disease-associated LRRK2 kinase. *The EMBO Journal*, *37*(1), 1–18. https://doi.org/10.15252/embj.201798099

Qi, C., Hasegawa, M., Takao, M., Sakai, M., Sasaki, M., Mizutani, M., Akagi, A., Iwasaki, Y., Miyahara, H., Yoshida, M., Scheres, S. H. W., & Goedert, M. (2023). Identical tau filaments in subacute sclerosing panencephalitis and chronic traumatic encephalopathy. *Acta Neuropathologica Communications*, *11*(1), 74. https://doi.org/10.1186/s40478-023-01565-2

Rajput, A., Dickson, D. W., Robinson, C. A., Ross, O. A., Dächsel, J. C., Lincoln, S. J., Cobb, S. A., Rajput, M. L., & Farrer, M. J. (2006). Parkinsonism, Lrrk2 G2019S, and tau neuropathology. *Neurology*, *67*(8), 1506–1508. https://doi.org/10.1212/01.wnl.0000240220.33950.0c

Raunio, A., Kivistö, V., Kero, M., Tuimala, J., Savola, S., Oinas, M., Kok, E., Colangelo, K., Paetau, A., Polvikoski, T., Tienari, P. J., Puttonen, H., & Myllykangas, L. (2022). Distribution of Lewy-related pathology in the brain, spinal cord, and periphery: The population-based Vantaa 85 + study. *Acta Neuropathologica Communications*, *10*(1), 178. https://doi.org/10.1186/s40478-022-01487-5

Ray, S., Bender, S., Kang, S., Lin, R., Glicksman, M. A., & Liu, M. (2014). The Parkinson Disease-linked LRRK2 Protein Mutation I2020T Stabilizes an Active State Conformation Leading to Increased Kinase Activity. *Journal of Biological Chemistry*, *289*(19), 13042–13053. https://doi.org/10.1074/jbc.M113.537811

Riederer, P., & Wuketich, St. (1976). Time course of nigrostriatal degeneration in parkinson's disease: A detailed study of influential factors in human brain amine analysis. *Journal of Neural Transmission*, *38*(3–4), 277–301. https://doi.org/10.1007/BF01249445

Rissman, R. A. (2009). Stress-Induced Tau Phosphorylation: Functional Neuroplasticity or Neuronal Vulnerability? *Journal of Alzheimer's Disease*, *18*(2), 453–457. https://doi.org/10.3233/JAD-2009-1153

Ritz, B. R., Paul, K. C., & Bronstein, J. M. (2016). Of Pesticides and Men: A California Story of Genes and Environment in Parkinson's Disease. *Current Environmental Health Reports*, *3*(1), 40–52. https://doi.org/10.1007/s40572-016-0083-2

Robinson, N., McComb, S., Mulligan, R., Dudani, R., Krishnan, L., & Sad, S. (2012). Type I interferon induces necroptosis in macrophages during infection with Salmonella enterica serovar Typhimurium. *Nature Immunology*, *13*(10), 954–962. https://doi.org/10.1038/ni.2397

Rocha, E. M., De Miranda, B. R., Castro, S., Drolet, R., Hatcher, N. G., Yao, L., Smith, S. M., Keeney, M. T., Di Maio, R., Kofler, J., Hastings, T. G., & Greenamyre, J. T. (2020). LRRK2 inhibition prevents endolysosomal deficits seen in human Parkinson's disease. *Neurobiology of Disease*, *134*, 104626. https://doi.org/10.1016/j.nbd.2019.104626

Rocha, E. M., Smith, G. A., Park, E., Cao, H., Brown, E., Hallett, P., & Isacson, O. (2015). Progressive decline of glucocerebrosidase in aging and P arkinson's disease. *Annals of Clinical and Translational Neurology*, *2*(4), 433–438. https://doi.org/10.1002/acn3.177

Ross, G. W., Petrovitch, H., Abbott, R. D., Nelson, J., Markesbery, W., Davis, D., Hardman, J., Launer, L., Masaki, K., Tanner, C. M., & White, L. R. (2004). Parkinsonian signs and substantia nigra neuron density in decendents elders without PD. *Annals of Neurology*, *56*(4), 532–539. https://doi.org/10.1002/ana.20226

Ross, O. A., Soto-Ortolaza, A. I., Heckman, M. G., Aasly, J. O., Abahuni, N., Annesi, G., Bacon, J. A., Bardien, S., Bozi, M., Brice, A., Brighina, L., Van Broeckhoven, C., Carr, J., Chartier-Harlin, M.-C., Dardiotis, E., Dickson, D. W., Diehl, N. N., Elbaz, A., Ferrarese, C., … Farrer, M. J. (2011). Association of LRRK2 exonic variants with susceptibility to Parkinson's disease: A case–control study. *The Lancet Neurology*, *10*(10), 898–908. https://doi.org/10.1016/S1474-4422(11)70175-2

Rudyk, C., Dwyer, Z., & Hayley, S. (2019). Leucine-rich repeat kinase-2 (LRRK2) modulates paraquat-induced inflammatory sickness and stress phenotype. *Journal of Neuroinflammation*, *16*(1), 120. https://doi.org/10.1186/s12974-019-1483-7

Rynda-Apple, A., Robinson, K. M., & Alcorn, J. F. (2015). Influenza and Bacterial Superinfection: Illuminating the Immunologic Mechanisms of Disease. *Infection and Immunity*, *83*(10), 3764–3770. https://doi.org/10.1128/IAI.00298-15

Sabikunnahar, B., Lahue, K. G., Asarian, L., Fang, Q., McGill, M. M., Haynes, L., Teuscher, C., & Krementsov, D. N. (2022). Sex differences in susceptibility to influenza A virus infection depend on host genotype. *PLOS ONE*, *17*(9), e0273050. https://doi.org/10.1371/journal.pone.0273050

Sadasivan, S., Zanin, M., O'Brien, K., Schultz-Cherry, S., & Smeyne, R. J. (2015). Induction of Microglia Activation after Infection with the Non-Neurotropic A/CA/04/2009 H1N1 Influenza Virus. *PLOS ONE*, *10*(4), e0124047. https://doi.org/10.1371/journal.pone.0124047

Sanchez-Contreras, M., Heckman, M. G., Tacik, P., Diehl, N., Brown, P. H., Soto-Ortolaza, A. I., Christopher, E. A., Walton, R. L., Ross, O. A., Golbe, L. I., Graff-Radford, N., Wszolek, Z. K., Dickson, D. W., & Rademakers, R. (2017). S tudy of *LRRK2* variation in

tauopathy: Progressive supranuclear palsy and corticobasal degeneration. *Movement Disorders*, *32*(1), 115–123. https://doi.org/10.1002/mds.26815

Sanchez-Guajardo, V., Barnum, C. J., Tansey, M. G., & Romero-Ramos, M. (2013). Neuroimmunological Processes in Parkinson's Disease and their Relation to α-Synuclein: Microglia as the Referee between Neuronal Processes and Peripheral Immunity. *ASN Neuro*, *5*(2), AN20120066. https://doi.org/10.1042/AN20120066

Sanyal, A., Novis, H. S., Gasser, E., Lin, S., & LaVoie, M. J. (2020). LRRK2 Kinase Inhibition Rescues Deficits in Lysosome Function Due to Heterozygous GBA1 Expression in Human iPSC-Derived Neurons. *Frontiers in Neuroscience*, *14*. https://doi.org/10.3389/fnins.2020.00442

Sardi, S. P., Clarke, J., Kinnecom, C., Tamsett, T. J., Li, L., Stanek, L. M., Passini, M. A., Grabowski, G. A., Schlossmacher, M. G., Sidman, R. L., Cheng, S. H., & Shihabuddin, L. S. (2011). CNS expression of glucocerebrosidase corrects α-synuclein pathology and memory in a mouse model of Gaucher-related synucleinopathy. *Proceedings of the National Academy of Sciences*, *108*(29), 12101–12106. https://doi.org/10.1073/pnas.1108197108

Sardi, S. P., Singh, P., Cheng, S. H., Shihabuddin, L. S., & Schlossmacher, M. G. (2012). Mutant *GBA1* Expression and Synucleinopathy Risk: First Insights from Cellular and Mouse Models. *Neurodegenerative Diseases*, *10*(1–4), 195–202. https://doi.org/10.1159/000335038

Scherzer, C. R., Grass, J. A., Liao, Z., Pepivani, I., Zheng, B., Eklund, A. C., Ney, P. A., Ng, J., McGoldrick, M., Mollenhauer, B., Bresnick, E. H., & Schlossmacher, M. G. (2008). GATA transcription factors directly regulate the Parkinson's disease-linked gene α-synuclein. *Proceedings of the National Academy of Sciences*, *105*(31), 10907–10912. https://doi.org/10.1073/pnas.0802437105

Schittone, S. A., Dionne, K. R., Tyler, K. L., & Clarke, P. (2012). Activation of Innate Immune Responses in the Central Nervous System during Reovirus Myelitis. *Journal of Virology*, *86*(15), 8107–8118. https://doi.org/10.1128/JVI.00171-12

Schlossmacher, M., Cullen, V., & Muthing, J. (2005). The Glucocerebrosidase Gene and Parkinson's Disease in Ashkenazi Jews. *New England Journal of Medicine*, *352*(7), 728–731. https://doi.org/10.1056/NEJM200502173520719

Schlossmacher, M. G., Tomlinson, J. J., Santos, G., Shutinoski, B., Brown, E. G., Manuel, D., & Mestre, T. (2017). Modelling idiopathic Parkinson disease as a complex illness can inform incidence rate in healthy adults: The P R EDIGT score. *European Journal of Neuroscience*, *45*(1), 175–191. https://doi.org/10.1111/ejn.13476

Schröder, J. B., Pawlowski, M., Meyer Zu Hörste, G., Gross, C. C., Wiendl, H., Meuth, S. G., Ruck, T., & Warnecke, T. (2018). Immune Cell Activation in the Cerebrospinal Fluid of Patients With Parkinson's Disease. *Frontiers in Neurology*, *9*, 1081. https://doi.org/10.3389/fneur.2018.01081

Semchuk, K. M., Love, E. J., & Lee, R. G. (1992). Parkinson's disease and exposure to agricultural work and pesticide chemicals. *Neurology*, *42*(7), 1328–1328. https://doi.org/10.1212/WNL.42.7.1328

Shahmoradian, S. H., Lewis, A. J., Genoud, C., Hench, J., Moors, T. E., Navarro, P. P., Castaño-Díez, D., Schweighauser, G., Graff-Meyer, A., Goldie, K. N., Sütterlin, R., Huisman, E., Ingrassia, A., Gier, Y. D., Rozemuller, A. J. M., Wang, J., Paepe, A. D., Erny, J., Staempfli, A., … Lauer, M. E. (2019). Lewy pathology in Parkinson's disease

consists of crowded organelles and lipid membranes. *Nature Neuroscience*, *22*(7), 1099–1109. https://doi.org/10.1038/s41593-019-0423-2

Shao, X., Shou, Q., Felix, K., Ojogho, B., Jiang, X., Gold, B. T., Herting, M. M., Goldwaser, E. L., Kochunov, P., Hong, L. E., Pappas, I., Braskie, M., Kim, H., Cen, S., Jann, K., & Wang, D. J. (2024). *Age-Related Decline in Blood-Brain Barrier Function is More Pronounced in Males than Females in Parietal and Temporal Regions*. https://doi.org/10.1101/2024.01.12.575463

Sharma, S., Bandopadhyay, R., Lashley, T., Renton, A. E. M., Kingsbury, A. E., Kumaran, R., Kallis, C., Vilariño-Güell, C., O'Sullivan, S. S., Lees, A. J., Revesz, T., Wood, N. W., & Holton, J. L. (2011). LRRK2 expression in idiopathic and G2019S positive Parkinson's disease subjects: A morphological and quantitative study. *Neuropathology and Applied Neurobiology*, *37*(7), 777–790. https://doi.org/10.1111/j.1365-2990.2011.01187.x

Sheng, Z., Zhang, S., Bustos, D., Kleinheinz, T., Le Pichon, C. E., Dominguez, S. L., Solanoy, H. O., Drummond, J., Zhang, X., Ding, X., Cai, F., Song, Q., Li, X., Yue, Z., Van Der Brug, M. P., Burdick, D. J., Gunzner-Toste, J., Chen, H., Liu, X., … Zhu, H. (2012). Ser ^{1292} Autophosphorylation Is an Indicator of LRRK2 Kinase Activity and Contributes to the Cellular Effects of PD Mutations. *Science Translational Medicine*, *4*(164). https://doi.org/10.1126/scitranslmed.3004485

Shu, L., Zhang, Y., Sun, Q., Pan, H., & Tang, B. (2019). A Comprehensive Analysis of Population Differences in LRRK2 Variant Distribution in Parkinson's Disease. *Frontiers in Aging Neuroscience*, *11*, 13. https://doi.org/10.3389/fnagi.2019.00013

Shutinoski, B., Hakimi, M., Harmsen, I. E., Lunn, M., Rocha, J., Lengacher, N., Zhou, Y. Y., Khan, J., Nguyen, A., Hake-Volling, Q., El-Kodsi, D., Li, J., Alikashani, A., Beauchamp, C., Majithia, J., Coombs, K., Shimshek, D., Marcogliese, P. C., Park, D. S., … Schlossmacher, M. G. (2019). Lrrk2 alleles modulate inflammation during microbial infection of mice in a sex-dependent manner. *Science Translational Medicine*, *11*(511). https://doi.org/10.1126/scitranslmed.aas9292

Sian, J., Youdim, M., Riederer, P., & Gerlach, M. (1999). MPTP-Induced Parkinsonian Syndrome. In *Basic Neurochemistry: Molecular, Cellular and Medical Aspects. 6th edition.* Lippincott-Raven. https://www.ncbi.nlm.nih.gov/books/NBK27974/

Sidransky, E., & Lopez, G. (2012). The link between the GBA gene and parkinsonism. *The Lancet Neurology*, *11*(11), 986–998. https://doi.org/10.1016/S1474-4422(12)70190-4

Sidransky, E., Nalls, M. A., Aasly, J. O., Aharon-Peretz, J., Annesi, G., Barbosa, E. R., Bar-Shira, A., Berg, D., Bras, J., Brice, A., Chen, C.-M., Clark, L. N., Condroyer, C., De Marco, E. V., Dürr, A., Eblan, M. J., Fahn, S., Farrer, M. J., Fung, H.-C., … Ziegler, S. G. (2009). Multicenter Analysis of Glucocerebrosidase Mutations in Parkinson's Disease. *New England Journal of Medicine*, *361*(17), 1651–1661. https://doi.org/10.1056/NEJMoa0901281

Smeyne, R. J., Eells, J. B., Chatterjee, D., Byrne, M., Akula, S. M., Sriramula, S., O'Rourke, D. P., & Schmidt, P. (2022). COVID -19 Infection Enhances Susceptibility to Oxidative Stress–Induced Parkinsonism. *Movement Disorders*, *37*(7), 1394–1404. https://doi.org/10.1002/mds.29116

Smeyne, R. J., Noyce, A. J., Byrne, M., Savica, R., & Marras, C. (2021). Infection and Risk of Parkinson's Disease. *Journal of Parkinson's Disease*, *11*(1), 31–43. https://doi.org/10.3233/JPD-202279

Smith, L. J., Lee, C.-Y., Menozzi, E., & Schapira, A. H. V. (2022). Genetic variations in GBA1 and LRRK2 genes: Biochemical and clinical consequences in Parkinson disease. *Frontiers in Neurology*, *13*, 971252. https://doi.org/10.3389/fneur.2022.971252

Sobu, Y., Wawro, P. S., Dhekne, H. S., Yeshaw, W. M., & Pfeffer, S. R. (2021). Pathogenic LRRK2 regulates ciliation probability upstream of tau tubulin kinase 2 via Rab10 and RILPL1 proteins. *Proceedings of the National Academy of Sciences*, *118*(10), e2005894118. https://doi.org/10.1073/pnas.2005894118

Soudani, N., Hage-Sleiman, R., Karam, W., Dbaibo, G., & Zaraket, H. (2019). Ceramide Suppresses Influenza A Virus Replication *In Vitro*. *Journal of Virology*, *93*(7), e00053-19. https://doi.org/10.1128/JVI.00053-19

Spanaki, C., Latsoudis, H., & Plaitakis, A. (2006). *LRRK2* mutations on Crete: R1441H associated with PD evolving to PSP. *Neurology*, *67*(8), 1518–1519. https://doi.org/10.1212/01.wnl.0000239829.33936.73

Spillantini, M. G., Schmidt, M. L., Lee, V. M.-Y., Trojanowski, J. Q., Jakes, R., & Goedert, M. (1997). α-Synuclein in Lewy bodies. *Nature*, *388*(6645), 839–840. https://doi.org/10.1038/42166

Spriggs, D. R., & Fields, B. N. (1982). Attenuated reovirus type 3 strains generated by selection of haemagglutinin antigenic variants. *Nature*, *297*(5861), 68–70. https://doi.org/10.1038/297068a0

Steger, M., Tonelli, F., Ito, G., Davies, P., Trost, M., Vetter, M., Wachter, S., Lorentzen, E., Duddy, G., Wilson, S., Baptista, M. A., Fiske, B. K., Fell, M. J., Morrow, J. A., Reith, A. D., Alessi, D. R., & Mann, M. (2016). Phosphoproteomics reveals that Parkinson's disease kinase LRRK2 regulates a subset of Rab GTPases. *eLife*, *5*, e12813. https://doi.org/10.7554/eLife.12813

Stojdl, D. F., Lichty, B. D., tenOever, B. R., Paterson, J. M., Power, A. T., Knowles, S., Marius, R., Reynard, J., Poliquin, L., Atkins, H., Brown, E. G., Durbin, R. K., Durbin, J. E., Hiscott, J., & Bell, J. C. (2003). VSV strains with defects in their ability to shutdown innate immunity are potent systemic anti-cancer agents. *Cancer Cell*, *4*(4), 263–275. https://doi.org/10.1016/S1535-6108(03)00241-1

Su, B., Wang, X., Drew, K. L., Perry, G., Smith, M. A., & Zhu, X. (2008). Physiological regulation of tau phosphorylation during hibernation. *Journal of Neurochemistry*, *105*(6), 2098–2108. https://doi.org/10.1111/j.1471-4159.2008.05294.x

Sulzer, D., Alcalay, R. N., Garretti, F., Cote, L., Kanter, E., Agin-Liebes, J., Liong, C., McMurtrey, C., Hildebrand, W. H., Mao, X., Dawson, V. L., Dawson, T. M., Oseroff, C., Pham, J., Sidney, J., Dillon, M. B., Carpenter, C., Weiskopf, D., Phillips, E., … Sette, A. (2017). T cells from patients with Parkinson's disease recognize α-synuclein peptides. *Nature*, *546*(7660), 656–661. https://doi.org/10.1038/nature22815

Sumikura, H., Takao, M., Hatsuta, H., Ito, S., Nakano, Y., Uchino, A., Nogami, A., Saito, Y., Mochizuki, H., & Murayama, S. (2015). Distribution of α-synuclein in the spinal cord and dorsal root ganglia in an autopsy cohort of elderly persons. *Acta Neuropathologica Communications*, *3*(1), 57. https://doi.org/10.1186/s40478-015-0236-9

Surface, M., Balwani, M., Waters, C., Haimovich, A., Gan-Or, Z., Marder, K. S., Hsieh, T., Song, L., Padmanabhan, S., Hsieh, F., Merchant, K. M., & Alcalay, R. N. (2022). Plasma Glucosylsphingosine in *GBA1* Mutation Carriers with and without Parkinson's Disease. *Movement Disorders*, *37*(2), 416–421. https://doi.org/10.1002/mds.28846

Suzumura, A., Takeuchi, H., Zhang, G., Kuno, R., & Mizuno, T. (2006). Roles of Glia-Derived Cytokines on Neuronal Degeneration and Regeneration. *Annals of the New York Academy of Sciences*, *1088*(1), 219–229. https://doi.org/10.1196/annals.1366.012

Sy, M., Kitazawa, M., Medeiros, R., Whitman, L., Cheng, D., Lane, T. E., & LaFerla, F. M. (2011). Inflammation Induced by Infection Potentiates Tau Pathological Features in Transgenic Mice. *The American Journal of Pathology*, *178*(6), 2811–2822. https://doi.org/10.1016/j.ajpath.2011.02.012

Takken, F. L. W., & Tameling, W. I. L. (2009). To Nibble at Plant Resistance Proteins. *Science*, *324*(5928), 744–746. https://doi.org/10.1126/science.1171666

Taxman, D. J., Huang, M. T.-H., & Ting, J. P.-Y. (2010). Inflammasome Inhibition as a Pathogenic Stealth Mechanism. *Cell Host & Microbe*, *8*(1), 7–11. https://doi.org/10.1016/j.chom.2010.06.005

Tayebi, N. (2003). Gaucher disease with parkinsonian manifestations: Does glucocerebrosidase deficiency contribute to a vulnerability to parkinsonism? *Molecular Genetics and Metabolism*, *79*(2), 104–109. https://doi.org/10.1016/S1096-7192(03)00071-4

Tayebi, N., Callahan, M., Madike, V., Stubblefield, B. K., Orvisky, E., Krasnewich, D., Fillano, J. J., & Sidransky, E. (2001). Gaucher Disease and Parkinsonism: A Phenotypic and Genotypic Characterization. *Molecular Genetics and Metabolism*, *73*(4), 313–321. https://doi.org/10.1006/mgme.2001.3201

Thaler, A., Gurevich, T., Bar Shira, A., Gana Weisz, M., Ash, E., Shiner, T., Orr-Urtreger, A., Giladi, N., & Mirelman, A. (2017). A "dose" effect of mutations in the GBA gene on Parkinson's disease phenotype. *Parkinsonism & Related Disorders*, *36*, 47–51. https://doi.org/10.1016/j.parkreldis.2016.12.014

Tiwari, D., Mittal, N., & Jha, H. C. (2022). Unraveling the links between neurodegeneration and Epstein-Barr virus-mediated cell cycle dysregulation. *Current Research in Neurobiology*, *3*, 100046. https://doi.org/10.1016/j.crneur.2022.100046

Tokarew, J. M., El-Kodsi, D. N., Lengacher, N. A., Fehr, T. K., Nguyen, A. P., Shutinoski, B., O'Nuallain, B., Jin, M., Khan, J. M., Ng, A. C. H., Li, J., Jiang, Q., Zhang, M., Wang, L., Sengupta, R., Barber, K. R., Tran, A., Im, D. S., Callaghan, S., … Schlossmacher, M. G. (2021). Age-associated insolubility of parkin in human midbrain is linked to redox balance and sequestration of reactive dopamine metabolites. *Acta Neuropathologica*, *141*(5), 725–754. https://doi.org/10.1007/s00401-021-02285-4

Tomlinson, J. J., Shutinoski, B., Dong, L., Meng, F., Elleithy, D., Lengacher, N. A., Nguyen, A. P., Cron, G. O., Jiang, Q., Roberson, E. D., Nussbaum, R. L., Majbour, N. K., El-Agnaf, O. M., Bennett, S. A., Lagace, D. C., Woulfe, J. M., Sad, S., Brown, E. G., & Schlossmacher, M. G. (2017). Holocranohistochemistry enables the visualization of α-synuclein expression in the murine olfactory system and discovery of its systemic anti-microbial effects. *Journal of Neural Transmission*, *124*(6), 721–738. https://doi.org/10.1007/s00702-017-1726-7

Tong, Y., Yamaguchi, H., Giaime, E., Boyle, S., Kopan, R., Kelleher, R. J., & Shen, J. (2010). Loss of leucine-rich repeat kinase 2 causes impairment of protein degradation pathways, accumulation of α-synuclein, and apoptotic cell death in aged mice. *Proceedings of the National Academy of Sciences*, *107*(21), 9879–9884. https://doi.org/10.1073/pnas.1004676107

Trinh, J., Schymanski, E. L., Smajic, S., Kasten, M., Sammler, E., & Grünewald, A. (2022). Molecular mechanisms defining penetrance of *LRRK2* -associated Parkinson's disease. *Medizinische Genetik*, *34*(2), 103–116. https://doi.org/10.1515/medgen-2022-2127

Trottier, M. D., Lyles, D. S., & Reiss, C. S. (2007). Peripheral, but not central nervous system, type I interferon expression in mice in response to intranasal vesicular stomatitis virus infection. *Journal of Neurovirology*, *13*(5), 433–445. https://doi.org/10.1080/13550280701460565

Tuerde, D., Kimura, T., Miyasaka, T., Furusawa, K., Shimozawa, A., Hasegawa, M., Ando, K., & Hisanaga, S. (2018). Isoform-independent and -dependent phosphorylation of microtubule-associated protein tau in mouse brain during postnatal development. *Journal of Biological Chemistry*, *293*(5), 1781–1793. https://doi.org/10.1074/jbc.M117.798918

Tysnes, O.-B., & Storstein, A. (2017). Epidemiology of Parkinson's disease. *Journal of Neural Transmission*, *124*(8), 901–905. https://doi.org/10.1007/s00702-017-1686-y

Ubamadu, E., Betancur, E., Gessner, B. D., Menon, S., Vroling, H., Curcio, D., Rozenbaum, M., Kurosky, S. K., Aponte, Z., & Begier, E. (2024). Respiratory Syncytial Virus Sequelae Among Adults in High-Income Countries: A Systematic Literature Review and Meta-analysis. *Infectious Diseases and Therapy*, *13*(7), 1399–1417. https://doi.org/10.1007/s40121-024-00974-7

Vilariño-Güell, C., Wider, C., Ross, O. A., Dachsel, J. C., Kachergus, J. M., Lincoln, S. J., Soto-Ortolaza, A. I., Cobb, S. A., Wilhoite, G. J., Bacon, J. A., Behrouz, B., Melrose, H. L., Hentati, E., Puschmann, A., Evans, D. M., Conibear, E., Wasserman, W. W., Aasly, J. O., Burkhard, P. R., … Farrer, M. J. (2011). VPS35 Mutations in Parkinson Disease. *The American Journal of Human Genetics*, *89*(1), 162–167. https://doi.org/10.1016/j.ajhg.2011.06.001

Virgin, H. W., Bassel-Duby, R., Fields, B. N., & Tyler, K. L. (1988). Antibody protects against lethal infection with the neurally spreading reovirus type 3 (Dearing). *Journal of Virology*, *62*(12), 4594–4604. https://doi.org/10.1128/jvi.62.12.4594-4604.1988

Vitner, E. B., Achdout, H., Avraham, R., Politi, B., Cherry, L., Tamir, H., Yahalom-Ronen, Y., Paran, N., Melamed, S., Erez, N., & Israely, T. (2021). Glucosylceramide synthase inhibitors prevent replication of SARS-CoV-2 and influenza virus. *Journal of Biological Chemistry*, *296*, 100470. https://doi.org/10.1016/j.jbc.2021.100470

Vitner, E. B., Farfel-Becker, T., Eilam, R., Biton, I., & Futerman, A. H. (2012). Contribution of brain inflammation to neuronal cell death in neuronopathic forms of Gaucher's disease. *Brain*, *135*(6), 1724–1735. https://doi.org/10.1093/brain/aws095

Vivaldi, G., Pfeffer, P. E., Talaei, M., Basera, T. J., Shaheen, S. O., & Martineau, A. R. (2023). Long-term symptom profiles after COVID-19 vs other acute respiratory infections: An analysis of data from the COVIDENCE UK study. *eClinicalMedicine*, *65*, 102251. https://doi.org/10.1016/j.eclinm.2023.102251

Wagner, S. K., Romero-Bascones, D., Cortina-Borja, M., Williamson, D. J., Struyven, R. R., Zhou, Y., Patel, S., Weil, R. S., Antoniades, C. A., Topol, E. J., Korot, E., Foster, P. J., Balaskas, K., Ayala, U., Barrenechea, M., Gabilondo, I., Schapira, A. H. V., Khawaja, A. P., Patel, P. J., … Zheng, Y. (2023). Retinal Optical Coherence Tomography Features Associated With Incident and Prevalent Parkinson Disease. *Neurology*, *101*(16). https://doi.org/10.1212/WNL.0000000000207727

Wallings, R., Connor-Robson, N., & Wade-Martins, R. (2019). LRRK2 interacts with the vacuolar-type H+-ATPase pump a1 subunit to regulate lysosomal function. *Human Molecular Genetics*, *28*(16), 2696–2710. https://doi.org/10.1093/hmg/ddz088

Wallings, R. L., McFarland, K., Staley, H. A., Neighbarger, N., Schaake, S., Brüggemann, N., Zittel, S., Usnich, T., Klein, C., Sammler, E. M., & Tansey, M. G. (2023). *The* R1441C-LRRK2 *mutation induces myeloid immune cell exhaustion in an age- and sex-dependent manner*. https://doi.org/10.1101/2023.10.12.562063

Wang, S., Unnithan, S., Bryant, N., Chang, A., Rosenthal, L. S., Pantelyat, A., Dawson, T. M., Al-Khalidi, H. R., & West, A. B. (2022). Elevated Urinary Rab10 Phosphorylation in Idiopathic Parkinson Disease. *Movement Disorders*, *37*(7), 1454–1464. https://doi.org/10.1002/mds.29043

Wang, W., Fu, Y. J., Zu, Y. G., Wu, N., Reichling, J., & Efferth, T. (2009). Lipid rafts play an important role in the vesicular stomatitis virus life cycle. *Archives of Virology*, *154*(4), 595–600. https://doi.org/10.1007/s00705-009-0348-2

Wei, S., Huang, J., Liu, Z., Wang, M., Zhang, B., Lian, Z., Guo, Y., & Han, H. (2019). Differential immune responses of C57BL/6 mice to infection by *Salmonella enterica* serovar Typhimurium strain SL1344, CVCC541 and CMCC50115. *Virulence*, *10*(1), 248–259. https://doi.org/10.1080/21505594.2019.1597496

Weindel, C. G., Bell, S. L., Vail, K. J., West, K. O., Patrick, K. L., & Watson, R. O. (2020). LRRK2 maintains mitochondrial homeostasis and regulates innate immune responses to Mycobacterium tuberculosis. *eLife*, *9*, e51071. https://doi.org/10.7554/eLife.51071

West, A. B., Cowell, R. M., Daher, J. P. L., Moehle, M. S., Hinkle, K. M., Melrose, H. L., Standaert, D. G., & Volpicelli-Daley, L. A. (2014). Differential LRRK2 expression in the cortex, striatum, and substantia nigra in transgenic and nontransgenic rodents. *Journal of Comparative Neurology*, *522*(11), 2465–2480. https://doi.org/10.1002/cne.23583

Wickham H (2016). ggplot2: Elegant Graphics for Data Analysis. Springer-Verlag New York. ISBN 978-3-319-24277-4, https://ggplot2.tidyverse.org/. (version 3.4.4)

Willis, A. W., Roberts, E., Beck, J. C., Fiske, B., Ross, W., Savica, R., Van Den Eeden, S. K., Tanner, C. M., Marras, C., on behalf of the Parkinson's Foundation P4 Group, Alcalay, R., Schwarzschild, M., Racette, B., Chen, H., Church, T., Wilson, B., & Doria, J. M. (2022). Incidence of Parkinson disease in North America. *Npj Parkinson's Disease*, *8*(1), 170. https://doi.org/10.1038/s41531-022-00410-y

Winner, B., Melrose, H. L., Zhao, C., Hinkle, K. M., Yue, M., Kent, C., Braithwaite, A. T., Ogholikhan, S., Aigner, R., Winkler, J., Farrer, M. J., & Gage, F. H. (2011). Adult neurogenesis and neurite outgrowth are impaired in LRRK2 G2019S mice. *Neurobiology of Disease*, *41*(3), 706–716. https://doi.org/10.1016/j.nbd.2010.12.008

Wisniewski, H. M., Dymecki, J., Wegiel, J., Kulczycki, J., Schmidt-Sidor, B., Grundke-Iqbal, I., & Strojny, P. (1991). Neurofibrillary Pathology in Subacute Sclerosing Panencephalitis. *Dementia and Geriatric Cognitive Disorders*, *2*(3), 133–141. https://doi.org/10.1159/000107188

Wüllner, U., Borghammer, P., Choe, C., Csoti, I., Falkenburger, B., Gasser, T., Lingor, P., & Riederer, P. (2023). The heterogeneity of Parkinson's disease. *Journal of Neural Transmission*, *130*(6), 827–838. https://doi.org/10.1007/s00702-023-02635-4

Xu, L., Bao, L., Li, F., Lv, Q., Ma, Y., Zhou, J., Xu, Y., Deng, W., Zhan, L., Zhu, H., Ma, C., Shu, Y., & Qin, C. (2011). Adaption of Seasonal H1N1 Influenza Virus in Mice. *PLoS ONE*, *6*(12), e28901. https://doi.org/10.1371/journal.pone.0028901

Xu, Y.-H., Quinn, B., Witte, D., & Grabowski, G. A. (2003). Viable Mouse Models of Acid β-Glucosidase Deficiency. *The American Journal of Pathology*, *163*(5), 2093–2101. https://doi.org/10.1016/S0002-9440(10)63566-3

Yao, X.-Y., Guan, L.-N., Chen, Q., & Ren, C. (2023). LRRK2 G2019S and Parkinson's disease: Insight from Neuroinflammation. *Postgraduate Medical Journal*, *100*(1179), 4–11. https://doi.org/10.1093/postmj/qgad080

Zhang, C., Pei, Y., Zhang, Z., Xu, L., Liu, X., Jiang, L., Pielak, G. J., Zhou, X., Liu, M., & Li, C. (2022). C-terminal truncation modulates α-Synuclein's cytotoxicity and aggregation by promoting the interactions with membrane and chaperone. *Communications Biology*, *5*(1), 798. https://doi.org/10.1038/s42003-022-03768-0

Zahr Eddin, K. (2024, August 23). Fiji-based quantification of glial parameters from IHC-stained mouse brain sections. *Protocols.io*. https://www.protocols.io/view/fiji-based-quantification-of-glial-parameters-from-261ge52qyg47/v1

Zhang, N., Zuo, Y., Jiang, L., Peng, Y., Huang, X., & Zuo, L. (2022). Epstein-Barr Virus and Neurological Diseases. *Frontiers in Molecular Biosciences*, *8*, 816098. https://doi.org/10.3389/fmolb.2021.816098

Zhang, Q., Cheng, X., Wu, W., Yang, S., You, H., Ye, Z., Liu, N., Chen, X., & Pan, X. (2022). Age-related LRRK2 G2019S Mutation Impacts Microglial Dopaminergic Fiber Refinement and Synaptic Pruning Involved in Abnormal Behaviors. *Journal of Molecular Neuroscience*, *72*(3), 527–543. https://doi.org/10.1007/s12031-021-01896-6

Zhang, Q., Pan, Y., Yan, R., Zeng, B., Wang, H., Zhang, X., Li, W., Wei, H., & Liu, Z. (2015). Commensal bacteria direct selective cargo sorting to promote symbiosis. *Nature Immunology*, *16*(9), 918–926. https://doi.org/10.1038/ni.3233

Zhang, Y., Tian, Q., Zhang, Q., Zhou, X., Liu, S., & Wang, J.-Z. (2009). Hyperphosphorylation of microtubule-associated tau protein plays dual role in neurodegeneration and neuroprotection. *Pathophysiology*, *16*(4), 311–316. https://doi.org/10.1016/j.pathophys.2009.02.003

Zhang, Y., Zhou, X., Cheng, F., Qi, Y., Hou, P., Zhao, M., & Zhang, H. (2017). Autophagy-related gene *LRRK2* is likely a susceptibility gene for systemic lupus erythematosus in northern Han Chinese. *Oncotarget*, *8*(8), 13754–13761. https://doi.org/10.18632/oncotarget.14631

Zheng, C., Zhou, X.-W., & Wang, J.-Z. (2016). The dual roles of cytokines in Alzheimer's disease: Update on interleukins, TNF-α, TGF-β and IFN-γ. *Translational Neurodegeneration*, *5*(1), 7. https://doi.org/10.1186/s40035-016-0054-4

Zimprich, A., Biskup, S., Leitner, P., Lichtner, P., Farrer, M., Lincoln, S., Kachergus, J., Hulihan, M., Uitti, R. J., Calne, D. B., Stoessl, A. J., Pfeiffer, R. F., Patenge, N., Carbajal, I. C., Vieregge, P., Asmus, F., Müller-Myhsok, B., Dickson, D. W., Meitinger, T., … Gasser, T. (2004). Mutations in LRRK2 Cause Autosomal-Dominant Parkinsonism with Pleomorphic Pathology. *Neuron*, *44*(4), 601–607. https://doi.org/10.1016/j.neuron.2004.11.005

Zucca, F. A., Giaveri, G., Gallorini, M., Albertini, A., Toscani, M., Pezzoli, G., Lucius, R., Wilms, H., Sulzer, D., Ito, S., Wakamatsu, K., & Zecca, L. (2004). The Neuromelanin of Human Substantia Nigra: Physiological and Pathogenic Aspects. *Pigment Cell Research*, *17*(6), 610–617. https://doi.org/10.1111/j.1600-0749.2004.00201.x